ISBN 0-7794-8652-8

THESE TERMS GOVERN YOUR USE OF THIS DOCUMENT

Your use of this Ontario Geological Survey document (the "Content") is governed by the terms set out on this page ("Terms of Use"). By downloading this Content, you (the "User") have accepted, and have agreed to be bound by, the Terms of Use.

Content: This Content is offered by the Province of Ontario's *Ministry of Northern Development and Mines* (MNDM) as a public service, on an "as-is" basis. Recommendations and statements of opinion expressed in the Content are those of the author or authors and are not to be construed as statement of government policy. You are solely responsible for your use of the Content. You should not rely on the Content for legal advice nor as authoritative in your particular circumstances. Users should verify the accuracy and applicability of any Content before acting on it. MNDM does not guarantee, or make any warranty express or implied, that the Content is current, accurate, complete or reliable. MNDM is not responsible for any damage however caused, which results, directly or indirectly, from your use of the Content. MNDM assumes no legal liability or responsibility for the Content whatsoever.

Links to Other Web Sites: This Content may contain links, to Web sites that are not operated by MNDM. Linked Web sites may not be available in French. MNDM neither endorses nor assumes any responsibility for the safety, accuracy or availability of linked Web sites or the information contained on them. The linked Web sites, their operation and content are the responsibility of the person or entity for which they were created or maintained (the "Owner"). Both your use of a linked Web site, and your right to use or reproduce information or materials from a linked Web site, are subject to the terms of use governing that particular Web site. Any comments or inquiries regarding a linked Web site must be directed to its Owner.

Copyright: Canadian and international intellectual property laws protect the Content. Unless otherwise indicated, copyright is held by the Queen's Printer for Ontario.

It is recommended that reference to the Content be made in the following form:

Ayer, J.A., Thurston, P.C., Bateman, R., Dubé, B., Gibson, H.L., Hamilton, M.A., Hathway, B., Hocker, S.M., Houlé, M.G., Hudak, G., Ispolatov, V.O., Lafrance, B., Lesher, C.M., MacDonald, P.J., Péloquin, A.S., Piercey, S.J., Reed, L.E. and Thompson, P.H. 2005. Overview of results from the Greenstone Architecture Project: Discover Abitibi Initiative; Ontario Geological Survey, Open File Report 6154, 146p.

Use and Reproduction of Content: The Content may be used and reproduced only in accordance with applicable intellectual property laws. *Non-commercial* use of unsubstantial excerpts of the Content is permitted provided that appropriate credit is given and Crown copyright is acknowledged. Any substantial reproduction of the Content or any *commercial* use of all or part of the Content is prohibited without the prior written permission of MNDM. Substantial reproduction includes the reproduction of any illustration or figure, such as, but not limited to graphs, charts and maps. Commercial use includes commercial distribution of the Content, the reproduction of multiple copies of the Content for any purpose whether or not commercial, use of the Content in commercial publications, and the creation of value-added products using the Content.

Contact:

FOR FURTHER INFORMATION ON	PLEASE CONTACT:	BY TELEPHONE:	BY E-MAIL:
The Reproduction of the EIP or Content	MNDM Publication Services	Local: (705) 670-5691 Toll Free: 1-888-415-9845, ext. 5691 (inside Canada, United States)	Pubsales@ndm.gov.on.ca
The Purchase of MNDM Publications	MNDM Publication Sales	Local: (705) 670-5691 Toll Free: 1-888-415-9845, ext. 5691 (inside Canada, United States)	Pubsales@ndm.gov.on.ca
Crown Copyright	Queen's Printer	Local: (416) 326-2678 Toll Free: 1-800-668-9938 (inside Canada, United States)	Copyright@gov.on.ca

Ontario

Ontario Geological Survey
Open File Report 6154

Overview of Results from the Greenstone Architecture Project: Discover Abitibi Initiative

2005

Ontario

ONTARIO GEOLOGICAL SURVEY

Open File Report 6154

Overview of Results from the Greenstone Architecture Project: Discover Abitibi Initiative

by

J.A. Ayer, P.C. Thurston, R. Bateman, B. Dubé, H.L. Gibson, M.A. Hamilton, B. Hathway, S.M. Hocker, M.G. Houlé, G. Hudak, V.O. Ispolatov, B. Lafrance, C.M. Lesher, P.J. MacDonald, A.S. Péloquin, S.J. Piercey, L.E. Reed and P.H. Thompson

2005

Discover Abitibi
A project of innovation, cooperation and revitalization

Découvrons l' Abitibi
Un projet d' innovation, de coopération et de renouvellement

Discover Abitibi Initiative
The Discover Abitibi Initiative is a regional, cluster economic development project based on geoscientific investigations of the western Abitibi greenstone belt. The initiative, centred on the Kirkland Lake and Timmins mining camps, will complete 19 projects developed and directed by the local stakeholders. FedNor, Northern Ontario Heritage Fund Corporation, municipalities and private sector investors have provided the funding for the initiative.

Initiative Découvrons l'Abitibi
L'initiative Découvrons l'Abitibi est un project de développment économique régional dans une grappe d'industries, projet fondé sur des études géoscientifiques de la ceinture de roches vertes de l'Abitibi occidental. Cette initiative, centrée sur les zones minières de Kirkland Lake et de Timmins, mènera à bien 19 projets élaborés et dirigés par des intervenants locaux. FedNor, la Société de gestion du Fonds du patrimoine du Nord de l'Ontario, municipalités et des investisseurs du secteur privé ont fourni les fonds de cette initiative.

FedNor Canada

Timmins

KIRKLAND LAKE
THE RIGHT ENVIRONMENT

Ontario
Northern Ontario Heritage Fund
Fonds du patrimoine du Nord de l'Ontario

Open File Reports of the Ontario Geological Survey are available for viewing at the Mines Library in Sudbury, at the Mines and Minerals Information Centre in Toronto, and at the regional Mines and Minerals office whose district includes the area covered by the report (see below).

Copies can be purchased at Publication Sales and the office whose district includes the area covered by the report. Although a particular report may not be in stock at locations other than the Publication Sales office in Sudbury, they can generally be obtained within 3 working days. All telephone, fax, mail and e-mail orders should be directed to the Publication Sales office in Sudbury. Use of VISA or MasterCard ensures the fastest possible service. Cheques or money orders should be made payable to the *Minister of Finance.*

Mines and Minerals Information Centre (MMIC) Macdonald Block, Room M2-17 900 Bay St. Toronto, Ontario M7A 1C3	Tel:	(416) 314-3800
Mines Library 933 Ramsey Lake Road, Level A3 Sudbury, Ontario P3E 6B5	Tel:	(705) 670-5615
Publication Sales 933 Ramsey Lake Rd., Level A3 Sudbury, Ontario P3E 6B5	Tel: Fax: E-mail:	(705) 670-5691(local) 1-888-415-9845(toll-free) (705) 670-5770 pubsales@ndm.gov.on.ca

Regional Mines and Minerals Offices:

Kenora - Suite 104, 810 Robertson St., Kenora P9N 4J2

Kirkland Lake - 10 Government Rd. E., Kirkland Lake P2N 1A8

Red Lake - Box 324, Ontario Government Building, Red Lake P0V 2M0

Sault Ste. Marie - 70 Foster Dr., Ste. 200, Sault Ste. Marie P6A 6V8

Southern Ontario - P.O. Bag Service 43, 126 Old Troy Rd., Tweed K0K 3J0

Sudbury - Level B3, 933 Ramsey Lake Rd., Sudbury P3E 6B5

Thunder Bay - Suite B002, 435 James St. S., Thunder Bay P7E 6S7

Timmins - Ontario Government Complex, P.O. Bag 3060, Hwy. 101 East, South Porcupine P0N 1H0

Toronto - MMIC, Macdonald Block, Room M2-17, 900 Bay St., Toronto M7A 1C3

Cette publication est disponible en anglais seulement.

Parts of this report may be quoted if credit is given. It is recommended that reference be made in the following form:

Ayer, J.A., Thurston, P.C., Bateman, R., Dubé, B., Gibson, H.L., Hamilton, M.A., Hathway, B., Hocker, S.M., Houlé, M.G., Hudak, G., Ispolatov, V.O., Lafrance, B., Lesher, C.M., MacDonald, P.J., Péloquin, A.S., Piercey, S.J., Reed, L.E. and Thompson, P.H. 2005. Overview of results from the Greenstone Architecture Project: Discover Abitibi Initiative; Ontario Geological Survey, Open File Report 6154, 146p.

Contents

FIGURES

PHOTOS

TABLES

CHART

Miscellaneous Release—Data 155

Digital Compilation of Maps and Data from the Greenstone Architecture Project in the Timmins–Kirkland Lake Region: Discover Abitibi Initiative

by J.A. Ayer, P.C. Thurston, R. Bateman, H.L. Gibson, M.A. Hamilton, B. Hathaway, S.M. Hocker, G. Hudak, B. Lafrance, V. Ispolatov, P.J. MacDonald, A.S. Péloquin, S.J. Piercey, L.E. Reed, P.H. Thompson and H. Izumi.

This digital release was produced as part of the Discover Abitibi Initiative and contains digital data from the Greenstone Architecture Project carried out by the Mineral Exploration Research Centre of Laurentian University and the Ontario Geological Survey under the Discover Abitibi Initiative. The digital data included in this compilation includes the digital maps, field collection data and lithogeochemical data from 8 Ontario Geological Survey preliminary maps (P.3543—Revised, P.3544—Revised, P.3546—Revised, P.3547—Revised, P.3555, P.3556, P.3557, and P.3558); a metamorphic map and tabular metamorphic data from Ontario Geological Survey, Open File Report 6162; and a lithostratigraphic assemblages map and tabular geochronological data from Ontario Geological Survey, Open File Report 6154. Data files in this compilation are provided as ArcView® shape (SHP) files. Users with limited access to software and hardware, limited knowledge or experience with GIS (Geographical Information Systems) can access the compiled maps listed above using ArcReader®, a free viewer available for download from ESRI®. Experienced users can access the data files and compiled map files using ESRI ArcGIS® version 8.x. Legends of the original maps are provided in portable document format (PDF). All data sets are in Universal Transverse Mercator co-ordinates using North American Datum 1983 (NAD83) Zone 17. The data and user documentation are available on one CD-ROM.

This MRD is available separately from this report.

Abstract

The Greenstone Architecture Project was funded by the Discover Abitibi Initiative to provide a multidisciplinary approach to better understanding metallogeny in the Abitibi greenstone belt. Its objective is to improve knowledge of the stratigraphy, volcanology, geochemistry, metamorphic petrology, and structural geology of the greenstone belt, emphasizing selected mineralized and barren areas in order to better understand base metal and gold metallogeny and geological architecture in the Timmins to Kirkland Lake region.

This report provides a regional prospective of the geological architecture of the region and a synthesis of the results of the nine subprojects that constitute the Architecture project, each of which also have their own publications. It also represents the first comprehensive multidisciplinary synthesis at greenstone belt scale since the widespread acceptance of autochthonous models for greenstone belt evolution. As such, it considerably advances understanding of Abitibi greenstone belt architecture and metallogeny with specific emphasis on Cu-Zn, Ni-Cu-PGE and gold mineralization and with numerous insights and recommendations that are directly applicable to exploration for these commodities.

We have considerably changed and improved our knowledge of Abitibi stratigraphy and belt-scale architecture utilizing 34 new TIMS and 11 SHRIMP U/Pb zircon ages to further subdivide and refine the distribution and age ranges for the volcanic and sedimentary assemblages, the intrusions and the timing of metallogenic and structural events. New xenocrystic evidence indicates that the Pacaud and Deloro assemblages were widespread basal units, but are now only found wrapped around the margins of external batholiths and in the cores of domes. A series of inter-formational unconformities in the volcanic "Keewatin" stratigraphic assemblages have been documented locally at the top of Pacaud, Deloro, Stoughton–Roquemaure and Kidd–Munro assemblages. The TIMS and SHRIMP data have also provided an improved understanding of the late sedimentary assemblages indicating that detritus for the Porcupine assemblage in the Timmins area was of local derivation with detrital zircon input peaking at approximately 2700 to 2690 Ma, coincident with the onset of D1. Detritus for the Timiskaming assemblage sedimentary rocks were derived from both local Abitibi-age, and external pre-Abitibi sources indicating a more widespread provenance. The Timiskaming assemblage detrital zircon input peaked at 2690 to 2670 Ma, coincident with D2 and D3 folding and faulting.

The project has resulted in an improved understanding of the stratigraphy, facies associations and metallogeny at township scales within volcanogenic massive sulphide (VMS) bearing assemblages in the Kamiskotia area by correlating the stratigraphy and the contained VMS mineralization to the upper Blake River assemblage, tracing mineralized stratigraphy from the Kam-Kotia to the Jameland deposits, recognizing, for the first time, the alteration signatures of the various Kamiskotia deposits, and relating a number of the Kamiskotia VMS deposits to synvolcanic faults; in the Ben Nevis area, by developing stratigraphic and geochemical correlations with the uppermost part of the Blake River assemblage and comparisons with the Noranda and LaRonde camps, and documenting overprinting relations between VMS and porphyry style mineralization associated with the Clifford stock; in the Munro Township area, by documenting the regional setting of VMS mineralization in the Kidd–Munro assemblage at the Potter and Potterdoal deposits and constructing a stratigraphy in the central part of the assemblage in Munro Township, and by documenting lithologies, geochemical patterns and structural overprinting of the upper Tisdale and lower Blake River assemblages in Currie Township.

We have improved understanding of the stratigraphy, facies associations and metallogeny in the Shaw Dome area by documenting the regional setting of Ni-Cu-PGE mineralization in the Tisdale assemblage, indicating the presence of important criteria for the generation of magmatic sulphide deposits including fertile komatiitic magma (metal source), proximity to sulphide iron formation (sulphur source), abundant olivine cumulate (heat source and dynamic system), and footwall embayments (physical traps).

The Timmins area and Kirkland Lake–Larder Lake area gold and intrusion subprojects utilized detailed mapping and structural studies, lithogeochemistry and geochronology to provide an improved understanding of the relationships between, and the ages of, the various assemblages, and the timing of intrusions, structural, alteration and epigenetic gold mineralization episodes. The results of these studies documented the existence of multiple gold mineralizing events at both Timmins and Kirkland Lake.

In the Timmins area, the main structural and gold mineralization events included D1 uplift and excision of upper Tisdale assemblage stratigraphy with formation of an angular unconformity predating deposition of Porcupine assemblage at 2690 Ma; an early, lower grade gold mineralizing event predating the Timiskaming unconformity was probably synchronous with D2 thrusting and folding and early south-over-north dip-slip movement on the Porcupine–Destor deformation zone (PDDZ) between 2685 and 2676 Ma. Main stage gold mineralization was associated with a protracted D3 event which coincided with the opening of the Timiskaming basin, but also overprinted the Timiskaming sediments. Rhenium–osmium geochronology on molybdenite associated with main stage gold mineralization at the McIntyre Mine provide an age of 2672±7 Ma and 2670±10 Ma at the Dome Mine. The D4 event included folding and faulting that preserved the Timiskaming assemblage in synclines along the PDDZ and is associated with a late stage gold mineralization event along the Pamour Mine trend.

In the Kirkland Lake–Larder Lake area, the main structural and gold mineralization events are post-Timiskaming and include a D2 event corresponding with movement along the Larder Lake–Cadillac deformation zone and the deposits spatially associated with this deformation zone (possibly correlative with the D3 event in Timmins). The D3 event was related to the east-west shortening. The Kirkland Lake gold deposits are associated with the brittle to brittle-ductile Kirkland Lake fault (Main Break) and its subsidiary splays. The presence of open-space-filling textures in veins, and the association of veins with brittle faults suggest relatively shallow crustal levels of mineralization. Distinct metal signature and mineralization style suggest that the Kirkland Lake deposits probably represents a stand-alone hydrothermal system that is unrelated to gold deposits along the Larder Lake–Cadillac deformation zone and its splays. A deep magmatic fluid source appears most probable for the Kirkland Lake mineralization. Gold-bearing veins could have formed early in the D4 event, synchronously with south over north reverse-dextral to reverse movement along the Main Break. Alternatively, mineralization could have predated the D4 event. Gold mineralization in the Narrows Break, north of the Kirkland Lake Main Break, was synchronous with northwest-southeast shortening during the D4 event.

A new metamorphic framework has provided additional constraints on the setting of gold deposits and a new tool for gold exploration. The metamorphic pattern in the study area is the result of superposition of regional metamorphism on narrow higher grade contact metamorphic aureoles that formed at different times immediately adjacent to granitic intrusions, indicating that most of the granitoids are older than the regional metamorphic event. Pre-Timiskaming phases of deformation were less penetrative and occurred at shallower depths in the crust and at lower temperatures than post-Timiskaming deformation, whereas post-Timiskaming deformation, when peak regional metamorphic conditions prevailed, was most conducive to formation of large synmetamorphic (orogenic) gold deposits. There is a striking spatial relationship of the boundary between the lower and upper greenschist metamorphic zones and a significant number of gold mines. Newly identified high priority targets are defined by the coincidence of metamorphic anomalies with major structural features, specific rock compositions, and moderate to intense deformation.

Regional structural patterns are now better understood, in part based upon improved knowledge of the distribution of the stratigraphy and intrusions in conjunction with detailed and regional scale geophysical surveys including magnetic, gravity and reflection seismic surveys. Major external intrusive units such as the Round Lake and Kenogamissi batholiths include synvolcanic phases that occupy

anticlinal culminations, whereas the later syntectonic intrusions had a relatively minor localized structural effect on the surrounding supracrustal rocks. Regional deformation zone are the locus of major faults which have been reactivated repeatedly and have exerted some control on the distribution of early volcanic ("Keewatin") and late sedimentary assemblages. All assemblages were constructed in an autochthonous fashion and have been locally juxtaposed along regional structures during major ductile deformation events that involved predominantly north-south transpressional shortening. Our geophysical inversions of magnetic and gravity data have demonstrated the sense of dip on a number of major structures and lithological units.

Overview of Results from the Greenstone Architecture Project: Discover Abitibi Initiative

J.A. Ayer[1], P.C. Thurston[2], R. Bateman[2], B. Dubé[3], H.L. Gibson[2], M.A. Hamilton[4], B. Hathway[2], S.M. Hocker[2], M.G. Houlé[1], G. Hudak[5], V.O. Ispolatov[2], B. Lafrance[2], C.M. Lesher[2], P.J. MacDonald[2], A.S. Péloquin[2], S.J. Piercey[2], L.E. Reed[6] and P.H. Thompson[7]

Ontario Geological Survey
Open File Report 6154
2005

---

[1]Precambrian Geoscience Section, Ontario Geological Survey, Sudbury, Ontario
[2]Mineral Exploration Research Centre, Laurentian University, Sudbury, Ontario
[3]Geological Survey of Canada, Québec, Québec
[4]Jack Satterly Geochronology Laboratory, Department of Geology, University of Toronto, Toronto, Ontario
[5]Department of Geology, University of Wisconsin Oshkosh, Oshkosh, Wisconsin
[6]L.E. Reed geophysical consultant, Rockwood, Ontario
[7]Peter H. Thompson Geological Consulting Ltd., Ottawa, Ontario

Introduction

The western part of the southern Abitibi greenstone belt (SAGB) contains some of the world's largest copper-zinc and gold deposits and significant amounts of nickel-copper-platinum group element (PGE) mineralization. Early discoveries were made by classical prospecting with subsequent discoveries commonly resulting from diamond drilling targeted by electromagnetic surveys. The next generation of deposits will be found at greater depth, principally beneath the extensive overburden that covers most of the Abitibi greenstone belt. Thus, exploration will require improved knowledge of the geological characteristics of the existing deposits, the stratigraphic, plutonic, structural and metamorphic architecture of the region and will rely more heavily on expensive geophysical and geochemical techniques, verified by diamond drilling.

The Abitibi greenstone belt is typical of many mineralized environments in that there is excellent knowledge of the immediate surroundings of the mineral deposits and knowledge of the regional scale setting. The understanding of the geology at the subregional and district scales is less clear, because of regional-scale stratigraphic variations and, in some cases, complex metamorphic and structural overprints. The objective of this project is to improve knowledge of the stratigraphy, volcanology, geochemistry, metamorphic petrology, and structural geology of the greenstone belt, emphasizing selected mineralized and barren areas in order to better understand the geological architecture of the belt. The project has increased our knowledge of the stratigraphy, lithological variation, structural patterns, geochemical variation, and alteration, and metamorphic overprints involved in the localization and genesis of Cu-Zn, Ni-Cu-PGE and Au deposits, and will aid in the development of new concepts for discovering deposits.

The purpose of this project was to provide new field-based geological and geochemical data and new concepts that can be used to more effectively and efficiently explore for gold and base metal deposits in the Timmins–Kirkland Lake region of the Abitibi greenstone belt (Figure 1). The project will contribute directly to new base metal and gold discoveries by 1) providing a better understanding of the stratigraphic, plutonic, structural and metamorphic architecture of the region, 2) identifying fundamental controls on localization and genesis of gold and base metal mineralization utilizing a variety of "state of the art" approaches, and 3) developing new geological tools for more effective exploration, thereby reducing exploration risk, especially in poorly exposed areas.

Although detailed mapping has been a key component of the project applied to the critical parts of the greenstone belt, the results of this detailed research have been extended to provide complete and equal coverage of, and generate an enhanced level of knowledge of, the entire Timmins–Kirkland Lake area. This overview report summarizes the various individual subproject results reported through the stream of maps, reports and workshops, culminating in this synthesis.

APPROACH

The approach taken was to mount thematic subprojects with emphasis on the following:

1. Improving knowledge of the stratigraphic framework for the greenstone belt as a whole. This has involved development of stratigraphic sections in the Kidd–Munro, Blake River, Tisdale, Porcupine and Timiskaming assemblages followed by expansion outward to the scale of the entire belt using geochemistry, geochronology, tracing of key marker horizons and structural relationships as tools in the stratigraphic and structural interpretation.
2. Understanding the fabric relations and their relative timing in the development of lode gold deposits and applying this understanding to regional-scale structures, plutonic event chronologies and metamorphism.

3. The geophysical subproject functioned as an adjunct to the geological subprojects. Custom plots of aeromagnetic data were used to trace marker units. Potential field inversion techniques were applied to both magnetic and gravity data to constrain the dip of stratigraphy and major structures to aid in regional-scale interpretation.
4. The VMS-related projects emphasized volcanological and stratigraphic mapping associated with VMS mineralization in the Kidd–Munro, Tisdale and Blake River assemblages. Work was conducted at both the deposit scale and the assemblage scale.
5. The Ni-Cu-PGE-related project emphasized volcanological and stratigraphic mapping associated with komatiite-associated mineralization within the Tisdale assemblage in the Shaw Dome area. The major contribution by the Architecture Project in support of this project involved geochronological data and three-dimensional (3D) geophysical inversions. This subproject, combined with the regional bedrock mapping carried by the OGS as in-kind contribution to the Greenstone Architecture Project, has improved knowledge of the stratigraphic, structural and volcanic architecture of Cu-Ni-PGE mineralization in the Shaw Dome area.

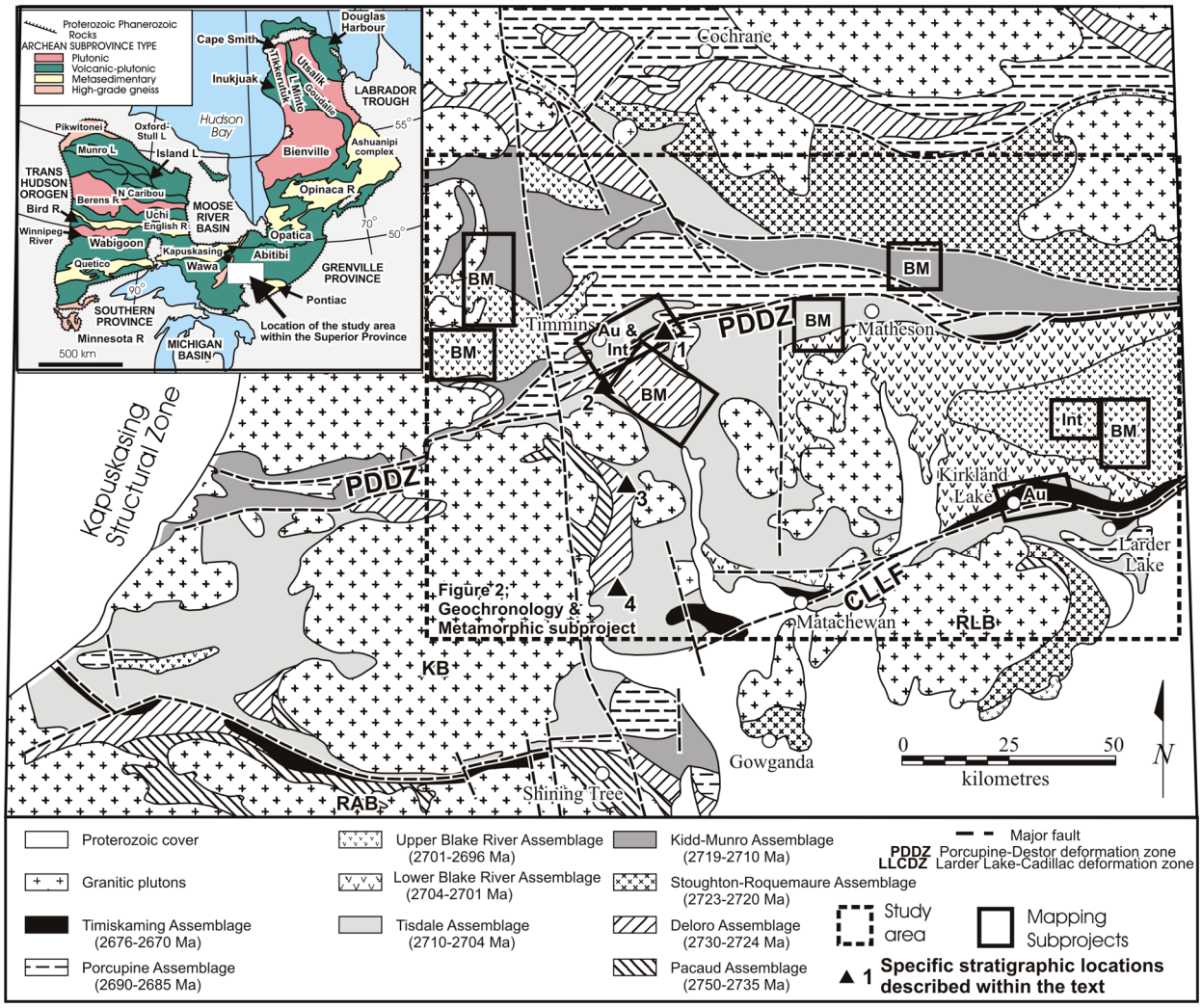

Figure 1. Assemblage map for the Ontario portion of the Abitibi greenstone belt with location of the study area, subproject areas (Au represents gold subprojects; BM, base metal subprojects and Int, intrusion subprojects) and stratigraphic locations discussed in the text. Abbreviations: KB, Kenogamissi batholith; RAB, Ramsey–Algoma batholith; RLB, Round Lake batholith.

6. The metamorphic subproject, based on examination of 2500 thin sections distributed throughout the study area, provides thermal and depth constraints on deposition, plutonism, deformation and mineralization in the region. At a regional scale and in the form of kilometre-scale metamorphic anomalies, the previously unrecognized boundary between the lower and upper greenschist zones highlights areas favourable for gold exploration.
7. This overview report attempts to synthesize the results of our investigations. Readers should make reference to the individual subproject maps and reports for full details. Thus far, we have focussed our products to exploration-oriented considerations. We will be emphasizing considerations such as deposit genesis and other theoretical considerations in a forthcoming special issue of *Economic Geology*.

PRODUCTS

The Greenstone Architecture Project has generated a large number of reports, maps and digital products over its two-year span, all of which have all been released as Ontario Geological Survey publications. Interim reports were provided as 20 Ontario Geological Survey, *Summary of Field Work* articles: 10 in 2003, and 10 in 2004. In addition, the following Open File Reports have been published:

1. OFR **6154** (this report): *Overview of Results from the Greenstone Architecture Project: Discover Abitibi Initiative* by J.A. Ayer, P.C. Thurston, R. Bateman, B. Dubé, H.L. Gibson, M.A. Hamilton, B. Hathaway, S.M. Hocker, M.G. Houlé, G. Hudak, B. Lafrance, C.M. Lesher, V.O. Ispolatov, P.J. MacDonald, A.S. Péloquin, S.J. Piercey, L.E. Reed, and P.H. Thompson
2. OFR **6155**: *Geological Setting of Volcanogenic Massive Sulphide Mineralization in the Kamiskotia area: Discover Abitibi Initiative* by B. Hathway, G. Hudak and M.A. Hamilton
3. OFR **6156**: *Volcanic Stratigraphy and Controls on Mineralization in the Genex Mine Area, Kamiskotia Area: Discover Abitibi Initiative* by S.M. Hocker, P.C. Thurston and H.L. Gibson.
4. OFR **6157**: *Geology of the Kidd–Munro Assemblage in Munro Township, and the Tisdale and Lower Blake River Assemblages in Currie Township: Discover Abitibi Initiative* by A.S. Péloquin, M.G. Houlé and H.L. Gibson.
5. OFR **6158**: *The Timmins–Porcupine Gold Camp, Northern Ontario: the Anatomy of an Archaean Greenstone Belt and its Gold Mineralization: Discover Abitibi Initiative* by R. Bateman, J.A. Ayer, B. Dubé and M.A. Hamilton.
6. OFR **6159**: *Geology, Structure, and Gold Mineralization, Kirkland Lake and Larder Lake Areas (Gauthier and Teck Townships): Discover Abitibi Initiative* by V. Ispolatov, B. Lafrance, B. Dubé, M.A. Hamilton and R.A. Creaser.
7. OFR **6160**: A*n Integrated Study of Intrusive Rocks Spatially Associated with Gold and Base Metal Mineralization in the Abitibi Greenstone Belt, Timmins Area and Clifford Township: Discover Abitibi Initiative* by P.J. MacDonald, S.J. Piercey and M.A. Hamilton.
8. OFR **6161**: *Geology and Base Metal Mineralization in Ben Nevis, Clifford and Katrine Townships: Discover Abitibi Initiative* by A.S. Péloquin and S.J. Piercey
9. OFR **6162**: *A New Metamorphic Framework for Gold Exploration in the Timmins–Kirkland Lake Area, Western Abitibi Greenstone Belt: Discover Abitibi Initiative* by P.H. Thompson.
10. OFR **6163**: *Gravity and Magnetic Three-Dimensional (3D) Modelling: Discover Abitibi Initiative* by L.E. Reed.

The following Preliminary Maps have been published:

1. Map **P.3543—Revised**: Precambrian Geology of Ben Nevis and Katrine Townships by A.S. Péloquin.
2. Map **P3544—Revised**: Precambrian Geology, Parts of Godfrey, Turnbull, Carscallen and Bristol Townships by B. Hathway and S.M. Hocker.
3. Map **P.3546—Revised**: Precambrian Geology of Gauthier Township Transect by V.O. Ispolatov and B. Lafrance.
4. Map **P.3547—Revised**: Precambrian Geology, Parts of Whitney and Hoyle Townships by R. Bateman.
5. Map **P.3555**: Precambrian Geology of Tisdale Township and Parts of Deloro, Mountjoy and Ogden Townships by R. Bateman.
6. Map **P.3556**: Precambrian Geology, Parts of Godfrey, Robb, Jamieson, Loveland, Macdiarmid and Thorburn Townships by B. Hathway.
7. Map **P.3557**: Precambrian Geology of Munro Township by A.S. Péloquin, M.G. Houlé and H.L.Gibson.
8. Map **P.3558**: Precambrian Geology of Teck Township Transect by V.O. Ispolatov.

The following Miscellaneous Release—Data (MRDs) of digital data have been published:

1. MRD **144**: *Geochemical, Petrographic and Compilation Data from the Genex Mine Area, Kamiskotia Area: Discover Abitibi Initiative* by S.M. Hocker, P.C. Thurston and H.L. Gibson.
2. MRD **155**: *Digital Compilation of Maps and Data from the Greenstone Architecture Project: Discover Abitibi Initiative* by J.A. Ayer, P.C. Thurston, R. Bateman, H.L. Gibson, M.A. Hamilton, B. Hathaway, S.M. Hocker, G. Hudak, B., Lafrance, V., Ispolatov, P.J. MacDonald, A.S. Péloquin, S.J. Piercey, L.E. Reed, P.H. Thompson and H. Izumi
3. MRD **162**: *Magnetic and Gravity 3D Modelling Products: Discover Abitibi Initiative* by L.E. Reed.

GEOLOGICAL SETTING

The Superior Province is the nucleus of the North American continent and consists of a collage of east-trending primarily Neoarchean sedimentary and granite-greenstone subprovinces surrounding a central nucleus of Mesoarchean gneissic units with minor greenstone belts. The Abitibi Subprovince is the southernmost of the subprovinces. The subprovince is bounded to the north by sedimentary rocks of the Opatica Subprovince, to the south by sedimentary rocks of the Pontiac Subprovince and to the southeast by rocks of the Mesoproterozoic Grenville Province. The Abitibi Subprovince is interrupted by the north-northeast-trending Kapuskasing structural zone, a west-dipping thrust of Paleoproterozoic age, which exposes granulite facies mid-crustal equivalents of the Abitibi Subprovince (Percival and West 1994).

This southern part of the greenstone belt consists of 6 major volcanic lithotectonic assemblages and two unconformably overlying primarily metasedimentary assemblages (Ayer, Amelin et al. 2002). The volcanic assemblages range in age from the ca. 2750 Ma Pacaud assemblage to the 2703 to 2696 Ma Blake River assemblage. In the following sections, the stratigraphy of the southern Abitibi greenstone belt is reviewed, emphasizing revisions to the stratigraphy established during the course of this project.

Geochronology

The Greenstone Architecture Project has resulted in the processing of 52 samples for age determinations by the following methods:

1. 36 samples collected during the 2003 and 2004 field seasons were processed to extract suitable minerals at the Jack Satterly Geochronology Laboratory (JSL), Department of Geology, University of Toronto. Of these samples, 29 were found to contain suitable minerals for U/Pb geochronology using thermal ionization mass spectrometry (TIMS).
2. 5 samples that had received TIMS analysis prior to this project were selected for additional zircon analysis using the TIMS at the JSL. These samples were selected to provide more precise ages in areas relevant to the goals of the project.
3. 11 samples that had received TIMS analysis either prior to, or during the project, were selected for additional analysis using the sensitive high-resolution ion microprobe (SHRIMP) at the Geological Survey of Canada. This was done to better understand zircon inheritance and provenance in volcanic, sedimentary and intrusive units relevant to the goals of the project.

THERMAL IONIZATION MASS SPECTROMETRY (TIMS) RESULTS

A summary of the new thermal ionization mass spectrometry (TIMS) age results is presented in Table 1. The locations and ages of all U/Pb geochronology samples are shown on Figure 2 (back pocket) with new geochronology results highlighted and numbered to correlate with the numbers on Table 1 and are presented in graphical form (concordia diagrams) in Figures 3 to 8. These results are also discussed in "Stratigraphic Framework" and "Intrusion Framework" below. The analytical methodology, reports on each sample (including samples without minerals suitable for geochronological analyses) and detailed analytical results for individual analyzed fractions from each sample are provided in Appendix 1 (Table A1).

SENSITIVE HIGH-RESOLUTION ION MICROPROBE (SHRIMP) RESULTS

Ion microprobe U-Th-Pb isotopic analyses were carried out using the SHRIMP II facility at the Geological Survey of Canada, Ottawa, on representative zircon grains from 11 samples from the southern Abitibi greenstone belt in order to address two principal issues. First, we sought to understand better the occasional patterns of xenocrystic inheritance revealed, sometimes cryptically, in several magmatic samples for which ages were obtained using conventional isotope dilution thermal ionization mass spectrometry (TIMS). Secondly, the relatively rapid analytical routine possible with the SHRIMP allows for a far greater canvassing of detrital zircon populations present within any given metasedimentary unit and, thus, more statistically valid variations in provenance source patterns could be characterized by this method compared to TIMS.

Detailed backscattered electron and cathodoluminescence imaging of a large number of zircons (typically 75–100 grains) from igneous lithologies allowed for the rapid identification of a number of zircons suspected to contain inherited, xenocrystic cores. In most cases, these were present as texturally distinct, rounded cores (with or without signs of internal growth or compositional zoning) or as embayed grain centres occasionally with truncated growth zoning, surrounded most commonly by oscillatory-zoned (magmatic) subhedral mantles or sharply prismatic euhedral igneous overgrowths. Rounded or subrounded cores were frequently surrounded by a series of radial cracks that propagate out to the grain exteriors.

Samples with zircons analyzed by SHRIMP II are discussed below with their results presented in graphical form (concordia diagrams and histograms showing age probabilities) in Figures 9 to 12. The analytical methodology and the data from each individual zircon analysis by the SHRIMP are presented in Appendix 2.

Table 1. Summary of Discover Abitibi TIMS results.

Number on Fig. 2	Sample Number	Rock Type	Primary Age (Ma)	Inheritance or Provenance Age(s) (Ma)	Assemblage or Intrusion
1	04BHA-0333	Felsic debris flow	2712.3±2.8	2861.4±3.4	upper Kidd–Munro
2	04BHA-0297	Quartz+feldspar felsic flow	2714.6±1.2		upper Kidd–Munro
3	04BHA-0462	Granophyre	2704.8±1.4		Kamiskotia Gabbroic complex
4	03BHA-0382	Rhyolite	2700.0±1.1		upper Blake River
5	03BHA-0384	Felsic lapilli tuff	2701.1±1.4		upper Blake River
6	03BHA-0345	Felsic lapilli tuff	2698.6±1.3		upper Blake River
7	03BHA-0047	Felsic lapilli tuff	2703.1±1.2		lower Blake River
8	96JAA-0094	Rhyolite	2712.2±0.9	2853.6±1.4	upper Kidd–Munro
9	04JAA-0004	Conglomerate	<2684.4±1.7	2684–2685, 2705, 2713–2716, 2726–2728	Timiskaming
10	04PCT-0062	Felsic lapilli tuff	2724.1±3.7		Deloro
13	SM85-60	Albitite	2672.8±1.1	2694.4±3.6	McIntrye Mine dike
14	KCR.52	Wacke	<2690.9±2.5	2691, 2692, 2696, 2698, 2699.5	Porcupine, Hoyle Fm.
15	04JAA-0003	Wacke	<2687.2±1.6	2687, 2692, 2708, 2720, 2726	Porcupine, Beatty Fm.
16	04ED-0198	Quartz porphyry	2687.6±2.2		Hoyle Pond Mine porphyry sill
17	03ED-096A	Quartz- feldspar porphyry	2684.4±1.9	2695.1±3.3	Hoyle Pond Mine porphyry intrusion
18	03RJB-18973-10	Sandstone	<2688.2±1.9	2688, 2690, 2704, 2712, 2725	Porcupine, Hoyle Fm.
19	03PJM-131	Quartz- feldspar porphyry	2677.5±2.0	ca. 2680–2703	Pamour porphyry intrusion
20	04JAA-0010	Albitite	2676.5±1.6		Dike proximal to PDDZ
21	03RJB-18972-6	Sandstone	<2689.5±1.7	2689–2692, 2723, 2726	Porcupine, Whitney Fm.
22	C88-17	Felsic volcanic	2724.6±0.8		Deloro
23	03LAH-0627	Quartz porphyry	2689.0±1.4	2692.3±1.7	Mount Logano porphyry
24	03LAH-0161	Felsic flow	2727±12		Deloro
26	96TB-099	Felsic fragmental	2723.1±1.3	2725.8±0.8	Deloro
27	04MGH-0283	Quartz- feldspar porphyry	2686.2±1.1		Redstone Mine, porphyry
28	04PCT-0064	Quartz-phyric gabbro	2705.7±4		Dike cutting Deloro volcanic rocks
30	03JAA-0006	Feldspar porphyry	<2690	2690–2701	Syenite cut by gold veins
31	03VOI-0422-1	Trachytic lava	2669.6±1.4	2676.6±4.3; 2694.2±2.8	Timiskaming
32	03VOI-0570-1	Sandstone	<2677.7±3.1	2678–2682, 2770	Timiskaming
33	03SJP-059-1	Feldspar porphyry	2688.5±2.3	2694	dike next to Clifford stock
34	03SJP-115-1	Monzonite	2686.9±1.2		Clifford stock
35	03ASP-0130-1	Porphyritic rhyolite	2699.8±3.6		upper Blake River
36	03ASP-0179-1	Massive rhyolite	2696.6±1.3		upper Blake River
38	C89-7	Gabbro	2712.4±1.1		Ghost Range sill
39	04JAA-0002	Leucogabbro	2706.8±1.2		Centre Hill complex

"<" indicates the maximum (inferred) depositional age based on the youngest detrital zircon analyzed.

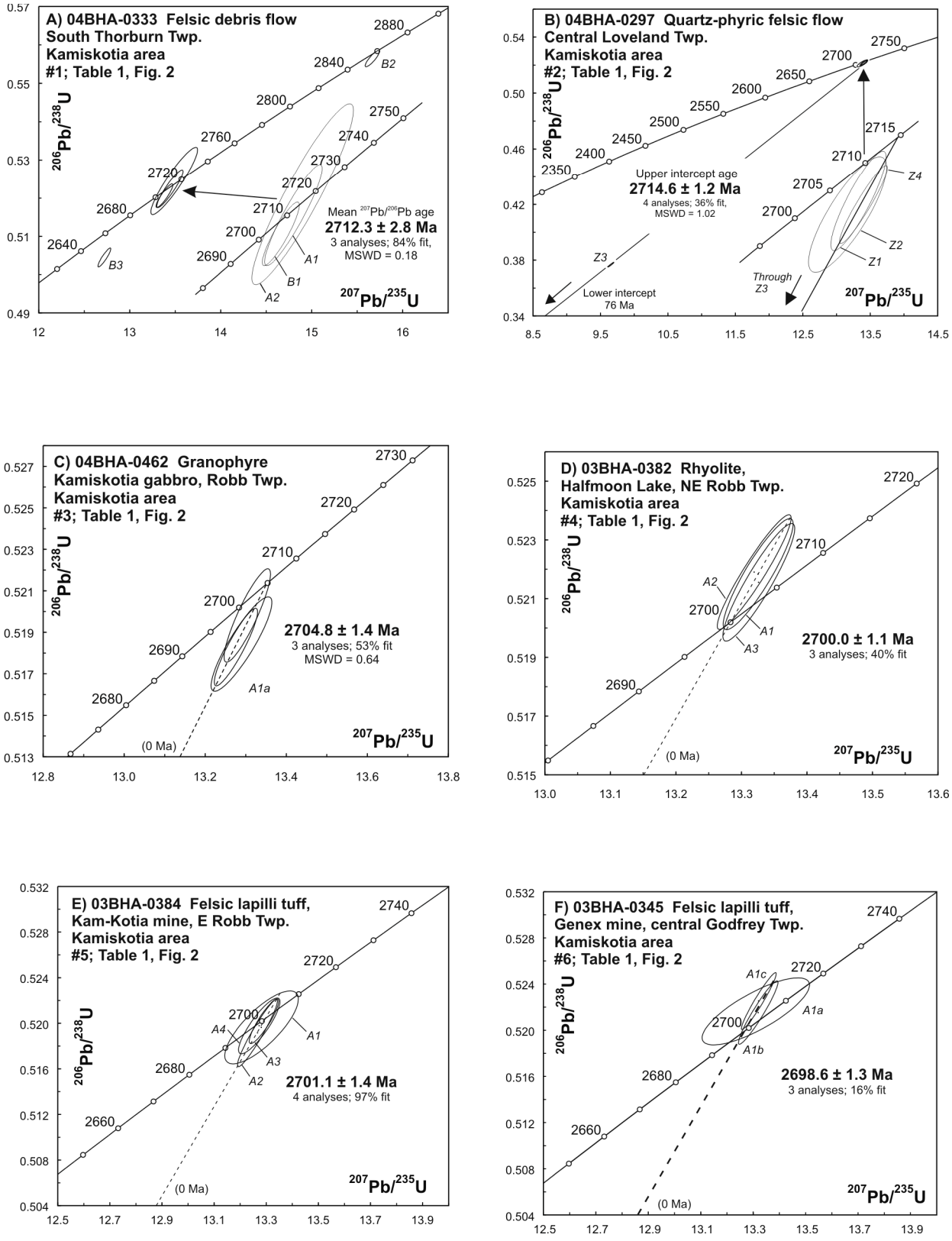

Figure 3. U/Pb concordia plots of TIMS results from the Kamiskotia area.

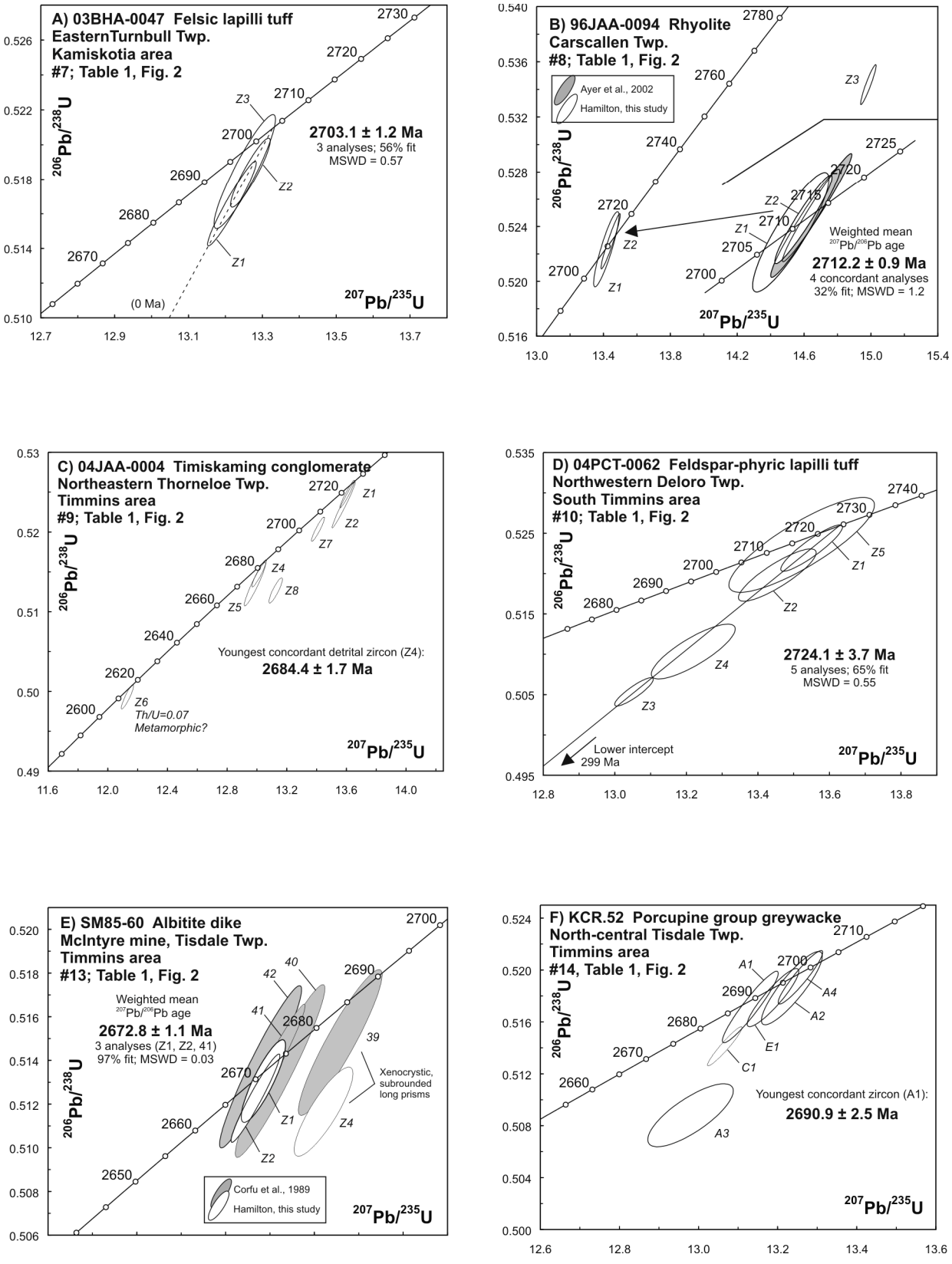

Figure 4. U/Pb concordia plots of TIMS results from the Kamiskotia and Timmins areas.

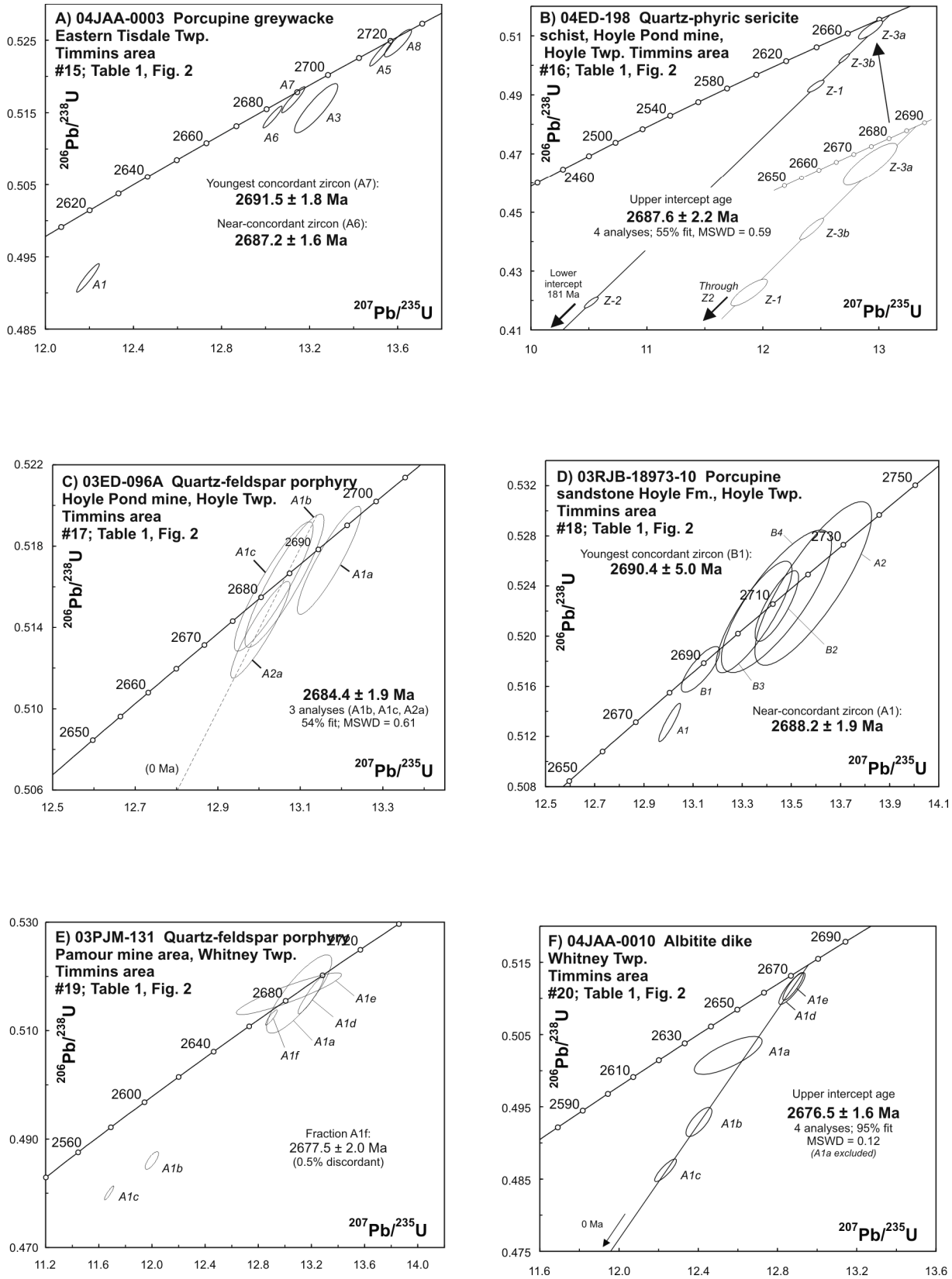

Figure 5. U/Pb concordia plot of TIMS results from the Timmins area.

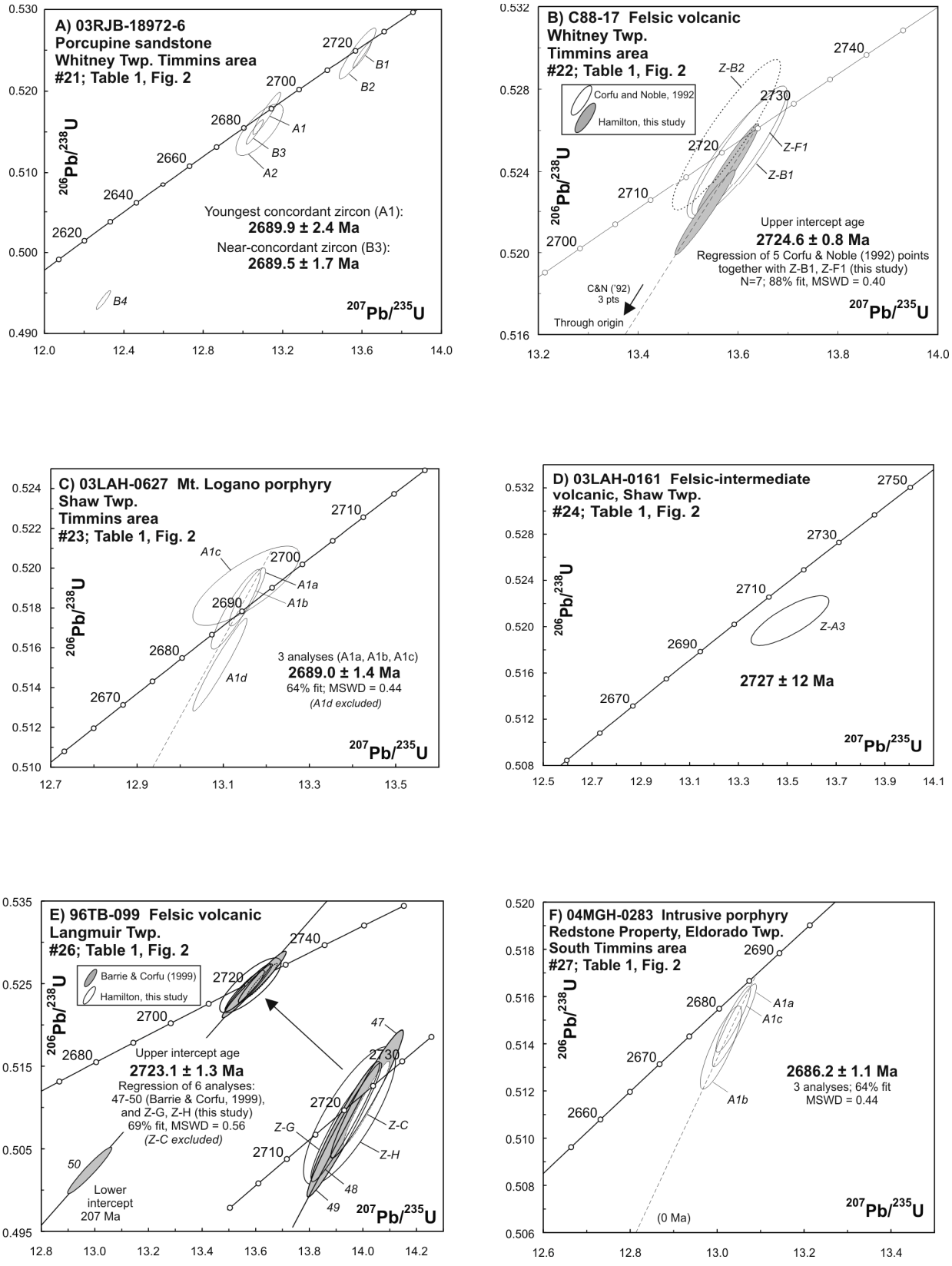

Figure 6. U/Pb concordia plot of TIMS results from the Timmins and Shaw Dome areas.

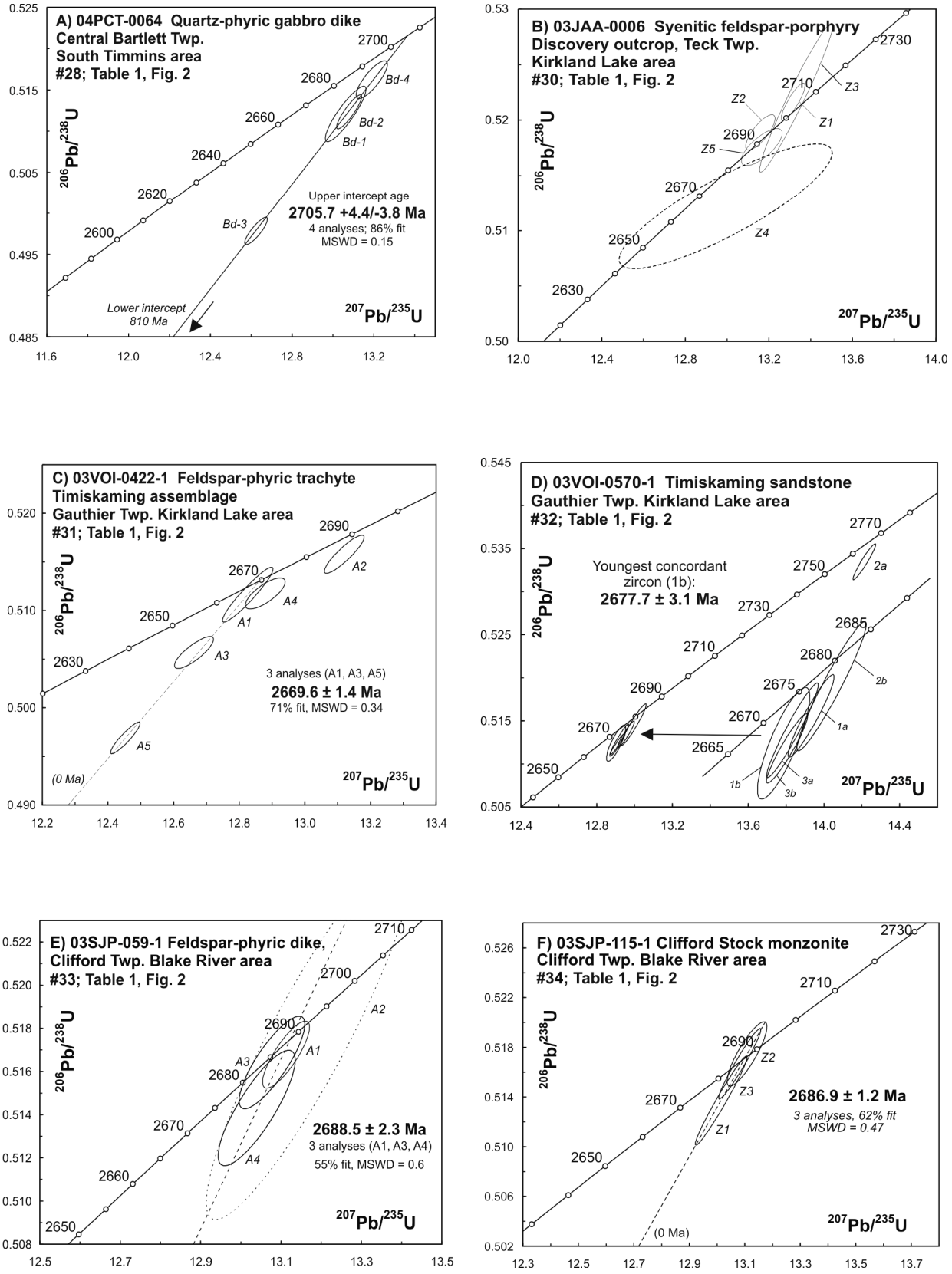

Figure 7. U/Pb concordia plots of TIMS results from Bartlett, Teck, Gauthier and Clifford townships.

Targeting of several of these overgrowth domains reinforced the earlier conclusions from TIMS studies that the inferred magmatic crystallization ages were correct, since texturally referenced, unambiguous igneous domains were analyzed and a larger population of grains were involved in this distinction. For example, the principal age mode present in zoned igneous mantles from a Deloro assemblage rhyolite from the Shining Tree area, 97JAA-106, is approximately 2725 Ma (Figure 9A), in agreement with the interpreted primary age of crystallization at 2726.5±1.1 Ma (Ayer, Amelin et al. 2002). In contrast, the age of distinct core domains, as well as occasional whole, discrete zircon xenocrysts ranged up to approximately 2750 Ma, in accord with earlier TIMS results suggesting inheritance from 2741 to 2744 Ma source materials from the underlying Pacaud assemblage.

SHRIMP analyses of zircons from the dacitic footwall of the Langmuir #2 Ni-Cu mine, 96TB-079, yield a unimodal age distribution whose principal age mode is also approximately 2725 Ma (Figure 9B), in good agreement with the age of an inferred inherited component constrained by a single TIMS analysis at 2724±4 Ma (Barrie and Corfu 1999). The distribution is heavily skewed towards analysis of core domains, which have ages ranging up to at least 2767 Ma (though slightly discordant). The few spot analyses targeting thin magmatic overgrowths yielded ages that are less precise than, but indistinguishable from, the primary magmatic age determined by Barrie and Corfu (1999) at 2708±2 Ma, confirming that the unit has a Tisdale assemblage affinity.

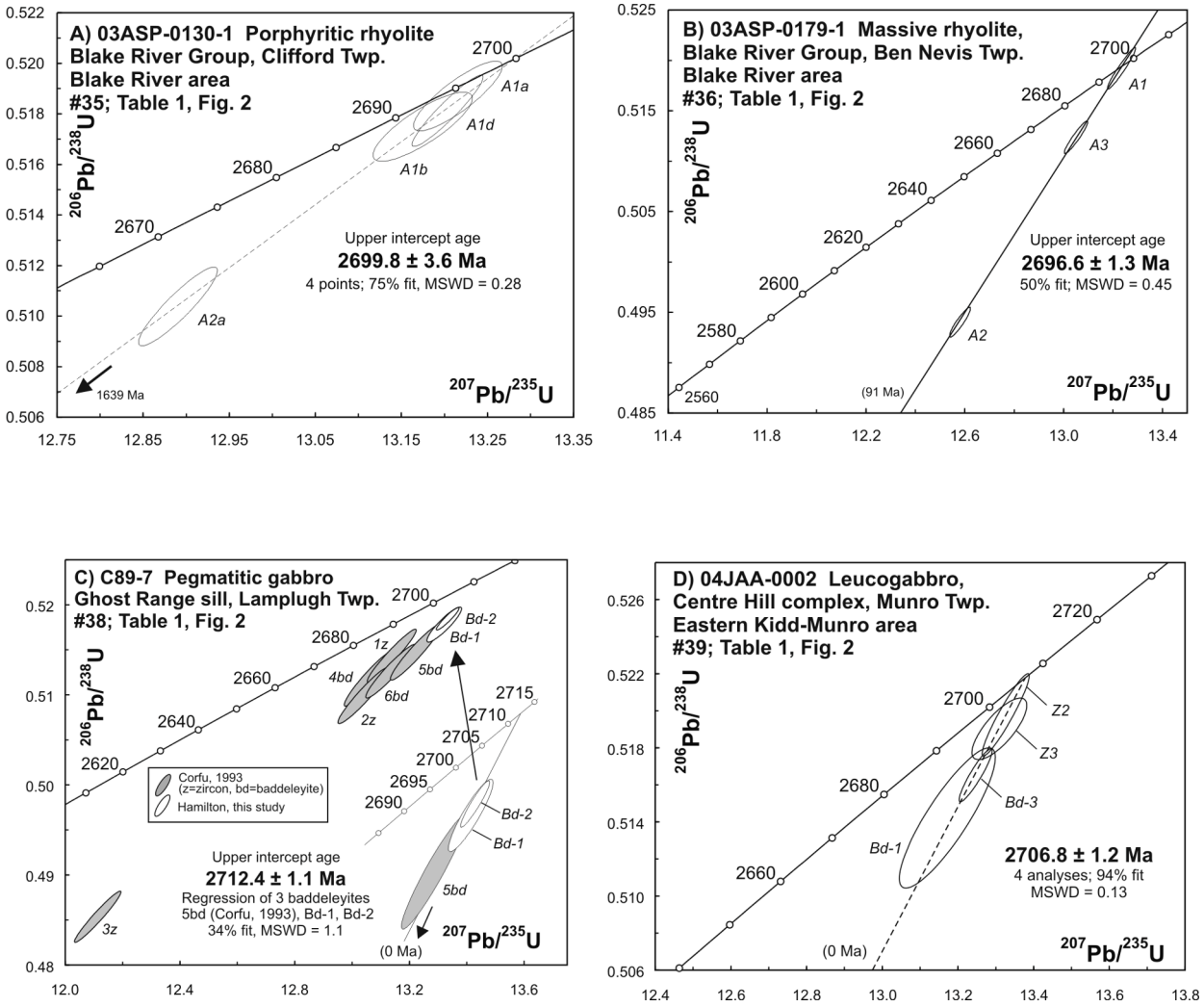

Figure 8. U/Pb concordia plots of TIMS results from Ben Nevis, Lamplugh and Munro townships.

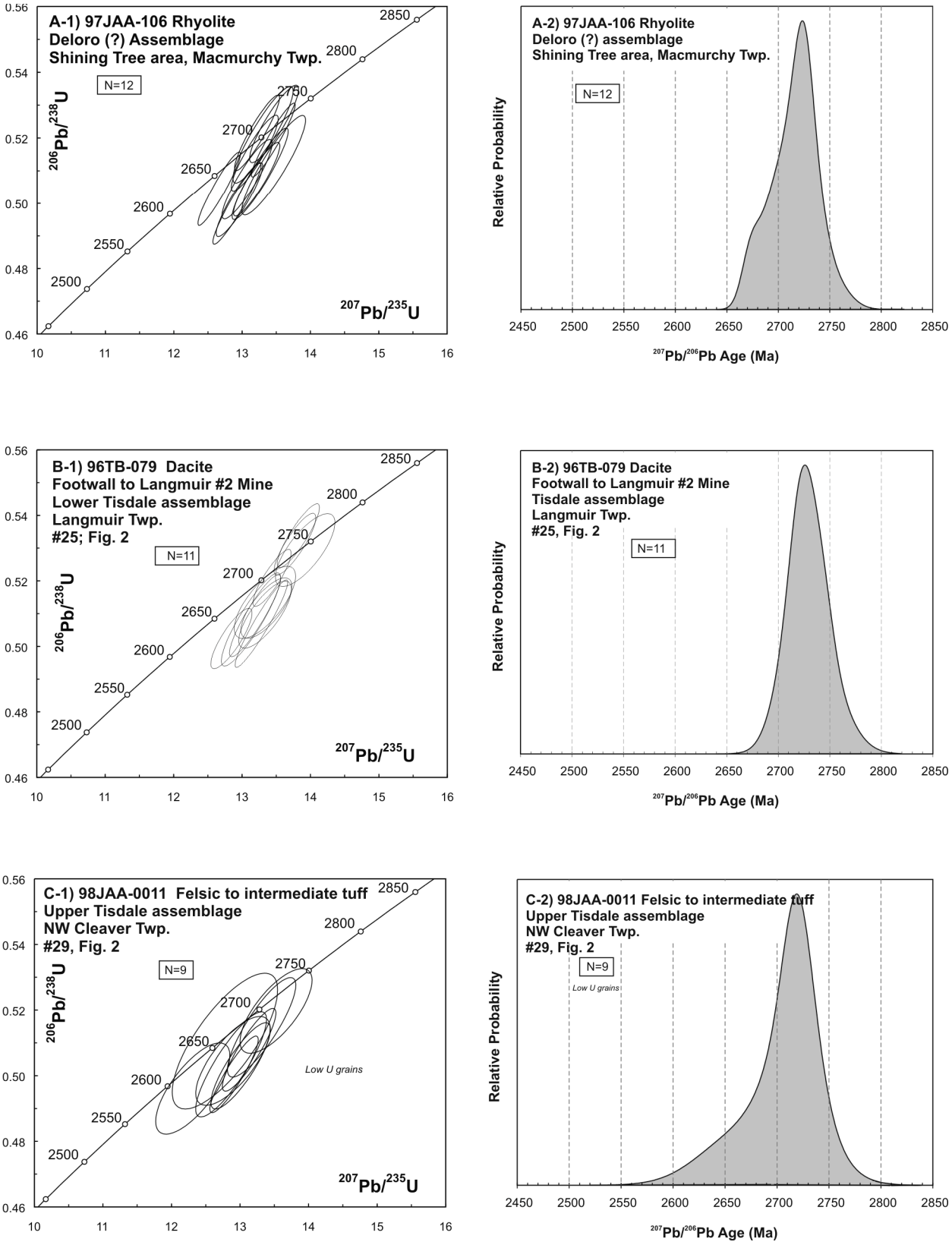

Figure 9. U/Pb SHRIMP results from "Keewatin" assemblage volcanic samples from the A) Shining Tree, B) Langmuir Township and C) Cleaver Township areas.

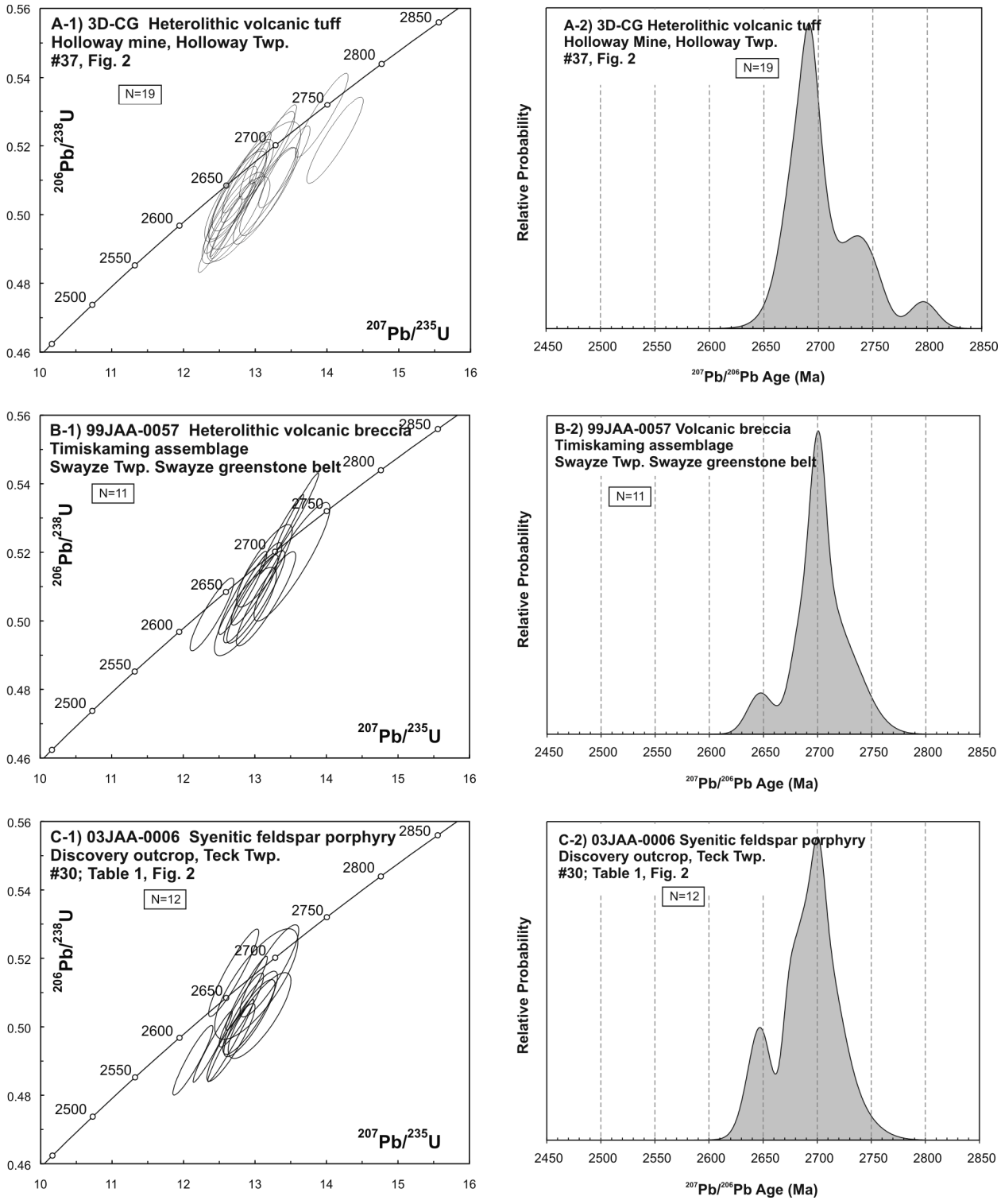

Figure 10. U/Pb SHRIMP results from the Timiskaming volcanic rocks and intrusions in the study area (A and C) and the Swayze greenstone belt (B).

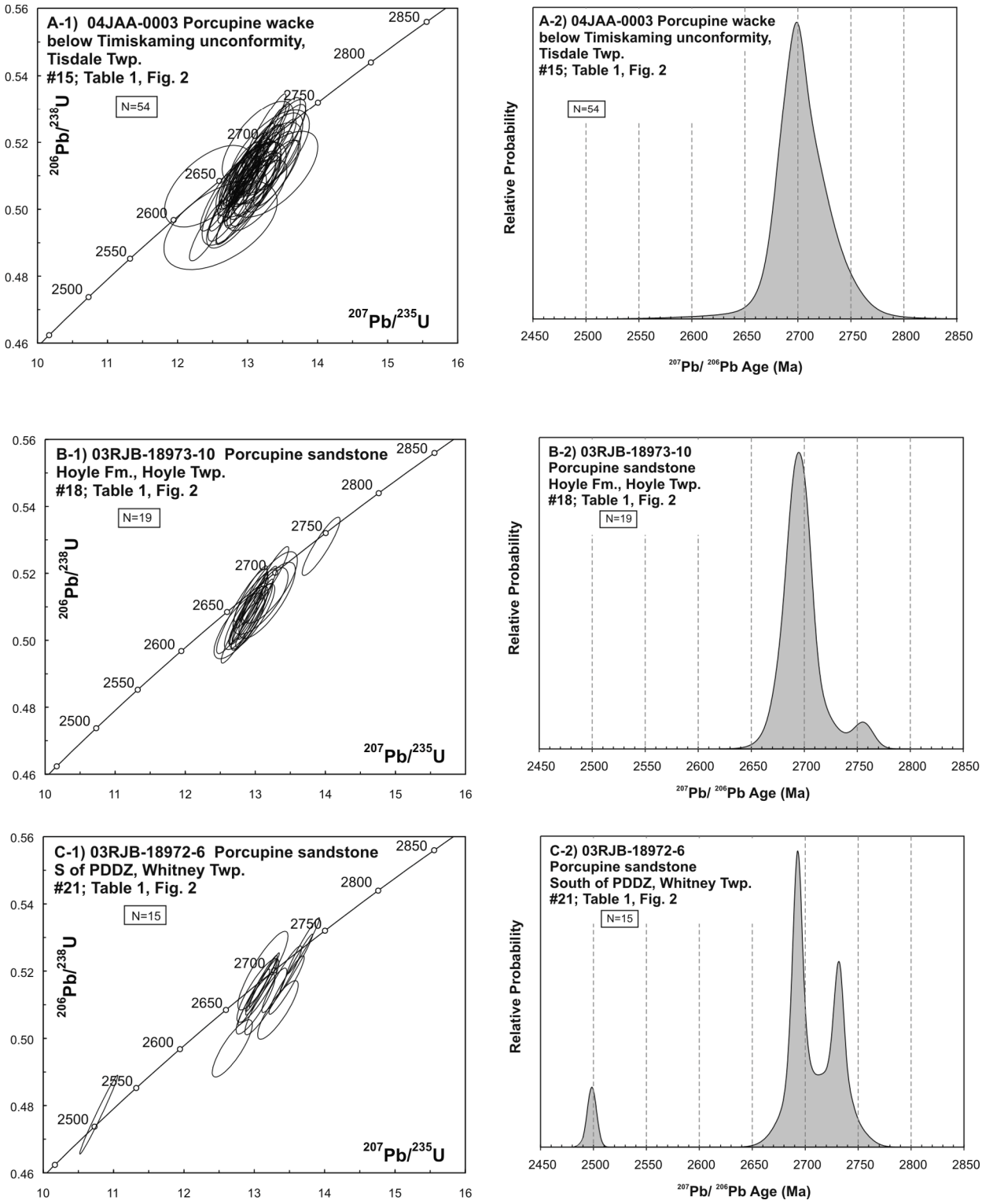

Figure 11. U/Pb SHRIMP results from Porcupine assemblage sedimentary rocks in the Timmins area.

In northwest Cleaver Township, a felsic to intermediate tuff of the upper Tisdale assemblage has an age of 2702±3 Ma, while a single grain yielded a concordant (inherited) age of approximately 2723 Ma (98JAA-0011; Ayer, Amelin et al. 2002). SHRIMP analyses of sector and oscillatory-zoned domains within these grains confirm a primary magmatic age at ca. 2700 Ma, but uranium concentrations in most grains were too low to yield sufficient age resolution for a more precise conclusion using this method. Despite this uncertainty, the presence of a significant population of zircon cores with ages in excess of the primary, magmatic age is likely confirmed, and have $^{207}Pb/^{206}Pb$ ages ranging from approximately 2720 to 2735 Ma (Figure 9C; Appendix 2).

In northwestern Holloway Township, a heterolithic volcanic tuff breccia or debris flow unit within the Porcupine–Destor deformation zone is a local host to the Lightning Zone gold mineralization at the Holloway Mine. A sample of this unit (3D-CG) has been shown by Ropchan et al. (2002), on the basis of the youngest analyzed zircon present, to be as young as 2686.8±1.8 Ma, or younger if the zircons are recycled, while the presence of older zircon populations at ca. 2694 Ma and 2712 Ma attests to the possible involvement of Porcupine (2685–2690 Ma) and Kidd–Munro (2712–2718 Ma) assemblage components as xenocrysts or detritus. Spot age determinations carried out using the SHRIMP on approximately 20 zircon grains from this sample confirm the presence of young, concordant age domains near 2680 Ma and reinforce earlier conclusions that this sample was likely deposited as a component of Timiskaming assemblage sedimentation (Figure 10A; Appendix 2). The cumulative probability plot

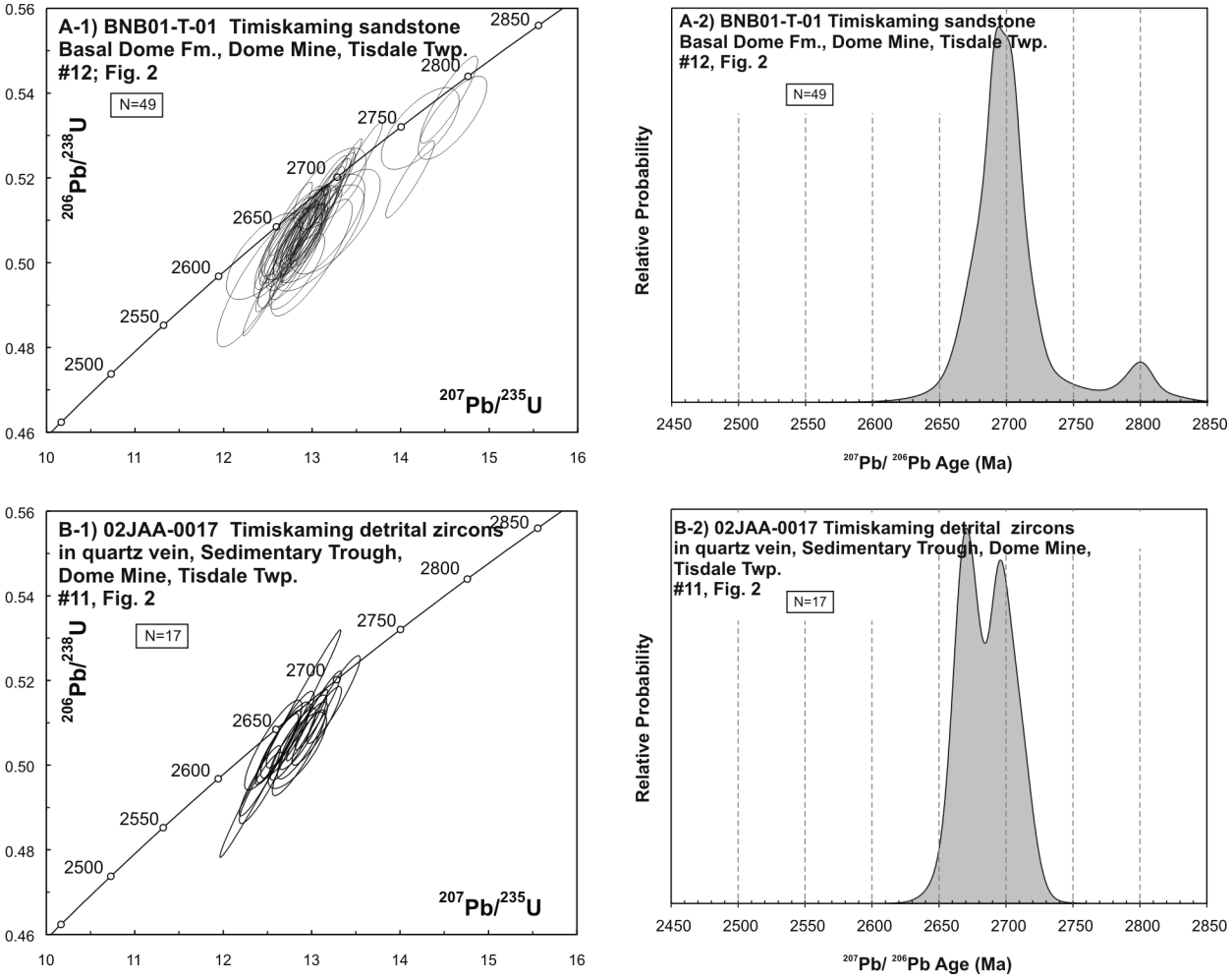

Figure 12. U/Pb SHRIMP results from Timiskaming assemblage sedimentary rocks in the Timmins area.

(Figure 10A-2), with a peak age mode at approximately 2691 Ma, also shows a significant proportion of Porcupine assemblage detritus, or debris analogous in age to the Krist formation or the broadly age-equivalent regional porphyry intrusions at ca. 2685 to 2692 Ma. An important grain age subpopulation also appears to be present at ca. 2730 to 2740 Ma, while a single spot analysis, from a concentrically zoned grain, is slightly discordant (4%) with a $^{207}Pb/^{206}Pb$ age of 2796 Ma. The sharply euhedral nature of many of the older grains argues against significant degrees of transport for these specific populations.

Sample 99JAA-0057 represents a second Timiskaming assemblage volcanic breccia, from Swayze Township, previously analyzed by Ayer, Ketchum and Trowell (2002). Zircons from this sample define a full range of morphological types, ranging from elongate and sharply prismatic to short, stubby, subrounded or even very well-rounded grains. The most reliable younger ages from this sample come from analyses of distinct overgrowths or thin embayments, constraining deposition generally at, or younger than, 2672 to 2683 Ma. This conclusion is in accord with the TIMS results of Ayer, Ketchum and Trowell (2002), who, on the basis of a slightly discordant single grain, inferred that the maximum age of deposition was 2669.8±1.7 Ma. Concordant or nearly concordant spot analyses from interior igneous domains mostly define a narrow age spectrum between ca. 2695 to 2705 Ma, with a peak age mode near 2700 Ma (Figure 10B; Appendix 2). Older ages occur near 2730 Ma, 2740 Ma and 2765 Ma. The range of SHRIMP spot ages reflects very closely the age populations defined by the TIMS age determinations on abraded single grains, and support the earlier observations that the inherited components in this fragmental volcanic were derived from underlying lithologies within the Pacaud, Deloro, Tisdale and Blake River assemblages (Ayer, Ketchum and Trowell 2002).

At the Kirkland Lake Discovery Outcrop in Teck Township, a syenitic porphyry crosscuts Timiskaming assemblage sediments and is itself cut by the "Main Break" gold vein system. Conventional isotope dilution analysis of single zircon grains from a sample of this porphyry (03JAA-0006, *see* Table 1) yielded a scattered array with ages as old as 2701 Ma and a youngest identifiable grain population at ca. 2690 Ma. However, as the unit is known to intrude Timiskaming assemblage sediments that must, on independent evidence, be younger than ca. 2678 Ma (#32: Figure 2), all of the measured TIMS ages must be concluded to be from inherited, xenocrystic grains—possibly all reflecting Timiskaming assemblage provenance sources.

Detailed scanning electron microscope (SEM) imaging of zircon grains from the syenitic porphyry show that most grains have sharply prismatic forms preserving broad internal zoning or have large, locally rounded cores surrounded by very thin, high-U, oscillatory-zoned shells or overgrowths. Ion microprobe spot age determinations on grain centres or cores range up to as old as ca. 2725 Ma, but are dominated by an age population centred on ca. 2700 Ma (Figure 10C; Appendix 2), much like that seen in the TIMS data. Very few grains had overgrowths thick enough to analyze, but these sparse analyses suggest magmatic overgrowth near 2685 Ma. A preliminary interpretation of these ages is that they represent grains derived from the regional suite of ca. 2685 to 2692 Ma porphyry intrusions found elsewhere in the southern Abitibi Subprovince. A single analysis of the core of a ragged, heavily cracked grain yields an age of 2674±6 Ma, but the age likely reflects some degree of secondary Pb-loss. Two very young SHRIMP spot analyses, in one case from a diffuse, embayed, structureless (unzoned) rim, yield ages near 2645 Ma; these are provisionally interpreted as possibly reflecting late hydrothermal or metamorphic recrystallization. The temporal relationship of this event to the Main Break gold vein system is unknown with any certainty and remains speculative.

The body of SHRIMP data obtained for the syenite porphyry at the Discovery Outcrop are currently too sparse and imprecise to reliably define an age of igneous emplacement. It is also conceivable that the syenitic magma never precipitated magmatic zircon. As the vast majority of the age determinations are older than the age of the Timiskaming sediments that the intrusion cuts, these zircons must be considered to be xenocrystic in origin.

SHRIMP U/Pb dating was carried out on detrital zircons from Porcupine assemblage units from three localities. Sample 04JAA-0003 represents a fine-grained wacke of the Beatty formation occurring immediately below an angular unconformity with overlying Timiskaming assemblage sandstones in eastern Tisdale Township. Conventional TIMS analysis of six air-abraded single detrital zircon grains from this sample demonstrated the presence of a range of ages spanning ca. 2687 to 2726 Ma, with the youngest, reliable near-concordant analysis suggesting that sedimentary deposition postdated 2687.2±1.6 Ma (2σ). The sample comprises a variety of zircon grain shapes and sizes, from 4-5:1 elongate prisms to equant crystals, with slightly subrounded varieties representing approximately 20 to 25% of the entire population, the rest being sharply faceted. SEM imaging of approximately 125 zircons reveals a variety of concentric, oscillatory zoned and straight- or weakly zoned igneous grain types. SHRIMP analyses for 54 zircons from this sample are shown in Appendix 2 and presented graphically in Figures 11A-1 and 11A-2. Most of the reliable concordant or near concordant ion probe spot age determinations cluster between ca. 2680 and 2750 Ma, with no consistent correlation between grain morphology or degree of rounding, except that sedimentary abrasion is not evident in the very youngest detrital grains analyzed. The slightly skewed but essentially unimodal age distribution has a relative probability peak near 2700 Ma. The SHRIMP data reveal that a slightly older age population is probably present in this sample than was suggested by the TIMS results. Because of the comparatively larger SHRIMP analytical errors, particularly associated with analyses of low-U grains or domains within grains, the significance of this should be regarded with some caution. The ion probe data also suggest that the depositional age for this sample might be near 2680 Ma, though the most robust and precise estimate remains the <2687 Ma constraint from TIMS.

A second sample of Porcupine assemblage sandstone, locally interbedded with conglomerate, was collected from Whitney Township south of the Porcupine–Destor deformation zone (Porcupine Joint Venture drill hole 18972). Single-grain TIMS U/Pb analyses carried out on zircons from sample 03RJB-18972-6 indicated populations having ages of ca. 2689 to 2692 Ma, 2723 Ma, and 2726 Ma. Detailed SEM imaging of over 120 additional grains reveals a diversity of textures dominated by concentric oscillatory zonation preserved within euhedral to subrounded and well-rounded morphologies. Ion probe analyses were carried out on a random selection of these grains. SHRIMP data for approximately 15 zircons are presented in Figures 11C-1 and 11C-2 and Appendix 2, and show that the dominant age populations span a range from ca. 2690 to 2745 Ma, in general agreement with, but extending beyond, the range revealed by TIMS. Although the total number of analyses is small, the data suggest two principal clusters centred near 2690 Ma and 2730 Ma, which may reflect sourcing within, or recycling of, underlying Krist formation felsic volcanic rocks (lowermost Porcupine assemblage) and Deloro assemblage units, respectively. The younger ages are also comparable to the emplacement ages of numerous calc-alkaline porphyries in the Timmins area and elsewhere (mostly 2688–2691 Ma: Hamilton, this study; Ayer, Barr et al. 2003; Gray and Hutchinson 2001; Corfu et al. 1989). Because of the larger analytical errors for the SHRIMP age determinations, the most reliable maximum age of deposition for this sandstone remains that determined by TIMS, at 2689.5±1.7 Ma (2σ). Ion probe analysis also yielded a single spot age determination for a grain interior at 2499±9 Ma; although the analysis is concordant (100.3%), this domain is characterized by anomalously high U (ca. 1200 ppm) and the significance of this age remains unclear. Further analytical work is required to elucidate the nature of this apparent age.

A third Porcupine assemblage sample represents a sandstone member from the Hoyle formation in Hoyle Township (03RJB-18973-10). Conventional U/Pb analysis of zircons this unit revealed detrital age populations at 2725 Ma, 2712 to 2713 Ma, 2704 Ma, and 2688 to 2690 Ma. Detailed SEM imaging of a broader selection of zircons (n>120) from this sample shows simple short prismatic and equant crystal forms dominated by magmatic, oscillatory internal zoning and minor subrounding of exterior prism faces. Initial, *in situ* SHRIMP analysis was carried out on 19grains and the data are presented in Appendix 2 and shown graphically in Figures 11B-1 and 11B-2. The data show a distinct clustering on or near concordia, ranging mostly between ca. 2680 and 2705 Ma, and have a prominent age mode at ca. 2690 Ma. Although

the youngest ages are not sufficiently precise to constrain a maximum age of deposition with great certainty, the bulk of the younger zircon detritus clusters near 2690 Ma and clearly substantiates in greater number the results determined by isotope dilution. A single spot analysis within a slightly subhedral, oscillatory-zoned 2:1 prism, yielded an age of 2756 Ma, consistent with a provenance from one of the oldest assemblages of the southern Abitibi greenstone belt.

As described earlier, the similarity of the youngest detrital grain ages (at ca. 2690 Ma) with the established ages for Krist formation felsic magmatism (2685–2691.5 Ma: Ayer, Barr et al. 2003) suggests that fragmental, calc-alkalic volcanism may have been contemporaneous with parts of early, conformable Porcupine assemblage sedimentation. Subsequent greywacke turbidite deposition likely followed shortly after initial Krist formation magmatism and, in part, represents reworking of the ca. 2690 Ma fragmental debris.

Conventional isotope dilution U/Pb analysis of approximately 12 single detrital zircon grains from two samples of the lower Timiskaming assemblage (Dome formation) at the Dome Mine were presented by Ayer, Barr et al. (2003). Six detrital grains from a wacke collected from the basal Dome formation in the "Greenstone Nose" (BNB01-T-01) yielded ages ranging from ca. 2710 to 2679 Ma, with approximately half the grains having ages near 2690 Ma, while the youngest detrital grain analyzed provided a maximum age of deposition at 2679±4 Ma (2σ). Detailed SEM imaging of approximately 130 additional, randomly selected, relatively non-magnetic zircons shows that almost all grains have sharply facetted or only weakly subrounded short prismatic forms, and are mostly characterized by igneous, concentric, oscillatory internal zonation. SHRIMP analysis of 49 representative grains from this sample yielded a spectrum of ages, dominantly between ca. 2670 and 2730 Ma, with a principal age mode near 2690 Ma (Figures 12A-1 and 12A-2; Appendix 2), which is similar to the TIMS results. However, a demonstrably older, distinctly pre-Abitibi, population of zircon is also present in this wacke, with ages clustering near 2780 Ma, and ca. 2795 to 2810 Ma. A single, young spot analysis near 2660 Ma (sample BNB01-T-01 spot 39.1, Appendix 2) characterizes a low-U grain, but is too imprecise to provide a robust estimate of the maximum age of deposition; the best constraint for a depositional age remains that determined earlier by TIMS (<2679 Ma: Ayer, Barr et al. 2003). The generally sharply facetted external grain morphologies, even among the older grain populations, attest to relatively restricted transport or reworking of these sediments.

The second sample, 02JAA-0017, was collected from an auriferous quartz vein cutting Timiskaming assemblage sediments in the "sedimentary trough" at the Dome Mine. Morphological and conventional TIMS U/Pb analyses of zircons from this sample led Ayer, Barr et al. (2003) to conclude that all the zircons present in the vein were xenocrystic, likely derived from the host conglomerate. Six analyzed grains yielded ages ranging from 2674 to 2695 Ma, with a single older zircon at 2814 Ma. The abraded, single grain data constrain the Timiskaming assemblage conglomerate deposition and the age of the crosscutting quartz vein to <2673.9±1.8 Ma (2σ). SEM imaging of >100 zircons from this sample shows that the grains have very similar morphologies, internal structure and low degrees of sedimentary abrasion as those described for the previous Dome formation wacke, sample BNB01-T-01. Rapid ion probe study of a representative suite of grains shows a spread of ages mostly between ca. 2668 and 2713 Ma, with a possible bimodal grouping of ages near 2670 Ma and 2695 Ma, although there is considerable overlap in errors and the statistical population is small (n<20; Figures 12B-1 and 12B-2; Appendix 2). The SHRIMP results support the earlier TIMS evidence for a slightly larger proportion of younger grains in this Timiskaming assemblage sample than in the basal Dome formation wacke, though both share a large proportion of ca. 2695 Ma detritus.

Stratigraphic Framework

In this section of the report, we present a revised stratigraphic framework for the study area concentrating upon changes in our understanding of Abitibi greenstone belt stratigraphy based on 1) new geochronologic results reported above; 2) stratigraphic mapping within the subprojects summarized below; and 3) reconnaissance mapping by the principal investigators (e.g., Ayer, Thurston et al. 2004). The lithostratigraphic assemblage age ranges, contact relationships, dominant rock types and chemical affinities as modified after Ayer, Amelin et al. (2002) are presented in Table 2. Figure 2 (*see* back pocket) provides a map of the interpretation of assemblages, intrusions, structures and all U/Pb ages within the study area based upon the 1:250 000 lithological compilation map of the central Abitibi greenstone belt in Ontario (Ayer, Berger et al. 2005).

ASSEMBLAGE CONTACT RELATIONSHIPS AND THE SIGNIFICANCE OF IRON FORMATION CONGLOMERATE AND CHERT BRECCIA UNITS

Crystallization ages of lithotectonic assemblages within representative greenstone belts in the North Caribou Terrane of northwestern Ontario are separated by intervals of up to approximately 100 million years (my) (Williams, Stott and Thurston 1992), whereas 3 to 10 my intervals in greenstone belts of the Pilbara craton (e.g., Hickman and Van Kranendonk 2004) and the western Abitibi greenstone belt (Ayer, Amelin et al. 2002) are more common. These differing durations for accumulation of lithotectonic assemblages bear upon models for greenstone belt development. Contacts between lithotectonic assemblages may be tectonic, intrusive, or unconformable (Williams, Stott and Thurston 1992). Contacts between "Timiskaming-style" assemblages in Superior Province greenstone belts are subaerial unconformities marked by development of regoliths or paleosols e.g. (Jackson and Fyon 1991). However, in Superior Province greenstone belts, contacts between "Keewatin" assemblages have, until recently, been assumed to be tectonic (e.g., Williams, Stott and Thurston 1992). However, the recent recognition of isotopic inheritance in some Superior Province greenstone belts (Ayer, Amelin et al. 2002; Thurston 2002 and references therein) and the younging of assemblage ages away from batholiths throughout the Superior Province (Thurston 2002) requires re-examination of the character of assemblage contacts for the "Keewatin-style" assemblages.

Shanmugam (1988) summarized the features of subaerial and submarine unconformities (Table 3). It is useful to note that the features of submarine and subaerial unconformities are not mutually exclusive. In deformed Precambrian orogens, such as the Pilbara craton (Blake 2001) and the Kaapvaal craton (Cheney and Winter 1995), subtle discordances of dip and regional scale truncations mark subaerial unconformities. Similar relationships can develop in submarine settings, however, the dominantly volcanic environment represented by the Abitibi greenstone belt has lens-like facies distribution (Mueller 1991; Bleeker 1999; Mueller and Mortensen 2002); therefore, regional-scale marker horizons used to map dip discordances and large-scale subtle, low-angle truncations are difficult to document. Features indicative of submarine unconformities are a function of a model of basin development in which basins have continuous inputs of detritus from the basin margins, resulting in continuous development of stratigraphy over time. Horizons such as glauconitic sands or manganese nodules represent intervals of non-deposition with or without weathering. Similarly, debris flows and slump deposits in the stratigraphy of a given basin represent an interval of non-deposition in the central part of the basin which is taken up by slump deposits from the basin margin. In the normal deformed metamorphosed Archean greenstone belts, only debris flows and slump deposits have preservation potential.

Table 2. Summary of southern Abitibi greenstone belt supracrustal assemblage names, ages, basal contacts, rock types and chemical affinities.

Assemblage Name (Age in Ma)	Includes Previously Identified Formations and Groups Within Study Area	Basal Contact Relationships	Dominant Rock Types	Volcanic Chemical Affinity
Timiskaming (2676–2670)	Timiskaming, Dome, Three Nations, Hearst	Angular unconformity	Conglomerate, sandstone, mafic to intermediate volcanic	Alkalic to calc-alkalic
Porcupine (2690–2685)	Porcupine, Krist, Beatty, Hoyle, Whitney, Hearst	Angular unconformity	Turbidite, minor conglomerate and iron formation	Calc-alkalic
Upper Blake River (2701–2696)	Blake River, Kamiskotia, Skead	Conformable	Mafic to felsic volcanic	Tholeiitic and calc-alkalic
Lower Blake River (2704–2701)	Kamiskotia, Kinojevis, Garrison	Conformable	Mafic and minor felsic volcanic	Tholeiitic
Upper Tisdale (2706–2704)	Tisdale, Marker Horizon, Duff, Coulson, Gauthier	Conformable to unconformable	Intermediate to felsic volcanic	Calc-alkalic
Lower Tisdale (2710–2707)	Tisdale, Bowman, Larder Lake	Conformable to unconformable	Ultramafic, mafic, felsic volcanic and iron formation	Komatiitic, tholeiitic and calc-alkalic
Upper Kidd–Munro (2717–2711)	Munro,	Conformable to unconformable	Ultramafic, mafic, felsic volcanic and iron formation	Komatiitic, tholeiitic
Lower Kidd–Munro (2719–2717)	Munro, Coulson, Rand	Conformable to unconformable	Intermediate to felsic volcanic	Calc-alkalic
Stoughton–Roquemaure (2723–2720)	Stoughton–Roquemaure, Kinojevis, Wabewawa, Catherine	Conformable to unconformable	Ultramafic, mafic, intermediate and felsic volcanic	Komatiitc, tholeiitic and calc-alkalic
Deloro (2730–2724)	Upper Deloro, Redstone River	Unconformable	Mafic, intermediate and felsic volcanic and iron formation	Tholeiitic and calc-alkalic
Pacaud (2750–2735)	Pacaud, lower Deloro	Unknown – removed by intrusions	Ultramafic, mafic and felsic volcanic	Komatiitic, tholeiitic and calc-alkalic

Table 3. Features of subaerial and submarine unconformities (*from* Shanmugam 1988).

Subaerial Unconformities	Submarine Unconformities
Discordance of dip	Debris flows, slump deposits, and hemi-pelagic mudstones in submarine canyons
Erosional surface	Glauconitic minerals
Regional truncation	Manganese nodules
Deformational contrasts	
Fluvial valleys	
Basal conglomerates	
Weathered units (chert etc.)	
Seismic reflection patterns	
Isotopes	
Paleosol, duricrust, regolith	

The western part of the Abitibi greenstone belt consists of "Keewatin" assemblages varying in age from ca. 2750 to 2696 Ma (Ayer, Amelin et al. 2002). A number of these assemblages include an uppermost unit of iron formation and/or graphitic argillite. Within the Keewatin stratigraphy of the Abitibi greenstone belt, Heather (1998) mapped a major iron formation unit overlying the circa 2730 Ma Deloro assemblage in the main part of the belt and overlying the correlative Marion group in the Swayze area. He postulated the iron formation to be regional-scale marker horizon. Heather obtained U/Pb zircon ages on units immediately underlying and overlying the major iron formation unit documenting a interval of about 6 my (2731±2 to 2724±2 Ma) for accumulation of the iron formation. Therefore, this Deloro–Tisdale assemblages contact is considered here to be a contact of regional significance. Details of this contact are discussed in the Deloro assemblage section below.

PACAUD ASSEMBLAGE

The 2750 to 2735 Ma Pacaud assemblage is the oldest outcropping supracrustal unit identified to date in the southern Abitibi greenstone belt (Ayer, Amelin et al. 2002). It consists predominantly of tholeiitic volcanic rocks with calc-alkaline intermediate to felsic volcanic rocks and minor komatiites. The assemblage crops out on the margins of the major batholiths such as the Round Lake and Kenogamissi batholiths. The base of the assemblage is cut by batholiths and, thus, its relationship to any older assemblage, such as the 2790 Ma unit in the northern Abitibi Subprovince within Quebec, is unknown (Rhéaume et al. 2004). The recently discovered presence of 2860 to 2800 Ma zircon xenocryst in isolated volcanic units within the study area (e.g., samples 96JAA-0094, 04BHA-0333 and 3D-CG) in conjunction with similar-age xenocrysts in isolated synvolcanic batholith samples (Ketchum et al., in press) indicated that older crust was locally sampled by the Abitibi-age magmas, but the precise nature of the relationship to the older basement remains elusive as other radiogenic isotopic systems, such as Nd and Hf, display signatures that typically indicate these magmas were derived from juvenile-depleted mantle, but also with some isolated samples indicating minor contamination by ancient crust (e.g., Corfu and Noble 1992; Ayer, Amelin et al. 2002; Ketchum et al., in press).

Our new SHRIMP data confirm speculation by Ayer, Amelin et al. (2002) that the Pacaud assemblage was more widespread than its present known outcrop distribution indicates (*see* Figures 1 and 2). This is indicated by xenocrystic zircon cores found within samples scattered across the southern Abitibi greenstone belt, including within a Deloro assemblage sample (97JAA-0106) overlying the Pacaud assemblage in the Shining Tree area; a Tisdale assemblage sample (96TB-079) overlying the Deloro assemblage in Langmuir Township, south of Timmins; and within Timiskaming assemblage volcanic units within the Swayze area (99JAA-0057) and Holloway Township (3D-CG) (*see* Figures 9 and 10).

DELORO ASSEMBLAGE

The 2730 to 2724 Ma Deloro assemblage (Ayer, Amelin et al. 2002) is composed primarily of calc-alkaline volcanic rocks. In the study area, it is exposed on the eastern flanks of the Kenogamissi batholith, the east flank of the Nat River batholith, in the core of the Shaw dome and north of Timmins (*see* Figure 2). It is also found on the north flank of the Ramsey–Algoma granitoid complex in the Shining Tree and Swayze areas and the western flank of the Kenogamissi batholith in the Swayze belt (*see* Figure 1). A similar age range is displayed by rocks of the Hunter Mine Group (Mueller and Mortensen 2002) to the east in Quebec, which we equate with the Deloro assemblage. In most instances, the assemblage is underlain by rocks of the slightly older Pacaud assemblage. The age range of the 2 assemblages suggests a gap of about 5 my. The Deloro assemblage is underlain by chert breccia in the Shining Tree area (Johns and Amelin 1998; Johns 1999). This chert breccia may be indicative of a basal unconformity for the Deloro assemblage. The assemblage is capped by a regionally extensive unit of oxide facies iron formation in the Woman River and Hanrahan antiforms of the Swayze greenstone belt and in the localities listed above.

New U/Pb TIMS analyses of zircons from felsic tuff intercalated with iron formation and ultramafic volcanic rocks in the northern part of the Shaw Dome yielded an age of 2724.1±3.7 Ma (#10: Table 1, Figure 4D). Based on this new Deloro-age sample from the northern margin of the Shaw Dome (#10: Figure 2), we have revised the interpretation of a Krist formation unit occurring immediately south of the Porcupine–Destor deformation zone (PDDZ) in Deloro and Ogden townships, which was based on the 2685.1±1.3 Ma age for a foliated quartz-feldspar porphyritic felsic rock in Ogden Township (Ayer, Barr et al. 2003). We now believe this nondescript quartz feldspar porphyritic rock is a porphyry intrusion cutting a package of structurally interleaved Deloro, Tisdale and Timiskaming assemblage units proximal to the PDDZ in Deloro and Ogden townships. This porphyry age fits quite well with the age of the slightly younger porphyry intrusion found at the Hoyle Pond Mine (*see* "Intrusion Framework").

Table 4. Locations of chert breccia and iron formation conglomerate units.

Township	UTM Co-ordinates (NAD83)		Notes
	Easting (m)	Northing (m)	
Carscallen	452248	5358479	Wire Gold Occurrence: IF breccia above pillowed flows
Whitney	485716	5367536	BIF, 1 m arkose, IF conglomerate with clasts to 60 cm in ferruginous chert matrix, capped with BIF
Deloro	479437	5364304	Heterolithic IF conglomerate in 2.5 m thick unit above BIF. Overlain by 2724 Ma feldspar phyric lapilli tuff at 478510E, 5364034N
English	482873	5327000	IF chert breccia overlain by heterolithic pyroclastic breccia debris flows and heterolithic conglomerate with chert clasts
Bartlett	482000*	5332042*	Feldspathic arkose beds with graphitic argillite tops
Hutt	485698	5314994	Heterolithic volcaniclastic units with intercalated chert and/or graphitic argillite units in lower Tisdale

* NAD27. Abbreviations: BIF, banded iron formation; IF, iron formation.

A second felsic sample intercalated with iron formation on the eastern side of the Shaw Dome yielded a less precise age of 2727±12 Ma (#24: Table 1, Figure 6D). These 2 samples provide geochronological confirmation that the central part of the Shaw Dome is of Deloro age (e.g., Pyke 1982; Corfu 1993; Ayer, Amelin et al. 2002). Two previously analyzed geochronology samples of felsic volcanic rocks from the outer flanks of the Shaw Dome were selected for additional zircon analyses to check for inheritance because they yielded Deloro ages in units considered to lie outside the Deloro-age core of the Dome. The new results have yielded slightly more precise Deloro assemblage ages of 2724.6±0.8 Ma and 2723.1±1.3 Ma for these 2 samples (#22 and #26: Table 1, Figures 6B and 6E) (cf. Corfu and Noble 1992; Barrie and Corfu 1999). This confirms structural repetition of Deloro assemblage units interleaved within the Tisdale assemblage on both the northeastern and southeastern margins of the Dome (Figure 2) (*see* Barrie and Corfu 1999). This feature is interpreted to be caused by early strata-parallel D2 folding and thrusting, similar to the D2 folding and thrusting of Tisdale and Porcupine assemblage units documented north of the Porcupine–Destor deformation zone in the Timmins camp (*see* "Timmins Subproject").

The iron formation capping the Deloro assemblage is typically iron-poor chert-magnetite, but hematite, siderite, pyrite, pyrrhotite, carbonaceous chert, and minor ferruginous and siliceous argillite units are also present (Heather 2001). Field investigation reveals that the iron formation unit includes intercalations of arkosic conglomerate and minor graphitic argillite in Whitney Township (Table 4). On a regional scale, the iron formation unit varies in thickness from a few metres to hundreds of metres. Most of the iron formation is typically well-bedded material with the bedding rarely deformed by synsedimentary and tectonic processes (Photo 1).

Chert breccia and iron formation conglomerate units occur in a number of locations in the Timmins area and are listed in Table 4.

The chert breccia units are massive, ungraded unbedded units with rare chert interbeds (Heather 2001). They contain re-sedimented chert and chert breccia clasts indicative of multiple generations of development (Photo 2).

Their regional extent along the eastern flank of the Swayze greenstone belt and the western flank of the Abitibi greenstone belt is interpreted to indicate that the iron formation and chert breccia unit is a regional marker unit (Heather 1998). Indeed, extensions of the unit exist in Quebec where mass flow units lie above metavolcanic rocks of ca. 2730 Ma age at Joutel (Legault et al. 2002). The unbedded, ungraded nature of the chert breccia indicates that the units are mass flow deposits.

The iron formation and chert breccia unit forming the upper part of the Deloro assemblage stratigraphy was examined in several locations, as listed in Table 4, and shown by the triangles on Figure 1. In Whitney Township adjacent to the Pamour pit haul road, the iron formation at the top of the Deloro assemblage consists of banded oxide-facies iron formation intercalated with metre-scale beds of

Photo 1. Banded iron formation in Deloro Township at location listed in Table 4.

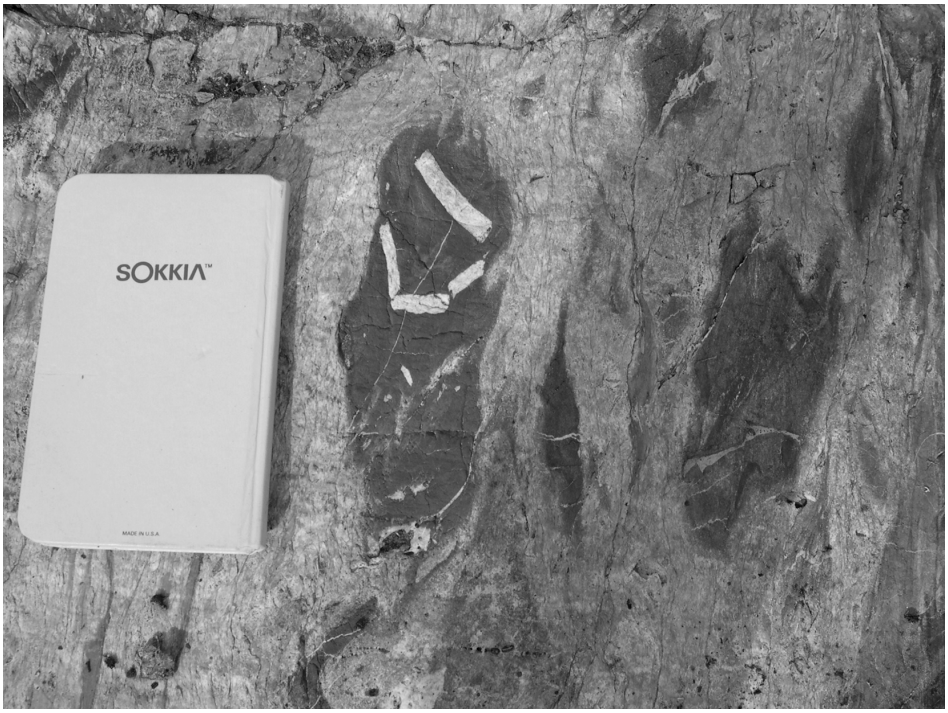

Photo 2. Clast in iron formation conglomerate containing chocolate-tablet-style fractured chert fragment in an iron formation clast.

arkosic conglomerate, and metre-scale units of iron formation conglomerate (triangle 1 on Figure 1). Along the power line in Deloro Township (triangle 2 on Figure 1), Deloro assemblage basalts are overlain by an iron formation unit succeeded by 2724.1±3.7 Ma feldspar phyric lapilli tuff of the Deloro assemblage. The iron formation is a finely laminated banded iron formation succeeded by iron formation conglomerate containing abundant arkose and chert clasts. Some clasts of iron formation contain tabular chert clasts indicating that there have been multiple episodes of iron formation sedimentation followed by cannibalization of the early formed iron formation units.

Triangle 3 on Figure 1 indicates the location of a representative section of the Deloro–Tisdale assemblages contact along the power line in northern English Township. Figure 13 is a schematic section of the Deloro–Tisdale assemblages contact in that location, which, from the base upward is 3 m

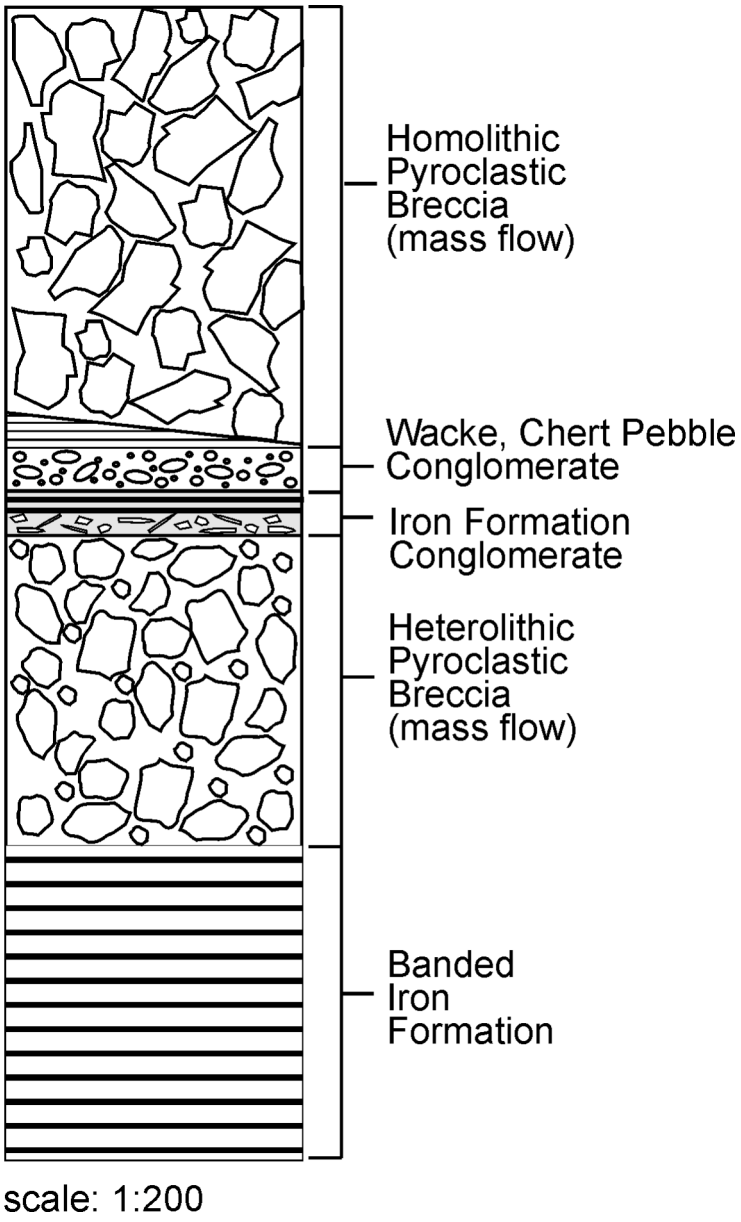

Figure 13. Schematic stratigraphic section of the Deloro–Tisdale assemblage contact in northern English township. Note the erosional contact between the wacke, chert pebble conglomerate unit and the homolithic pyroclastic breccia.

(thickness) of banded iron-poor iron formation, succeeded by approximately 60 m thickness of heterolithic, unbedded, ungraded felsic pyroclastic breccia, a 5 m thickness of iron-formation conglomerate, 2 to 3 m of wacke in erosional contact with approximately 60 m thickness of monolithic rhyolitic pyroclastic breccia. The felsic volcanic units, given their unbedded, non-graded nature are considered mass-flow deposits. The contact between the chert fragment-bearing wackes and the upper pyroclastic breccia unit is an erosional surface transecting the wacke unit.

North of English Township in Bartlett Township, the Deloro–Tisdale assemblages contact is marked by metre-scale feldspathic arkose beds with graphitic arkose tops. It is presumed that this is a more proximal facies of the relationships described in the preceding paragraph.

In Carscallen Township at the Wire Gold occurrence (Hall and Smith 2002; *see* Table 4), iron formation breccia occurs at the contact between the Deloro assemblage and the overlying Upper Unit of the Kidd–Munro assemblage. This contact is interpreted to be a submarine unconformity based on these relationships.

In summary, at each of the Deloro–Tisdale assemblages contacts shown on Figure 1, the "iron formation" actually consists of conventional banded iron formation, and/or iron formation conglomerate or other units deposited by mass-flow processes. Using the criteria of Shanmugam (1988), this chert breccia unit in the upper part of the Deloro assemblage is then interpreted as a regional-scale unconformity between the Deloro assemblage in Whitney, Bartlett, Geikie, McArthur and English townships and the overlying Tisdale assemblage and between the Deloro assemblage and the overlying Kidd–Munro assemblage in Carscallen Township. Similarly, the chert breccia unit beneath the lowest Deloro assemblage metavolcanic unit in the Shining Tree area also may represent an unconformity between the Pacaud and Deloro assemblages.

STOUGHTON–ROQUEMAURE ASSEMBLAGE

The 2723 to 2720 Ma Stoughton–Roquemaure assemblage consists of mafic volcanic rocks with subordinate felsic volcanic rocks and komatiites (~1%) (Sproule et al. 2002). The assemblage has been identified in both the northern and the southeastern parts of the study area (*see* Figure 2). In the north, the assemblage is conformably underlain by the Hunter Mine group of the Deloro assemblage east of Lake Abitibi batholith in Quebec (Mueller and Mortensen 2002). In the part of the assemblage that crops out south of Kirkland Lake, the basal contact is with the Pacaud assemblage. This contact represents an age gap of about 20 my and, thus, is interpreted to be unconformable. Iron formation in the upper part of the Stoughton–Roquemaure assemblage in this area (i.e., the Catharine group: Jackson and Fyon 1991), and crystallization ages of 2701 Ma with 2720 Ma zircon xenocryst in felsic volcanic rocks of the overlying upper Blake River assemblage (i.e., the Skead group) (Corfu 1993) indicate an unconformity also occurs at the top of this part of the Stoughton–Roquemaure assemblage.

KIDD–MUNRO ASSEMBLAGE

Lower Part

The lowermost part of the Kidd–Munro assemblage ranges in age from 2719 to 2717 Ma. It differs from the more extensive upper Kidd–Munro assemblage by being dominated by intermediate to felsic calc-alkalic volcanic rocks. It has been identified in 3 areas (*see* Figure 2): 1) in the northeast where it was

previously identified as the Coulson–Rand assemblage (Jackson and Fyon 1991). Here the lack of an age gap and the presence of xenocrystic zircons with an age of 2723 Ma indicates that it conformably overlies the Stoughton–Roquemaure assemblage located to the north, despite the presence of the North Branch Porcupine–Destor deformation zone at this contact. 2) In the north-central area, where it is complexly infolded with the upper Kidd–Munro assemblage rocks in Dundonald and Clergue townships; and 3) west of the Mattagami River fault in the northwest where a thick sequence of calc-alkalic volcanic rocks have an age of 2719.5±1.7 Ma (Ayer, Amelin et al. 2002). In the latter area, it lies in faulted contact with a northeast-facing unit of the upper part of the Kidd–Munro assemblage to the south, and has unknown contact relationships with rocks assumed to be part of the Blake River assemblage to the north.

Upper Part

The 2717 to 2711 Ma upper part of the Kidd–Munro assemblage is the traditionally known part of the Kidd–Munro assemblage as identified by Jackson and Fyon (1991). It extends across the northern part of the study area (*see* Figure 2) and is dominated by tholeiitic mafic and komatiitic rocks with localized accumulations of tholeiitic felsic volcanic rocks and graphitic sedimentary units. In the east, the basal contact is interpreted to be conformable with underlying calc-alkaline volcanic rocks of the lower Kidd–Munro assemblage to the north. To the west, the northern margin is in faulted contact with the Porcupine assemblage. The southern margin lies in faulted contact with sedimentary rocks of the Timiskaming assemblage along the Porcupine–Destor deformation zone (PDDZ) in the east, and the Porcupine assemblage (Pipestone fault) to the west. West of the Mattagami River fault, the assemblage has been sinistrally offset to the south by about 8 km. Here, both the northern and southern contacts are marked by faults. New geochronologic samples with crystallization ages of 2712.3±2.8 Ma and 2714.6±1.2 Ma from central Loveland and southern Thorburn townships (#1 and #2: Table 1, Figures 3A and 3B) confirm the mapping-based interpretation of a northeast-facing package in faulted contact with the lower Kidd–Munro assemblage in Thorburn Township to the north (*see* "Kamiskotia Area Subprojects"). In addition, one of these samples was found to contain a pre-Abitibi-age xenocryst with an age of 2861.4±1.7 Ma (#2: Table 1, Figure 3A).

A less extensive part of the upper Kidd–Munro assemblage also occurs south of the Kamiskotia area. Here, the assemblage faces to the northeast and unconformably overlies iron formations at the top of the Deloro assemblage to the south (see above). Newly extracted zircons from a previously sampled overlying felsic tuff in Carscallen Township (Ayer, Amelin et al. 2002) yielded a more precise crystallization age of 2712.2±0.9 Ma (#8: Table 1, Figure 4B). This indicates an age gap of approximately 12 my exists between the unconformably underlying Deloro and the upper Kidd–Munro assemblages at this locality. The newly analyzed zircons from this sample also revealed the presence of a discordant pre-Abitibi xenocryst with an age of 2853.6±1.4 Ma (*see* Figure 4B).

TISDALE ASSEMBLAGE

Lower Part

The lowermost part of the Tisdale assemblage ranges in age from 2710 to 2706 Ma. It consists predominantly of tholeiitic mafic volcanic rocks with localized accumulations of komatiite, intermediate to felsic calc-alkaline volcanic rocks and iron formation. It is widespread in the central part of the map area where it forms the nose and limbs of a broad west-closing synclinorium cored by the Blake River assemblage (*see* Figure 2). The basal contact of Tisdale assemblage is marked by iron formation and chert

clast conglomerates at the top of the underlying Deloro assemblage, which, in conjunction with an age gap of about 15 my, indicates the presence of a widespread submarine unconformity (*see* "Deloro Assemblage"). Felsic to intermediate volcanic rocks intercalated with ultramafic volcanic rocks and iron formation occupy the lowermost part of the assemblage exposed around the Shaw Dome, where Houlé and Guilmette (2004) have identified it as "Package B" (*see* "Shaw Dome Area"), and south of the study area where felsic volcanic rocks in the core of the Halliday anticline have an age of 2710.5±1.6 Ma and are surrounded by mafic volcanic rocks and komatiite with an age of 2707.8±1.2 Ma (Ayer, Ketchum and Trowell 2002). The Adam iron mine is also interpreted to occur in the lower Tisdale assemblage as indicated by an age of 2712±4 Ma from heterolithic volcanic rocks intimately intercalated with komatiite in the footwall of the iron formation, which are part of the Larder Lake group, south of Kirkland Lake (Ayer, Amelin et al. 2002).

SHRIMP analyses of zircons from a felsic volcanic unit with an age of 2708.2±2.1 Ma (Barrie and Corfu 1999) from the southeastern margin of the Shaw Dome in the "Package C" sequence indicates that both Pacaud- and Deloro-age zircon xenocrysts (Figure 14) are present in this sample (#25: Figure 2 (sample 96TB-079). This implies that, at the time of deposition of this unit, both the Deloro and the Pacaud assemblages underlay the Tisdale assemblage, thus, indicating that the Pacaud assemblage was a more widespread basal assemblage in the SAGB than its present outcrop distribution indicates (*see* Figures 1 and 2).

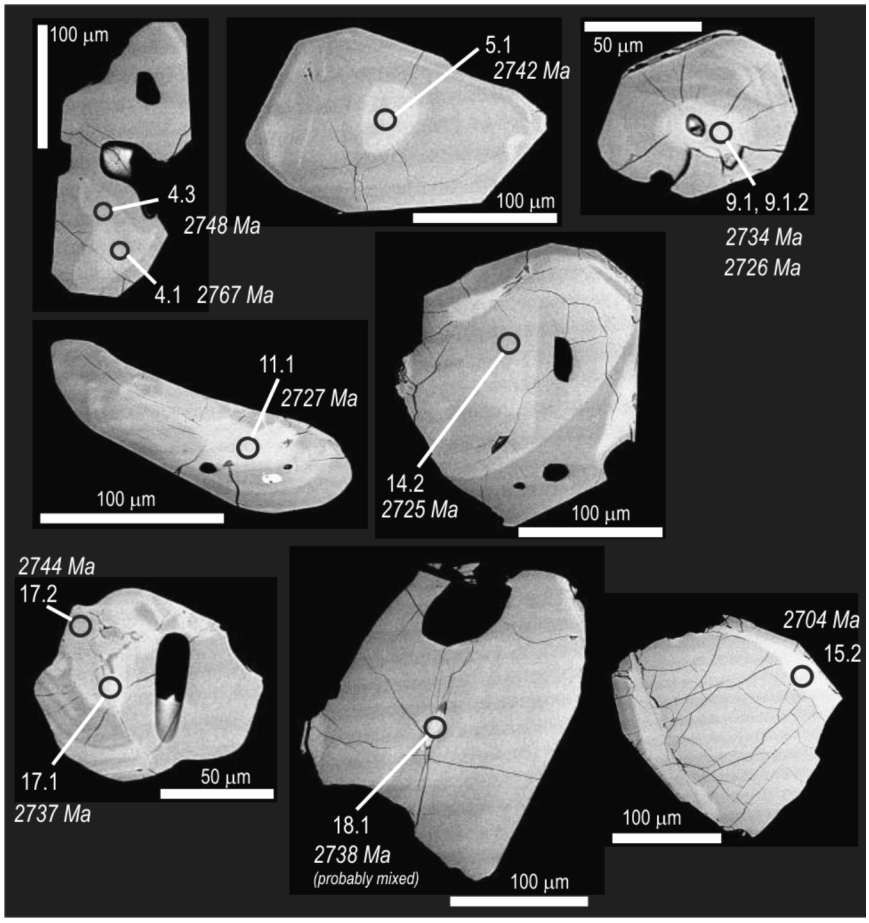

Figure 14. Backscattered electron images of the cores of inherited zircon and a zircon overgrowth from lower Tisdale assemblage volcanic sample 96TB-079. The spot locations, numbers and ages correspond with the SHRIMP II analyses in Appendix 2 (Table A2).

An internal contact within the lower Tisdale assemblage in Hutt Township (triangle 4 on Figure 1) displays heterolithic felsic volcanic debris flows and arkoses intercalated with finely laminated chert, oxide- and sulphides-facies iron formation. This intercalation of mass-flow units and iron formation would suggest that internal contacts within the lower unit of the Tisdale assemblage may represent a localized submarine unconformity.

The lower Tisdale assemblage also occurs in the western part of the study area, north of the Porcupine–Destor fault (PDF). Here, unlike the more extensive lower Tisdale unit south of the PDF (described above), the lowermost portion of the lower Tisdale and the upper Tisdale assemblage (and the Blake River assemblage) are absent. Instead, here, the Tisdale stratigraphy established by Ferguson et al. (1968) consists of komatiites and tholeiites of the Hershey Lake formation, in turn succeeded by the tholeiites of the Central formation, the variolitic tholeiites of Vipond formation (2706.9±3.1 Ma: Ayer, Amelin et al. 2002) and capped by the tholeiitic Gold Centre formation. Here, the Tisdale formations are unconformably overlain by, and complexly infolded with, the Porcupine assemblage (*see* "Timmins Subproject").

Upper Part

The upper part of the Tisdale assemblage ranges in age from 2706 to 2704 Ma. It is dominated by calc-alkaline felsic to intermediate volcanic rocks including amygdaloidal flows, heterolithic debris flows and volcaniclastic sedimentary rocks. This part of the Tisdale assemblage conformably overlies the lower Tisdale assemblage in the central part of the map area and includes the Marker Horizon (Corfu and Noble 1992) extending from Hislop to Michie townships, which is, in turn, conformably succeeded by the lower Blake River assemblage (*see* "Currie Township"). Other upper Tisdale assemblage units occur further to the west and south within the cores of easterly trending synclinorial folds. One such unit, centred in Argyle and Baden townships, was previously identified as part of the Blake River assemblage in Ayer, Amelin et al. (2002). Despite several unsuccessful attempts to directly obtain an age for this unit, it is herein reassigned to the upper Tisdale assemblage because of its lithological and geochemical characteristics and the fact that it is intruded by a synvolcanic granitic body with an age of 2699±3 Ma in northeastern Baden Township (*see* Figure 2). A synvolcanic intrusion of this age is considered to be more likely within the Tisdale assemblage than the Blake River assemblage.

A felsic volcanic unit with an age of 2702±3 Ma from Cleaver Township (#29: Figure 2) previously indicated the presence of Deloro-age inheritance in this part of the upper Tisdale assemblage (Ayer, Amelin et al. 2002). SHRIMP II analyses of additional zircons from this sample yielded a number of inherited zircons with ages of approximately 2735 to 2720 Ma as well as magmatic zircons with ages of approximately 2704 to 2698 Ma (Figure 15).

A unit of the upper Tisdale assemblage also occurs in the northern part of the map area. Its northern contact with the Stoughton–Roquemaure assemblage is marked by the North Branch of the Porcupine–Destor deformation zone (*see* "Structural Framework") and an age gap of about 15 my. However, the presence of the 2704±5 Ma mafic to ultramafic intrusive complex in Mann and McCart townships (Barrie 1999) intruding the contact between the 2 assemblages suggests an originally unconformable contact modified by faulting. The unit youngs southward where it is overlain in the east by tholeiitic basalts that also face south and are assumed to be part of the lower Blake River assemblage (see "Blake River Assemblage"). Further to the west, the southern margin is in fault contact with the Deloro assemblage across to the Buskegau River deformation zone.

BLAKE RIVER ASSEMBLAGE

Lower Part

The lower Blake River assemblage has an age range of 2704 to 2701 Ma. It was previously identified as the Kinojevis assemblage in Ayer, Amelin et al. (2002). However, its difference in age from the Kinojevis Group in Quebec that has an age of 2718±2 Ma (Zhang et al. 1993), which correlates with the Kidd–Munro assemblage in Ontario, has led to confusion in Abitibi stratigraphic nomenclature and, thus, this unit is herein identified as the lower part of the Blake River assemblage. This better fits its original identification as the Garrison subgroup of the Blake River group by Goodwin (1979). The unit consists predominantly of tholeiitic mafic volcanic rocks with isolated units of tholeiitic felsic volcanic rocks and turbiditic sedimentary rocks.

Based on our new mapping and geochronology, we have also revised stratigraphy in the Kamiskotia region (*see* "Kamiskotia Area Subprojects") where the southern part of this area is now interpreted to be underlain by the lower and upper parts of the Blake River assemblage (*see* Figure 2)—an area that was previously assigned to the Tisdale assemblage (Ayer, Amelin et al. 2002). We now also interpret that the lower Blake River assemblage underlies areas with poor exposure and limited geochronology in Mahaffy, Macdiarmid and Geary townships (*see* Figure 2).

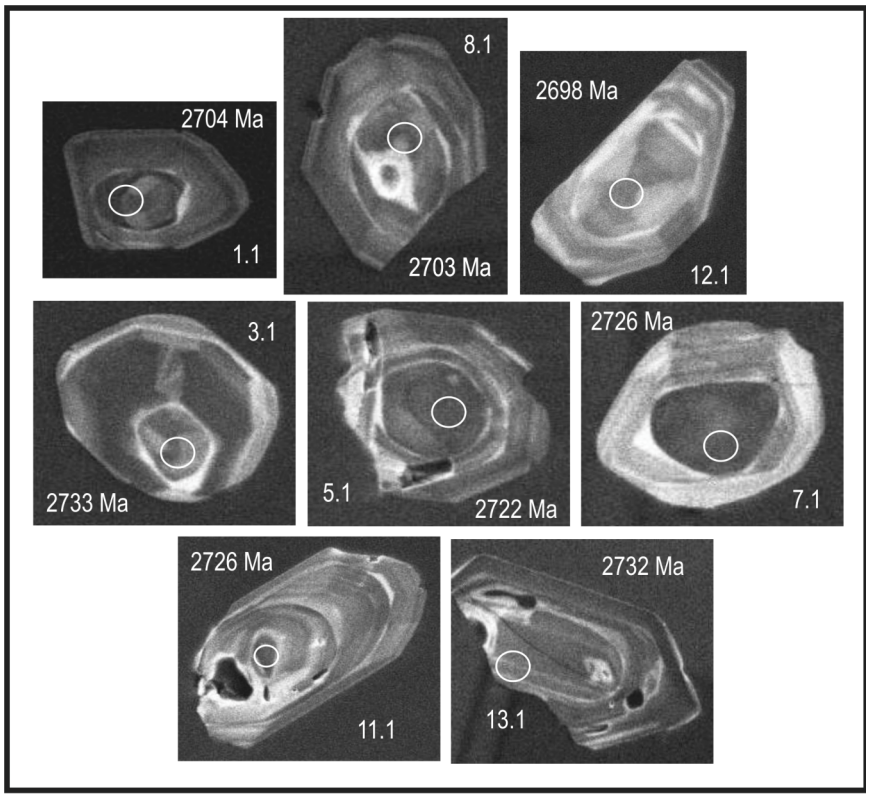

Figure 15. Cathodoluminescence images of inherited and magmatic zircon from upper Tisdale assemblage volcanic sample 98JAA-0011. The spot locations, numbers and ages correspond with the SHRIMP II analyses in Appendix 2 (Table A2).

Upper Part

The upper Blake River assemblage ranges in age from 2701 to 2696 Ma and consists predominantly of flows of calc-alkaline basalt and andesite, locally with bimodal tholeiitic basalt and rhyolite. The Blake River group occurs in the east-central part of the study area and is the most voluminous part of the assemblage (*see* Figure 1). Goodwin (1979) identified this part of the Blake River group as the Misema subgroup. New mapping and geochronology indicates that the Misema subgroup in Ben Nevis Township (*see* "Ben Nevis Area Subprojects") has a U/Pb age of 2696.6±1.3 Ma (Figure 4A). This is younger than the pre-cauldron phase of the Noranda subgroup (2701±1 Ma: Mortensen 1993b), younger than the Misema subgroup in Pontiac Township (2701±2 Ma: Corfu et al. 1989), and of the same age as the post-cauldron phase of the Noranda subgroup (the Reneault–Dufresnoy formation: 2697.9+1.3/–0.7 Ma (Mortensen 1993b) and 2696±1.1 Ma (Lafrance, Moorhead and Davis 2003; and the Bousquet formation: 2698.6±1.5 Ma, 2698.0±1.5 Ma and 2694±2 Ma (Lafrance, Moorhead and Davis 2003). Thus, the Ben Nevis–Clifford volcanic complex formed late in the Blake River group volcanic event.

The new mapping and geochronology in the Kamiskotia area has resulted in revision to the stratigraphy proposed in this area by Ayer, Amelin et al. (2002). The volcanic rocks in the southern part of this area are assigned to the Kamiskotia Volcanic Complex (KVC) (*see* "Kamiskotia Area Subprojects"). The known VMS deposits in the study area occur within a restricted, east-facing stratigraphic interval in the upper part of the KVC. New U/Pb ages for this interval, ranging from 2701.1±1.4 to 2698.6±1.3 Ma (Figures 3D, 3E and 3F) and, thus, indicate that it correlates better with the upper Blake River assemblage, rather than the Tisdale assemblage (cf. Ayer, Amelin et al. 2002). The VMS-bearing KVC unit is interpreted to unconformably overlie the upper part of the Kidd–Munro assemblage to the south based on an age gap of about 12 my (*see* Figure 2). An as yet unreported age of 2700 Ma from a heterolithic volcanic unit in the hanging wall west of the Kidd Creek deposit (W. Bleeker, Geological Survey of Canada, personal communication, 2005) suggests an interesting spatial association between VMS deposits and the proposed unconformable contact between the upper Blake River and the upper Kidd–Munro assemblages in both the Kamiskotia and Kidd Creek areas.

PORCUPINE ASSEMBLAGE

The Porcupine assemblage ranges in age from 2690 to about 2685 Ma and is, thus, similar to many of the porphyries and syntectonic intrusions (discussed below). The assemblage consists predominantly of wacke, siltstone and mudstone displaying Bouma sequence subdivisions indicating predominantly distal deposition by turbidity currents, but locally also containing calc-alkaline felsic volcanic rocks, conglomerates and iron formation. The age range has been revised from the previously published range of 2696 to 2692 Ma (Ayer, Amelin et al. 2002) based on a considerable amount of new geochronology over the past few years. However, the absolute minimum age limit of the assemblage is difficult to determine precisely because the uppermost portions of this assemblage are clastic sedimentary rocks in which the zircons are of detrital origin and, thus, provide only the maximum age of deposition of the units.

Timmins Area

A number of distinctive sedimentary and volcanic units that are now included within the Porcupine assemblage have been given stratigraphic names in the past including the Krist, Hoyle, Beatty and Whitney formations (Born 1995).

The Krist formation consists of calc-alkaline felsic fragmental volcanic rocks locally unconformably overlying the Tisdale assemblage. Recent geochronology has provided crystallization ages of 2687.5±1.3 Ma and 2687.3±1.6 Ma for samples in the Kayorum syncline and the nose of the Porcupine syncline in Timmins, and an age of 2691±1.5 Ma, south of the PDF in Whitney Township (Ayer, Barr et al. 2003). The ages and geochemical signatures of the Krist formation volcanic rocks, which are indistinguishable from those of the porphyry intrusions in the Timmins region, indicate that the abundant porphyry intrusions in the Timmins area represent subvolcanic intrusions coeval with Krist formation volcanism (*see* "Intrusion Subproject").

The Hoyle formation is a widespread unit of turbiditic sedimentary rocks with minor conglomerate restricted to north side of the PDDZ. It extend east as far as Guibord Township, and west as far as Denton Township. It unconformably overlies a number of older volcanic assemblages including the Tisdale and Blake River assemblages and is separated from the Kidd–Munro assemblage to the north by the Pipestone fault. Previous geochronology of detrital zircons from clastic samples indicate maximum depositional ages of 2684.7±6.3 Ma in Kidd Township (Bleeker, Parrish and Sager-Kinsman 1999) and 2691.3±1.5 Ma in Mountjoy Township (Bleeker 1999). New samples from Tisdale and Whitney townships, analyzed by TIMS, indicate maximum depositional ages of <2690.9±2.5 Ma in Tisdale Township and <2688.2±1.9 Ma in Whitney Township, in addition to older detrital ages of 2690 to 2704 Ma, 2712 to 2713 Ma, and 2725 Ma (#14 and #18: Table 1, Figures 4F and 5D). SHRIMP results from the latter sample indicate more numerous, but less precise detrital zircon ages from 2680 to 2756±9 Ma with a peak at about 2695 Ma (*see* Figure 11B).

The Beatty formation consists of a turbiditic sedimentary sequence restricted to the core of the Porcupine syncline where it conformably overlies the Krist formation. The youngest detrital zircons from a new geochronology sample of wacke underlying the Timiskaming assemblage unconformity in Tisdale Township provides a maximum depositional age of 2687.2±1.6 Ma, in addition to older detrital zircons with ages of 2692 Ma, 2708 Ma, 2720 Ma, and 2726 Ma (#15: Table 1, Figure 5A). SHRIMP results from this sample yielded a continuum of less precise detrital zircon ages from 2680 to 2750 Ma with a peak at about 2700 Ma (*see* Figure 11A).

The Whitney formation consists of turbiditic sedimentary rocks south of the PDDZ in Whitney and Cody townships. The formation is underlain by the Krist formation on the west limb of a syncline within the sediments, and by the Tisdale assemblage to the south and east (*see* Figure 2). The Whitney formation was previously considered to be part of the Tisdale group (Pyke 1982; Born 1995), but a new geochronological sample in Whitney Township yielded detrital zircons indicating a maximum depositional age of 2689.5±1.7 Ma and older detrital zircons with ages of 2692 Ma, 2723 Ma and 2726 Ma (#21: Table 1, Figure 6A). SHRIMP results from this sample indicate a continuum of less precise zircon ages from 2680 to 2750 Ma with a peak at about 2695 Ma (*see* Figure 11C). These ages confirm the Whitney formation is part of the Porcupine assemblage and, in conjunction with the presence of an underlying unit of the Krist formation, suggest it is most likely the eastward continuation of the Beatty formation (and the Porcupine syncline), sinistrally offset by about 13 km across the PDDZ (*see* Figure 2). These marker units thus provide the first direct evidence for both the sense and magnitude of post-D2 strike-slip displacement on the PDDZ in the Timmins area (i.e., postdating the F2 Porcupine syncline).

Northeast Area

Three turbiditic sequences occur in the northeastern part of the study area. Two of these units are minor and have not been dated. However, a more widespread sedimentary unit, extending from poorly exposed paragneisses northwest of Cochrane, to turbidites interbedded with iron formation (*see* Figure 1) extending approximately 200 km along strike to the east into Quebec, has been correlated with the

Porcupine assemblage (Ayer, Amelin et al. 2002). The southern margin of this unit occurs in Wesley and Moody townships within the study area. The youngest detrital zircons from sandstone in Purvis Township (just north of the study area) yielded a maximum age of deposition of 2698±2.4 Ma. Older detrital zircons from this sample yield ages of 2745 Ma, 2725 Ma and 2715 Ma suggesting provenance from the Pacaud, Deloro and Kidd–Munro assemblages, respectively. A significantly older detrital zircon with an age of 2825 Ma may have been derived from pre-Abitibi rocks of the Opatica Subprovince. All three of these sedimentary units are included within the Porcupine assemblage and are interpreted to have had unconformable basal contacts with older volcanic assemblages, but the contacts have been modified by subsequent deformation and many are now the locus of regional deformation zones (*see* "Structural Framework").

Larder Lake South Area

A unit interpreted to be part of the Porcupine assemblage occurs in the southeast corner of the study area. It was previously identified as part of the Hearst assemblage (Jackson, Fyon and Corfu 1994) and consists of turbidites and heterolithic conglomerate. It unconformably overlies, and is complexly infolded with the Larder Lake group volcanic rocks of the Tisdale assemblage. Two samples (a turbidite and a conglomerate) were analyzed from northern Skead Township (*see* Figure 2) and the youngest detrital zircon age detected was 2695.6±3.0 Ma with older detrital zircons at 2703 Ma, 2708 Ma, 2715 Ma and 2718 Ma (Ayer, Barr et al. 2003). Thus, the unit was deposited sometime after 2695.6±3.0 Ma. It is, therefore, interpreted to be part of Porcupine assemblage, but, unlike the samples from the Timmins area, the unit was lacking in a source for detrital zircons closer to the actual age of deposition (i.e., <2690 Ma).

The numerous zircons data now available from the Porcupine assemblage sedimentary rocks indicates that zircons were derived predominantly from the underlying Abitibi volcanic assemblages, the synvolcanic and the syntectonic intrusions and, thus, contrasts with the Timiskaming assemblage samples (see below) which commonly also contain pre-Abitibi-age zircons (i.e., 2860–2790 Ma). These Porcupine assemblage detrital data support an interpretation for a basal unconformity associated with considerable uplift, erosion and a relatively local provenance. Our SHRIMP data (*see* Figure 11) indicate the peak in detrital zircon concentration occurs at about 2695 Ma, thus, conforming with ages for the earliest members of a voluminous suite of syntectonic intrusions. This evidence, along with the abundance of syntectonic plutons intruded into the area at about this time (*see* "Intrusion Framework"), suggests that initiation of D1 compression and associated syntectonic plutonism were the likely causes of the uplift, erosion and sedimentation that occurred in deep submarine canyons associated with fault escarpments.

TIMISKAMING ASSEMBLAGE

The Timiskaming assemblage is the youngest supracrustal assemblage in the SAGB and ranges in age from about 2676 to 2670 Ma and, thus, is modified from 2687 to 2675 Ma as previously published in Ayer, Amelin et al. (2002). It is predominantly restricted to narrow corridors of clastic sedimentary rocks locally intercalated with alkaline and calc-alkaline volcanic rocks unconformably deposited on older assemblages in close proximity to regional deformation zones such as the Porcupine–Destor, Larder Lake–Cadillac and Ridout faults (*see* Figure 1). The clastic component of the assemblage consists of polymictic conglomerate and sandstone deposited in subaerial alluvial fan, fluvial and deltaic environments (Mueller, Donaldson and Doucet 1994; Born 1995).

Timmins Area

In the Timmins area, the Timiskaming assemblage is confined to a narrow east-trending unit of conglomerates and sandstone overlying the Tisdale and Porcupine assemblages. An angular unconformity occurs along the north contact of the Timiskaming assemblage and it is truncated by the PDDZ and/or the Dome fault to the south (*see* "Timmins Subproject"). Born (1995) subdivided the Timiskaming assemblage in this area into the lowermost Dome formation, consisting of alluvial sediments grading upwards into proximal and mid-fan turbidites, in turn overlain by the Three Nations formation grading upwards from alluvial to fluvial to shelf-facies sandstones. Two samples from the Dome formation at the Dome Mine were analyzed using the TIMS methods (Ayer, Barr et al. 2003): wacke from the basal part of the Dome formation in the "Greenstone Nose" contains detrital zircons with ages ranging from 2710 Ma to 2679±4 Ma, whereas conglomerate in the "sedimentary trough" yields a broader spectrum of detrital zircon ages ranging from 2814 Ma to 2674±2 Ma (#11 and #12: Figure 2). Less precise SHRIMP results from these 2 samples reveal bimodal age distributions with a significant pre-Abitibi population ranging in age from 2820 to 2780 Ma and an Abitibi-age population ranging from 2730 Ma to approximately 2670 Ma (*see* Figures 12A and 12B). Detrital zircons from a pebbly sandstone unit with the Three Nations formation in German Township about 25 km to the northeast indicate a considerably younger maximum depositional age of 2669±1 Ma. In addition, older detrital zircons ranging from 2700 to 2816 Ma are also present in this sample (Bleeker 1999).

Newly recognized portions of the Timiskaming assemblage consisting of conglomerate, sandstone, siltstone and heterolithic volcanic breccia have been identified along the PDDZ west of the Dome Mine (*see* Figure 2). A sample of heterolithic conglomerate from the Buffalo Ankerite Mine in Deloro Township yielded ages of ca. 2682±4 Ma and 2669±7 Ma and a fine-grained epiclastic unit at the Nabob Mine in Ogden Township yielded ages ranging from ca. 2673 Ma to 2722 Ma (Ayer, Barr et al. 2003). Further to the west in Thorneloe Township, the youngest detrital zircon age of 2684.4±1.7 Ma from a new geochronology sample of conglomerate closely associated with the PDDZ, in addition to older detrital zircons with ages of 2705 Ma, 2713 to 2716 Ma, 2726 to 2728 Ma (#9: Table 1, Figure 4C), suggest this unit may also be part of the Timiskaming assemblage, although the age of the youngest detrital zircon also allows for the possibility that it may alternatively be part of the Porcupine assemblage.

East of Matheson Area

Timiskaming assemblage clastic sedimentary rocks composed of conglomerate, wacke-sandstone, siltstone, argillite and schist are closely associated with the PDDZ from the Quebec border to Hislop Township. These rocks were originally lumped together with structurally interleaved older volcanic assemblages in a unit identified as the Destor–Porcupine Complex by Jensen and Langford (1985). Berger (2002) reported banded magnetite-hematite iron formation is complexly interbedded and structurally interleaved with clastic sedimentary rocks in Michaud Township, and sedimentary and alkalic volcanic rocks correlative with the Timiskaming assemblage underlie the southeast part of Hislop Township, south of the PDDZ, and display a close spatial relationship with the Hislop and Ross faults. Ropchan et al. (2002) reported TIMS geochronology results from Timiskaming assemblage units in Holloway Township. The youngest concordant detrital zircons from sandstone interbedded with conglomerate yielded an age of 2684±1.3 Ma, a second discordant zircon (1.8%) yielded an age of 2676.5±1.6 Ma, in addition to older detrital zircons with ages ranging from 2695 to 2724 Ma. The youngest detrital zircon from a heterolithic volcanic breccia closely associated with the Lighting Zone mineralization at the Holloway Mine (sample 3D-CG, #37: Figures 2 and 10A) yielded an age of 2686.6±1.8 Ma with older zircons ranging from 2695 to 2717 Ma. SHRIMP analysis of this sample has yielded less precise zircon ages ranging from 2682 to 2796 Ma (Figure 16).

The volcanic breccia sample from the Holloway Mine is texturally and compositionally similar to a Timiskaming assemblage volcanic breccia unit in Swayze Township in the Swayze belt, which yielded a variety of zircon ages based on TIMS analysis, the youngest being about 2669 Ma (Ayer, Ketchum and Trowell 2002). Zircons from this sample (99JAA-0057) were analyzed by SHRIMP and define a full range of morphological types, ranging from elongate and sharply prismatic to short, stubby, subrounded or even very well-rounded grains. The most reliable younger ages from this sample come from analyses of distinct overgrowths or thin embayments, constraining deposition generally at, or younger than, 2672 to 2683 Ma (Figure 17). Concordant or nearly concordant spot analyses from interior igneous domains mostly define a narrow age spectrum between ca. 2695 and 2705 Ma, with a peak age mode near 2700 Ma (*see* Figure 10B; Appendix 2). Older ages occur near 2730 Ma, 2740 Ma and 2765 Ma and support the earlier observations that the inherited components in this fragmental volcanic were derived from underlying lithologies within the Pacaud, Deloro, Tisdale and Blake River assemblages (Ayer, Ketchum and Trowell 2002).

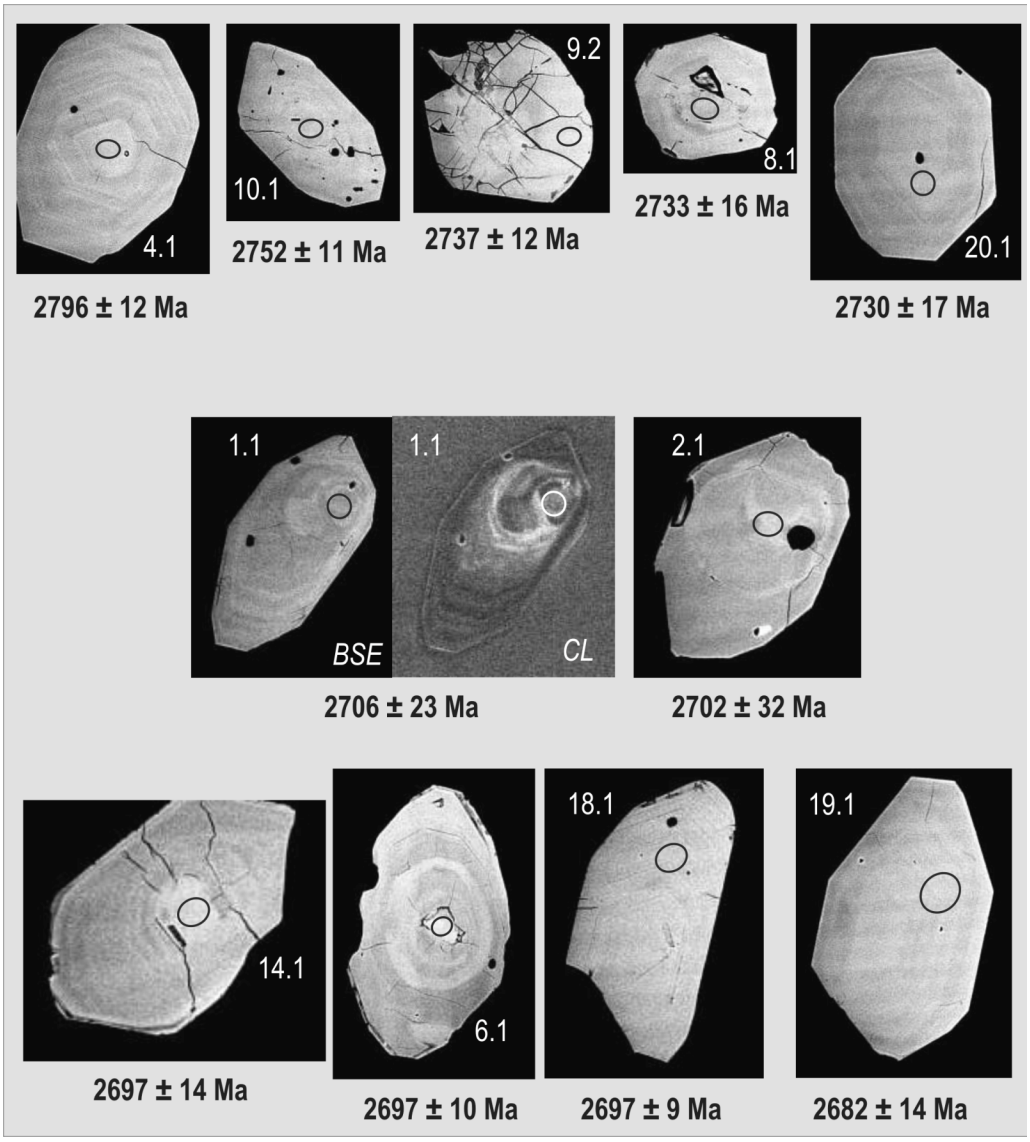

Figure 16. Backscattered electron (BSE) and cathodoluminescence (CL) images of the cores of inherited zircon and a zircon overgrowth from Timiskaming assemblage volcanic sample 3D-CG. The spot locations, numbers and ages correspond with the SHRIMP II analyses in Appendix 2 (Table A2).

Kirkland Lake–Larder Lake Area

Hyde (1980) subdivided sedimentary components of the Timiskaming Group in the Kirkland Lake–Larder Lake area into an early non-marine association dominated by conglomerates and sandstone of braided river origin. These are intimately intercalated with alkalic volcanic rocks consisting of pyroclastic and massive trachytic flows. He also interpreted a later re-sedimented association consisting of turbidites, turbiditic conglomerates and oxide-iron formation representing submarine fan deposits. However, the timing of the re-sedimented association is controversial as Jensen and Langford (1985), Corfu, Jackson and Sutcliffe (1991), and Mueller, Donaldson and Doucet (1994) all interpreted the turbidite sequences as part of an older sedimentary association, analogous to the relationship between the Porcupine and Timiskaming assemblages in the Timmins area. Jackson, Fyon and Corfu (1994) interpreted these turbiditic units as structurally overlying the Timiskaming assemblage and identified them as the part of the Hearst assemblage.

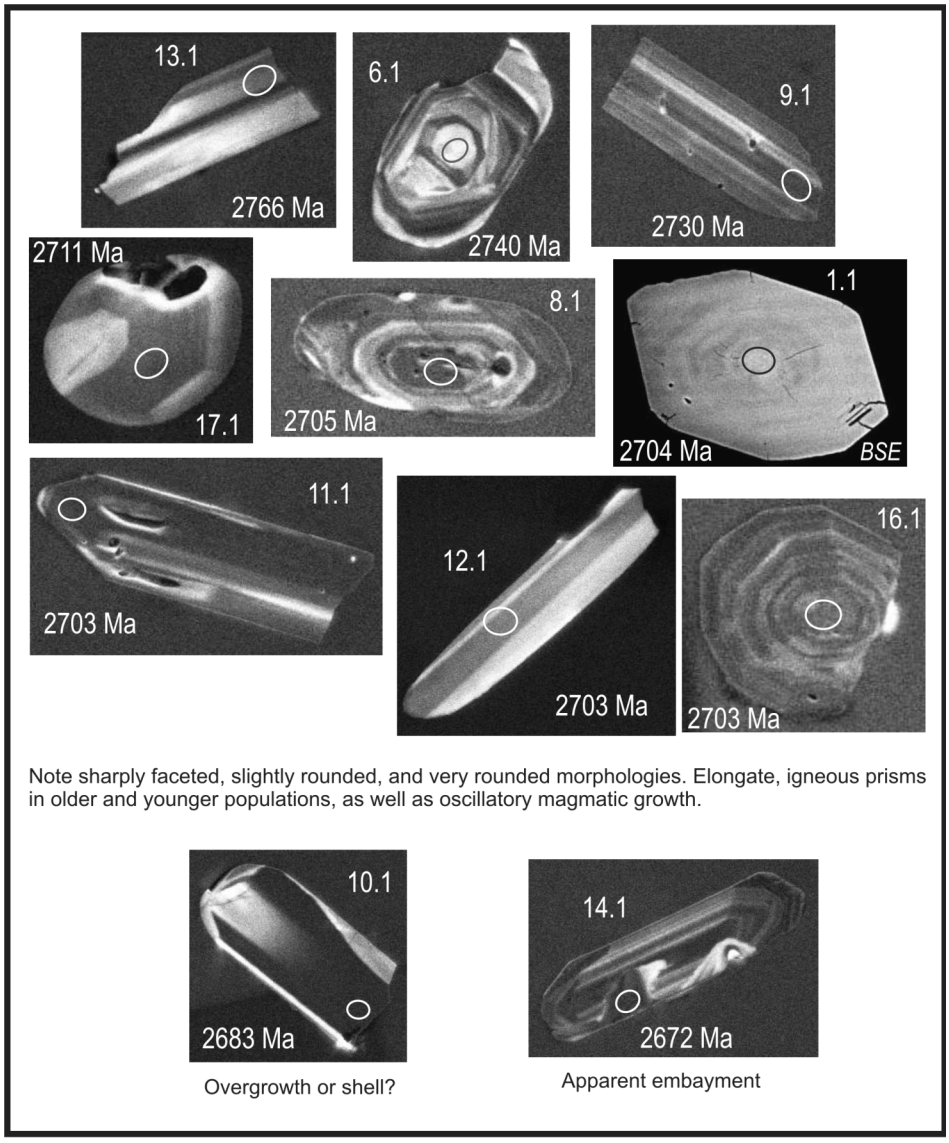

Figure 17. Backscattered electron images of the cores of inherited zircon and a zircon overgrowth from Timiskaming assemblage volcanic sample 99JAA-0057. The spot locations, numbers and ages correspond with the SHRIMP II analyses in Appendix 2 (Table A2).

Corfu, Jackson and Sutcliffe (1991) sampled a number of the non-marine association facies sedimentary rocks in the Kirkland Lake and Larder Lake areas and determined their maximum age of deposition to be about 2679 Ma. More recent geochronology from a turbidite sample interbedded with heterolithic conglomerate beds and minor oxide-iron formation from McVittie Township, east of the town of Larder Lake, yielded detrital zircon ages of 2674.3±3.7 Ma and 2684.9±1.9 Ma (Ayer, Ketchum and Trowell 2002) indicating that at least this part of the re-sedimented association belongs to the Timiskaming assemblage as was originally interpreted by Hyde (1980). New geochronology of a wacke sample from Gauthier Township yielded detrital zircons ranging from the youngest at 2677.7±3.1 Ma, to 2682 Ma and 2770 Ma (#32: Table 1, Figure 7D)and a sample of trachyte flow from this area yielded an even younger zircon age of 2669.6±1.4 Ma with inheritance zircons having ages of 2676.6±4.3 Ma and 2694.2±2.8 Ma (#31: Table 1, Figure 7C). These ages indicate that the upper part of the Timiskaming assemblage in this area is as young as 2670 Ma, similar to the age of the Three Nations formation east of Timmins (see above).

Matachewan Area

A unit of conglomerate and cross-bedded sandstone, locally associated with turbiditic sedimentary rocks, extends west from Cairo Township to south of Hutt Township (*see* Figure 2). A number of geochronology samples were analyzed from this unit in order to determine its age and provenance (Ayer, Ketchum and Trowell 2002). The youngest detrital zircon from a sandstone in Powell Township has an age of 2685.8±1.5 Ma, as well as older detrital zircons with ages of 2692.3±2.7 Ma, 2695.2±2.4 Ma and 2757±12 Ma. A second sample was collected from fine-grained wacke interbedded with conglomerate south of Montrose Township. The youngest zircon indicates a maximum deposition age of 2688.5±1.0 Ma, whereas a number of older detrital zircons range from 2690 to 2723 Ma. The youngest detrital zircons, from sandstone interbedded with conglomerate south of Hutt Township, indicate a maximum depositional age of 2690±3.0 Ma also with detrital zircons with ages of 2706 and 2715 Ma (Ayer, Amelin et al. 2002). The above U/Pb zircon data indicate that these sedimentary units were deposited sometime after 2685.8±1.5 Ma and that only Abitibi-age zircons have been detected to date. Thus, they could belong to either the Porcupine or the Timiskaming assemblages given the time limits established for these assemblages as discussed above. However, because of the facies association of localized fluvial conglomerates and cross-bedded sandstones and the strong spatial association with the Larder Lake–Cadillac deformation zone (LLCDZ), the unit is still considered to be part of the Timiskaming assemblage.

In contrast with the Porcupine, the Timiskaming assemblage samples (see below) commonly contain detrital zircons with pre-Abitibi ages (i.e., 2860–2790 Ma). These ages indicate a more widespread provenance that included source terrains older than the Abitibi. These sources could have included detritus from the Opatica Subprovince to the north, or unknown older terrains to the south or east which would have been subsequently removed by collision with the Grenville Province during the Proterozoic. However, new evidence of pre-Abitibi U/Pb ages of zircon xenocrysts, and ancient crustally contaminated Nd and Hf isotopes (Ketchum et al., in press) in some volcanic and plutonic samples only found to date in the westernmost part of the SAGB, suggests that pre-Abitibi crust, similar in age to the lowermost part of the Wawa supracrustal sequences, may have underlain the AGB in a wedge extending up to 80 km east of the Kapuskasing Structural Zone (Ketchum et al., in press). This suggests the strong possibility that the Wawa Subprovince may have contributed at least some of this pre-Abitibi detritus to the Timiskaming.

Intrusion Framework

The plutonic rocks of the SAGB fall into three broad groups or subdivisions: synvolcanic, syntectonic and posttectonic intrusions (Chown et al. 1992; Chown, Harrap and Moukhsil 2002; Sutcliffe et al. 1993; Heather 1998). Detailed geochronological studies of a number of the intrusive complexes indicate that they formed over about 90 million years by multiple intrusive events (Frarey and Krogh 1986; Mortensen 1993a, 1993b; Heather 1998; Davis et al. 2000; Ketchum et al., in press). These subdivisions are being applied to the major batholithic complexes for the first time in the study area. They are used in a broad-scale categorization to attempt to correlate with the much more extensive database on supracrustal rocks with synvolcanic intrusion interpreted to be pre-D1, the syntectonic intrusion interpreted to be coeval with the Porcupine and Timiskaming assemblages and the posttectonic intrusion interpreted to postdate the Timiskaming assemblage. In Figure 2, we have subdivided the intrusions into 4 broad categories: 1) mafic to ultramafic synvolcanic intrusions, 2) felsic to intermediate synvolcanic intrusions, 3) syntectonic intrusions, and (4) late-tectonic intrusions.

INTERMEDIATE TO FELSIC SYNVOLCANIC INTRUSIONS

Intermediate to felsic synvolcanic intrusions range in age from about 2745 to 2696 Ma. They are termed synvolcanic because they are coeval with the volcanic assemblages (i.e., Pacaud to Blake River). In addition, this intrusive group also predates significant compressional strain in the southern Abitibi Subprovince and they are geochemically similar to the calc-alkaline members of the coeval volcanic assemblages. The synvolcanic intrusions are typically foliated and are tonalitic to granodioritic in composition. They are found predominantly within the larger granitic complexes such as the Ramsey–Algoma, Kenogamissi and Round Lake batholiths (*see* Figure 1), often as sheets or laccoliths (Heather 2001). In the synvolcanic complex in the Rice Lake area on the southwestern margin of the Kenogamissi batholith, strongly foliated tonalite occurs around the margins and surrounding a supracrustal enclave in the central part of the batholith. The tonalite has crystallization ages of 2747 to 2742 Ma and contains inherited zircons dated at ca. 2.85 Ga (Becker and Benn 2003; Ketchum et al., in press). Here, the tonalite is intruded by weakly foliated granodiorite with an age of 2700 Ma, but also containing 2.85 Ga xenocrysts. Foliated synvolcanic tonalite and granodiorite with ages of 2713+2/–3 Ma and 2696±3 Ma, respectively (Heather 2001), occur in the central part of the Kenogamissi batholith and extend into the southwestern part of the study area (*see* Figure 2). The oldest units within the Round Lake batholith are gneissic to foliated tonalite with recently determined ages of 2743.6±0.9 Ma and 2713.2±1.2 Ma (Ketchum et al., in press). These tonalitic phases of the Round Lake batholith are cut by discrete granodiorite plutons, with ages of 2697 Ma and locally with 2715 Ma zircon xenocrysts, in the northern, western and eastern part of the batholith (Chown, Harrap and Moukhsil 2002). Synvolcanic intrusions within greenstones within the study area include a 2699±2.9 Ma quartz diorite on the southwestern margin of the Watabeag batholith (Frarey and Krogh 1986) and 2695±1.5 Ma tonalite intruding the Kamiskotia gabbroic complex, in which 2.93 Ga zircon xenocrysts were also found (Barrie and Davis 1990).

MAFIC TO ULTRAMAFIC SYNVOLCANIC INTRUSIONS

Mafic to ultramafic synvolcanic intrusions range from approximately 2740 to 2700 Ma in the SAGB (Corfu 1993; Heather 1998; Mortensen 1993a, 1993b). They mainly occur as sills or lenticular units that cut stratigraphy at a low angle. They are compositionally fractionated, ranging from peridotite to gabbro and diorite, commonly with igneous layering and magma-mixing textures and vary from massive to

strongly foliated. As these intrusions do not typically contain abundant zircons, the ages of oldest members of this suite are indirectly inferred to be similar in age to the 2740±2 Ma trondhjemite closely associated with dioritic phases of the Chester granitoid complex, and an age of 2731±3 Ma for a feeder dike cutting diorite and gabbro of the Rush River complex. Both of these complexes occur in the Swayze belt on the margins of the Ramsey–Algoma and Kenogamissi batholiths, respectively (Heather 2001), and are interpreted to be coeval with the Pacaud assemblage.

Within the study area, the oldest dated mafic to ultramafic synvolcanic intrusion is the Ghost Mountain sill. The intrusion is layered with a peridotitic base grading into a gabbroic top (Jensen and Langford 1985). New analyses of additional zircons from a gabbro sample within the intrusion (*see* Corfu 1993) now yield a more precise age of 2712.4±1.1 (#38: Table 1, Figure 8C). This new age indicates the sill is coeval with upper Kidd–Munro volcanism and this is also supported by an age of 2716.3±1.5 Ma (Ropchan et al. 2002) from calc-alkaline volcanic rocks immediately to the south, indicating the sill was intruded into the lower Kidd–Munro assemblage (*see* Figure 2).

All remaining dated synvolcanic intrusions within the study area are coeval with the Tisdale assemblage and include an age of 2707+3/–2 Ma for the Dundonald sill intruding the Kidd–Munro assemblage in Dundonald Township (Barrie and Corfu 1999); an age of 2704±4.9 Ma (Barrie and Corfu 1999; Barrie 1999) for the Mann ultramafic to mafic complex intruding the contact between the Stoughton–Roquemaure and the Tisdale assemblages in Little Township; an age of 2705±10 Ma for diorite intruding the lower Tisdale assemblage in Macklem Township (Corfu et al. 1989); and 2707+3/–2 Ma for an ultramafic intrusion intruding the Deloro assemblage in Deloro Township (Corfu and Noble 1992). A new age of 2706.8±1.2 Ma from gabbro near the top of the Centre Hill complex in Munro Township (#39: Table 1, Figure 8D) confirms that this mafic to ultramafic intrusion, which intrudes the upper Kidd–Munro assemblage, is about 10 my younger that the assemblage and was not the heat source for the stratigraphically overlying Potter Mine VMS mineralization (*see* "Munro Township"). The Centre Hill intrusion age is within error of the 2704.9±1.9 Ma age for the Warden–Munro Complex in northeastern Munro Township (Barrie 1999), thus indicating that they are both members of an extensive sill-like intrusive complex synclinally closing to the east in McCool Township (*see* Figure 2).

A new age of 2704.8±1.4 Ma from granophyric gabbro in the uppermost part of the Kamiskotia gabbroic complex intrusion in Robb Township (#3: Table 1, Figure 3C) correlates well with the 2707±2 Ma age for a pegmatitic gabbro from the lower middle zone of the complex in Turnbull Township (Barrie and Davis 1990). Both of these ages confirm this mafic intrusion is coeval with the upper Tisdale assemblage. However, the Kamiskotia gabbroic complex is interpreted to underlie the Blake River assemblage (*see* Figure 2), which is younger than the complex and, thus, the contact may be either unconformable and/or structurally modified.

On the eastern edge of the Kenogamissi batholith, the Pacaud and Deloro assemblages are intruded by the Muskasenda gabbro, which extends roughly conformable with the north-trending stratigraphy over a strike length of about 15 km in Bartlett, English and Beemer townships (Pyke 1978) (*see* Figure 2). The gabbro has not been directly dated, but numerous east-trending dikes emanate from the gabbro, cutting the overlying 2727 Ma Deloro assemblage and most likely represent feeder dikes for the overlying Tisdale assemblage mafic volcanic rocks to the east. These field relations of the Muskasenda gabbro and a new U/Pb zircon age of 2705.7+4.4/–3.8 Ma on an east-trending quartz gabbro dike emanating from the gabbro in Bartlett Township (#28: Table 1, Figure 7A) demonstrate that Tisdale assemblage age magmatism occurred in Deloro assemblage units. This is analogous to the relationship between the ~2.9 Ga Balmer assemblage and the stratigraphically overlying ~2.8 Ga Narrow Lake assemblage in the Confederation Lake area (Rogers et al. 2000). These field relationships and the U/Pb age demonstrate the autochthonous nature of the stratigraphically lower portion of the western Abitibi greenstone belt.

The youngest dated synvolcanic mafic to ultramafic intrusion in the SAGB in Ontario is the Montcalm gabbroic complex occurring west of the study area. This peridotitic to gabbroic intrusion hosts the Montcalm Ni-Cu deposit. A gabbro from this complex has an age of 2702±2 Ma and is cut by a granodiorite dike with an age of 2700+5/–4 Ma (Barrie and Davis 1990). These ages suggest the Montcalm gabbroic complex is coeval with Blake River assemblage volcanism in the Kamiskotia area.

SYNTECTONIC INTRUSIONS

Syntectonic plutons are coeval with some of the major deformation episodes in the Abitibi and, later in this report (*see* "Structural Framework"), we relate them to the various deformational events. This group ranges in age from about 2695 to 2670 Ma and occurs throughout the Abitibi greenstone belt (Chown et al. 1992; Corfu 1993; Mortensen 1993a, 1993b; Heather 1998; Davis et al. 2000). Early syntectonic intrusions range from about 2695 to 2685 Ma and consist predominantly of tonalite, granodiorite, diorite and feldspar±quartz porphyries, which are geochemically similar to the coeval Porcupine assemblage volcanic rocks and have adakitic geochemical affinity (*see* "Intrusion Subproject"). These intrusions range from foliated to massive and occur both as stocks within the greenstone belt and as major portions of the surrounding batholithic complexes such as the Lake Abitibi, Nat River and the northern part of the Kenogamissi batholiths. A new age of 2686.9±1.2 Ma from monzonite in the Clifford stock and 2688.5±2.3 Ma for an adjacent feldspar porphyritic dike (#34 and # 33: Table 1, Figures 7F and 7E, respectively), are coeval with an age of 2689±1 Ma for quartz diorite from the Claris Lake stock in Pontiac Township (Corfu and Noble 1992) and 2686.4±2.8 Ma for granodiorite in the Adams stock (Frarey and Krogh 1986).

Numerous porphyries have been dated in the Timmins region with most ages ranging from 2691 to 2687 Ma (Corfu et al. 1989; Ayer, Barr et al. 2003). New geochronology on porphyries as a part of this study include 2689.0±1.4 Ma from the Mount Logano porphyry in northeastern Shaw Township and 2686.2±1.1 Ma from a porphyry dike cutting Tisdale assemblage volcanic rocks in Adams Township (#23 and # 27: Table 1, Figures 6C and 6F), the latter age correlates well with an age of 2686.4±2.8 Ma in the adjacent Adams stock (Frarey and Krogh 1986). A number of porphyry ages now provide better constraints on the timing of deformation in the Timmins area (Bateman et al. 2005). These include an age of 2689.3±4.5 Ma for a syntectonic granodiorite dike folded in D2 within the PDDZ immediately north of the Kenogamissi batholith (Hall and Smith 2002); an age of 2687.2±2.2 Ma for a strongly foliated, quartz-phyric sill interpreted to pre- to syn-D2 and 2684.4±1.9 Ma from a crosscutting quartz feldspar porphyry intrusion, both of which occur at the Hoyle Pond Mine (Dinel and Fowler 2004) (#16 and #17: Table 1, Figures 5B and 5C); and an age of 2677.5±2.0 Ma from a porphyry intrusion in the vicinity of the Pamour Mine interpreted to be post-D3 (Bateman et al. 2005) (#19: Table 1, Figure 5E).

Late syntectonic intrusions range in age from about 2680 to 2672 Ma (Corfu 1993; Wilkinson, Cruden and Krogh 1999; Ropchan et al. 2002) and, thus, are broadly coeval with the Timiskaming assemblage. These intrusions are relatively small and occur in close proximity to the PDDZ and LLCDZ. Compositions are typically alkalic, consisting of monzonite, syenite and albitite with the more mafic phases consisting of diorite, gabbro, clinopyroxenite, hornblendite and lamprophyre. A previously unreported sample was selected from strongly foliated syenite within the LLCDZ at the southern margin of the Cairo stock in Cairo Township prior to this project (*see* Figure 2). The sample was selected in order to test the age of the intrusion and to provide a maximum age for development of the LLCDZ at this locality. The youngest zircons in the sample yield a crystallization age of 2676±1.4 Ma, but older inherited zircons with ages of 2689 and 2720 Ma are also present (J.A. Ayer, OGS, unpublished data, 2005). A new sample of feldspar-phyric syenite cut by the main ore-controlling structure of the Kirkland Lake fault (the Main Break), was collected from the Discovery Outcrop in Kirkland Lake (*see* "Kirkland Lake–Larder Lake Subproject"). This syenite porphyry is the youngest and volumetrically most abundant

phase of the composite intrusion that hosts the bulk of gold mineralization of the Kirkland Lake ore deposit. It was selected to provide a maximum age for development of the fault and the associated gold mineralization. Unfortunately, the only zircons found for TIMS analysis are considered to be xenocrysts ranging in age from ca. 2690 to 2701 Ma (sample 03JAA-0006, #30: Table 1, Figure 7B). SHRIMP analysis of this sample suggests the presence of younger, but considerably less precise zircon ages to about 2685 Ma and possible even younger grains to 2645 Ma which could be metamorphic or hydrothermal (Figure 18).

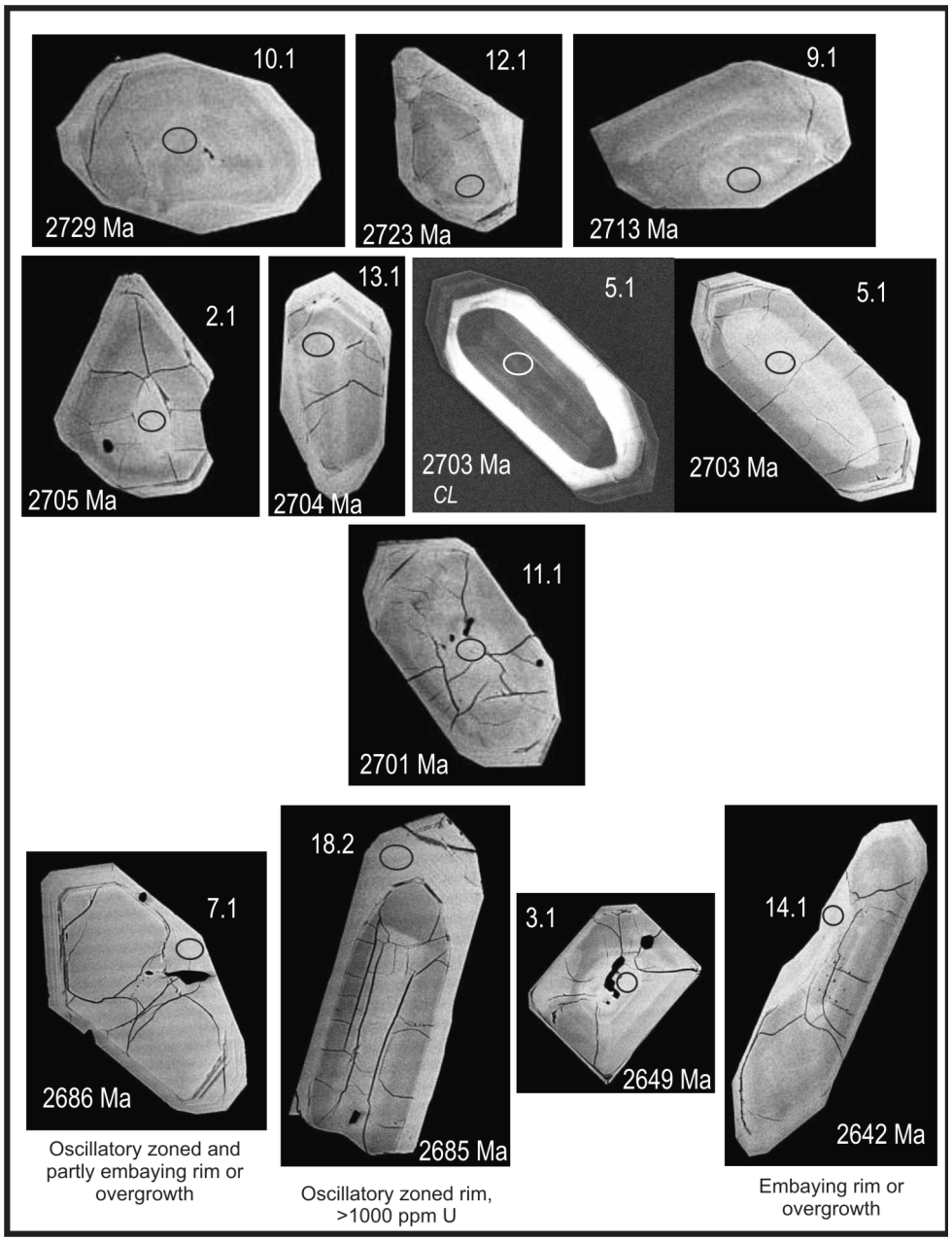

Figure 18. Backscattered electron and cathodoluminescence (CL) images of zircons from syenite porphyry sample 03JAA-0006. The spot locations, numbers and ages correspond with the SHRIMP II analyses in Appendix 2 (Table A2).

Albitite dikes are crosscut by gold-bearing veins in the Hollinger–McIntyre Mine (Burrows et al. 1993) and give a maximum age for the bulk of vein quartz gold mineralization. An albitite dike, which postdates the Cu-Au-Ag-Mo porphyry-style ore body hosted by the Pearl Lake porphyry at depth in the McIntyre Mine, provided an age of 2673+6/–4 Ma (Corfu et al. 1989). In order to further refine the timing of gold mineralization in Timmins, additional zircons were collected from this sample and now have provided a more precise age of 2672.8±1.1 Ma (#13: Table 1, Figure 4E). This age is within error of the 2671.5±1.9 Ma age for an inter-mineral lamprophyre dike cutting early replacement-style gold mineralization (Lightning zone) at the Holloway Mine and demonstrates that there is more than one age for Abitibi orogenic gold deposits (Ropchan et al. 2002). Albitite dikes were also observed to intrude sedimentary rocks and ultramafic volcanic rocks near the Destor–Porcupine deformation zone in Whitney Township (E. Barr, Placer Dome (CLA) Ltd., Porcupine Joint Venture, personal communication, 2004). An 8 m wide albitite dike cutting ultramafic volcanic rocks in this area yielded an age of 2676.5±1.6 Ma (#20: Table 1, Figure 5F). This age is within error of the Pamour porphyry age of 2677±2.0 Ma, but is slightly older than the McIntyre albitite dike.

LATE TECTONIC INTRUSIONS

Late-tectonic intrusions range in age from about 2670 to 2660 Ma and occur throughout the SAGB (Heather, 1998; Davis et al. 2000). They are typically massive and occur within batholiths and the greenstones. They consist of "Algoman" biotite granite, pegmatite and biotite-muscovite S-type granite. The only geochronology from this type of intrusion within the study area is an age of 2663.3±3.3. Ma from "porphyritic granitoid" of the Prosser stock in southwestern Prosser Township (Bleeker, Parrish and Sager-Kinsman 1999). An age of 2662±4 Ma from a massive biotite granite in Desrosiers Township (Heather 2001) occurs within the Algoman Somme pluton within the Kenogamissi batholith and extends into the southwestern corner of the study area (*see* Figure 2). On the Quebec side of the Abitibi, the latest Archean intrusions are the flat-lying, garnet-bearing, Pressiac and Lamotte monzonite intrusions which have been dated at 2660 Ma (Chown, Harrap and Moukhsil 2002).

Structural Framework

GEOPHYSICAL INTERPRETATIONS OF GREENSTONE BELT ARCHITECTURE AT DEPTH

Reflection Seismic Interpretation

Pre-existing and new Discover Abitibi geophysical data have improved our understanding of lithological and structural features at depth. The new Discover Abitibi reflection survey is the first seismic survey in the Abitibi where the acquisition parameters were designed to allow imaging of near-surface, economically important structures and stratigraphy. The Discover Abitibi reflection seismic profiles thus provide direct insight into the architecture of the greenstone belt, particularly in the Timmins region (Reed, Snyder and Salisbury 2005). The base of the greenstone belt is imaged at about 8 km depth in the northern part of the North Timmins–Crawchest seismic line (Reed, Snyder and Salisbury 2005). Major lithologic contacts such as the Tisdale – Kidd–Munro assemblages contact in central Tully Township and unconformable contacts such as the Kidd–Munro – Porcupine assemblages contact in Kidd Township are imaged. Splayed reflectors suggest the presence of numerous thrust duplex structures. Major faults such as the North Branch of the Porcupine–Destor deformation zone are also imaged. Both the South Timmins

and the North Timmins–Crawchest regional lines cross the Porcupine assemblage. On both profiles, several prominent reflective bands define an antiformal structure 3 to 6 km beneath the Porcupine assemblage. These features may represent the base of the Porcupine assemblage metasediments underlain by, and folded with mafic volcanic rocks of the Tisdale assemblage during regional shortening.

South of Timmins, the South Timmins regional line images the Adams stock as a shallow, pancake-shaped body. To the east, the South Porcupine regional line crosses the Shaw Dome. This profile displays a prominent band of reflections at 1 to 5 km depth within the Deloro assemblage in core of the Shaw structure. The dip of these reflectors change from shallowly northward to shallowly southward at an apex in the central part of Shaw Township and, thus, correlate well with a "Dome" structure (Reed, Snyder and Salisbury 2005). This band of reflection is underlain by a less reflective zone to a depth of about 7 km that may coincide with homogeneous crust typical of a granitic pluton (i.e., similar to the area underlain by the Adams stock).

The PDDZ is imaged by the Kettle Lakes line in German and Macklem townships, and the Shillington line in Taylor and Currie townships. Reed, Snyder and Salisbury (2005) report that both profiles show south-dipping reflectors underlying the lower Tisdale assemblage with their northernmost extent marked by the surface trace of the PDDZ. A marked transition to north-dipping reflectors occurs north of the PDDZ near the surface and this transition zone dips moderately southward beneath the Tisdale assemblage on both lines. Seismic lines crossing the PDDZ further to the west are less informative about the possible dip of this structure which may reflect a steeper orientation and/or less distinctive impedance contrast across the PDDZ in the Timmins area.

Potential Field Inversions

Computer-based interpretations of the geophysical data including magnetic and gravity inversions have also been done for each of the detailed mapping areas as part of this project. This has better constrained the distribution of rock units and structures for the mapping-based subprojects and has helped to visualize the dip and/or plunge of lithological units, folds and faults at depth. An example of the utility of the inversions can be seen for the southern Currie Township area (*see* "Geophysics Subproject") where inversions of the magnetic data suggest a syncline in the highly magnetic lower Blake River volcanic rocks (*see* Figure 2) and an overall southerly dip to this part of the assemblage in the gravity inversions. In Tully Township, the area underlain by ultramafic volcanic rocks in the southern part of the Kidd–Munro assemblage is associated with magnetic highs and gravity lows. This may be of economic significance as this might reflect extensive serpentinization related to the Pipestone deformation zone. This area is known to host a number of gold deposits (Berger 2002). In addition, Thompson (2005) identified this area as one which has a favourable metamorphic signature for hosting gold deposits. The inversions also indicate the ultramafic rocks are synformally folded with an overall dip to the north, a feature also suggested by north-dipping seismic reflectors on the South Timmins seismic profile in this general area.

Inversions in the Tisdale and Deloro township areas of the Timmins camp identify the PDDZ as a steeply north-dipping structure (Reed 2005a) in an area where the seismic profiles do not provide much information on the inclination of this structure. In addition, the magnetic inversion in the Teck Township area indicates a steep northerly dip to the LLCDZ.

Worming Geophysical Data Treatment and Display Technique

"Worming", which tracks the displacement of edge features in potential field data (gravity or magnetic data) by use of upward continuation, is a relatively new interpretive tool that was applied experimentally in the study area. The technique highlights contacts between units with contrasting physical properties and can give an indication of dip. Figure 19 (back pocket) combines computer-generated gravity worms (provided by P. Keating, Geological Survey of Canada) with the assemblage and structural map in an attempt to visualize the nature of contacts between regional-scale units of contrasting density at depth. In this figure, the grey-scale shaded image in the background is of the Bouguer gravity and dipping contacts are shown by gravity worms as progressive colour changes from dark blue (near surface) to red (deep). As one might expect given their differences in density, gravity contrast anomalies commonly conform to the surface contacts of many of the larger felsic intrusions within the supracrustal rocks. In many of these intrusions, the worms suggest the surrounding greenstones dip beneath the plutons, a phenomenon which is also evident on some of the Discover Abitibi reflection seismic profiles south of Timmins. In other cases, the worms only partially conform to the surface contacts, suggesting these intrusions may be larger at depth, or plunge in the direction of the offsets (*see* discussion of Clifford stock in "Geophysics Subproject").

The regional deformation zones are also commonly coincident with pronounced gravity worms. For example, both the Pipestone and north branch Porcupine–Destor deformation zones have worms which indicate moderate dips towards each other at depth (*see* Figure 19), thus suggesting a graben-like structure bounds the eastern part of the Kidd–Munro assemblage. Worms indicating a northerly dip also occur at the contact between the Porcupine and Kidd–Munro assemblages in Wark and Tully townships and likely represent the western extension of the Pipestone deformation zone. This feature is also confirmed by a seismic reflector dipping north beneath the Kidd–Munro assemblage from this general locality on the South Timmins regional seismic line. The PDDZ is associated with near-surface gravity worms which more or less conform to its surface location in Hislop Township, but which become progressively deflected to the southwest by up to 5 km in Macklem Township. On the other hand, near-surface gravity worms more or less conform to the LLCDZ west of Kirkland Lake, are progressively deflected to the northeast, following the trace of the Kirkland Lake fault and change to an easterly trend following the contact between the upper Tisdale and the lower Blake River assemblages in Gauthier Township (*see* Figure 2). It is possible these gravity worms are related to splays of the main gold-bearing deformation zones.

REGIONAL STRATIGRAPHIC AND STRUCTURAL INTERPRETATION

At a regional scale, supracrustal units in the SAGB are dominated by east-west striking volcanic and sedimentary assemblages (*see* Figure 1). The structural grain is also dominated by east-trending Archean deformation zones and folds (*see* Figure 2). The regional deformation zones commonly occur at assemblage boundaries and are spatially closely associated with long linear belts representing the sedimentary assemblages (i.e., Porcupine and Timiskaming). Ayer, Amelin et al. (2002) hypothesized that the regional association of the PDDZ and LLCDZ and major assemblage boundaries, in conjunction with the regional distribution of stratigraphic gaps between certain assemblages, indicates that the current locations of these regional deformation zone are proximal to the locus of early synvolcanic extensional faults dating as far back as the time of deposition of the upper part of the Deloro assemblage (i.e., 2724 Ma).

The larger batholithic complexes which are external to the supracrustal rocks such as the Kenogamissi and Round Lake batholiths contain the older members of the felsic to intermediate synvolcanic intrusion group (ca. 2745–2710 Ma). These batholiths have exerted control on the preservation of early stratigraphy as the volcanic assemblages uniformly wrap around and young away from their margins (*see* Figures 1 and 2). Thus, at the scale of the greenstone belt, the batholiths represent centres of structural domes and the intervening areas define belt-scale synclinoria such as the Blake River synclinorium.

The notion of a belt-scale synclinorium cored by the Blake River assemblage has a long history going back at least to the work of Jensen and Langford (1985). Benn and Peschler (2005) have recently proposed a detachment fold model for the development of the synclinorium during a single, belt-wide folding event that deformed the whole region. The model is based upon structural analysis and general interpretation of the previous generation of reflection seismic surveys. In our work, we are able to postulate a more detailed version of the belt-scale folding showing deformation was protracted and occurred in a number of distinct intervals based on geochronologic, stratigraphic, potential field geophysical data and high-resolution reflection seismic surveys.

This pattern is interrupted by the trends of Porcupine and Timiskaming assemblage rocks which unconformably overlie the older assemblages. These large-scale folds are visible in the reflection seismic profiles beneath the Porcupine assemblage on the Crawchest seismic line. Younger members of the felsic to intermediate synvolcanic intrusion group (2710–2696 Ma) appear to be relatively minor in extent and occur within both the supracrustal belt and the batholiths. The mafic to ultramafic synvolcanic intrusions have a pronounced affinity for the supracrustal belt indicating that they are most likely sills and/or upper crustal magma chambers coeval with volcanism.

The older group of the syntectonic intrusions (2695–2685 Ma) may be related to the compressive stresses that induced early folding and faulting related to the onset of continental collision between the Abitibi and older subprovinces to the north. These intrusions occur within the external batholiths, and as smaller batholiths, stocks and dikes internal to the supracrustal belt such as the Lake Abitibi and Watabeag batholiths, the Adams and Clifford stocks, and numerous porphyry intrusions and dikes. Regional deformation episodes have been identified based on overprinting relationships of folds and faults with D1 constrained by cessation of Blake River assemblage volcanism at 2696 Ma and onset of the deposition of the Porcupine assemblage at 2690 Ma. D1 folds are commonly refolded and transposed by later deformation and, therefore, it is often difficult to determine the original orientation of D1 structures. Within the study area, D1 folds do not appear to have any associated fabric and, thus, regional-scale folds of this generation have not been specifically identified. However, where F1 fold trends are discernible in other parts of the SAGB, they typically have a northerly orientation, such as the broad anticline cored by the Kenogamissi batholith (Ames et al. 1997) and northerly trending F1 folds with well-developed axial planar cleavages observed in outcrops in the Swayze belt (Heather 2001; Becker and Benn 2003).

Note, on Figure 2, specific fold generations have only been assigned in the Timmins and Kirkland-Larder Lakes areas, where the detailed structural studies associated with this project have been undertaken, and that the first (1^{st}), second (2^{nd}) and third (3^{rd}) generation folds correspond with D2, D3 and D4, respectively, in the Timmins area. Folds in the remaining parts of the study area have not been ascribed to specific generations because of a lack of detailed structural mapping. In the Timmins area, the base of the Porcupine assemblage is interpreted to be a low-angle unconformity that cuts progressively lower into the Tisdale assemblage stratigraphy eastward along the north limb of the Porcupine syncline (Bateman et al. 2005). This is likely the result of uplift and erosion and suggests the unconformity was caused by east-west oriented compression and/or extension related to D1 folding and the emplacement of syntectonic intrusions such as the broad northerly trending F1 antiform coring the Kenogamissi batholith (Ames et al. 1997).

In Timmins, the first generation of folding and faulting with an associated fabric is a series of stacked, south-over-north D2 thrust faults with hanging wall folds, located north of the PDDZ (Bateman et al. 2005). The D2 event is post-Porcupine assemblage in timing (i.e., <2685 Ma) as the assemblage is folded and faulted by D2 deformation, but pre-Timiskaming (i.e., >2676 Ma), because the Timiskaming unconformity truncates the D2 folds and thrust faults. Early ductile deformation, which is interpreted to be synchronous with D2, is evident as C-S structures in the PDDZ indicating south-over-north thrusting along a south-dipping zone, which was probably the root zone to the stacked thrusts to the north (Bateman et al. 2005). A post-Porcupine age for early thrusting coincides with the age data from the Duparquet Basin associated with the PDDZ in Quebec (Mueller et al. 1996).

Younger syntectonic intrusions (2680–2670 Ma) are small stocks, dikes and sills that are coeval with the Timiskaming assemblage and are spatially associated with the PDDZ and LLCDZ. Broadly synchronous with this magmatic event, syntectonic opening of the Timiskaming half-graben in a dilatational jog, was followed by foliation and folding, only the late stages of which affected the sediments. S3 foliation is strongly developed in Tisdale, Porcupine and Timiskaming assemblage rocks proximal to the PDDZ in the Timmins area, and is axial planar to a series of *en échelon* folds with curved axial surfaces along the PDDZ. The F3 fold axes do not affect the trace of the PDDZ, and do not extend directly across it to its southern side. These facts are interpreted to indicate development of F3 during left-lateral strike-slip movement along the PDDZ (Bleeker 1995). The magnitude of this sinistral displacement appears to be about 13 km as indicated by the offset of both the Krist formation and the F2 Porcupine syncline in Tisdale Township, eastward into Whitney and Cody townships. Here, the Krist formation underlies the Porcupine assemblage sediments on the western limb of an F2 syncline within the Whitney formation (*see* Figure 2). Therefore, it is hypothesized that both the Krist and Beatty formations and the F2 Porcupine syncline have been offset across the PDDZ during D3. This D3 event in Timmins may be correlative with early folding observed in Timiskaming assemblage wackes in Gauthier Township where it has been designated as pre-D2 (*see* "Kirkland Lake–Larder Lake Subproject").

The late tectonic intrusions (2670–2660 Ma) are minor, high crustal level intrusions which occur both within the external batholiths and the supracrustal belt. Possibly synchronous with this magmatic event, D4 folding created a syncline within the Timiskaming assemblage rocks in the Timmins area. Here, S4 foliation crenulates S3 and is axial planar to F4 folds that commonly have Z asymmetry. Minor structures suggest right lateral strike-slip along the PDDZ. The last significant event, D5, consists of an intense constrictional strain seen in Tisdale assemblage pillows, clasts in Krist formation volcaniclastic rocks and cobbles in Timiskaming assemblage conglomerates. The D4–D5 event represents the final stage in transpressional deformation along the PDDZ. This structural event may be correlative with the D2 event identified in the Kirkland Lake–Larder Lake area in which S2 overprints Timiskaming assemblage volcanic rocks with an age of 2670 Ma and is most strongly developed in proximity to the LLCDZ. Kinematic indicators in Gauthier Township suggest a reverse-dextral sense of movement along the LLCDZ during D2.

Subproject Results

VMS MINERALIZATION SUBPROJECTS

Kamiskotia Area Subprojects

The main goal of this subproject (Hathway, Hudak and Hamilton 2005) has been to understand the stratigraphy, volcanic facies, alteration and structural style of the Archean Kamiskotia Volcanic Complex, the volcanic succession that hosts copper-zinc volcanogenic massive sulphide (VMS) mineralization in the Kamiskotia area (Abitibi greenstone belt, Timmins region). With this aim, the study area was mapped at regional scale (1:10 000 and 1:20 000 scale), with focussed deposit-scale work on the main past-producing VMS deposits. 156 samples were analyzed for major oxides and selected trace elements in order to characterize the volcanic rock units of the mapped area, and 7 new U/Pb zircon ages were acquired. A detailed subproject by Hocker focussed on the Genex deposit and is discussed below.

KIDD–MUNRO ASSEMBLAGE

New U/Pb ages of 2714.6±1.2 and 2712.3±2.8 Ma indicate that the northeast-facing succession in the northern part of the study area (Loveland, Macdiarmid and Thorburn townships) forms part of the Kidd–Munro assemblage (2719–2710 Ma: Ayer, Amelin et al. 2002). A west-northwest-trending faulted contact is inferred between this older succession and the Kamiskotia Volcanic Complex to the south (Figure 20).

The lower part of the Kidd–Munro assemblage, in south-central Loveland and northernmost Robb townships, consists of high-silica FIIIb rhyolites with consistent, relatively flat REE patterns with strong negative Eu anomalies. All outcrops appear to consist of quartz- and feldspar-phyric, typically flow-banded coherent rhyolite. Minor felsic volcaniclastic intervals within the rhyolite succession have been intersected by drilling. The rhyolites are overlain by a thick succession of massive to pillowed, sparsely plagioclase-phyric mafic volcanic rocks. Pillow facing directions are to the east-northeast or northeast. These rocks largely plot in the calc-alkaline basalt and andesite fields on the Jensen cation plot. Chondrite-normalized REE patterns for most samples are similar, and distinct from other groups, with a flat pattern in the middle and heavy REE, a moderately steep negative slope in the light REE, and a slight negative Eu anomaly. Lenses of re-deposited felsic volcaniclastic rocks occur within the mafic volcanic succession. In northwestern Macdiarmid Township, northeast Loveland Township, and on the southern boundary of Thorburn Township, the mafic lavas are overlain by a thicker felsic to intermediate volcaniclastic succession. Here, exposed rocks are largely massive, poorly sorted breccias and tuff breccias, although thick sections of tuffaceous sandstone and graphitic argillite are seen in drill core. Sharp-based graded beds at several locations indicate facing to the north-northeast.

KAMISKOTIA VOLCANIC COMPLEX

The Archean volcanic rocks in the southern part of the study area are assigned to the Kamiskotia Volcanic Complex (KVC: Figure 20). The known VMS deposits in the study area occur within a restricted, east-facing stratigraphic interval in the upper part of the KVC. New U/Pb ages for this interval, ranging from 2701.1±1.4 to 2698.6±1.3 Ma, and an age of 2703.1±1.2 Ma from the lower part of the KVC, indicate that the KVC may better be regarded as part of the Blake River assemblage (2701–2697 Ma: Ayer, Amelin et al. 2002), rather than the Tisdale assemblage (2710–2703 Ma). Facing directions through most of the

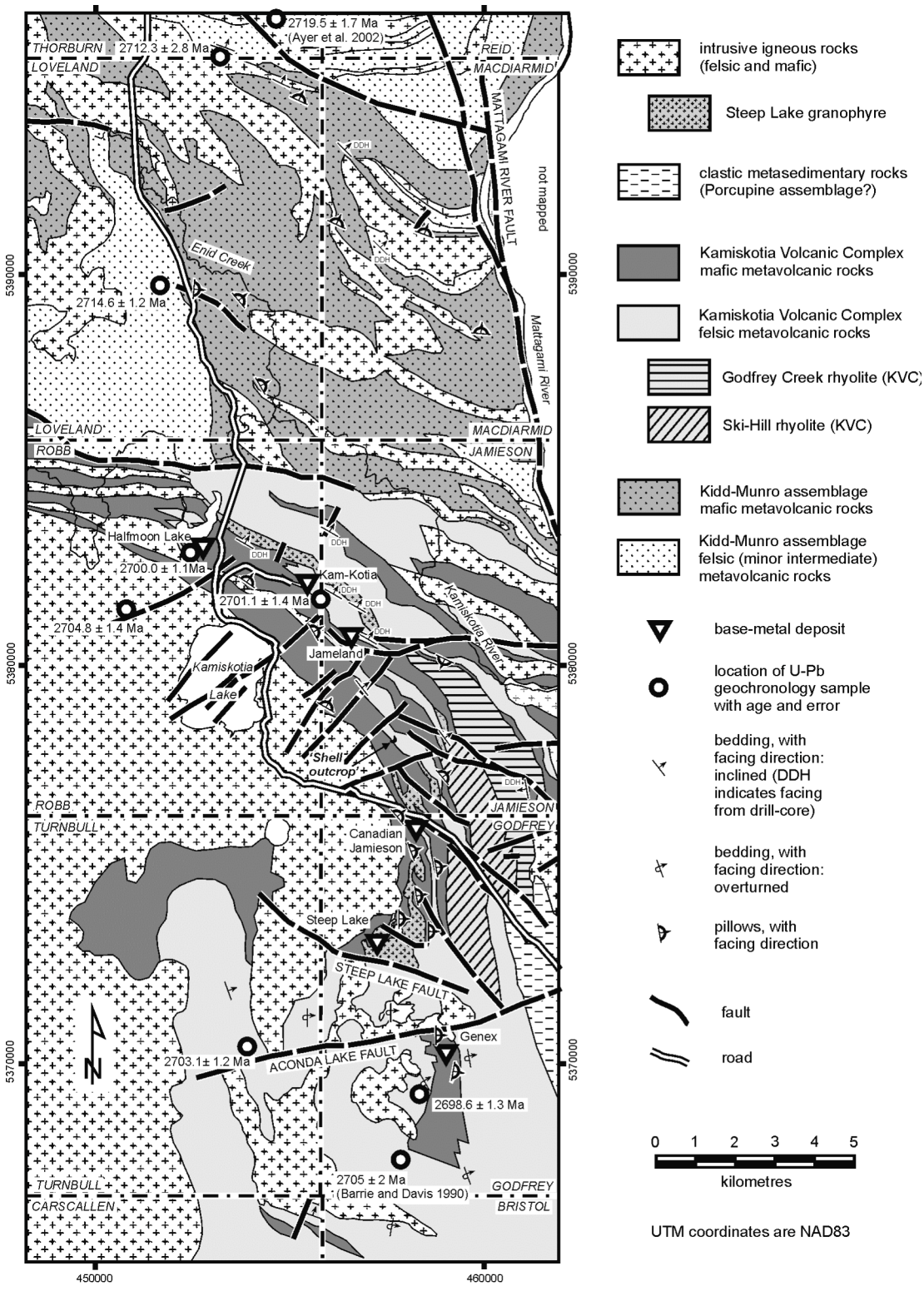

Figure 20. Geological sketch map of the Kamiskotia area, with locations of known VMS deposits and samples used for U/Pb geochronology (*from* Hathway, Hudak and Hamilton 2005, p.3). Age 2719.5±1.7 Ma (at very top of figure) is *from* Ayer, Amelin et al. (2002); 2705±2 Ma (near bottom of figure) is *from* Barrie and Davis (1990).

KVC are to the east or northeast, except in south-central Jamieson Township where southwest-facing indicators at outcrop (pillow packing) and in drill core (graded felsic tuff units) suggest the presence of a possible synclinal axis.

South of the Steep Lake fault (*see* Figure 20), the KVC consists largely of coherent rhyolite and associated rhyolitic breccia and lapilli tuff, with lenses of mafic lava in northeast Carscallen and northwest Bristol townships, and around and to the south of the Genex Mine. Farther north, the lower part of the KVC consists largely of pillowed and massive mafic lava, whereas the upper part is dominated by rhyolite (e.g., Ski-Hill and Godfrey Creek units: *see* Figure 20). A 150 to 200 m thick, northeast-facing interval of tuffaceous sandstone and conglomerate, with minor graphitic mudstone is present in a series of drill holes approximately 1 km northeast of the Kam-Kotia Mine. Similar sedimentary strata sectioned by several drill holes in southern Jamieson Township appear to lie broadly along strike from the sections northeast of Kam-Kotia and, if the westward facing reported from one Falconbridge core is discounted, could represent a southeastward extension of that interval. Similar clastic rocks also occur in the Genex Mine hanging wall (Hocker, Thurston and Gibson 2005a). As with re-deposited volcaniclastic facies throughout the KVC, these intervals all appear to have been deposited by sediment gravity flows, and there seems to be no evidence for deposition above storm wave base. The KVC sample set analyzed in the present study is strongly bimodal, with a compositional gap between 56 and 72 weight % SiO_2. Rhyolites in the lower part of the KVC and at the level of the VMS deposits include FII and low-Yb FIIIb types, with minor high-Yb FIIIb rocks, whereas rhyolites in the upper part of the KVC are uniformly of the high-Yb FIIIb type.

Hart (1984) divided the KVC mafic volcanic rocks in Godfrey, Jamieson and Robb townships into primitive and overlying, more evolved types. New geochemical data obtained in this study supports this division, which is clear on plots of TiO_2 against Zr and P_2O_5 (*see also* Hocker, Thurston and Gibson 2005a, p.18, Figure 6). The contact between the two types appears to coincide with the VMS-hosting interval at the Canadian Jamieson and Kam-Kotia mines. On the Jensen plot, both types fall in the tholeiitic basalt field, but lavas lying stratigraphically above the VMS deposits are more iron-rich than those below. Both types have relatively flat chondrite-normalized REE patterns, generally with slight to moderate negative Eu anomalies, but there is a consistent increase in total REE concentrations stratigraphically upward from the primitive into the more evolved lavas. The mafic lavas from Carscallen and Bristol townships fall in the alkali basalt field on the Nb/Y versus Zr/TiO_2 plot (*see also* Hathway et al. 2005, p.16, Figure 4). Their REE patterns are also unlike those seen in other groups, showing relatively steep, smoothly S-curved negative slopes in the middle and light REE, and no Eu anomaly. These rocks are geochemically distinct from the KVC tholeiitic basalts to the northeast. Given their stratigraphic position at or near the base of the KVC, it is possible that they may represent part of the Kidd–Munro assemblage, which is present farther to the southwest in Carscallen Township (Ayer, Amelin et al. 2002).

KAMISKOTIA GABBROIC COMPLEX

The Kamiskotia Gabbroic Complex (KGC) has generally been thought to be broadly coeval with the KVC, which it underlies and intrudes (e.g., Barrie 1992). Barrie (1992) divided the KGC into four zones, of which only the uppermost two are found in the present study area. Gabbro of the "Upper Zone" is exposed to the northeast and southwest of Kamiskotia Lake and in a small area to the northeast of Steep Lake. Remaining KGC rocks in the area are generally of felsic to intermediate composition and were included in the "granophyre zone", lying above and along strike with the Upper Zone, by Barrie (1992). A new age of 2704.8±1.4 Ma for a granophyric phase of the Upper Zone gabbro is younger than a previous age of 2707±2 Ma from the stratigraphically lower, Middle Zone gabbro in Turnbull Township (Barrie and Davis 1990). The new age is slightly older than (although within error of) the new age of 2703.1±1.2 Ma from the lower part of the KVC. However, it is significantly older than the 2700.0±1.1 Ma KVC rhyolite age

from Halfmoon Lake, only 2 km to the northeast, and it is possible that this part of the KGC may intrude an older succession (e.g., Kidd–Munro assemblage) with the KVC deposited on top of such a basement complex. Elsewhere, rocks of the "granophyre zone" undoubtedly intrude the upper part of the KVC, for instance in the Genex Mine area (*see also* Hocker, Thurston and Gibson 2005), where synvolcanic faults have localized the emplacement of intrusive rocks.

PORCUPINE ASSEMBLAGE

Although the contact is not exposed, bedding orientation suggests there may be an angular unconformity between the KVC and conglomerates exposed in central Godfrey Township, on the eastern margin of the study area (*see* Figure 20). It is suggested that the conglomerates may form part of the Porcupine assemblage (2696–2692 Ma: Ayer, Amelin et al. 2002).

KAM-KOTIA AND CANADIAN JAMIESON VOLCANOGENIC MASSIVE SULPHIDE DEPOSITS

Detailed deposit-scale mapping indicates a similar stratigraphic position for VMS mineralization at these two past-producing mines. At the Kam-Kotia Mine, two northeast-striking faults located immediately south-southwest of the open pit show evidence for synvolcanic movement, including the presence of dikes or apophyses of synvolcanic intrusions, abrupt changes in unit thicknesses, and offsets of a unit with subsequent units not offset. Numerous faults on this trend intersect the VMS-hosting interval in Robb and Jamieson townships. Field mapping and petrographic studies, suggest the presence of a northeast-oriented discordant iron-rich chlorite-rich±sericite alteration pipe that is at least 200 m wide and extends upward to the southwestern part of the Kam-Kotia open pit. At the Canadian Jamieson Mine, a synvolcanic diabase sill or dike occurs in the immediate vicinity of the ore lenses, suggesting the presence of an east-northeast-trending synvolcanic structure in this location. As at Kam-Kotia, rocks in the vicinity of the Canadian Jamieson orebodies are strongly chlorite and sericite altered.

GENEX VOLCANOGENIC MASSIVE SULPHIDE DEPOSIT SUBPROJECT

A detailed subproject focussed on the Genex deposit (Hocker, Thurston and Gibson 2005a, 2005b) has shown the metavolcanic rocks in the Genex Mine area are cut by numerous mafic and intermediate synvolcanic intrusions. The synvolcanic timing of the mafic intrusions is indicated by the presence of peperite, a pillowed base, irregular contacts, amoeboid dikes, and incorporation of felsic material. The synvolcanic nature of the intermediate intrusions is evidenced by the presence of a mixed zone near the upper contact, abundant spherulites and amygdules, and localization within synvolcanic faults. Synvolcanic faulting occurred after emplacement of the mafic synvolcanic intrusions, and provided conduits for the intermediate synvolcanic intrusions, as well as for the hydrothermal fluids responsible for the base-metal mineralization and alteration at the Genex Mine.

The Genex mineralization is distributed in 3 zones: the first in pillow breccia and hyaloclastite, the second at the contact between felsic tuff and intermediate intrusion, and the third within the intermediate intrusion. The mineralization represents subseafloor replacement sulphides localized within zones of higher permeability. All rocks have experienced hydrothermal alteration in the form of sericitization, chloritization, epidotization, silicification, and iron-carbonatization. The small size of the synvolcanic intrusions mitigates against them being the primary heat source associated with the hydrothermal system; however, their occurrence indicates the presence of a localized high heat-flow thermal regime. Mapping the distribution of these intrusions is important for defining synvolcanic structures, and potentially new zones of base metal sulphide mineralization.

Although no significant VMS mineralization has been found in the Genex area since the discovery of the initial deposit, the area still has potential to host significant VMS mineralization, especially along strike from the Genex deposit. Geochemically, the Genex felsic metavolcanic rocks are classified as FIIIa rhyolites, which, according to Lesher et al. (1986), are preferentially associated with Archean VMS mineralization. Furthermore, the presence of a mineralizing hydrothermal system has already been established in the area. Thus, many of the necessary components for a VMS deposit are present. Lastly, the presence of mineralized mudstone lapilli in the volcaniclastic rocks overlying the Genex area is of interest. Not only is the volcaniclastic sequence a good marker horizon, but the presence of mineralized fragments indicates that VMS mineralization was still occurring during the evolution of the stratigraphic package. The source of the mineralized mudstone fragments is not yet identified. In further exploration for VMS mineralization in the Kamiskotia area, an important feature that must be recognized is the presence of synvolcanic structures. In the Genex area, the identification of high-level synvolcanic intrusions is critical in defining the presence of synvolcanic structures. Thus, recognition of synvolcanic intrusions similar to those of the Genex area, which tend to utilize synvolcanic structures as conduits, is important in defining synvolcanic structures.

IMPLICATIONS FOR VOLCANOGENIC MASSIVE SULPHIDE EXPLORATION

New U/Pb ages indicate that the Kidd–Munro assemblage rocks in Loveland, Macdiarmid and Thorburn townships are coeval with the Kidd Volcanic Complex, which hosts the giant Kidd Creek VMS deposit 5 km to the east of the study area. The high-silica FIIIb rhyolites in south-central Loveland Township are geochemically similar to ore-associated FIIIb rocks from Kidd Creek (e.g., Lesher et al. 1986), and seem likely to represent the most prospective part of the succession. Volcaniclastic intervals representing lulls in volcanism during which VMS deposits may have developed have been intersected by drilling. Drilling has also indicated mineralization associated with the felsic-intermediate volcaniclastic rocks at the top of the Kidd–Munro assemblage succession, particularly along felsic–mafic contacts at the base of and within this interval.

Future exploration in the KVC is probably best focussed on the along-strike extension of the known VMS-hosting interval. Evidence for early movement on the Aconda Lake fault immediately north of the Genex deposit, and for increased alteration intensity along northeast-trending faults in the Kam-Kotia Mine area, suggests that synvolcanic faulting may have played an important role in localizing VMS mineralization. Areas where such faults intersect the VMS-hosting interval may provide a tighter focus for more detailed exploration. Mafic and felsic volcaniclastic strata, which can be replaced by VMS mineralization, and felsic coherent facies flows and/or domes, appear to be important potential targets. Chlorite and/or sericite alteration is associated with VMS orebodies at the Kam-Kotia, Canadian Jamieson and Genex mines. Although these alteration haloes represent a further exploration guide, they appear to be relatively areally restricted, and may prove difficult to locate given the sparse outcrop in much of the study area. Evidence of west-facing in northeast Godfrey and southeast Jamieson townships suggests the possibility of repetition of the VMS-hosting interval across a map-scale syncline in that area.

Ben Nevis Area Subproject

Katrine, Ben Nevis and Clifford townships are part of the Archean Blake River Group within the Blake River assemblage of the Abitibi Subprovince. The Blake River Group hosts one of the most significant mining camps in Canada—the Noranda camp—where the origin, localization, and distribution of deposits are relatively well understood. In contrast, very little is known about the Blake River Group in Ontario; hence, this subproject was conceived to improve our knowledge of the Blake River Group in Ontario and to use that knowledge to assess its potential for VMS mineralization.

The Blake River Group is divided into 3 subgroups: the Garrison, the Misema and the Noranda. The volcanic rocks of Katrine, Ben Nevis and Clifford townships belong to the Misema subgroup. The Misema subgroup in Ben Nevis Township has a U/Pb age of 2696.6±1.3 Ma. This is younger than the pre-cauldron phase of the Noranda subgroup (2701±1 Ma: Mortensen 1993b), younger than the Misema subgroup in Pontiac Township (2701±2 Ma: Corfu et al. 1989), and of the same age as the post-cauldron phase of the Noranda subgroup (the Reneault–Dufresnoy formation: 2697.9+1.3/–0.7 (Mortensen 1993b) and 2696±1.1 Ma (Lafrance, Moorhead and Davis 2003), and the Bousquet formation: 2698.6±1.5 Ma, 2698.0±1.5 Ma and 2694±2 Ma (Lafrance, Moorhead and Davis 2003)). Thus, the Ben Nevis–Clifford volcanic complex formed late in the Blake River Group volcanic event.

The Noranda cauldron sequence of the Noranda subgroup hosts the majority of VMS deposits in the Blake River Group (Gibson, Watkinson and Comba 1989; Gibson and Watkinson 1990). The volcanism in the Noranda cauldron is flow dominated (de Rosen-Spence 1976; Gibson, Watkinson and Comba 1989; Paradis 1990), as is the pre-cauldron volcanism (Péloquin, Verpaelst and Gaulin 1989a; Péloquin et al. 1989b; Péloquin 2000). However, pyroclastic rocks form an important part of the post-cauldron volcanism (Trudel 1978, 1979; Goutier 1997; Lafrance, Moorhead and Davis 2003).

The Ben Nevis–Clifford volcanic centre has a large pyroclastic component. Subaqueous andesite flows are the dominant rock type in the study area. In Katrine Township, pyroclastic rocks are rare, and felsic volcanic rocks even rarer. In Ben Nevis and Clifford townships, there is a spectrum of subaqueous volcanic rocks from basalt to rhyolite. Both flow and pyroclastic facies occur in all rock types, but the felsic volcanic rocks are dominantly pyroclastic with rare flow or dome facies. The large pyroclastic component of the Ben Nevis–Clifford volcanic centre suggests that it may be a subaqueous composite stratovolcano constructed on a mafic to intermediate volcanic "floor" represented by the Misema subgroup mafic to intermediate volcanic rocks in Katrine Township. The increase in pyroclastic rocks, and the pumiceous and scoriaceous nature of some of the fragments, indicates shallow depth of emplacement for the Ben Nevis–Clifford volcano.

The geochemistry of the Ben Nevis–Clifford volcanic centre also differs from the Noranda volcanism. Noranda has long been known to be bimodal (andesite–rhyolite) and to have 2 end-member andesite affinities: tholeiitic and calc-alkalic (or LREE-enriched) (e.g., Goodwin 1977; Gélinas et al. 1977; Laflèche, Dupuy and Bougault 1992; Péloquin 2000; Péloquin et al. 2001). In contrast, the Misema subgroup in the study area is unimodal (andesite dominant) with no silica gap, and there are no true tholeiites in the area.

Volcanogenic massive sulphide (VMS)-style alteration and mineralization occur in the study area indicating that a synvolcanic hydrothermal system existed. However, the mineralization is concentrated in synvolcanic dikes as veins or in the multiple injection margins, suggesting that the fluids were channelized within the dikes. This indicates that the present exposure may represent the feeder zone of the hydrothermal system. The area is structurally complex and the influence of faults and deformation zones on the stratigraphy of the area must be determined, as should the effect of possible folding.

High-level synvolcanic dikes, which can only be distinguished from extrusive rocks by their crosscutting relationships, occur in all rock types throughout the study area, as do mafic to intermediate dikes and irregular masses, which are comagmatic with the Blake River Group volcanism.

The differences between the Ben Nevis–Clifford volcanic centre and the Noranda cauldron indicate that mineral exploration in Ben Nevis and Clifford townships should not be limited strictly to Noranda-type Cu-Zn VMS deposits. The presence of VMS-style alteration and mineralization in the area indicates that a synvolcanic hydrothermal system existed. However, the apparent concentration of the mineralization in the synvolcanic dikes, as veins or in the multiple injection margins, suggests that the

fluids were channelized within the dikes. Thus, the present exposure may represent the feeder zone of the hydrothermal system (Figure 21). The structural complexity of the area must first be unravelled. The influence of faulting and the iron-carbonatized deformation zones on the stratigraphy of the area should be determined, and the possibility that the area is affected by complex folding examined.

The recognition of a porphyry system related to the Clifford stock in Clifford Township by Piercey (Piercey et al. 2004: MacDonald, Piercey and Hamilton 2005) opens up a new avenue for exploration. A gravity low in Ben Nevis Township, which is similar to that corresponding to the Clifford stock in Clifford Township, suggests a "Clifford-type" intrusion at depth. The occurrence of Clifford-event porphyry dikes in Ben Nevis Township confirms that the Clifford intrusive event extends south of the Murdoch Creek–Kennedy Lake fault.

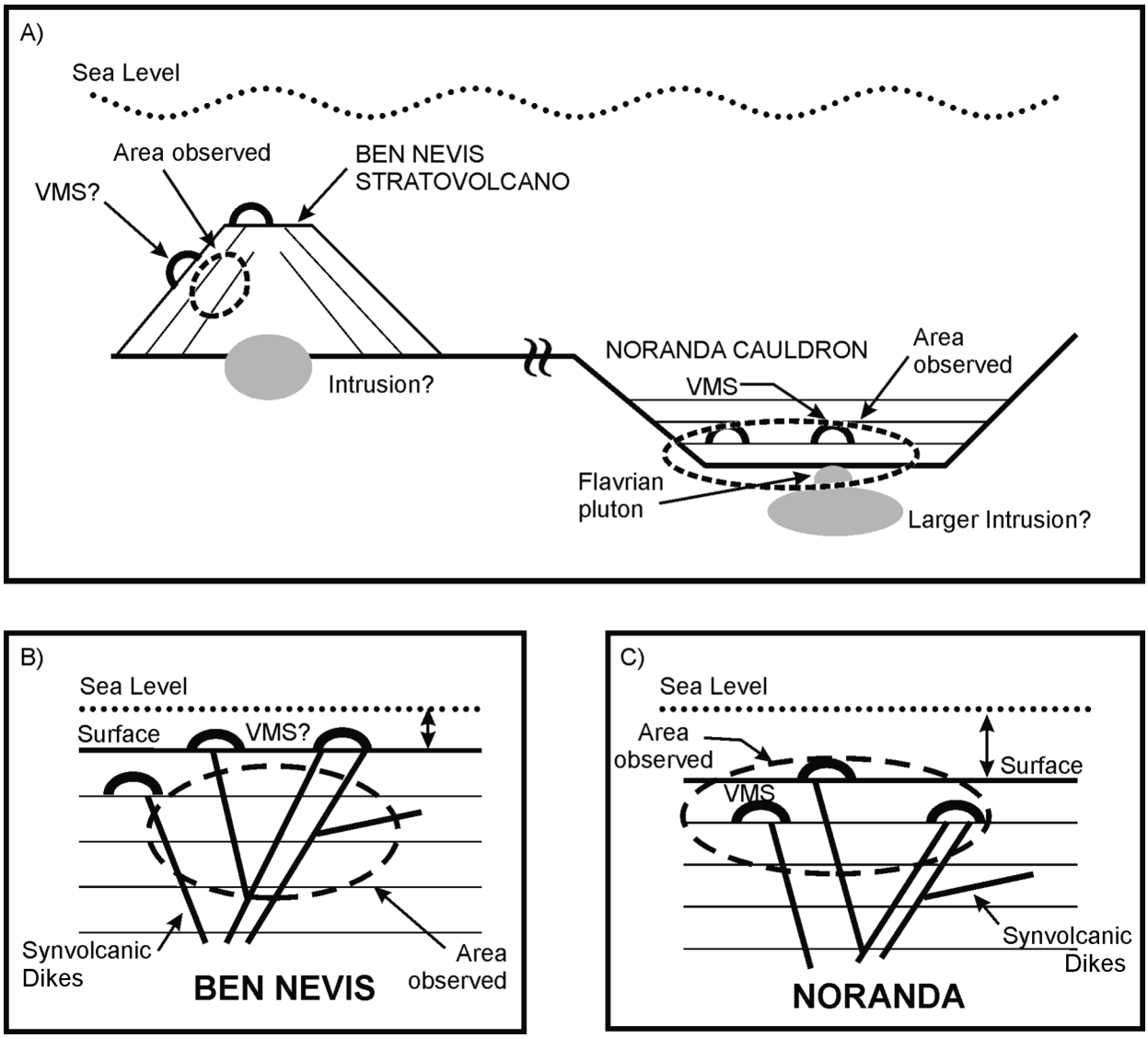

Figure 21. Schematic diagrams (not to scale) of a) the Ben Nevis–Clifford stratovolcano in relationship to the Misema mafic lava plain (Katrine township and western Quebec) and the Noranda cauldron, indicating possible areas of present exposure, b) the Ben Nevis–Clifford stratovolcano indicating the possible area of present exposure, and c) the Noranda cauldron indicating the possible area of present exposure (*from* Péloquin and Piercey 2005, p.47).

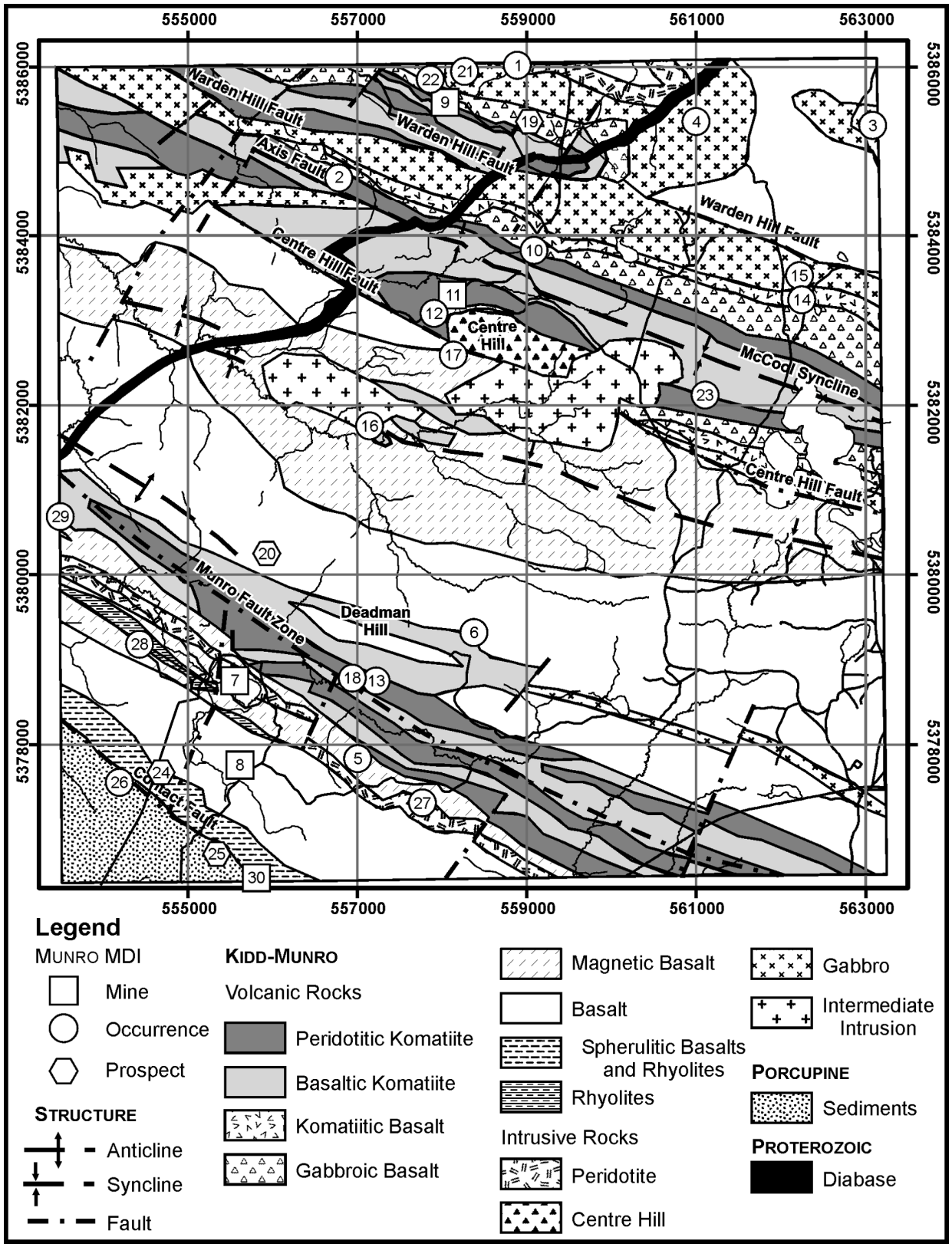

Figure 22. Geological map of Munro Township (*from* Péloquin, Houlé and Gibson 2005, p.4). Mineral occurrence and deposit numbers are listed in Péloquin, Houlé and Gibson (2005, Table 2); the Potter Mine (formerly known as the Centre Hill Mine) and Potterdoal Mine (numbers 11 and 9, respectively) are discussed in the text.

Munro–Currie Subproject

The goal of the Munro and Currie townships VMS subprojects of the Discover Abitibi Initiative is to reach a better understanding of the volcanic stratigraphy in the 2 townships, and of the stratigraphic position of the volcanogenic mineralization in both. In Munro Township, the mineralization at both the Potter Mine (formerly known as the Centre Hill Mine) and Potterdoal Mine is hosted in thin volcaniclastic and sedimentary units at mafic–ultramafic flow contacts; in Currie Township, the mineralization at the Currie (Tillex) occurrence is hosted in the volcaniclastic and sedimentary units of the upper Tisdale assemblage.

MUNRO TOWNSHIP

In Munro Township, the Kidd–Munro assemblage rocks consist of subaqueous tholeiitic basalt and ultramafic flows; felsic and intermediate volcanic rocks are rare. The area is divided into 3 blocks: South Munro, Central Munro and North Munro. The South Munro block corresponds to the area of the Kidd–Munro assemblage south of, and including, the southern ultramafic unit cut by the Munro fault zone, referred to as the "First Komatiitic Lava Succession" (after Johnstone 1991). The Central Munro block corresponds to the area located between the southern ultramafic unit and the Centre Hill fault. The North Munro block corresponds to the area located north of the Centre Hill fault (Figure 22; Péloquin, Houlé and Gibson 2005). The South Munro block is characterized by a basal interlayered spherulitic rhyolite and basalt unit, followed by a basaltic unit, within which a thin rhyolite unit (the Beatty rhyolite) occurs; the uppermost unit in the south block is the "First Komatiitic Lava Succession" of Johnstone (1991). The Central Munro block is characterized by basaltic to komatiitic basaltic units. The difference between the South and Central Munro blocks lies in the presence of rhyolites and andesites in the former. As the displacement along the Munro fault and the folding in the area appear to be of limited extent, it is possible that the South and Central Munro blocks form a continuous stratigraphic sequence consisting of a lower tholeiitic unit comprised of interlayered tholeiitic basalts, tholeiitic andesites and rhyolites capped by the "First Komatiitic Lava Succession" (South Munro block), and an upper tholeiitic basalt unit (Central Munro block) (Péloquin, Houlé and Gibson 2005). The Centre Hill fault between the Central and North Munro blocks constitutes a major stratigraphic break. In the North Munro block, ultramafic volcanic and intrusive rocks are dominant. The stratigraphic sequence is interpreted to be repeated 3 times within the block by folding (the McCool syncline) and faulting (the Warden Hill fault) (Arndt, Naldrett and Pyke 1977; Coad 1976; Johnstone 1991; Epp 1997; Péloquin, Houlé and Gibson 2005). The Potter and Potterdoal mines are located in the North Munro block: Potter Mine on the south limb of McCool syncline and Potterdoal in the Warden Hill fault repetition of the north limb of the syncline.

The most complete stratigraphic section is defined at Potter Mine on the south limb of McCool syncline. There, the volcanic succession is divided into 3 units: 1) a Lower Komatiitic Unit, 2) the Middle Tholeiitic Unit; and 3) the Upper Komatiitic Unit (Gamble 2000, Gibson and Gamble 2000). The mineralization at Potter Mine is hosted in the Middle Tholeiitic Unit, which consists of basaltic volcaniclastic rocks, intact and autobrecciated sills and/or dikes of basalt, thin argillaceous and carbonaceous sedimentary units, chert, massive sulphide, and lesser komatiitic flows. The sulphides are hosted within the lapillistone facies of the basaltic volcaniclastic rocks; this facies is interpreted to have accumulated within a primary graben (Gibson and Gamble 2000).

The magnetic signatures of the stratigraphic succession at Potter Mine can be traced around the closure of the McCool syncline. North of Potter Mine, on the north limb of the syncline, the succession observed is a mafic unit, overlain by an ultramafic unit. The units are massive, thick, and coarse grained and exhibit no internal structure. They were recognized as flows based on the presence of flow-top breccias (Arndt 1977; Arndt Naldrett and Pyke 1977). These flows, the lateral extensions of the Potter

Mine stratigraphic succession, have also been interpreted to be Theo's and Fred's flows, recognized at the Potterdoal Mine north of the Warden Hill fault (Arndt 1977, Arndt, Naldrett and Pyke 1977). Thus, the north limb of McCool syncline is interpreted to be repeated across the Warden Hill fault.

At Potterdoal Mine, the volcanic succession is divided into 2 units structurally repeated by the Buster fault (Epp 1997, Epp and Crocket 1999). The lowest unit in the area consists of thick layered tholeiitic flows: Theo's flow and the Ore flow. The upper unit is a thick layered komatiitic flow: Fred's flow. Theo's flow and the Ore flow are interpreted to be at the same stratigraphic level, the present superposition of the flows being due to movement along the Buster fault (Epp 1997, Epp and Crocket 1999). The mineralization at Potterdoal Mine occurs in a breccia unit within a sedimentary and volcaniclastic unit between the Ore flow and Fred's flow. The breccia was interpreted to be "tectonic" and to have formed in a scarp depression. Along strike from the "tectonic" breccia, mafic volcaniclastic deposits are observed similar to the pyroclastic rocks at Potter Mine (Epp 1997, Epp and Crocket 1999, Péloquin, Houlé and Gibson 2005).

The mafic to ultramafic volcanic contact favourable to volcanogenic massive sulphide deposits is structurally repeated in the North Munro block (Figure 23): 1) at Potter Mine north of the Centre Hill fault; 2) on the north limb of McCool syncline, south of the Warden Hill fault; and 3) at Potterdoal Mine

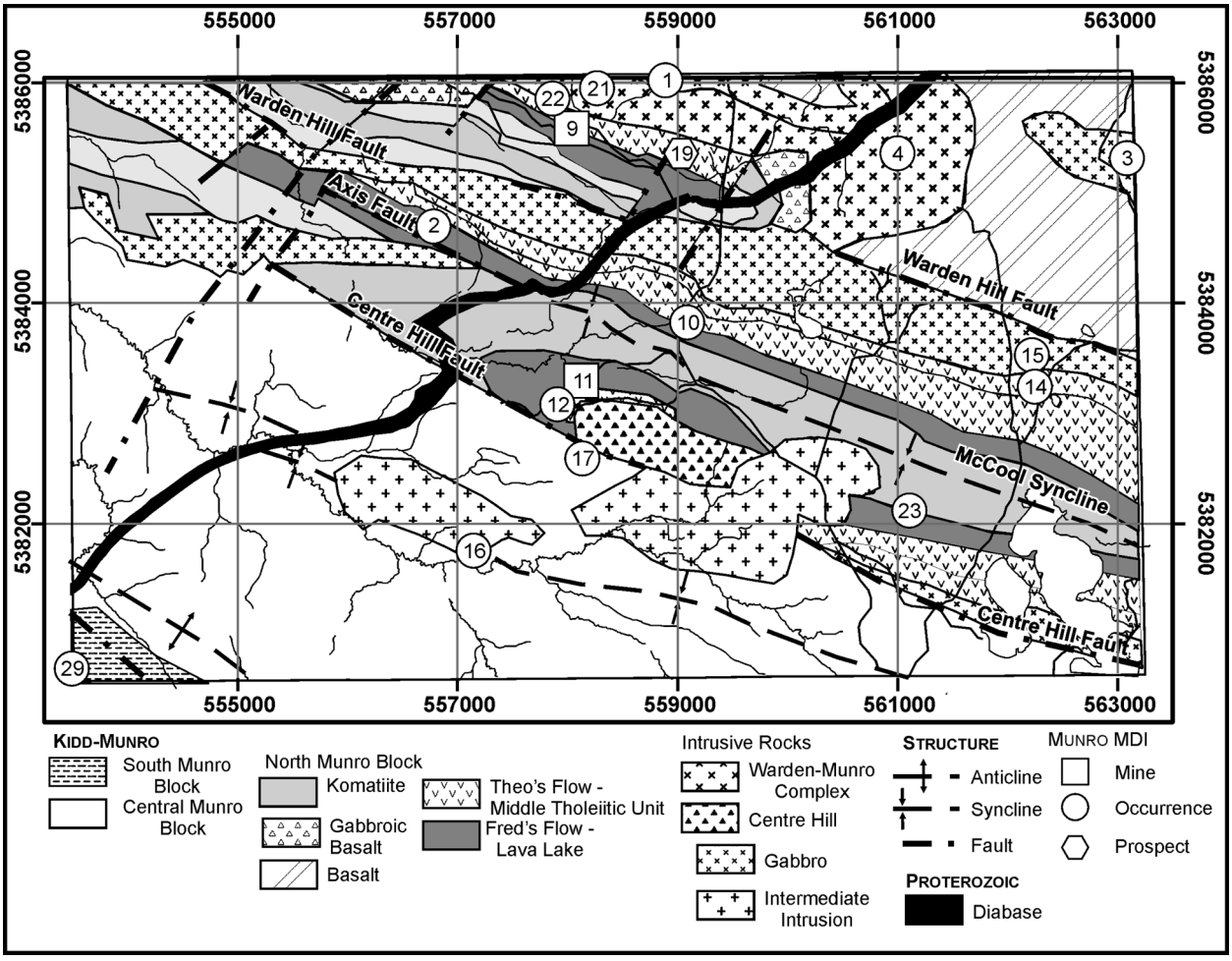

Figure 23. Map of the North Munro block showing the repetition of Fred's and Theo's flows (*from* Péloquin, Houlé and Gibson 2005, p.18). Mineral occurrence and deposit numbers listed are from Péloquin, Houlé and Gibson (2005, p.44, Table 2); the Potter Mine (formerly known as the Centre Hill Mine) and Potterdoal Mine (numbers 11 and 9, respectively) are discussed in the text.

north of the Warden Hill fault. Thus, the Potter and Potterdoal mines are interpreted to be time-stratigraphic equivalents (Arndt, Naldrett and Pyke 1977; Coad 1976; Epp 1997; Péloquin, Houlé and Gibson 2005). In both cases, the massive sulphides are related to volcanic fragmental rocks occurring at the contact between the tholeiitic and komatiitic units (Gamble 2000; Gibson and Gamble 2000; Epp 1997). The presence of interflow sedimentary and volcaniclastic units at the mafic–ultramafic contact along strike from the Potterdoal deposit, and between Theo's and Fred's flows on the north limb of the McCool syncline (south of the Warden Hill fault), as well as the extension of the mafic–ultramafic contact under the overburden to the east, indicates further potential for volcanogenic massive sulphide mineralization.

CURRIE TOWNSHIP

Currie Township is dominated by the basaltic rocks of the lower Tisdale and lower Blake River assemblages (Figure 24). Although, the intermediate to felsic volcaniclastic rocks, argillites and greywackes of the upper Tisdale assemblage are a lesser component of the geology of the township and very rarely crop out, they are important in that they host the Currie (Tillex) base metal showing. The assemblage boundaries are interpreted from the magnetic signature of the units and from drill core.

The stratigraphic succession in Currie Township is generally east-west striking, vertical to southward dipping and southward younging where facing directions were observed. The stratigraphic sequence from north to south is lower Tisdale, upper Tisdale and lower Blake River assemblages. The lower Tisdale and the lower Blake River assemblages are dominated by mafic flows. The upper Tisdale assemblage (including the "Marker Horizon") is dominated by felsic tuffs (including feldspar crystal tuffs), mafic to intermediate tuffs and sediments (argillites and greywackes). Proterozoic diabase dikes and Archean porphyry dikes crosscut the volcanic assemblages. The porphyry dikes resemble the feldspar crystal tuffs of the upper Tisdale assemblage.

Based on limited geochemistry, the basalts in the lower Tisdale and lower Blake River assemblages are dominantly tholeiitic. However, one sample from a porphyritic pillowed flow in the lower Blake River assemblage is geochemically similar to the upper Tisdale assemblage intermediate volcanic rocks. The geochemistry of the upper Tisdale assemblage tuffs shows them to be calc-alkalic in affinity. Multiple geochemical populations are recognized in the upper Tisdale assemblage, possibly due to variations at the source and/or in subsequent crustal contamination.

The volcanic rocks of Currie Township are deformed. In general, the rocks in all of the assemblages exhibit well-developed east-west subvertical schistosity. A large-scale fold is recognized in the magnetic signature of the lower Blake River assemblage. In drill core of the upper Tisdale assemblage, the schistosity is seen to be bedding parallel, and zones of strong deformation and fault gouges, also bedding parallel, were observed. In general, the upper Tisdale assemblage is more deformed than the lower Tisdale and lower Blake River assemblages. The upper Tisdale assemblage tuffs and sediments may have been more susceptible to deformation and acted as a corridor where higher strain was focussed; the existence of a strata-parallel fault occurring at or near the upper Tisdale–lower Blake River assemblages contact should not be ruled out.

In the upper Tisdale assemblage, the porphyritic dikes form 2 main geochemical populations equivalent to populations observed in the volcanic rocks of that assemblage. The porphyritic dikes from the lower Tisdale and lower Blake River assemblages are geochemically similar to the volcanic rocks and porphyry dikes of the upper Tisdale assemblage. This similarity between the porphyry dikes in all the assemblages and to the upper Tisdale assemblage volcanic rocks suggests that they are co-magmatic. The magmatic event responsible for the upper Tisdale assemblage volcanic rocks, therefore, has an intrusive expression, and the event continued during the deposition of the lower Blake River assemblage.

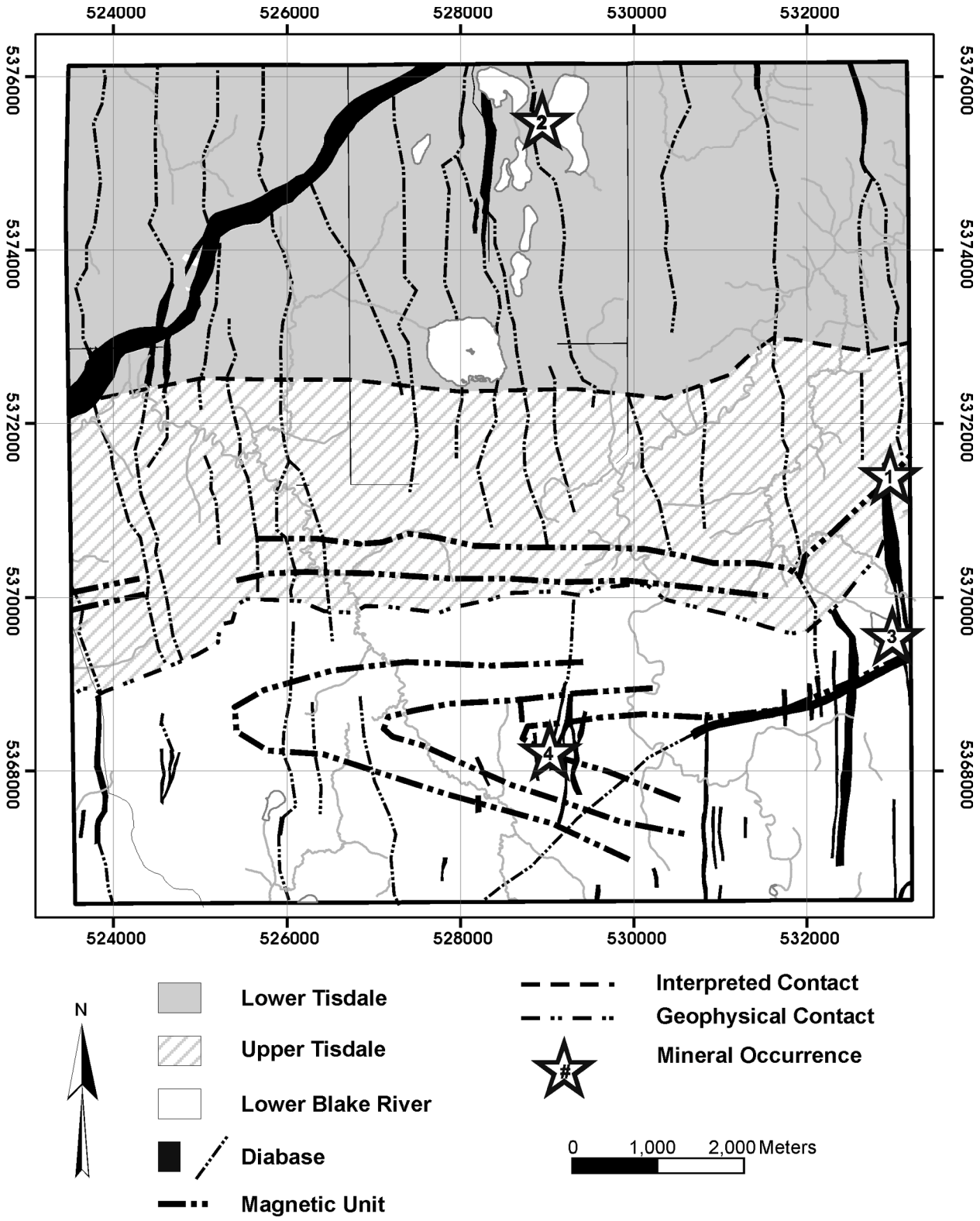

Figure 24. Geological map of Currie Township showing mineral occurrences (*from* Péloquin, Houlé and Gibson 2005, p.52). Mineral occurrences are 1) Currie (Tillex) (discussed in the text), 2) Anderson, 3) Foster, and 4) Reid.

The Currie (Tillex) showing occurs in the sediments and felsic tuffs of the upper Tisdale assemblage, and is within the same stratigraphic sequence that hosts the Cross Lake deposit (Ontario Geological Survey 2004b; Vaillancourt 2001). The mineralization described by Expatriate Resources, and described and observed in drill core from Kinross Gold Corporation and core in the Kirkland Lake Drill Core Library occurred as small stringers, and along bedding and foliation planes. The mineralized zones are commonly schistose, and numerous bedding parallel faults and sheared zones are observed in drill core.

The mineralization in the Marker Horizon (Corfu and Noble 1992) of the upper Tisdale assemblage in Currie Township appears to be integrally associated with the sediments and felsic tuffs. A unit of particular interest within this assemblage corresponds to a magnetic high on the magnetic map and can be traced with few breaks across the entire township (Ontario Geological Survey 2004a). A second unit with a high magnetic signature occurs 200 to 300 m south of the first. The generally east-west orientation of these magnetic highs is subparallel to the interpreted upper Tisdale–lower Blake River assemblage boundary. These magnetic units may be stratigraphic and used as "marker units" within the Marker Horizon of the upper Tisdale assemblage.

NICKEL-COPPER-PLATINUM GROUP ELEMENT MINERALIZATION SUBPROJECT

This subproject is an affiliated OGS project that has been designed to complement the Discover Abitibi Greenstone Architecture Project (base metal and gold subprojects) by focusing on nickel-copper-platinum group element (PGE) mineralization in the Abitibi greenstone belt, but more specifically in the Shaw Dome area in the vicinity of known komatiite-associated deposits. This project represents an in-kind OGS contribution, which is both part of the Ontario Geological Survey core program and part of an ongoing PhD study by M.G. Houlé based at Laurentian University (LU) and the University of Ottawa (UO) on the physical volcanology and metallogenesis of komatiites in the Abitibi greenstone belt. Because of the nature of this in-kind OGS–LU–UO contribution, the Ni-Cu-(PGE) subproject section has progressed along a different time frame, so this section represents a summary rather than a complete assessment of the exploration potential of komatiite-associated deposits in the Abitibi greenstone belt.

This part of the Discover Abitibi Greenstone Architecture subproject has focussed on the Shaw Dome for several reasons: 1) it is one of the areas in the Abitibi greenstone belt that contains known occurrences of komatiite-associated deposits, and 2) the Shaw Dome area provides an opportunity to examine the physical volcanology of komatiitic rocks at several scales (i.e., outcrop, property, and regional).

The goals of this subproject are three-fold:

1. to evaluate the subvolcanic–volcanic architecture of the ultramafic rocks in the Shaw Dome
2. to evaluate the Ni-Cu-(PGE) mineral potential of the komatiitic rocks in the Shaw Dome
3. to extend what we have learned about the physical volcanology and metallogenesis of komatiitic rocks in the Shaw Dome to the scale of the Abitibi greenstone belt

A multi-scale, integrated approach is critical in constraining the komatiite volcanic facies to aid in the interpretation of the volcanic architecture of komatiite flow fields and to assess the mineral potential for komatiite-associated Ni-Cu-(PGE) deposits.

Table 5. Simplified classification of primary mineralization types in komatiite-associated magmatic Ni-Cu-PGE deposits (*modified from* Lesher and Keays 2002) in the Abitibi greenstone belt.

Origin	Type		
Type	**I** **Stratiform Basal**	**II** **Stratabound Internal**	**III** **Stratiform "Reef-style"**
Sulphide distribution	At or near the bases of komatiitic peridotite or komatiitic dunite units	Within komatiitic peridotite or dunite units	At/near contact lower ultramafic cumulate zones and upper mafic zones
Sulphide textures	Massive, net-textured, disseminated	Disseminated, interstitial	Disseminated
Timing and paragenesis	Segregated prior to or during emplacement	Segregated during crystallization of cumulate host rock	Segregated in final crystallization stages of host rock
Examples in the Abitibi greenstone belt	- Shaw Dome (Langmuir #1, Langmuir #2, McWatters, Hart, Redstone, Galata) - Bartlett Dome (Texmont) - Halliday Dome (Sothman) - Bannockburn area (Thalweg, Rahn Lake, C-Zone) - Dundonald area (Alexo, Kelex, Dundeal, Dundonald South) - Munro area (Mickel) - Lamotte area (Marbridge Zone 1-4, Cubric–Bilson, Ataman, Quebec Moly)	- Bannockburn area (Bannockburn) - Lasarre–Amos area (Dumont Nickel)	Common, but uneconomic - Round Lake Dome (Boston Creek sill) - Munro area (Fred's flow)

Komatiite-Associated Deposits

Nickel-copper-(platinum group element) (PGE) sulphide mineralization associated with komatiitic rocks (komatiites and komatiitic basalts) in Archean and Proterozoic greenstone belts are an important part of the broader category of magmatic Ni-Cu-PGE mineralization. Although komatiitic basalts and komatiites occur in several greenstone belts worldwide, the majority of known Ni-Cu-(PGE) deposits occur in only a few of these belts, including the Abitibi and Cape Smith belts of Canada, the Norseman–Wiluna and Forrestania belts of Western Australia, the Bindura–Shamva and Shangani–Filabusi belts of Zimbabwe, and the Crixas and Minas Gerais belts in Brazil.

Komatiite-hosted Ni-Cu-(PGE) deposits contain a variety of mineralization types (Lesher and Keays 2002), which may be subdivided into 3 broad genetic categories: magmatic, mobilized metamorphically hydrothermally, and mobilized tectonically. Each of these categories may be subdivided into several types and subtypes (Table 5; Lesher and Keays 2002). The most favourable Ni-Cu-(PGE) primary mineralization types in the Shaw Dome area are, in order of economic potential, stratiform basal (Type I: Kambalda-type), stratabound internal (Type II: Mt. Keith type), and stratiform internal (Type III: "reef-type").

In the past decades, researchers have recognized that the physical volcanology of komatiites is the single most important parameter in assessing the mineral potential of komatiites (e.g., Lesher, Arndt and Groves 1984; Lesher 1989; Hill et al. 1990, 1995; Barnes et al. 1999). Furthermore, a recent study on chalcophile elements geochemistry reveals that all komatiitic rocks are a favourable magma source for Ni-Cu-(PGE) mineralization in the Abitibi greenstone belt, regardless of age. These results corroborate that the physical volcanology is more important than magma composition in determining the prospectivity of komatiitic rocks (Sproule et al., in press). Thus, several factors are considered to be critical to the genesis of economically significant magmatic sulphide deposits (e.g., Lesher and Keays 2002, Naldrett 2004), including:

1. **Source of Metal**: The magma must be initially undersaturated in sulphide so that it contains sufficient concentrations of Ni, Cu, and PGE;

2. **Source of Sulphur**: The magma must have access to an external sulphur source to achieve early sulphide saturation and to segregate significant abundances of immiscible sulphides at a high (crustal) level;
3. **Dynamic System**: The ores must form in a dynamic system where the magmas can interact with country rocks (to extract S) and where the sulphides can equilibrate with a sufficient amount of magma to generate high chalcophile element contents in the sulphides (i.e., high R factor);
4. **Physical Trap**: The sulphides must be concentrated in some type of physical trap (embayment, inflection).

Abitibi Greenstone Belt

NICKEL SULPHIDE DEPOSITS

Nickel-copper-(platinum group element)(PGE) discoveries in the Abitibi greenstone belt occurred sporadically, including several periods of intense exploration and discovery alternating with other periods with only minimal mineral exploration (Figure 25): Period I (1907–1915) included the discovery of the Alexo Mine; Period II (1950–1951) included the discovery of the Texmont Mine; Period III (1960–1977) included the discovery of Langmuir Mine (#1 and #2); and Period IV (1989–1998) included the discovery of the Dundeal Horizon, and Period V (2003 to current) includes the discovery of C-Zone in the Bannockburn area. Thus, Ni-Cu-(PGE) mineralization continues to be discovered whenever there is sufficient exploration activity.

Komatiite-associated Ni-Cu-(PGE) deposits, prospects and showings in the Abitibi greenstone belt occur exclusively in the 2719 to 2710 Ma Kidd–Munro assemblage (e.g., Alexo, Dundonald South, Dumont, Marbridge) and the 2710 to 2703 Ma Tisdale assemblage (e.g., Langmuir, McWatters, Redstone, Texmont, Sothman, Bannockburn). No deposits have been discovered in the 2750 to 2735 Ma Pacaud assemblage and 2723 to 2720 Ma Stoughton–Roquemaure assemblage. The likely reasons for this are discussed below.

The deposits almost always occur in clusters. For example, there are 6 known deposits in the Shaw Dome, 4 in the Bannockburn area, 5 in the Dundonald area, and at least 4 in the Lamotte area. This is the normal pattern for komatiite-associated Ni-Cu-(PGE) deposits worldwide, exemplified by the deposits in the Kambalda–St. Ives–Tramways–Widgiemooltha–Carnilya Hill district in Western Australia (Barnes 2004). Clearly, areas where only one or two deposits have been discovered, such as the Bartlett and Halliday domes, have significant potential for discovery of additional deposits.

KOMATIITE PHYSICAL VOLCANOLOGY

Interpreting volcanic environments is difficult as it may be complicated by primary factors (e.g., more than one eruptive centre in each assemblage, differences in eruption rate and style, differences in mode and environment of emplacement) and secondary factors (e.g., metamorphism, alteration, structural complexity). However, there are clear lithological, geochemical, textural, and volcanological differences between the komatiitic rocks in the different assemblages of the Abitibi greenstone belt (Table 6).

The Pacaud assemblage is dominated by sheet-like flows with lesser pillowed flows. These sheet-like flows include abundant differentiated flows (ortho- to mesocumulate lower zones and poorly developed spinifex-textured upper zones) and less abundant massive flows (olivine-phyric or ortho- to

mesocumulate). The Stoughton–Roquemaure assemblage is dominated by pillowed flows with lesser sheet-like flows. Massive flows are frequently associated with pillowed flows, whereas differentiated flows only occur in specific parts of the Stoughton–Roquemaure assemblage. The Tisdale and Kidd–Munro assemblages contain more sheet-like flows than pillowed flows. Both massive and differentiated flows are frequently present in these assemblages, however, the massive flows are characterized by abundant ortho- to adcumulate lithologies with fewer olivine-phyric lithologies and differentiated flows are characterized by thick orthocumulate lower zones with thin spinifex-textured upper zones.

Volcaniclastic komatiitic rocks occur in the Kidd–Munro and Tisdale assemblages, and are typically autoclastic (i.e., flow-top breccia hyaloclastite or reworked hyaloclastite rather than pyroclastic rock). Only the Kidd–Munro and Tisdale assemblages contain a large proportion of komatiitic peridotite and

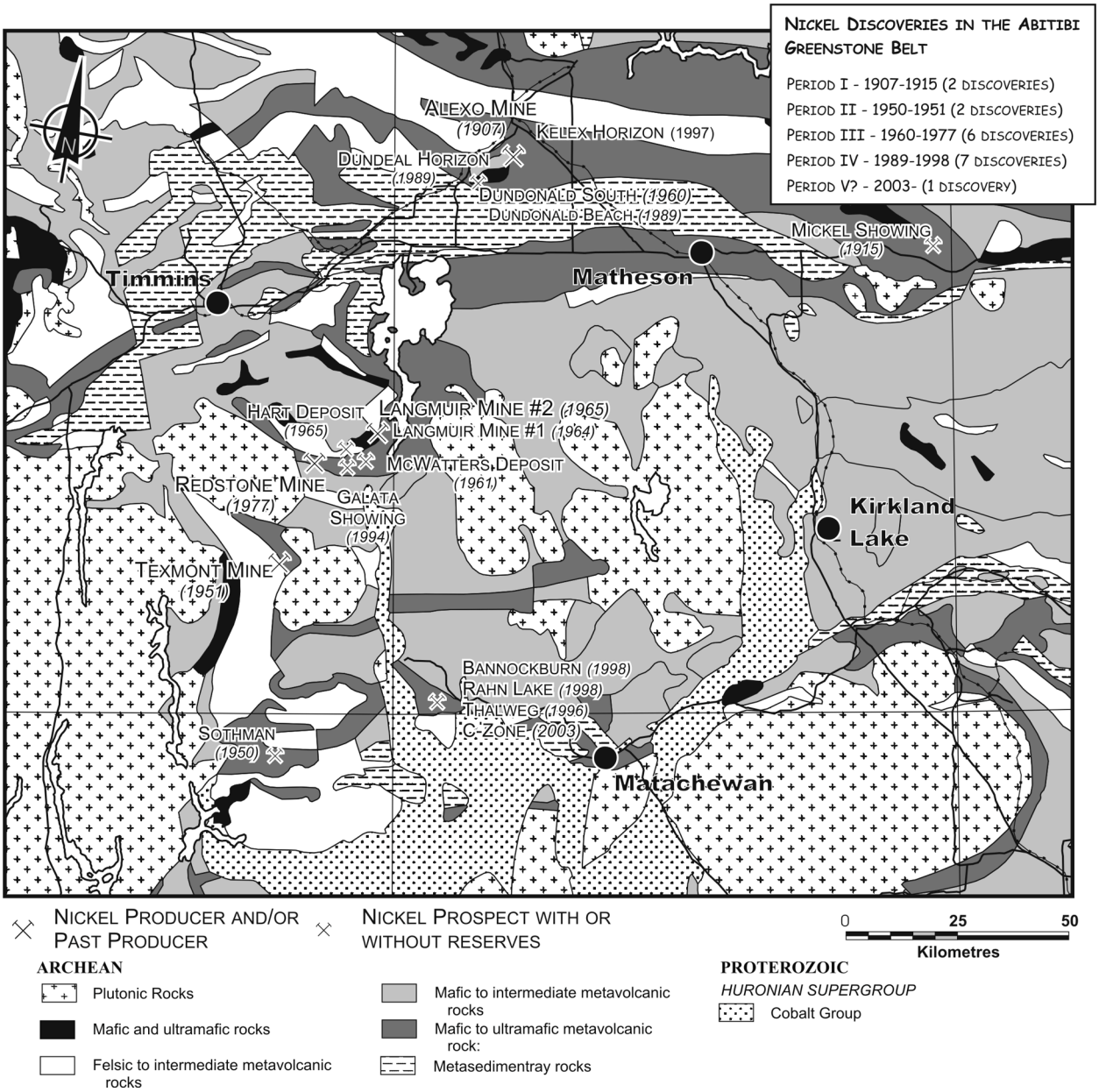

Figure 25. General geology of the Abitibi greenstone belt around Timmins showing the different nickel showings or deposits with the year of discovery.

komatiitic dunite in massive cumulate lithologies, which are interpreted to represent lava channels or the channel-flow facies of channelized sheet flows and high-level sills. These environments are important, as they are the favoured facies to host Ni-Cu-(PGE) mineralization (Lesher 1989). This is consistent with the presence of komatiite-hosted Ni-Cu-(PGE) deposits only within the Kidd–Munro (e.g., Marbridge, Alexo, and Dundonald) and Tisdale assemblages (e.g., Texmont, Redstone, Hart, and Langmuir deposits).

Table 6. Summary of geochemical (or lithological) and textural facies for the komatiitic rocks in different assemblages of the Abitibi greenstone belt (*modified from* Houlé 2001).

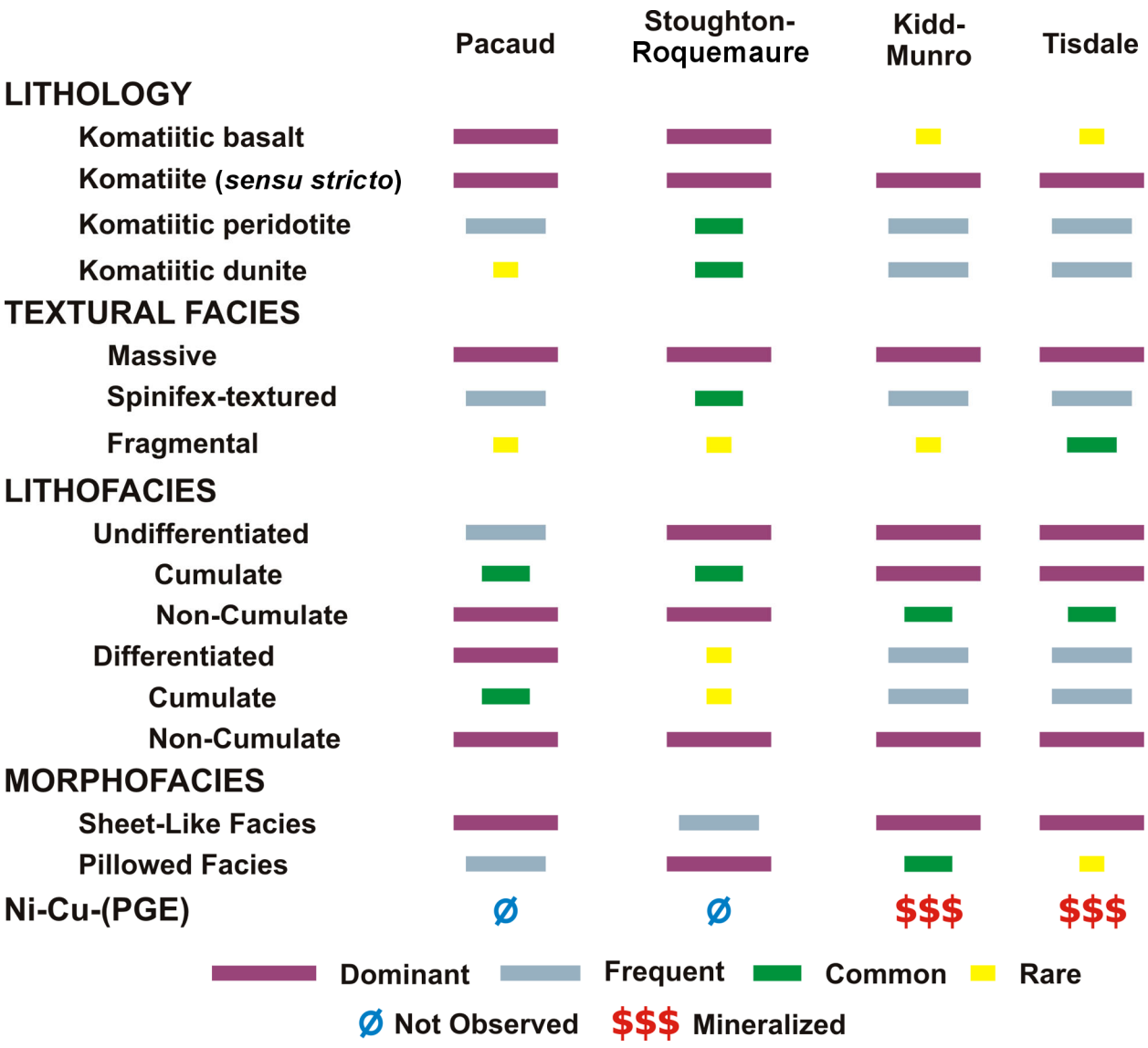

Shaw Dome Area

GEOLOGICAL SETTING

The Shaw Dome area (Pyke 1974) is outlined by an outward-facing stratigraphic contact between the Deloro and Tisdale assemblages, and comprises three packages. “Package A” (Deloro assemblage): The core of the domal structure is composed dominantly of massive and pillowed calc-alkalic intermediate to mafic metavolcanic lava flows with lesser intermediate volcaniclastic rocks and ultramafic intrusive rocks (dikes, sills and plutons). Several horizons of iron formations occur at different stratigraphic levels within this sequence, but dominantly within the upper part. “Package B” (Tisdale assemblage): The middle part of the sequence is composed of intermediate to felsic fragmental metavolcanic rocks (with lesser massive and pillow lavas), iron formations, and ultramafic flows and intrusions. Several horizons of iron formations occur at different stratigraphic levels within this sequence. “Package C” (Tisdale assemblage): The peripheral part of the sequence is composed of massive and pillowed tholeiitic mafic metavolcanic rocks intercalated with massive and pillowed komatiitic basalt and komatiite metavolcanic rocks.

The metavolcanic and metasedimentary rocks in the Shaw Dome have been metamorphosed to lowermost greenschist to lowermost amphibolite facies, depending on proximity to later intrusions. Deformation is strongly partitioned and many rocks exhibit well-preserved primary structures (e.g., pillows, polyhedral jointing) and textures (e.g., cumulate and spinifex textures). Within ultramafic rocks in the area, olivine is normally serpentinized whereas pyroxene and plagioclase (in gabbroic facies) are frequently preserved. Some rocks have been intensely and pervasively carbonated (calcite, magnesite, and siderite), which has destroyed most primary textures. Nevertheless, cumulate and spinifex textures are often preserved even in these highly altered rock.

KOMATIITIC ROCKS

The ultramafic rocks in the Shaw Dome area consist of intimately associated flows and high-level intrusive components. Determination of the intrusive versus extrusive origin of these rocks and the implications of these emplacement mechanisms is one of the goals of the Ni-Cu metallogenic theme of the collaborative subproject being conducted between OGS and the Discover Abitibi Initiative. Distinguishing between an intrusive or extrusive origin is difficult because of the scarcity of large, well-preserved outcrops. Nonetheless, the ultramafic rocks in this area have been subdivided into two groups: an intrusive “Lower Komatiitic Horizon” and an extrusive “Upper Komatiitic Horizon” (Muir 1975; Pyke 1982; Larson 1996; Stone and Stone 2000).

Lower Komatiitic Horizon

The Lower Komatiitic Horizon is composed of two types of intrusive ultramafic rocks: a) discordant ultramafic bodies and b) subconcordant ultramafic bodies. However, both of these types have essentially the same textural characteristics and exhibit pale orange-brown or bone-white weathered surfaces and dark green or pale green fresh surfaces. Most exposures consist of komatiitic dunite to peridotite, but some pyroxenitic and gabbroic units are locally present in association with the other more ultramafic components.

Upper Komatiitic Horizon

The Upper Komatiitic Horizon is characterized by komatiitic ultramafic metavolcanic rocks that exhibit pale orange-brown or bone-white weathered surfaces and dark green or pale green fresh surfaces, quite similar to the ultramafic rocks observed within the Lower Komatiitic Horizon.

The rocks in the lower part of the Upper Komatiitic Horizon are primarily massive komatiitic dunites and peridotites, but some olivine spinifex-textured komatiites are also present. In some areas, the ultramafic rocks are less magnesian komatiitic basalts and exhibit pyroxene spinifex textures and pillow morphologies.

The rocks in the upper part of the Upper Komatiitic Horizon include both olivine spinifex-textured komatiites and massive komatiitic peridotites. They display a wider range of primary structures (polyhedral jointing, flow breccias, spinifex-textured veins and/or sills) and textures (cumulus and spinifex textures). The thicknesses of the flows decreases upwards through the stratigraphy from approximately 30 to approximately 2 m.

Nickel Sulphide Deposits

Numerous occurrences of nickel, copper and platinum-group element mineralization associated with intrusive and extrusive komatiites have been identified in the Shaw Dome area (Hall, McDonald and Dinel 2003; Hall, Houlé and Tremblay 2004; Houlé, Hall and Tremblay 2004; Houlé and Guilmette 2005). Of the most significant occurrences, the Galata prospect and possibly the McWatters deposit occur in the Lower Komatiitic Horizon, whereas the Langmuir #1 and #2 mines, the Redstone mine, and the Hart prospect occur in the Upper Komatiitic Horizon. All of these deposits are associated with very magnesian, olivine-rich units, which have been interpreted as channelized lava flows or sills. All are also closely related spatially to sulphide-bearing iron formation, and all are localized in some type of footwall embayment (e.g., Pyke 1975; Green and Naldrett 1981; Robinson and Hutchinson 1982; Jiricka 1984; Schuster 1995). Sproule et al. (2002, in press) concluded that all of the host rocks were undersaturated in sulphide prior to emplacement. As noted above, these features are all critical in the formation of magmatic Ni-Cu-(PGE) mineralization.

Thus, the combination of a fertile komatiitic magma (metal source), proximity to sulphide-bearing iron formations (sulphur source), abundant olivine cumulate rocks indicating high magma flux (heat source and dynamic environment), and embayments (localization) provide an excellent environment for forming komatiite-associated Ni-Cu-(PGE) deposits in the Shaw Dome area.

Implications for Komatiite-Associated Deposits

A review of chalcophile element data (PGE, Ni, Cu, Co) of barren komatiitic rocks throughout the Abitibi greenstone belt reveals that all komatiitic rocks, regardless of age, display the same overall unfractionated trends (Sproule et al., in press). Thus, the komatiitic magmas that generated these rocks were sulphide-undersaturated when they were erupted and did not lose any sulphide mineral phases or PGEs during ascent through the crust. Thus, all komatiitic rocks, regardless of assemblage, represent favourable magma sources for Ni-Cu-PGE mineralization.

Several researchers have recognized the importance of volcanological processes in the genesis and localization of Ni-Cu-(PGE) mineralization associated with komatiites. Volcanic facies may be established by detailed mapping at the outcrop scale, stratigraphic mapping at the property and camp scale, and by inference on a larger scale. Volcanic facies that have been identified include vent pyroclastic facies,

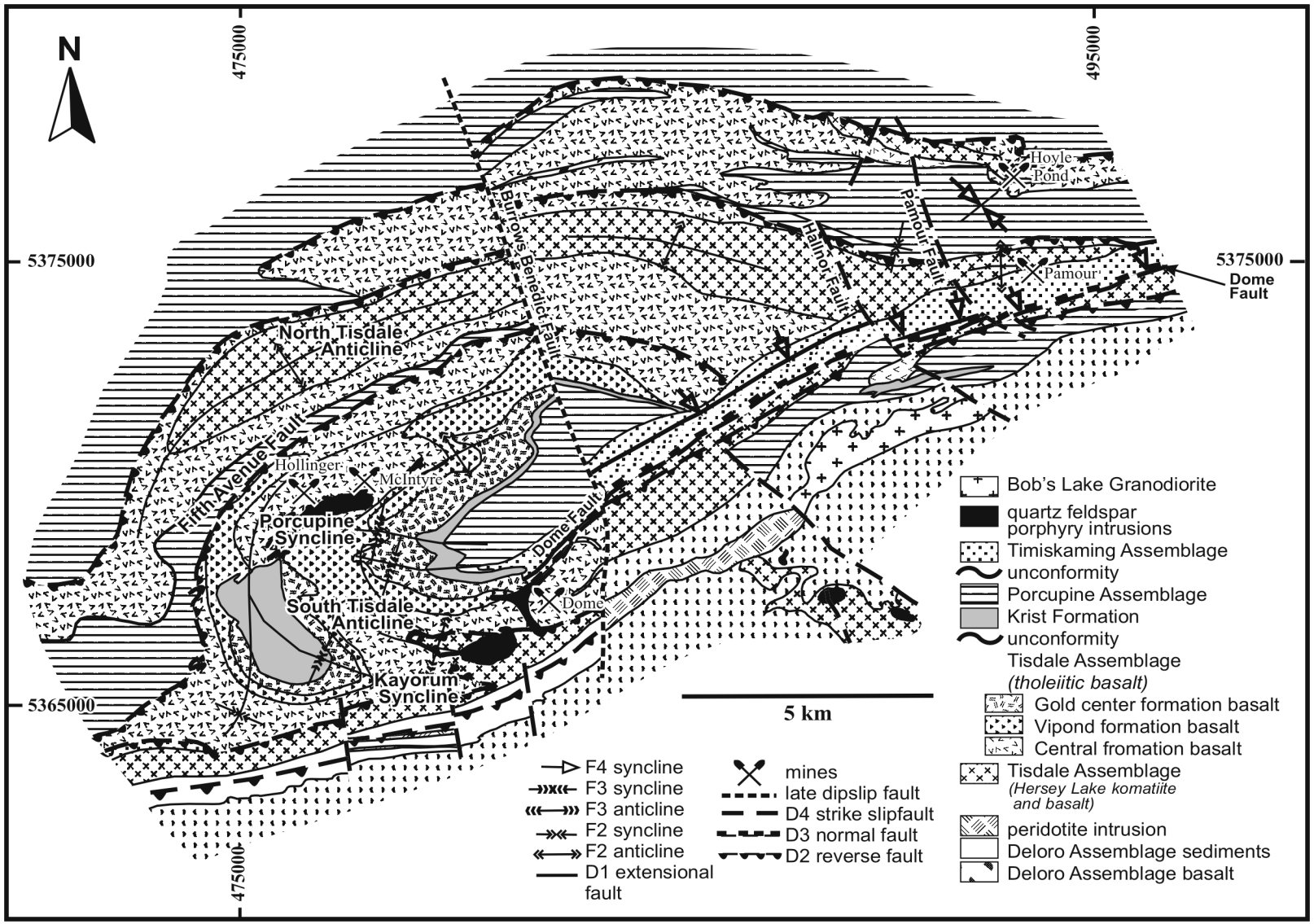

Figure 26. A generalized map of the Timmins–Porcupine gold camp, covering Tisdale, Deloro, Mountjoy, Ogden, Whitney and Hoyle townships (*modified from* Bateman et al 2005, p.7; *modified after* Ferguson et al. 1968).

sheet flow facies, channelized sheet flow facies, lava channel facies, lava pond facies, lava lobe facies, and distal pyroclastic and/or epiclastic facies. Worldwide, most Ni-Cu-PGE mineralization is hosted by lava channels, channelized sheet flows and, rarely, within vent facies. Komatiite flow fields have never been mapped directly, but komatiite volcanic facies have been interpreted to vary on the scale of an entire flow field and also on the scale of individual flow units. This complexity of lava facies makes it difficult to predict the locations of mineralized lava channel or channelized sheet flows, except that they most often (but not always) occur at or near the bases of individual komatiite sequences. Our work suggests that the identification of variations within barren volcanic facies is particularly important as it can potentially vector toward ore-forming environments. As these types of deposits are usually found within deformed Archean and Proterozoic greenstone belts, a multidisciplinary approach including geological mapping, volcanic facies mapping, geophysical surveys, and geochemical studies are required to aid in the exploration for these deposits and to facilitate the recognition of favourable volcanic sequences that may host magmatic Ni-Cu-(PGE) sulphide mineralization.

GOLD MINERALIZATION SUBPROJECTS

Timmins Subproject

The Timmins–Porcupine gold camp is the largest lode gold camp in Earth's Archean greenstone belts (Witwatersrand aside). It hosts several deposits are dispersed over 35 km, and together produced 63.7 million ounces gold, which is far ahead of other districts in the province (Groves et al. 2005). These deposits are distributed along the northern margin of an originally south-dipping Porcupine–Destor deformation zone (PDDZ). Herein lies one of the structural anomalies to be resolved: Why the gold deposits apparently lie in the footwall of this shear zone, contrary to other Archean gold camps such as Val d'Or and Kalgoorlie? Other uncertainties concerning these gold deposits include the kinematics and timings of deformations; the presence or absence of foliation predating the deposition of the Timiskaming assemblage; the relative timing of the several generations of quartz-carbonate veins and styles that have long been known (at least in general terms) in this camp; and the way in which an evolving orogenesis determines the geometry and kinematics of coeval gold mineralization. Research carried out involved mapping, and geochemical analysis of samples north of the PDDZ, principally in Tisdale, Hoyle and Whitney townships. A structural scheme, with refinements to the stratigraphic column and geochronology, has been constructed for the Timmins–Porcupine gold camp in order to develop the constraints applying to these matters (Figure 26; Bateman et al. 2005).

Unconformities or disconformities have been identified between each assemblage (Ayer, Amelin et al. 2002) mapped in the gold camp: between Tisdale and Deloro; between Porcupine and Tisdale; and a long recognized unconformity between the Timiskaming and the Porcupine–Tisdale assemblages. Some formations have been shown to be correlatives: the terms Beatty and Hoyle formations apply to turbidites that occur in different parts of the camp, and have been shown to be of the same age (~2688 Ma). The age of the albitite dikes at the McIntyre Mine has been confirmed at 2672.8±1.1 Ma, and a second albitite dike and a porphyry intrusion in the vicinity of the Pamour Mine have ages of 2676.5±1.6 Ma and 2677.5±2.0 Ma, respectively, the latter being considerably younger than the 2685 to 2690 Ma age of the other dated porphyries and the Krist formation. Geochemical sampling and analysis (compared with unpublished Porcupine Joint Venture data) of basalts and komatiites have allowed the subdivision of the Tisdale assemblage into 4 formations that have been traditionally defined on lithological and textural grounds. These formations—the Hersey Lake komatiite (2 subgroups), Central formation (3 subgroups), Vipond formation and Gold Centre formation—are distinguished on the basis of Fe_{total}-MgO-TiO_2-V-Zr-Y-Ni-Cr-REE. Lavas in one Central formation subgroup show distinct boninitic affinities (Kerrich et al.

1999) in their REE patterns and other trace element signatures, and provide the basis for refining the map-scale distribution of these formations and, hence, definition of the earliest folding in D2. These data also lead to inference of the tectonic setting, involving plate–plume interference.

Early stratigraphic excision (or non-deposition) resulted in an incomplete Tisdale assemblage sequence below Porcupine assemblage sediments. To the north of a septum of Porcupine assemblage sediments, Tisdale assemblage basalts lack the upper (geochemically defined) Gold Centre and Vipond formations. Below the Porcupine syncline sediment, there is a contact truncating early folds (Buffam 1948), and this unconformity cuts down the Tisdale assemblage section to the east. These facts are interpreted to indicate an angular unconformity between Tisdale and Porcupine assemblages, and that it represents an extensional or normal faulting event that excised some Tisdale assemblage stratigraphy, and possibly all of the Blake River assemblage if it was deposited here. These contacts are folded by F2 folds.

A D2 foliation has been systematically mapped in Tisdale assemblage rocks that is not identified in rocks above the Timiskaming unconformity. Folds are defined by geochemical-stratigraphic patterns of basalt formations and foliation trends with overprinting relationships. Folds associated with D2 strike east-west, and are refolded by F3 in S-asymmetrical folds (*see* Figure 26). They are interpreted as representing hanging-wall anticlines in 3 or 4 stacked south-over-north thrust panels. The Porcupine assemblage is affected by this deformation, since it is involved in these same folds. The earliest element of the PDDZ is C-S structures indicating south-over-north thrusting along a south-dipping zone, which is probably the root zone to the stacked thrusts. A post-Porcupine age for thrusting coincides with age data from the Duparquet Basin, Quebec (Mueller et al. 1996).

The F3 folds and S3 foliation are strongly developed in Tisdale assemblage rocks, and consist of a series of *en échelon* folds with curved axial surfaces along the PDDZ. The F3 fold axes do not affect the trace of the PDDZ, and do not extend across it to its southern side. In contrast to the Tisdale assemblage, F3 folding is quite minor, yet S3 foliation in Timiskaming rocks is strong. The Timiskaming assemblage occupies a syncline or half-graben with an faulted southern margin (the early formed Dome fault) adjacent to a counterclockwise deviation of the PDDZ from its east-northeast trend. These facts are interpreted to indicate formation of F3 and S3 during left lateral strike-slip movement along the shear zone, and the syntectonic opening of the Timiskaming half-graben in a dilatational jog, followed by foliation and folding, only the late stages of which affected the sediments, an interpretation which shares analogies to that of Bleeker (1995).

Folding in D4 created the syncline that preserves the Timiskaming assemblage rocks. Foliation S4 crenulates S3 and is axial planar to F4 folds that commonly have Z asymmetry. Minor structures suggest right lateral strike-slip along the PDDZ (Bleeker 1995). As part of this event, shortening strain was partitioned on the local scale around the Timiskaming unconformity into relatively small-scale reverse faults. The last significant event, D5, consists of an intense constrictional strain seen in Tisdale pillows, clasts in Krist formation volcaniclastic rocks and cobbles in Timiskaming assemblage conglomerates. Deformation event D4–D5 represents the final stage in transpressional deformation along the PDDZ. Reversal of strike-slip direction along the shear zone converted an initially dilatational jog into a compressional jog, accounting for constriction adjacent to the jog in the shear zone trend. The larger scale significance of the shift from left lateral to right lateral strike-slip is unclear from this study at the scale of the gold camp. One of either the D3 or D4 episodes may have been overall coaxial shortening with differing strike-slip during different orientation intervals, and the other episode may have been more strictly non-coaxial strain with a constant sense of strike-slip, as along the Larder Lake–Cadillac deformation zone (LLCDZ)(Wilkinson, Cruden, and Krogh 1999). The solution to this question lies in further structural analysis along the trace of the PDDZ.

Deformation postdating D4 is minor. A conjugate set of strike-slip faults, indicating north-south shortening, postdate the last phase of mineralization and S4. Two phases of crenulations have had no map-scale effect, but are locally strong. A set of flat-lying D6 crenulations may be related to gravitational collapse of the thickened orogen, and D7 chevron folds and conjugate kinks, best developed in well-foliated rocks along the PDDZ, indicate orogen-parallel shortening. Some quartz veining is related to this last event, but there is no evidence that gold was introduced in D6 or D7 episodes.

GOLD MINERALIZATION

The general belief has long been that mineralization in the Timmins–Porcupine camp postdated Timiskaming sedimentation. However, the presence of clasts of ankerite vein material (Dubé, Williamson and Malo 2003) within Timiskaming assemblage conglomerate is unambiguous evidence for pre-Timiskaming gold-related hydrothermal activity. It has also been suggested, and disputed, that gold-bearing clasts also occur in the Timiskaming assemblage (Gray and Hutchinson 2001; Poulsen, Robert, and Dubé 2000). There is also extensive evidence from across the Abitibi Subprovince for protracted gold mineralization (Bateman et al. 2005).

Ankerite veining is widespread as an early generation of veins in deposits strung along the PDDZ, and at the Dome Mine. Large (500 m strike, 900 m vertical), sheeted ankerite±quartz tourmaline veins lie parallel to lithological layering, and appear to be restricted to Tisdale assemblage volcanic rocks (Pressacco 1999). These do not carry large amounts of gold. The quartz-fuchsite vein (Moritz and Crocket 1990) is the highest grade ore of the Dome Mine, and is also apparently restricted to Tisdale assemblage rocks, although no definitive crosscutting relationships precisely establish its relative age. Quartz-ankerite-pyrite-minor gold veins at the Aunor–Delnite Mine have been compared with the Dome ankerite veins. They are relatively early, being cut by later quartz-tourmaline veins.

Other mineralization that represent the bulk of Timmins–Porcupine gold clearly postdates Timiskaming assemblage sedimentation. At the McIntyre Mine, early stage Cu-Au-Ag-Mo mineralization is crosscut by albitite dikes (Burrows et al. 1993). Molybdenite associated with this mineralization has an age of 2672±7 Ma using the Re/Os isotopic method and our refined age for the McIntyre Mine albitite dike is 2672.8±1.1 Ma (#13: Table 1, Figure 4E). Main-stage Hollinger–McIntyre mineralization, which hosts half of the Timmins–Porcupine area gold, consists of arrays of extension fractures infilled with quartz and gold. These arrays cut the albitite dikes and are formed synchronously with D3–S3, and are overprinted by S4 crenulations (Bateman et al. 2005). Veining at Vedron Mine, close to the PDDZ, also has quartz veins strongly folded and foliated in the D3 event.

Syn- to late-D4 mineralization is represented by the Pamour Mine, and other deposits found along the trace of the PDDZ and the Timiskaming trough. Veins formed during north-northwest–south-southeast shortening are represented by conjugate reverse faults occupied by fault-fill veins and shallowly inclined quartz extension veins. These veins are generally undeformed, but are crosscut by S4, which, locally, has folded some veins.

Thus, there is a protracted period of gold mineralization in the Timmins–Porcupine gold camp that extends from before Timiskaming assemblage sedimentation. Its relationship with D2 thrusting is unclear, but alteration appears to overprint S2. The bulk of gold mineralization phases extend through D3 and D4. These deformation phases constitute a transpressional orogenesis (Bleeker 1995) with mineralization coinciding with the transition from coaxial-thrusting strain to strike-slip non-coaxial strain, spanning the time of the opening of the Porcupine and Timiskaming assemblage sedimentary basins, which are focussed along the trace of the PDDZ. The protracted history of deformation, alteration and gold mineralization suggests a long-lived or multi-stage auriferous hydrothermal system, and indicates a

plumbing system geometrically stable for long enough to feed gold into a relatively small volume of rock throughout a period of transpressional deformation. This is similar to the deformation–mineralization history recorded in the one gold camp comparable with the Timmins–Porcupine camp: Kalgoorlie (Bateman and Hagemann 2004).

Kirkland Lake–Larder Lake Subproject

Work in Kirkland Lake–Larder Lake gold belt (cf. Thomson 1950) was concentrated in 26 km^2 transect in Gauthier Township (west of the town of Larder Lake) and 36 km^2 transect in Teck Township (west of the town Kirkland Lake, including the town). Both areas straddle the Larder Lake–Cadillac deformation zone (LLCDZ), and a 3 to 4 km wide belt of Timiskaming assemblage metavolcanic and metasedimentary rocks located north of it. In the north, Timiskaming assemblage rocks are in contact with lower Blake River (Teck Township transect) and upper Tisdale (Gauthier Township transect) assemblages.

The most significant structural feature of both areas is the ductile LLCDZ, a high-strain zone generally corresponding to the south boundary of the Timiskaming volcanic-sedimentary belt. The overall trend of the deformation zone is approximately east to west, with broad deviations to northeast and southeast orientations. In the transect areas, the LLCDZ is 400 to 600 m wide; deformation is notably more intense in Gauthier Township transect area.

Another ductile high-strain zone is the northeast-trending (~070°) Upper Canada deformation zone in Gauthier Township transect. Although this structure is only locally exposed, it is at least 150 m wide and most likely represents a north splay of the LLCDZ (Toogood 1989). There is no notable difference in strain intensity or deformation style between the LLCDZ and the Upper Canada deformation zone.

The brittle to brittle-ductile northeast-striking, steeply south-dipping Kirkland Lake fault (the Main Break) crosscuts clastic and volcanic rocks and syenitic stocks of the Timiskaming assemblage approximately 2 km north of LLCDZ (Teck Township transect area). Gold mineralization of the Kirkland Lake camp occurs along this fault and its immediate splays. In the western part of the camp, mineralization is controlled by the ’04 Break, a northeast-striking, south-dipping fault located 120 to 140 m north of the Main Break (Charlewood 1964; Still 2001).

DEFORMATION FABRICS

All deformation features documented in this project affect Timiskaming assemblage rocks. Previously, Wilkinson, Cruden and Krogh (1999) classified the oldest fabric in the Timiskaming assemblage as corresponding to the second deformation event (D2); the earlier event (D1) was interpreted as responsible for pre-Timiskaming thrusting and folding that did not produce penetrative fabrics. In this study, we document evidence for an early, not fabric-forming deformation that affected Timiskaming rocks and predated the D2 event. In the east of the Gauthier Township transect area, there are bedding facing reversals in predominantly northwest-striking, northeast-dipping Timiskaming (≥2677 Ma) turbidites. The oldest foliation, S2, overprints both directly facing and overturned beds with consistent counterclockwise orientation. This implies that facing reversals could not have resulted from D2 folding, but are instead related to an older deformation event. It is possible that the early deformation that was previously interpreted as entirely pre-Timiskaming spanned into Timiskaming time, or there could be a separate syn-post-Timiskaming non-foliation-forming deformation pulse that predated the formation of the earliest fabric. Since the presently available data are inconclusive in this respect, we follow the nomenclature of Wilkinson, Cruden and Krogh (1999) in which the earliest deformational fabric in Timiskaming assemblage rocks is attributed to D2.

S2 is the earliest regional fabric and the main foliation of the Larder Lake and Upper Canada deformation zones. It is defined by flattened clasts in conglomerates and tuffs, and by penetrative schistosity and compositional banding of secondary chlorite, talc, white mica, fuchsite and carbonate in hydrothermally altered mafic, ultramafic and alkalic metavolcanic rocks. In Teck Township, S2 occurs within the 400 to 500 m wide Larder Lake–Cadillac deformation zone. In Gauthier Township, the fabric occurs within a broader (~1300–2100 m wide) halo that extends from the southern flank of the Larder Lake–Cadillac deformation zone to the Upper Canada deformation zone and about 400 to 500 m further north. S2 is a steeply dipping fabric, orientation of which varies broadly from northeast (~060–070°, e.g., Upper Canada deformation zone) to east (e.g., at the Teck–Lebel townships border) and to southeast (~110–150°, e.g., eastern part of Gauthier Township transect). Within the LLCDZ, S2 appears to generally follow the orientation of the deformation zone. Stretching lineation (L2), associated with S2, is defined by stretched clasts in conglomerates and tuffs, varioles in mafic metavolcanic rocks, and rod-like secondary mineral aggregates in hydrothermally altered rocks. Lineation L2 is particularly well developed in Gauthier Township where it plunges moderately (35–60°) to the east.

S3 is a north-trending (~340–020°) steeply dipping crenulation cleavage. It is best documented in the Upper Canada deformation zone and also identified in several other locations in Gauthier Township. Structural timing of the cleavage is constrained by relationships with S2 and S4: S3 crenulates S2, is axial planar to symmetric and S-asymmetric folds of S2, and is overprinted by S4. Similarly oriented, north-trending cleavage axial planar to symmetric and Z-asymmetric folds of S2 was mapped in Teck Township, in carbonate-fuchsite-altered ultramafic rocks within the LLCDZ. No unequivocal overprinting by S4 was documented there, and the north-trending fabric was assigned to S3 based on similarity in orientation with the S3 foliation of the Gauthier Township transect.

Foliation S4 trends northeast in the Gauthier Township (060–080°) and the Teck Township (040–060°) transects. It is a steeply dipping regional foliation axial planar to outcrop-scale Z-asymmetric and, more rarely, symmetric F4 folds. Locally, foliation changes orientation to east and even east-southeast, due to deflection along narrow high strain zones. However, on a regional scale, the orientation of S4 is relatively constant, and there is no systematic change in the S4 trend with increasing or decreasing distance to the LLCDZ. Most commonly, S4 is a discrete crenulation cleavage axial planar to microfolded bedding and S2 fabric; in Timiskaming assemblage conglomerates in Teck Township, S4 is defined by pebble flattening.

A late crenulation cleavage, S5, was observed in the Larder Lake–Cadillac deformation zone, in the eastern part of the Gauthier Township transect. It strikes 130 to 170°, dips 30 to 80°W, overprints S2 and S4 and is commonly axial planar to S-shaped folds of S2. No map-scale structure is associated with this fabric.

KINEMATIC INDICATORS IN THE LARDER LAKE–CADILLAC DEFORMATION ZONE

Asymmetric shear sense indicators were mapped at two locations along the Larder Lake–Cadillac deformation zone in Gauthier Township. In the northern wall of the flooded McBean open pit, where highly strained Timiskaming assemblage conglomerates with well-developed stretching lineation (L2) are exposed. On the surface that is parallel to L2 and perpendicular to S2, some of the least strained pebbles show asymmetric pressure shadows indicating oblique reverse-dextral slip (south side over north and to the west) along the direction of stretching lineation.

The other location is the stripped outcrop at the Princeton property, eastern part of the Gauthier Township transect. Here, shear sense is indicated by a combination of dextral Z-shaped drag folds, asymmetrical recrystallized tails around pebbles, the clockwise orientation of extensional quartz-carbonate veins with respect to foliation (S2), and offsets of these veins along S2. The interpreted movement direction is similar to that documented at the McBean pit, that is, oblique reverse-dextral slip parallel to the L2 stretching lineation.

GOLD MINERALIZATION

Production commenced in 1915 and, through the 20th century, the Macassa, Kirkland Lake Gold (later Kirkland Minerals), Teck–Hughes, Lake Shore, Wright–Hargreaves, Sylvanite and Toburn mines collectively produced 758.3 metric tonnes of gold with an average grade of 15.21 g/t (Gosselin and Dubé 2005) from one giant gold deposit (the Kirkland Lake deposit). Underground workings extend to ~2.5 km below the surface in the central part of the orebody, and mineralization remains open to depth (Charlewood 1964). The Upper Canada Mine produced 43.49 tonnes of gold at a grade of 10.3 g/t. Gold mineralization examined in this study includes the gold lodes of the Kirkland Lake deposit (underground in Macassa Mine and surface exposures on Wright–Hargreaves, Lake Shore, and Teck–Hughes properties), the past-producing Upper Canada Mine (L zone), and occurrences hosted by the LLCDZ.

Mineralization of the Upper Canada Mine (Gauthier Township) is confined to a ductile Upper Canada deformation zone. In the L zone, the most productive mineralized zone of the mine, gold occurs in thin (2–5 mm) S2-parallel, quartz-carbonate bands or veinlets in quartz-sericite-carbonate-pyrite pervasively altered and foliated Timiskaming assemblage tuff. Strong bulk carbonatization is characteristic of the mineralized zone. As evident from relationships of alteration assemblages and deformational fabrics, hydrothermal activity spanned through three deformation stages (D2 to D4). Gold mineralization was emplaced relatively early, during D2, and was overprinted by subsequent deformation. The D4 overprint is particularly notable: the mineralized zone as a whole and individual gold-bearing quartz-carbonate bands and veinlets are folded into Z-asymmetric folds with locally developed axial planar S4.

Gold occurrences at the Anoki and McBean properties are localized within, or in immediate proximity to, the first-order LLCDZ. Mineralized zones are not exposed at surface and were observed in drill core. Mineralization occurs as 1) sulphidized Fe-tholeiite flows (Anoki Main zone); 2) quartz stockworks in carbonate- and carbonate-fuchsite-altered ultramafic rocks (“green carbonate” McBean and Anoki Deep zones); 3) sulphidation and quartz veining with visible gold in Timiskaming clastic rocks, spatially associated with feldspar-phyric dikes (40 East zone); and 4) quartz veining with native gold and sulphides in cherty to graphitic exhalite horizons in basalts (Anoki South). Mineralization is typically accompanied by strong host-rock carbonatization. Relationships between carbonate-fuchsite alteration assemblage and deformational fabrics present in drill core from the footwall of the McBean zone are compatible with broad syn-D2 timing of alteration.

Mineralized zones of the McBean and Anoki properties constitute part of a regional-scale hydrothermal system that corresponds to an approximately 20 km long segment of the Larder Lake–Cadillac deformation zone from the Kerr–Addison–Chesterville gold deposit (McGarry Township) in the east to the Anoki area (Gauthier Township) in the west. Other gold deposits of this group include Cheminis and Omega occurrences in McVittie Township. Sulphide-rich replacement ores in mafic (mostly tholeiitic) metavolcanic rocks (“flow ore”) account for most production and resources, native gold-bearing quartz stockworks in carbonate-fuchsite-altered meta-ultramafic rocks (“green carbonate ore”) rank second.

Gold deposits and occurrences of the Larder Lake–Cadillac and Upper Canada deformation zones are likely related. The Upper Canada deformation zone is interpreted as a splay of the Larder Lake–Cadillac deformation zone, both structures were active during D2 and likely were hydraulically connected. Geochemical signatures of gold occurrences hosted by two deformation zones are generally compatible. Plunge of ore zones at the Upper Canada Mine and the McBean, Cheminis and Kerr–Addison deposits is approximately parallel to L2, which supports similar structural timing of Upper Canada and Larder Lake–Cadillac gold mineralization. Syn-D2 timing of Upper Canada mineralization documented in this study, and evidence supporting close relationships between the Upper Canada and Larder Lake–Cadillac mineralized systems suggest that gold mineralization hosted by LLCDZ probably was broadly synchronous with D2.

Mineralization of Kirkland Lake camp (i.e., Toburn, Sylvanite, Wright–Hargreaves, Lake Shore, Teck–Hughes, Kirkland Lake Gold and Macassa mines) consists of gold and telluride-bearing quartz veins associated with brittle to brittle-ductile Kirkland Lake fault (Main Break) and the '04 Break, as well as with immediate splays of with these two faults. Presence of open-space-filling textures in veins, and the association of veins with brittle faults suggest relatively shallow crustal levels of mineralization. Relationships of gold-bearing veins, intra-mineral alkalic dikes and deformational fabrics, as well as presence of S4-parallel syn-mineralization stylolites and cataclastic breccias in gold-bearing quartz veins suggest that mineralization could have formed early in the D4 event synchronous with south-over-north reverse-dextral to reverse movement along the Main Break. However, the presently available evidence supporting temporal overlap of mineralization and D4 is relatively sparse, and it is possible that mineralization predated the D4 event.

The positive correlation between high tellurium and gold content and the fact that the deposit is hosted within an alkalic multiphase intrusive complex clearly indicate that the Kirkland Lake gold deposit shares very strong analogies with gold deposits related to alkalic magmatism (e.g., Jensen and Barton 2000). The key geological parameters that support such an analogy include 1) location of the mineralized system in an area characterized by protracted multi-stage alkalic magmatism (both volcanic and intrusive) and its spatial association with a multi-phase alkalic stock; 2) gold- and telluride-rich high-grade mineralization; 3) base metal-poor quartz-carbonate veins with high Au/Ag ratio; 4) carbonatization and K metasomatism (sericite alteration); 5) enrichment in molybdenum; and 6) structurally focussed zones of high-grade mineralization.

If the Kirkland Lake gold deposit is indeed related to alkalic magmatism, the parent intrusion is yet to be identified. At present, it is impossible to establish a definite genetic link between gold mineralization and any specific magmatic phase. Direct structural relationships imply that mineralization postdated the emplacement and, most likely, complete crystallization of the syenite porphyry stock, because the ore-controlling Main Break and subsidiary structures cut and displace the intrusion in a brittle fashion. Moreover, the ≥2.5 km vertical extent of mineralization in the syenite porphyry, consistent association of gold-bearing veins with discrete brittle faults throughout this vertical interval, and apparent lack of zoning and features indicative of magmatic–hydrothermal transition within the intrusion, imply that hydrothermal fluids probably were not derived directly from the syenite porphyry host. A deep magmatic source (i.e., larger intrusion or magmatic chamber at depth) is more probable. Whether syenitic intrusions exposed at present erosional level and mineralizing fluids of the Kirkland Lake gold deposit were derived from a single deep magmatic source, or they instead represent two different magmatic "events" within the Timiskaming-type, predominantly alkalic magmatic cycle, remains completely unclear. This is mainly because the length of the time gap between emplacement of the syenite porphyry and formation of gold-bearing veins is unknown, due to inconclusive nature of presently available geochronological data. The occurrence of intra-mineral alkalic dikes is important. Even though these very small dikes are unlikely to be genetically related to mineralization, their presence indicates that alkalic magmatism overlapped in time with hydrothermal activity, and thus the existence of a deep magmatic chamber (i.e., potential fluid source) is geologically feasible.

However, regardless of the timing of Kirkland Lake mineralization and many uncertain details of its genesis, the distinct metal inventory (Te>Au, Mo, Pb, Ag, high Au/Ag, low As) of gold-bearing veins indicates a distinct fluid source, that is, different from the source that contributed fluids for gold deposits and occurrences clustering along the Larder Lake–Cadillac deformation zone and its splays. Based on presently available data, a deep alkaline magmatic fluid source (magmatic chamber or intrusion at depth) for Kirkland Lake gold mineralization appears most probable.

The Narrows Break mineralized zone, located approximately 350 m north of the Main Break, consists of sheeted gold-bearing carbonate-quartz veinlets enclosed in carbonatized and sulphidized (pyrite) Timiskaming assemblage sandstones, reworked tuffs, and mafic syenites. This mineralization differs in style, alteration and geochemistry from typical Kirkland Lake gold-bearing veins, and probably represents a separate hydrothermal system. Relationships between S4 and sheeted veinlets of the Narrows Break mineralized zone imply syn-D4 timing of mineralization.

INTRUSION SUBPROJECT

The Intrusion Subproject (MacDonald, Piercey and Hamilton 2005) is aimed at understanding the relationship of intrusions to gold and base metal mineralization in the Abitibi greenstone belt of Ontario, and was subdivided into 2 smaller projects: 1) intrusions associated with gold in the Timmins Camp, and 2) the relationship of the Clifford stock and the Blake River Group in eastern Ontario to base metal and gold mineralization in Clifford Township (*see* Figure 1).

Porphyry intrusions in the Timmins camp were studied from Bristol Township, west of Timmins, through the Timmins camp proper, across to Carr Township, east of Timmins, so as to compare porphyries within the main gold camp to those outside of the main camp. The porphyry intrusions in the Timmins camp and area have been subdivided into 5 trends depending on geographic location. These trends are east-trending belts ranging from 4 to 20 km long that are typically composed of numerous intrusions ranging from small dikes a few hundred metres long to oval bodies that are up to 11 km long. The porphyry intrusions generally intrude into the Vipond Formation of the Tisdale assemblage, but also at the Deloro–Tisdale and Tisdale–Porcupine assemblages contacts; the porphyry intrusions are generally semi-conformable to stratigraphy. The majority of the porphyry intrusions were emplaced predominantly at 2687 to 2691 Ma (Ayer, Barr et al. 2003; Corfu et al. 1989), although the Aquarius porphyry was emplaced at 2705 Ma (Corfu et al. 1989), and the Pamour porphyry was emplaced at 2677.5 Ma (this study). The bulk of the gold-associated intrusions are high-aluminum (high-Al) tonalite-trondhjemite-granodiorite (TTG) suite intrusions with light rare earth element (LREE)-enrichment, heavy rare earth element (HREE) and yttrium depletion, and high Al_2O_3 contents; these signatures are very similar to modern-day adakitic magmas. The porphyry intrusions in the Timmins camp, even though spatially associated with gold and copper mineralization, have no genetic relationship to gold largely because 1) gold-bearing veins crosscut both the porphyry intrusions and the rocks that host the porphyries; 2) they are hosted in structurally controlled vein arrays; and 3) recent Re/Os ages obtained from gold-associated molybdenite (Ayer, Barr et al. 2003) illustrate that the porphyries are 17 to 30 million years younger than the gold mineralization event. Nonetheless, gold mineralization is typically associated with 1) clusters of porphyry intrusions (e.g., Dome and Hollinger–McIntyre mines) with high-Al TTG signatures; 2) porphyries that have strong associations with major structures; and 3) porphyries that have undergone sericite (±carbonate) alteration (significant sodium losses and potassium metasomatism).

The rocks of the Blake River Group in Clifford Township consist predominantly of basalt to andesite with lesser rhyolite, and associated synvolcanic, high level rhyolitic intrusive rocks, and synvolcanic gabbro and diabase. The Blake River Group rocks have lithogeochemical signatures similar to modern enriched mid-ocean ridge basalt (E-MORB) and many have evidence for crustal contamination (contaminated E-MORB). The Clifford stock and age equivalent east-northeast-trending dikes from Clifford Township crosscut the Blake River Group and represent a distinctively younger pulse of magmatic activity within northeastern Ontario. Contrary to previous assertions, the Clifford stock has yielded a U/Pb zircon age of 2686.9±1.2 Ma, and an age equivalent east-northeast-trending dike has yielded an age of 2688.5±2.3 Ma. These ages are younger than the Blake River Group magmatism in this

area (ca. 2700–2696 Ma: Péloquin and Piercey 2005), but are similar to other late tectonic TTG plutons in the southeastern Abitibi greenstone belt (e.g., Clarice Lake, Lac Dufault; Corfu and Noble 1992; Mortensen 1993). The Clifford stock and equivalent rocks have very distinctive lithogeochemical signatures typical of high-Al TTG suites, and have very distinctively low Y (<10 ppm) and Yb (<2 ppm), and high Zr/Y (>7), Nb/Y (>0.4), Al_2O_3/Yb (>10), and La/Yb (>10) ratios, as compared to the older Blake River Group rocks; these features can be used to geochemically discriminate felsic magmatism associated with the Blake River Group from younger TTG-related magmatism associated with the Clifford stock and other TTG magmatism (ca. 2690 Ma).

Mineralization in Clifford Township consists of an older VMS-related style of mineralization, and a younger, overprinting porphyry copper-molybdenum-gold (Cu-Mo-Au) style of mineralization. The VMS-related mineralization consists of epidote-quartz-pyrite-chlorite assemblages, typical of semi-conformable-style alteration associated with permeable zones (e.g., amygdules, pillow margins and interpillow regions) in the volcanic rocks of the Blake River Group. There are also some zones of higher temperature chlorite-quartz-chalcopyrite-pyrite assemblages typical of pipe-like alteration. The younger porphyry Cu-Mo-Au style mineralization occurs as a series of breccia pipes and stockwork vein systems. This latter style of mineralization is associated with a complex array of veinlet and vein-styles of alteration that is quite distinctive from VMS mineralization. The fact that this mineralization is hosted in the Clifford stock and associated dikes that are circa 2690 million years old suggests that this mineralization represents a distinctly younger magmatic-hydrothermal event, distinctive from the early VMS-related event.

METAMORPHIC SUBPROJECT

The Metamorphic Subproject of the Greenstone Architecture Project, Discover Abitibi Initiative, is designed to address a significant gap in knowledge of the geological setting of gold deposits and of the application of metamorphic data and concepts to gold exploration in the Timmins–Kirkland Lake area. There are three reasons why this gap should be filled. First, some metamorphic zone boundaries may be themselves valid gold exploration targets (Hall 1998, using data from Mikucki and Roberts 2004; Thompson 2002, 2003, 2005). Second, metamorphic data and the concepts developed to explain the origin of metamorphic rocks impose constraints on the geological setting of gold deposits and the mineralization and alteration therein. Third, this project provides a basis for comparison of the metamorphic settings of the Timmins and Kirkland Lake gold camps with each other and with the less productive adjacent parts of the greenstone belt. Map-scale variations of metamorphic grade combined with textures and mineral assemblages are the basis for analysis and interpretation of the spatial and temporal relationships between metamorphism and magmatism, deformation, alteration, and gold mineralization. The resulting metamorphic framework (Thompson 2005) advances knowledge of known gold deposits and helps to define new exploration targets.

Subdivision of the greenschist zone using the appearance of biotite in metamorphosed quartzofeldspathic and aluminous rocks and the appearance of amphibole in metamorphosed ultramafic rocks (Table 7) reveals a striking spatial relationship between the metamorphic zone boundary and a significant number of past and presently producing gold mines (Figure 27). Higher priority targets are defined by the coincidence of metamorphic anomalies defined by the boundary with major structural features, particular rock compositions, and moderate to intense deformation and/or alteration. For example, in Tully, Prosser, and Wark townships, a lenticular zone of upper greenschist grade rocks surrounded by lower greenschist zone rocks is associated with a northeast-trending fault zone, a small alkalic pluton and, at the northeast end, numerous gold occurrences. On a smaller scale, the linear array of metamorphic “hot” spots located between two branches of the Destor–Porcupine fault in Whitney Township may be significant. A more detailed examination of the relationship between a metamorphic

Table 7. Diagnostic mineral assemblages (point data) are the basis for the definition of metamorphic grade in each metamorphic zone. Metamorphic zones (*see also* Thompson 2005, Figure 2, back pocket) are derived from the grade in one or more rock associations. The first digit of the two-digit number in each cell indicates the rock association. The second digit indicates the relative metamorphic grade for the rock association (higher number, higher grade). The relative positions of the boundaries in rock associations 2 to 7 that correspond approximately to the lower/upper greenschist zone boundary on the map are inferred. The precise positions of these boundaries relative to each other have yet to be calibrated. Mineral name abbreviations: ab - albite, act - actinolite, am – amphibole undifferentiated, and - andalusite, bt - biotite, cb – carbonate (ankerite, calcite, dolomite, magnesite, siderite), cht - chlorite, crd - cordierite, ctd - chloritoid, cum - cummingtonite, diop - diopside, epg - epidote group, grt - garnet, gru - grünerite, hn - hornblende, kf - potassium-feldspar, mt - magnetite, plg - plagioclase, se - serpentine, sil - sillimanite, st - staurolite, tlc - talc, trm - tremolite, wm - white mica (muscovite, paragonite, talc).

Rock Association	**Metamorphic Grade**				
	Sub-greenschist Facies	Greenschist Facies			Amphibolite Facies
	Metamorphic Zones on Map				
	Sub-greenschist Zone	Lower Greenschist Zone	Upper Greenschist Zone	Transition Zone	Amphibolite Zone
	Diagnostic Mineral Assemblages				
1) Metabasites: metabasalt/gabbro/diabase, greenstone, amphibolite, meta-andesite	10 prn, prn-pu	11 act-cht-epg-ab		12 act-hn	13 hn-plg(calcic)
2) Metaquartzofeldspathic rocks: metarhyolite/dacite, qtz-fp metaporphyry, felsic metavolcaniclastite, metawacke	20 prn, prn-pu cht-wm	21 cht-wm cht-kf cht-wm-cb	22 bt epg-act		23 bt-hn
3) Metamorphosed ultramafic rocks: metakomatiite, metaperidotite/dunite	30	31 cht-tlc-cb, se-cht cht-tlc-se-cb	32 clinoamphibole (trm, cum)		
4) Metamorphosed aluminum-rich rocks: metashale/siltstone, metahydrothermal alteration	40	41 cht-wm	42 bt, bt-grt, ctd-cht		43 crd-and/sil-bt st-and/sil-bt, crd orthoamphibole
5) Chemical metasedimentary rocks, meta-iron formation	50 minesotaite greenalite	51 qtz-cht, cht-cb, mt-qtz	52 clinoamphibole (cum/gru), am-grt, two am		
6) Metamorphosed granitoids: metagranite to metatonalite	60 prn, prn-pu	61 cht-kf, cht-wm	62 bt, bt-epg, bt-epg-am		
7) Metamophosed carbonate-rich rocks: carbonate metasediments, meta-interpillow rock, metahydrothermal alteration, cht-cb schist	70	71 cht-cb-qtz cht-cb-wm-qtz	72 bt-cht-cb epg-cht-am-cb		73 diop-am-grt, hn-bt-qtz
8) Unmetamorphosed granitoids: granite to tonalite	80 no metamorphic minerals				

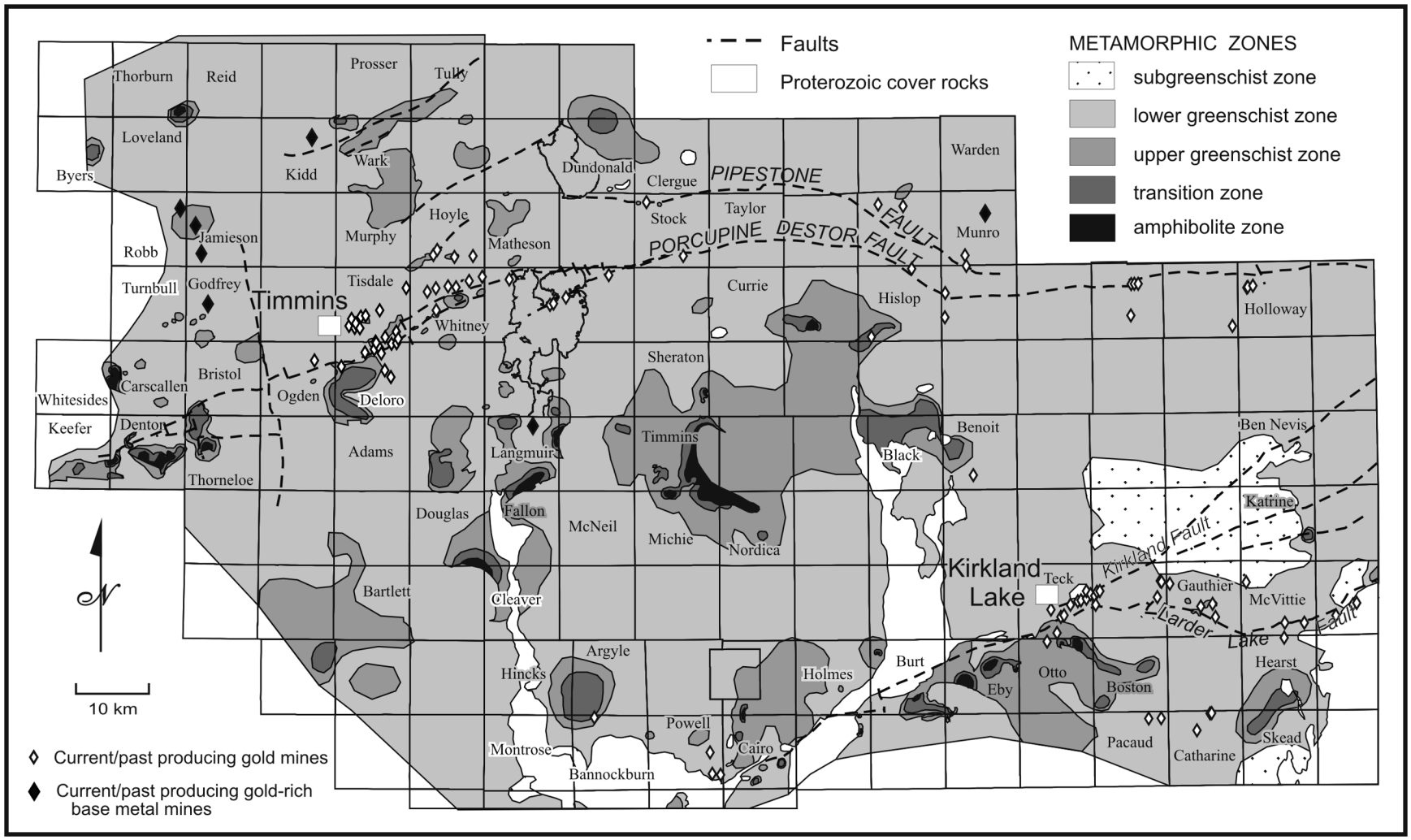

Figure 27. Simplified page-size version of the metamorphic map of the Timmins–Kirkland Lake area (*from* Thompson 2005, p.6). To improve clarity, the metamorphosed granitoids, the UTM grid, and gold occurrences have been omitted. Note, for example, the spatial relationship between metamorphic anomalies defined by the boundary between the lower and upper greenschist zones and current and past-producing gold mines east and northeast of Timmins and east of Kirkland Lake.

anomaly and the Dome Mine (Figures 28 and 29) raises the possibility that metamorphic anomalies indicate which segment of a regional scale deformation or alteration zone has the highest potential to contain a large gold deposit. One of the two small metamorphic anomalies mapped along the Pipestone fault in Stock Township is spatially associated with the Clavos Mine.

The irregular metamorphic pattern in the project area is attributed to superposition of subgreenschist- and greenschist-grade regional metamorphism on narrow higher grade contact metamorphic aureoles that formed at different times immediately adjacent to felsic porphyries, felsic to intermediate granitoids and alkalic intrusions. The metamorphosed plutonic, volcanic and sedimentary rocks now at the surface reached maximum pressures (depths of 8–10 km) and temperatures (350 to 450°C) during the main phase of ductile deformation that occurred after deposition of the Timiskaming assemblage. Metamorphic data are consistent with the idea that the pre-Timiskaming phase of deformation was less penetrative and occurred at shallower depths and lower temperatures in the crust.

Metamorphic mineral assemblages indicate that rocks in the study area were well within the range of temperature and pressure that is favourable for gold deposition for tens of millions of years (Figure 30). Clearly, the period when peak metamorphic conditions prevailed and the predominant second phase of ductile deformation was in progress was the most conducive for synmetamorphic (orogenic) gold mineralization. At this time, metamorphic fluid production was at a maximum and ongoing deformation increased the potential for formation of structural conduits and traps. However, in view of the metamorphic data indicating pre-metamorphic ages for most of the intrusive plutonic rocks that are prominent in the southwest half of the project area, perhaps gold exploration models related to granite- and porphyry-related gold should be considered in this part of the area.

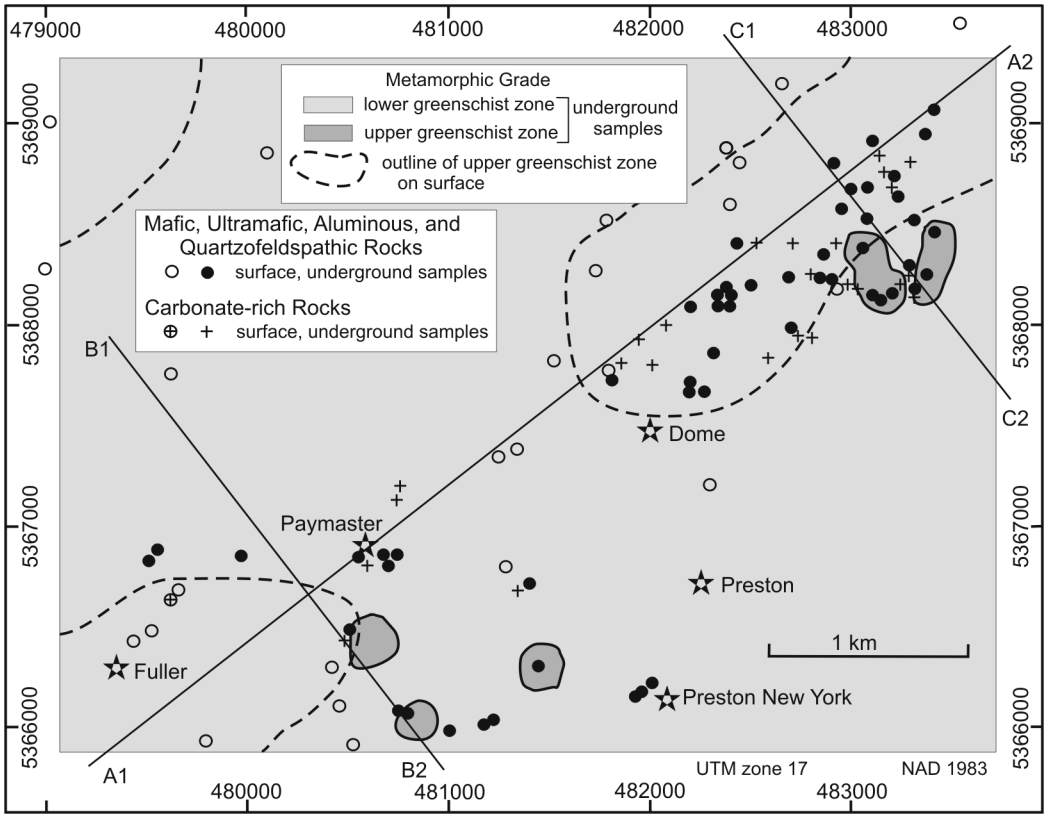

Figure 28. Metamorphic map in the vicinity of the Dome and Paymaster mines (*after* Thompson 2005, p.19). See Figure 29 for profiles A_1–A_2, B_1–B_2 and C_1–C_2. Underground samples and inferred upper greenschist zone metamorphic anomalies projected to the surface along vertical lines.

A regional-scale project of this kind must balance the conflicting demands of covering the designated area and of obtaining a data density adequate to define reasonably well-constrained metamorphic exploration targets. Definition of many of the metamorphic anomalies with gold potential that are outlined on the metamorphic map of Timmins–Kirkland Lake area (*see* Figure 27; Thompson 2005) can and should be improved with additional sampling in key target areas. More complete analysis and interpretation of the spatial relationships between the intensity of strain, the type and intensity of alteration, and metamorphic zone boundaries is required. Future work should address also the low density or absence of data in the northwest, south-central and northeast sectors of the map presented here and extend metamorphic mapping to the north and southwest in Ontario and eastward into Quebec.

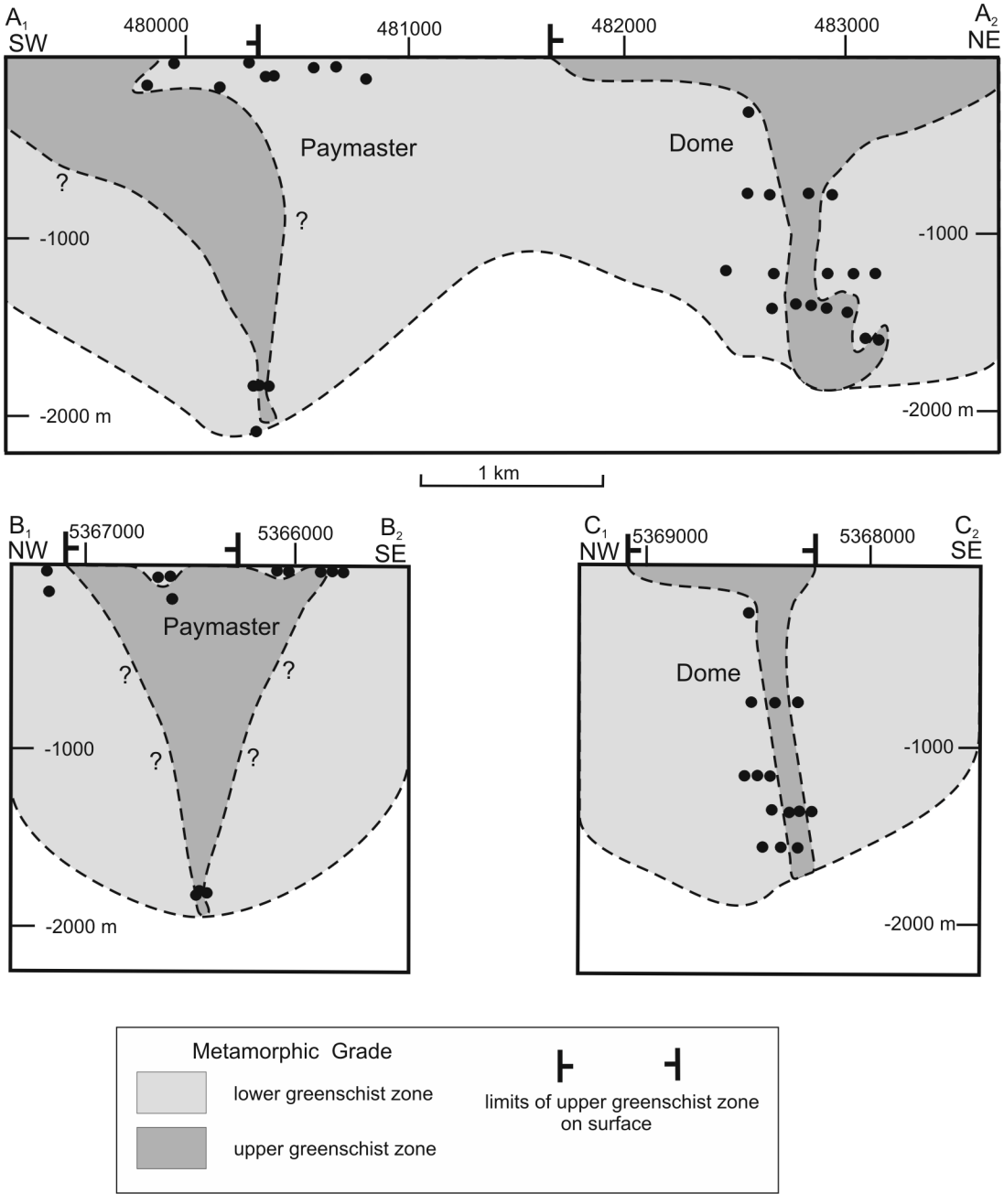

Figure 29. Underground data projected onto vertical profiles oriented parallel and perpendicular to the main structural trend through the Dome and Paymaster mines indicates that metamorphic anomaly is a linear feature (*from* Thompson 2005, p.19).

Recommendations

- Further testing of metamorphic tools for gold exploration should be done by increasing the density of data in and around metamorphic anomalies that are associated with known gold deposits and by exploring metamorphic anomalies in areas where gold mines have not yet been found (e.g., 20 km north and 10 km south of Timmins; Pipestone fault).

- The low density of metamorphic data in the northwest, south-central, and northeast sectors of the metamorphic map should be improved and metamorphic mapping extended to the north and southwest in Ontario and eastward into Quebec.

- More comprehensive analysis and interpretation of the spatial relationships between the intensity of strain, type and intensity of hydrothermal alteration and metamorphic zone boundaries should be done.

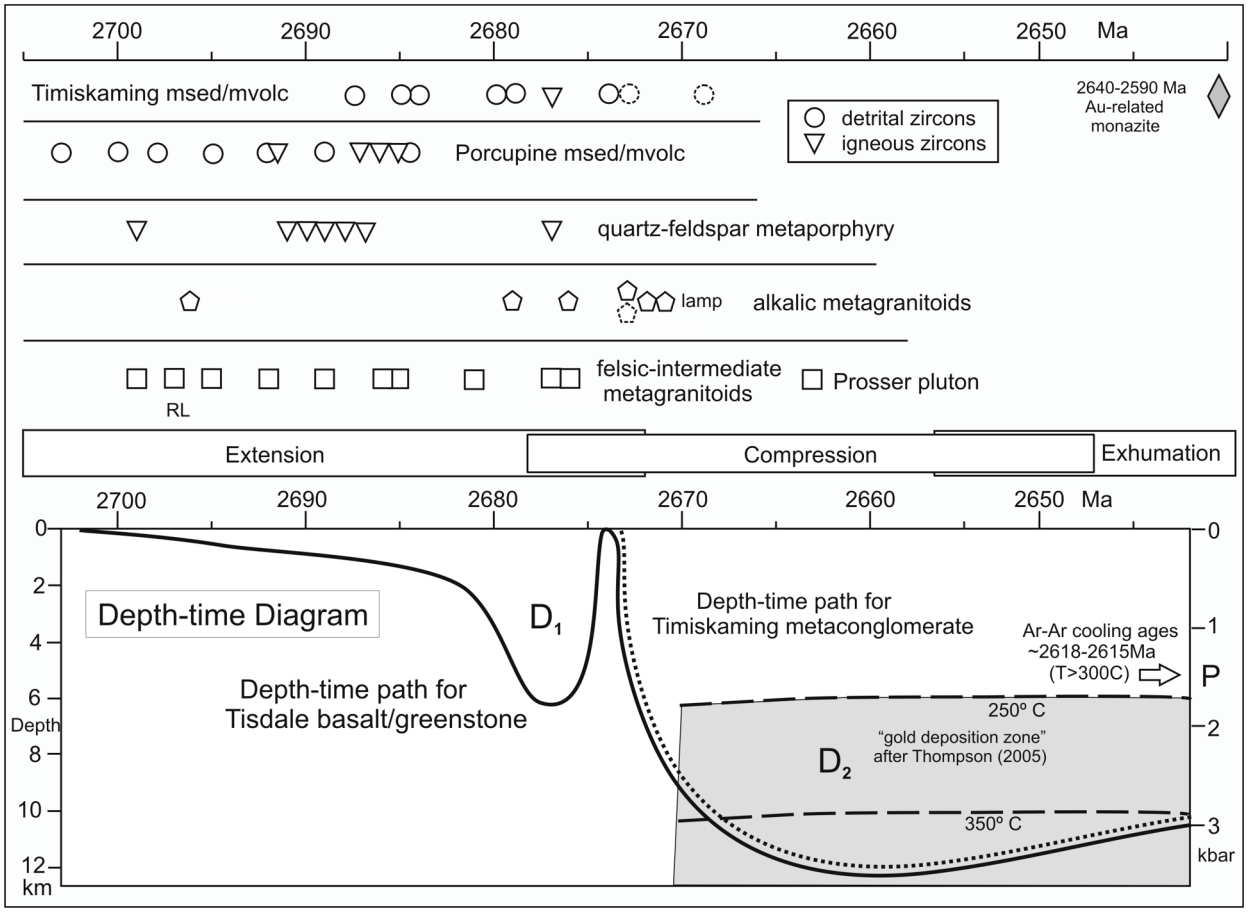

Figure 30. Depth–time diagram illustrating history of 2 hypothetical samples (Tisdale basalt or greenstone, Timiskaming conglomerate or metaconglomerate) with respect to a simple three-stage model of the tectonic evolution of part of the western Abitibi greenstone belt (*from* Thompson 2005, p.23). Geochronology *after* Ayer et al. (this report), Ayer, Barr et al. (2003), Hanes et al. (1989) and Schandl et al. (1991).

GEOPHYSICS SUBPROJECT

Magnetic and Gravity Three-Dimensional (3D) Modelling

In this study, three-dimensional (3D) inversions of magnetic and gravity data were carried out on 10 areas, which extend from the Kamiskotia area, west of Timmins, to Gauthier Township, east of Kirkland Lake (Reed 2005a, 2005b). Geophysical data for the Tully–Prosser townships area was included in the 3D inversions, but was not studied geologically. The 3D inversions were carried out using the University of British Columbia Geophysical Inversion Facility (UBC–GIF) inversion codes (MAG3D 1998; GRAV3D 2001) and were run as uncontrolled inversions. The starting points for these inversions were magnetic maps from various airborne surveys (OGS Operation Treasure Hunt and Discover Abitibi surveys) and ground and airborne gravity surveys from the Ontario Geological Survey gravity database and recent airborne surveying done under the Discover Abitibi Initiative. The products of the 3D inversions present magnetic susceptibility or density contrasts as isosurfaces in defined three-dimensional blocks that correspond with a software-generated model of the 3D source of the surface response.

The Timmins–Kirkland Lake area of the Abitibi greenstone belt holds considerable promise for the development of views into the third dimension using geophysical data and 3D imaging. Many of the data sources appear coherent and well defined, which are ideal for inversions as produced in this program. The geological interpretation is enhanced through integration of the surface geology with the three-dimensional view of stratigraphy and lithology derived from the geophysics.

Responses in the potential field data at surface represent volumes with contrasting magnetic or density parameters. Simple interpretative models such as 2 or 2.5 dimensional models have become insufficient to describe the three-dimensional potential field earth. At present, three-dimensional inversion of potential fields is being used to develop images of source bodies (Li and Oldenburg 1996, 1998a, 1998b). Three-dimensional potential field imaging has been used to interpret regional and mineral deposit-scale environments (Boulanger and Chouteau 2001; Oldenburg, Li and Ellis 1997). While 3D images presented as magnetic susceptibility or density contrasts need to be treated with some care and caution, as a number of solutions are possible with potential field data, they represent a significant advance over previous simple modelling methods.

Some processing has been done to optimize the gravity and magnetic data for 3D inversion. The magnetic data are delivered with the International Geomagnetic Reference Field (IGRF) removed, and the grid has been levelled to the Ontario master magnetic grid. The total Bouguer gravity response has been filtered to remove a broad regional field, leaving local anomalies produced by relatively near-surface sources. The filter used was a 10 kilometre bandpass (Geosoft® processing). This filter processes the gridded Bouguer response to remove all wavelengths longer than 10 km. The resultant response shows sources having widths of up to 5 km and having depths and depth extents of 2.5 km or larger. It will be noted that these maps correlate reasonably with generalized surface geology. It has proven beneficial to use flat-map gridded data with the regional field removed (for both magnetic and gravity data) for the 3D inversions (Gupta and Ramani 1980). The inversions then focus on the near surface events.

Filtering of the gravity data results in a map with both positive and negative Bouguer residual values, which depart from a zero background. These represent high and low density contrasts from an average background and can be represented as high and low density isosurfaces in the imaging. Extraction of the negative component for imaging has been accomplished here by multiplying the residual anomaly by –1 and re-running the 3D inversion. (Note the Tisdale–Deloro example discussed below).This was needed for imaging the low density components in the model. Alternatively, the same result may be achieved by multiplying the positive inversion by –1, but this has proven computationally difficult because of the size

of the inversion product. (Recent additions to the WinDisp software permits converting the inversion model directly to negative components; other imaging systems may handle this differently.)

The 3D inversions have been imaged using viewer software (WinDisp 3DViewer, Scientific Computing and Applications) and presented as freeze-frame images (bitmaps) displaying various aspects of the view. The viewer can see the selected product images, without loading the viewing software, provided with the report of this work (Reed 2005a). The image shown here is from the Currie Township area (Figure 31, Chart A, back pocket). The magnetic model (orange to red) extends to a depth of 3.75 km (as seen by the upper wire frame). The positive gravity model in green extends to a depth of 5 km (lower wire frame). The image also contains amplitude-enhanced magnetic data on and above the surface of the model (an additional product developed in WinDisp, but not a part of the 3D process). The view looks west from slightly below the surface. The 3D magnetic image suggest a syncline in mafic volcanic rocks on the south (left) side. The gravity image suggests an overall south dip. The conflict between the northerly dipping magnetic images at the south edge and the southerly dipping gravity is not resolved. It has been recognized that different mafic volcanic rocks north of the magnetic unit have bimodal densities but low magnetic response. The more dense unit to the north (right) appears to dip steeply to the north.

The amount of point data used to construct the primary images determines the resolution achieved in the inversion. The magnetic data have the highest resolution (survey lines spaced 50 to 150 m apart), and show dips, plunges and extensions to depth in the inversions (a few hundred metres to several kilometres). The gravity inversions are less detailed as the primary data represents data points spaced an average of 1 km apart. These inversions show broad features commonly with substantial depth extent (several kilometres in the Currie Township example), which may complement or, in places, contrast with the magnetic inversions. A byproduct of this subproject has been the development of magnetic, gravity and geologic maps which have been brought together in various viewing relationships. These provide the ability to refine the surface geologic maps and distinguish among rock units not easily separated in the existing mapping. Geological interpretation, structure and stratigraphy in the third dimension are suggested by these results.

Three-dimensional inversion images may be presented together. Figure 32 (Chart A, back pocket) is an example from the Tisdale–Deloro townships area—the core zone of Timmins camp gold production—containing the Hollinger–McIntyre gold mines in the west-central area and the Dome Mine towards the southeast corner. The 3D magnetic inversions are represented in apple green, with yellow and red cores (succeeding isosurfaces). The 3D gravity inversion is represented by aquamarine (positive shell) and light green (negative shell). The positive gravity expression, to the north and south, and associated magnetic highs correlate with mafic to ultramafic volcanic rocks of the Tisdale assemblage. This view from above helps visualize some of the features extracted from the surface maps by the 3D process. Near the centre of the image, a magnetic feature extends into a trough within a large, low density feature. Some caution is needed because of the differences in resolution of the magnetic and gravity data, but there is an appearance of magnetic and perhaps more dense volcanic rocks overlying lower density felsic volcanic rocks and/or sedimentary rocks of the Porcupine assemblage.

The WinDisp software permits the presentation of geology on top of the 3D inversion. Products from the Clifford–Ben Nevis–Arnold–Katrine townships area are displayed in a view looking north (Figure 33, Chart A, back pocket). The geology has been made transparent to better view the 3D inversion of the negative or low density component of the gravity underneath. The geology used is from Ayer, Berger and Trowell (1999). The core of the Clifford stock is identified by the red feature over the larger 3D gravity low event. Surrounding the stock are felsic volcanic units that are the likely source of the low gravity field.

The Clifford stock sits in a depression in the density low, or higher density event, as can be seen in Figure 34 (Chart A, back pocket) showing a north-south slice through the stock and surrounding volcanic

rocks looking east. Note the geology at the surface. The low-density 3D shell is seen in light blue. The red element is a shell of the 3D magnetic inversion, which closely corresponds spatially to the Clifford stock. The magnetic body appears to be plunging to the south (right), but this needs to be viewed with the full 3D imaging system to see the full three-dimensional shape. Higher density elements identifying more intermediate volcanic rocks surrounding the felsic volcanic rocks are seen as light green in the section. Magnetic elements (red) to the south associate with these denser elements.

The detailed report on this work (Reed 2005a) is supplemented by a separate digital products (Reed 2005b) that contains binary files that can be opened using WinDisp 3DViewer to show the full 3D movable images; bitmap images showing many freeze-frame views of the 3D inversions (similar to Figures 31 to 34); and bitmap images of associated surface magnetic and gravity data and geology used in the inversions; and georeferenced tiff images of the area geology.

Discussion of Greenstone Belt Development

The evolutionary history of the SAGB extends from 2750 to 2660 Ma, a span of 90 Ma, and includes volcanism, sedimentation and plutonism (Figure 35). The U/Pb zircon data and mapping demonstrates a belt-wide distribution of lithostratigraphic assemblages and supports coherent, upward facing, autochthonous stratigraphy as previously suggested (e.g., Goodwin 1977; Pyke 1982; Jensen and Langford 1985; Heather 1998; Ayer, Amelin et al. 2002). Zircon inheritance in the Abitibi greenstone belt was first documented by Corfu (1993) and later by Heather (1998). Inherited zircons with ages similar to those of underlying assemblages have been detected in all but the Pacaud assemblage and most of the plutonic suites. Zircon inheritance is present in 20% to almost 40% of samples analyzed for this study (Ayer, Amelin et al. 2002) with inherited zircons at least 10 my older than their crystallization age, 2 of which are pre-Abitibi in age. This pattern of isotopic inheritance together with greater amounts of crustal contamination in the younger komatiites (Sproule et al. 2002), and field relations (Muskasenda gabbro) are all features consistent with autochthonous stratigraphic evolution, rather than allochthonous juxtaposition of exotic terranes.

The oldest major stratigraphic unit in the SAGB is the 2750 to 2735 Ma Pacaud assemblage. Although not much of the Pacaud assemblage currently crops out, or has been directly dated because of its lack of zircon-bearing volcanic units, our new inheritance data in younger volcanic assemblages suggests the Pacaud assemblage was considerably more widespread. The zircon data also support an age gap of about 5 my with the overlying Deloro assemblage (2730–2724 Ma; *see* Figure 35) in those parts of the Pacaud assemblage intruded by Ramsey–Algoma and the Kenogamissi batholiths in the west. A more significant gap of about 20 my occurs with the overlying Stoughton–Roquemaure assemblage where the Pacaud assemblage is intruded by the Round Lake batholith (*see* Figure 2). These age gaps and localized chert breccia units observed in the Pacaud assemblage directly underlying the Deloro assemblage could represent submarine unconformities as a result of crustal displacement caused by tonalitic plutons intruding lower in the crust during and postdating deposition of the Pacaud assemblage rocks. Evidence for this are the lenticular bodies and small screens of gneissic tonalite and trondhjemite ranging in age from 2747 to 2740 Ma occurring as remnants on the margins, or within the larger batholithic complexes such as the Ramsey–Algoma, Kenogamissi and Round Lake batholiths (Ketchum et al., in press). The early volcanic assemblages uniformly face away and wrap around these batholiths. However, the original nature of these early suites has been obscured by intrusion of extensive younger synvolcanic, syntectonic and posttectonic suites.

Thus, the Pacaud and Deloro assemblages are considered to have been regional basal supracrustal units within the SAGB. We are uncertain what may have originally underlain the Pacaud assemblage as

the evidence for pre-Pacaud strata is only available indirectly as isolated inherited zircons, which, to date, have only been found in the westernmost part of the SAGB (along with rare pre-Abitibi zircons found in plutonic samples), and isolated Nd and Hf isotopic evidence for localized contamination by older crustal sources (Ketchum et al. in press). The Pacaud assemblage may have been underlain by back-arc basin- or oceanic-mantle, which was subsequently subducted into the Archean mantle, as Nd isotopes from volcanic samples of all ages predominantly suggest magma derived from juvenile undepleted sources (Ayer, Amelin et al. 2002; Ayer, Ketchum and Trowell 2002; Ketchum et al., in press).

The Stoughton–Roquemaure and Kidd–Munro assemblages (2724–2710 Ma) are only found north of the PDDZ and south of the LLCDZ (Kidd–Munro assemblage also found in the Shining Tree and south Swayze areas), but no volcanism nor any inherited zircons of this age are present in the central area in the time interval between the Deloro and Tisdale assemblages. Truncation of these volcanic units by the deformation zones implies that horst and graben style synvolcanic faulting predated ductile deformation with uplift of the central area resulting in non-deposition in this area from 2724 to 2710 Ma, whereas voluminous volcanism (predominantly rift-related mafic and ultramafic in composition) occurs in the areas north and south of these postulated early faults. Although granitoids in the SAGB have not been extensively dated, tonalitic synvolcanic intrusions with ages of 2723 to 2713 Ma have been found in the Kenogamissi and Round Lake batholiths. This suggests this area may have been uplifted by intrusion of granitic rocks underlying the central area, which may have been partially responsible for the age gap.

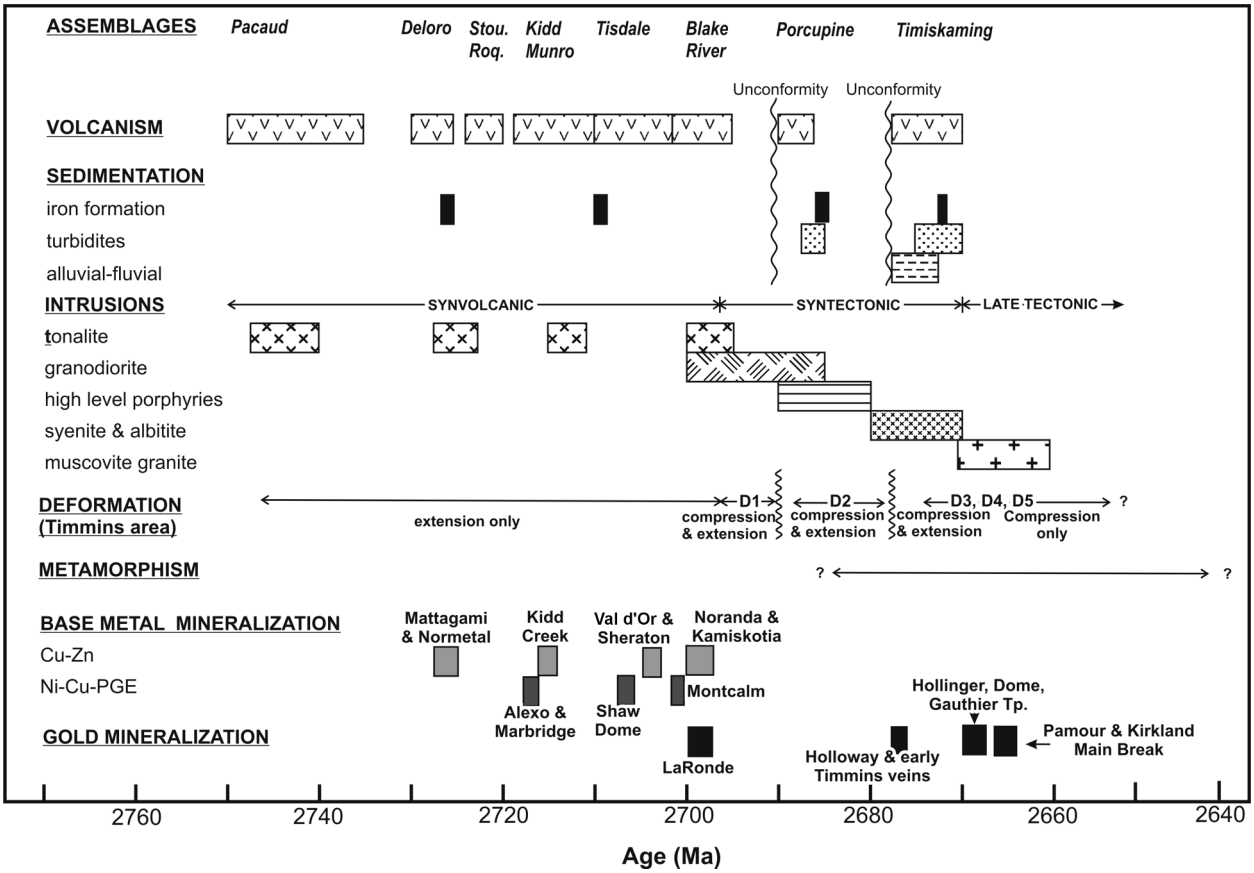

Figure 35. Timeline for the evolution of southern Abitibi greenstone belt including the volcanic and sedimentary assemblages, intrusions, deformation, metamorphism and the main mineralization episodes (*modified from* Bateman et al. 2005, p.3). Geochronological data are from numerous sources including the new results in this report (Corfu 1993; Mortensen 1993a, 1993b; Powell, Carmichael and Hodgson 1995; Bleeker, Parrish and Sager-Kinsman 1999; Davis et al. 2000; Heather 2001; Ayer, Amelin et al. 2002; Ayer, Ketchum and Trowell 2002; Ropchan et al. 2002; Ayer, Barr et al. 2003; Dubé et al. 2004; Ketchum et al., in press).

In contrast, the volcanic rocks of the Tisdale and Blake River assemblages (2710–2696 Ma) are thickest and most extensive, have complete stratigraphic sections and are also locally truncated by the PDDZ and LLCDZ in the central area (*see* Figure 2). This suggests that dip-slip displacement on the regional faults changed with the central area of the greenstone belt experiencing greater subsidence during this period. Although there are numerous sill-like mafic to ultramafic intrusions of this age within the supracrustal assemblages, it is assumed that these were subvolcanic intrusions conformable with stratigraphy and were unlikely to have caused major amounts of uplift. However, synvolcanic granodiorite and tonalite ranging in age from 2700 to 2695 Ma have been found in the Nat River, Kenogamissi and Round Lake batholiths and may be responsible for localized uplift and the age gaps. Significant age gaps, which are interpreted as submarine unconformities, occur outside the central area: between the Stoughton–Roquemaure and Tisdale assemblage in the northern part of the study area; between the Kidd–Munro and Blake River assemblages in the Kamiskotia area; and between the Stoughton–Roquemaure and Blake River assemblages east of the Round Lake batholith.

After 2696 Ma, the tectonic regime shifted from volcanic construction to one dominated by deformation, plutonism and erosion accompanied by development of localized basins infilled by sedimentary and volcanic rocks. The Porcupine assemblage was deposited with angular unconformity on older volcanic assemblages from about 2690 to 2685 Ma. Porcupine assemblage volcanic centres occurred at both Timmins and in the northeastern part of the Shining Tree area, regions which are also marked by extensive porphyry intrusions of similar adakitic chemistry and age to the volcanic rocks. The volcanic accumulations grade upwards and laterally into turbiditic sediments and localized iron formation deposited below wave base in east-west trending basins typically bound by ductile deformation zones postdating deposition. The early phases of syntectonic plutonism ranges from approximately 2695 to 2685 Ma, during which time, an early episode of regional D1 deformation predated the Porcupine angular unconformity at 2690 Ma and locally (in the Swayze area) resulted in F1 folds with well-developed axial planar cleavage (Heather 2001; Becker and Benn 2003).

SHRIMP and TIMS geochronological investigations on the Porcupine wackes in the Timmins area indicate that zircons were derived from a terrane with similar ages to the underlying volcanic and plutonic groups (see Figs 4F, 5A, 5D and 6A). Based on the larger zircon populations analyzed by the SHRIMP, the Hoyle formation sample in Hoyle Township exhibits a major narrow peak at 2695 Ma and a minor second one at 2750 Ma (*see* Figure 11B). The Beatty formation sample, immediately underlying the Timiskaming unconformity in Tisdale Township, has a broader single peak at 2698 Ma (*see* Figure 11A), whereas the Whitney Township sample, south of the PDDZ, has a narrow peak at 2693 Ma and a second smaller one at 2730 Ma (*see* Figure 11C). These data suggest that while the Porcupine formations in the Timmins area had the majority of their zircons supplied from the syntectonic intrusive group and/or the Blake River assemblage, there are some differences in the secondary zircon supply. This ranges from a minor but distinguishable secondary supply of Pacaud-age zircons in the Hoyle formation in Hoyle Township; significant secondary supply of Deloro-age zircons in the Whitney formation, south of the PDDZ; and predominantly syntectonic intrusive group and/or Blake River-age zircons for the Beatty formation in Tisdale Township.

The Duparquet, Lac Caste, Kewagama, Cadillac and the Pontiac groups in Quebec have similar maximum depositional ages (Davis 2002) to the Porcupine assemblage units in Ontario and, thus, are thought to be correlative. However, basins hosting the Duparquet Group seem to be most similar to the Porcupine formations in the Timmins area and the Porcupine unit south of Larder Lake, in that their provenance appears to be only from sources within the Abitibi Subprovince. The other groups in Quebec are similar to the Scapa sediments in that they all contain pre-Abitibi zircons (i.e., >2.8 Ga) (Ayer, Amelin et al. 2002; Davis 2002). The Scapa sediments are a very widespread unit, extending northwest of the study area (*see* Figure 2), and over 150 km to the east into the Quebec portion of the Abitibi Subprovince. The presence of zircons from older more distal terranes, in conjunction with D1 folding and

plutonism suggests the onset of regional compression and collision with an older Superior Province craton to the north (Davis et al. 1995).

The D2 event postdates the Porcupine assemblage as it is deformed by it, but D2 structures are unconformably truncated by, and thus predate, the Timiskaming. D2 resulted in localized folding and thrusting and early south-side up, dip-slip, ductile deformation on regional deformation zones.

The Timiskaming assemblage ranges from 2676 to 2670 Ma and consists of conglomerate and sandstone, locally with volcanic rocks. It was deposited with angular unconformity on the older volcanic and sedimentary assemblages, typically in long linear basins with unconformable contacts along the north margin and in faulted contact with the PDDZ and LLCDZ to the south. Facies studies indicate the basal portions were deposited subaerially and include alluvial–fluvial environments, whereas the upper portions are more typically deeper water sediments that include turbidites and iron-poor iron formation. The supracrustal rocks are broadly coeval with small syntectonic alkalic intrusions, ranging from 2680 to 2672 Ma, also found in close proximity to the major deformation zones. The period during which the Timiskaming assemblage formed is thought to represent extensional to transpressional tectonism associated with continental island arc magmatism and sedimentation in which the supracrustal units were unconformably deposited in subaerial alluvial fan and fluvial environments closely associated to regional-scale faults (Ayer, Amelin et al. 2002).

Broadly synchronous with the syntectonic opening of Timiskaming basins in dilatational jogs, was D3 folding, only the late stages of which affected the assemblage. Left-lateral strike-slip movement along the PDDZ accompanied D3 and is interpreted to be associated with up to 13 km of sinistral offset of markers across the PDDZ in the Timmins area.

The D4 folding created synclines within the Timiskaming assemblage rocks and right-lateral strike-slip displacement along the PDDZ. This event may be correlative with oblique reverse-dextral slip along the LLCDZ which has been identified as a post-Timiskaming “D2” event in the Kirkland Lake–Larder Lake area (*see* “Timmins Subproject” and “Kirkland Lake–Larder Lake Subproject”). A late tectonic magmatic event consists of Algoman granites and S-type granitic plutons, ranging in age from 2670 to 2660 Ma, postdates the Timiskaming assemblage. These plutons occur both within the batholiths and the supracrustal rocks. They appear to be temporally associated with D4 folding (D2 deformation along the LLCDZ), and dextral strike-slip displacement on the major deformation zones. The D4–D5 event represents the final stage in transpressional deformation along the PDDZ in Timmins and are thought to be similar to D3 and D4 documented in the Kirkland Lake–Larder Lake area. These deformation events are associated with the generation of crenulation cleavages, minor folds and brittle faulting, but do not appear to be associated with regional scale folding.

The irregular metamorphic patterns in the study area (*see* Figure 27) are attributed to superposition of subgreenschist- and greenschist-grade regional metamorphism on narrow higher grade contact metamorphic aureoles that formed at different times adjacent to the various felsic to intermediate intrusions. The metamorphosed plutonic, volcanic and sedimentary rocks now at the surface reached maximum pressures (depths of 8–10 km) and temperatures (350 to 450°C) during the main phase of ductile deformation (D4 to D6) that occurred after deposition of the Timiskaming assemblage and are estimated to have reached peak conditions in the range of 2665 to 2655 Ma (*see* Figure 30). Direct evidence for the timing of metamorphism may be evident in some of the SHRIMP U/Pb zircon analyses as indicated by ages of approximately 2650 Ma. A possible metamorphic zircon with a low Th/U ratio from a conglomerate in Thorneloe Township yielded an age of 2618±2 Ma (*see* Figure 4C). SHRIMP analyses of a number of monazite crystals with low Th/U ratios in the vicinity of the Dome Mine yielded ages of 2640±5 Ma which could be hydrothermal or metamorphic (Ayer, Barr et al. 2003) and are synchronous with the minimum age of 2643 Ma for regional metamorphism in the Noranda area (Powell,

Carmichael and Hodgson 1995). Rocks subjected to peak metamorphic conditions that ended up at the earth's surface yielded $^{40}Ar/^{39}Ar$ cooling ages in the range 2615 to 2617 Ma (Hanes et al. 1989). These rocks were at depths in the crust where temperatures in excess of 300°C prevailed 40 my after cooling began at the onset of exhumation (*see* Figure 30; Thompson 2005).

Discussion of Metallogenesis

VOLCANOGENIC MASSIVE SULPHIDE AND NICKEL-COPPER-PLATINUM GROUP ELEMENT MINERALIZATION

There are four distinct base metal-bearing (VMS±Ni-Cu-PGE) volcanic assemblages in the Abitibi greenstone belt (Ayer, Berger and Trowell 1999). Two distinct types of VMS mineralization occur within the Deloro assemblage: 1) massive sulphide deposits in mafic to felsic calc-alkaline volcanic rocks spatially associated with tholeiitic rhyolites, and 2) base metal mineralization in sulphide-facies iron formations representing proximal exhalative mineralization localized within regional-scale oxide-facies iron formations. The economically more significant type 1 VMS deposits have all been found to date within the northern Abitibi greenstone belt in Quebec and include the Mattagami, Joutel and Normetal mines. The Shunsby deposit within the Shining Tree belt is an example of the type 2, iron formation-hosted, Cu-Zn deposits (Heather 1998).

The upper Kidd–Munro assemblage is host to a major VMS epoch, which includes the giant Kidd Creek Mine, associated with high silica rhyolites and ultramafic volcanic rocks and smaller deposits, such as the Potter and Potterdoal mines in Munro Township, associated with ultramafic and mafic volcanic rocks (*see* "Munro Subproject"). The ultramafic rocks in this assemblage are also considered to be highly prospective targets for magmatic Ni-Cu mineralization, such as the Alexo Mine and other deposits in Dundonald Township, and the Marbridge deposit in Quebec (*see* "Nickel-Copper-Platinum Group Element Mineralization Subproject").

The Tisdale assemblage contains a number of past-producing Ni-Cu-PGE mines and deposits associated with the komatiitic rocks (*see* "Nickel-Copper-Platinum Group Element Mineralization Subproject"). Thus, the lower part of the Tisdale assemblage is considered to have high potential for new magmatic Ni-Cu deposits as it includes a number of past-producing mines in the Shaw Dome area of Timmins. Geochronologic results suggest the lower Tisdale assemblage is a very widespread unit in the study area (*see* Figure 2) and that much of this area may have good potential for Ni-Cu discoveries associated with komatiites. Examples include the past-producing Texmont Mine, in McArthur Township, and undeveloped deposits in Sothman and Bannockburn townships.

A number of VMS deposits are known to occur in upper Tisdale-age units in Quebec. These deposits, which include the Louvicourt Mine, occur in the 2704±2 Ma Val d'Or formation that consists of calc-alkaline intermediate to felsic volcanic rocks (Scott, Mueller and Pilote 2002). There are large areas underlain by calc-alkaline rocks of the upper Tisdale assemblage within the study area (*see* Figure 2) and the recently discovered Zn-Cu-Pb mineralization in Sheraton Township, with an age of 2703.7±1.5 Ma (Ayer, Amelin et al. 2002) and the Cu-Zn-Au mineralization found along strike to the east in Currie Township (*see* "Currie Subproject") suggest that the upper Tisdale assemblage is worthy of additional VMS exploration.

The youngest base metal episode occurs in the upper Blake River Assemblage. The Noranda cauldron sequence of the Noranda subgroup hosts the majority of VMS deposits in the Blake River Group (Gibson,

Watkinson and Comba 1989; Gibson and Watkinson 1990). However, pyroclastic rocks form an important part of the post-cauldron volcanism (Trudel 1978, 1979; Goutier 1997; Lafrance, Moorhead and Davis 2003). The abundance of base metals associated with highly elevated precious metals in deposits such as the Horne Mine in Noranda, Quebec, and the gold deposits to the east, led Robert and Poulsen (1997) to suggest that some of the gold mineralization in the Blake River Group was related to volcanism. The gold-rich VMS deposits that were formed before main-stage deformation include the LaRonde Penna deposit and the Doyon Mine located between Noranda and Val d'Or in the Doyon–Bousquet–LaRonde gold camp (Dubé et al. 2003). LaRonde is a giant pre-deformation gold-rich synvolcanic VMS deposit (Mercier-Langevin et al. 2004; Dubé, Mercier-Langevin et al. 2004), whereas Doyon is a world-class gold-copper sulphide-rich vein-type deposit. The gold-bearing stockwork and sheeted veins at the Doyon deposit are deformed by the main foliation and mineralized veins in the West Zone are cut by pre-D2 deformation diorite dikes. These features suggest that the mineralization is pre- or early main-stage deformation. The Doyon deposit may be associated with the emplacement of a late magmatic phase (tonalite) of the multistage Mooshla pluton (Gosselin 1998; Galley, Pilote, and Davis 2003).

Copper-zinc mineralization in the Ben Nevis area occurs within the upper part of the Blake River assemblage, which has a U/Pb age of 2696.6±1.3 Ma. This is younger than the pre-cauldron phase of the Noranda subgroup (2701±1 Ma: Mortensen 1993b), younger than the Misema subgroup in Pontiac Township (2701±2 Ma: Corfu et al. 1989), and of the same age as the post-cauldron phase of the Noranda subgroup (the Reneault–Dufresnoy formation: 2697.9+1.3/–0.7 (Mortensen 1993b) and 2696±1.1 Ma (Lafrance, Moorhead and Davis 2003, and the Bousquet formation: 2698.6±1.5 Ma, 2698.0±1.5 Ma and 2694±2 Ma (Lafrance, Moorhead and Davis 2003). Thus, the Ben Nevis–Clifford volcanic complex formed late in the Blake River Group volcanic event, an area in which gold-rich VMS deposits may also be present.

The VMS deposits of the Kamiskotia deposit were previously believed to be part of the Tisdale assemblage, based on an age of 2705±2 Ma from Godfrey Township (Barrie and Davis 1990). However, they are associated with bimodal tholeiitic basalts and rhyolites and occur with a single stratigraphic horizon that has an age of 2700 Ma, all of which indicate they are more similar to the Blake River age and style of VMS mineralization. Unconformable juxtaposition of the VMS-rich Kidd–Munro and Blake River assemblages indicates that the northwestern part of the study areas had a long history of formation of significant VMS deposits and, thus, is an area that is worthy of focussed exploration for new Cu-Zn deposits (*see* "Kamiskotia Subprojects").

West of the Kamiskotia area, the Montcalm gabbroic complex is a peridotitic to gabbroic intrusion which hosts the Montcalm Ni-Cu deposit. A gabbro from this complex has an age of 2702±2 Ma and is cut by granodiorite dike with an age of 2700+5/–4 Ma (Barrie and Davis 1990). These ages suggest the Ni-Cu mineralization in the Montcalm gabbroic complex is coeval with Blake River assemblage volcanism in the Kamiskotia area.

EPIGENETIC GOLD MINERALIZATION

There were several phases of hydrothermalism and gold mineralization in the Timmins–Porcupine gold camp. Clasts of colloform-crustiform ankerite vein in conglomerate of the Dome formation at Dome Mine (Dubé, Williamson and Malo 2003) demonstrate early hydrothermal low-grade mineralization. Ankerite veining and minor mineralization in Dome and Aunor mines predate the Timiskaming unconformity, and may be related to D2 thrusting. Copper-gold-silver-molybdenum mineralization in the Pearl Lake porphyry predates main-stage quartz-gold veins in the Hollinger Mine and is post-Timiskaming sedimentation. This gold mineralization, which is perhaps coeval with Lightning zone replacement-style gold mineralization at the Holloway Mine, overprints a Timiskaming-age volcanic unit. At the Holloway Mine, the gold mineralization is itself cut by an inter-mineral dike with an age of 2671.5±1.9 Ma, which

is, in turn, overprinted by a later auriferous quartz-carbonate veining event (Ropchan et al. 2002). The bulk of the gold mineralization in Timmins, however, corresponds to auriferous quartz veining in extensional fracture arrays interpreted as syn- to late-S3 foliation. Consequently, this main-stage gold-quartz mineralization at Hollinger–McIntyre and Dome mines and in other deposits was the result of late D3 events. The geometry of a significant proportion of quartz veins is structurally compatible with oblique (right lateral, south block up) shear (Bateman, Ayer and Dubé 2005). Regionally, D3 was left lateral, so these vein systems may represent antithetic R′ shear arrays. The extensional network of quartz-gold veins at Pamour Mine crosscut S4 foliation with a minimum of deformation, and formed during north-south shortening, dip-slip fault movement (D4). The D5 constriction generated local quartz ladder veins, but probably no new stage of gold mineralization was introduced.

This protracted history of deformation and alteration indicate a long-lived or multistage auriferous hydrothermal system, and a plumbing system geometrically stable for long enough to feed gold into a relatively small volume of rock. Variability in timing is reflected in diverse styles of gold mineralization (vein type, vein mineralogy, disseminated, sulphide-rich mineralization), alteration mineralogy (massive ankerite, albite, sericite), sulphide and ore minerals (pyrite, tellurides) and metals (Au, Ag, Cu, Mo, W). Syn-deformation quartz-carbonate vein deposits are commonly spatially associated at the regional scale with Timiskaming-like regional unconformities and suggest an empirical relationship between large-scale greenstone quartz-carbonate gold deposits, deformation opening of these basins, and regional unconformities (Hodgson 1993; Robert 2000; Dubé, Williamson and Malo 2003). This is similar to the deformation–mineralization history recorded in the Archean Kalgoorlie gold camp in southwestern Australia (Bateman and Hagemann 2004).

In the Kirkland Lake–Larder Lake camp, gold mineralization in Gauthier Township represents a hydrothermal event distinct from the Kirkland Lake gold lodes. Mineralization at the Upper Canada Mine occurs in a high-strain ductile deformation zone that probably represents a splay of the Larder Lake–Cadillac deformation zone. Although hydrothermal activity spanned three deformation phases (which, in Kirkland Lake–Larder Lake chronology, are identified as D2, D3 and D4), gold was introduced relatively early, during D2 (probably equivalent to D3 in Timmins) and was accompanied by strong bulk carbonatization. Subsequent deformation and, possibly, hydrothermal activity overprinted gold mineralization.

Gold occurrences of the Anoki and McBean properties are localized within or in the immediate proximity of the first-order Larder Lake–Cadillac deformation zone. Gold occurs in sulphidized Fe-tholeiite flows (Anoki Main zone), in quartz stockworks within carbonate- and carbonate-fuchsite-altered ultramafic rocks (“green carbonate”, McBean and Anoki Deep zones), in quartz-sulphide zones hosted by Timiskaming assemblage clastic rocks and locally associated with feldspar-phyric dikes (40 East zone), and in quartz veining with sulphides in cherty to graphitic exhalite horizons enclosed in basalts (Anoki South). In all cases, mineralization is accompanied by extensive carbonatization. Drill cores from the McBean zone show that mineralization and alteration are most likely synchronous with the development of D2 fabrics. Mineralized zones at the Anoki and McBean properties are part of a regionally extensive hydrothermal system that affected an approximately 20 km long segment of the Larder Lake–Cadillac deformation zone from the Kerr–Addison–Chesterville gold deposit (east) to the Anoki occurrences (west). Other similar gold deposits include the Cheminis and Omega deposits in McVittie Township. Most gold production and reserves are from sulphide-rich replacement ores in mafic (mostly tholeiitic) volcanic rocks, whereas native gold-bearing quartz stockworks in carbonate-fuchsite-altered meta-ultramafic rocks (“green carbonate ore”) are second in importance. Gold deposits and occurrences along the Larder Lake–Cadillac and Upper Canada deformation zones are probably related because they have similar geochemical signatures and similar ore zone plunges roughly parallel to L2. The Upper Canada deformation zone is interpreted as a splay of the Larder Lake–Cadillac deformation zone, and as both structures are syn-D2, they were likely hydraulically connected during the introduction of gold-bearing fluids along these structures.

The Kirkland Lake giant gold deposit is clearly a structurally controlled syn-deformation gold- and telluride-rich high-grade hydrothermal system characterized by steeply to moderately dipping fault-fill veins hosted by brittle to brittle-ductile faults (primarily the Main Break and the 04 Break). The gold-bearing veins were formed at relatively shallow crustal levels, probably simultaneously with reverse-dextral to reverse movement on the Main Break. The deposit shares strong analogies with high-grade gold-telluride deposits linked to alkalic magmatic systems (Jensen and Barton 2000). Because the exact timing of hydrothermal activity and gold mineralization and development of the Main Break and 04 Break structures relative to alkaline magmatism remain speculative, it is impossible to establish a definite genetic link between gold mineralization and any known magmatic phase. In a structural sense, gold-bearing veins postdate the Timiskaming assemblage clastic-volcanic sequence and the syenite porphyry stock as both are cut by the gold-bearing Main Break, 04 Break and associated structures. The structural timing of Kirkland Lake mineralization is not entirely clear. Using the relative chronology between the intra-mineral dikes, the quartz veins and the foliations, we propose that the mineralization could be syn-D4 (D5 in Timmins?), however, we recognize that evidence supporting this timing is not 100% conclusive and additional work is needed to provide more reliable constraints. It is possible that mineralization entirely predated D4. The distinct metal inventory (Te>Au, Mo, Pb, Ag, high Au/Ag, low As) of Kirkland Lake mineralization indicates a separate fluid source, different from gold deposits and occurrences clustering along the Larder Lake–Cadillac deformation zone and its splays. A deep alkaline magmatic fluid source (magmatic chamber or intrusion at depth) appears most probable.

As reported by Sillitoe (2002), several giant gold deposits related to alkaline rocks may be considered unique in term of combination of geological characteristics and, as shown by its geological parameters, the Kirkland Lake gold deposit fits such a statement. The interpretation of Kirkland Lake as a stand-alone hydrothermal system related to alkalic magmatism and unrelated to gold mineralization along the Larder Lake–Cadillac deformation zone agrees with the interpretation of Robert (2003).

Conclusions

The objective of this project was to improve knowledge of the stratigraphy, volcanology, geochemistry, metamorphic petrology, and structural geology to better understand the metallogeny and architecture of the Abitibi greenstone belt in the Timmins–Kirkland Lake study area. We have, thus, considerably changed and improved our knowledge of Abitibi stratigraphy and belt-scale architecture by

- utilizing 34 new TIMS and 11 SHRIMP U/Pb zircon ages to further subdivide and refine the distribution and age ranges for the volcanic and sedimentary assemblages, the intrusions and the timing of metallogenic and structural events.
- providing new evidence in the form of xenocrystic zircons that the Pacaud and Deloro assemblages were widespread basal units, but are now restricted to units only found wrapped around the margins of external batholiths and in the cores of domes. The data also provide evidence for pre-Abitibi-age inheritance in volcanic assemblage samples, proving early (pre-D1) interaction with an older (>2.85 Ga) crustal precursor to the Abitibi greenstone belt.
- documenting a series of interformational unconformities in the volcanic “Keewatin” stratigraphic assemblages. Submarine unconformities are preserved locally at the top of Pacaud, Deloro, Stoughton–Roquemaure and Kidd–Munro assemblages.

- providing an improved understanding of the late sedimentary assemblages indicating that detritus for the Porcupine assemblage sedimentary rocks in the Timmins area was of local derivation with detrital zircon input peaking at approximately 2700 to 2690 Ma, coincident with the onset of D1. Detritus for the Timiskaming assemblage sedimentary rocks were derived from both local Abitibi-age, and external pre-Abitibi sources indicating a more widespread provenance. The detrital zircon input peaked at 2690 to 2670 Ma, coincident with D2 and D3 folding and faulting.
- revising the stratigraphic nomenclature to make a more straightforward correlation with Quebec-based Abitibi stratigraphy by establishing a lower Kidd–Munro assemblage, a lower Tisdale assemblage and a lower Blake River assemblage.

We have improved understanding of the stratigraphy, facies associations and metallogeny at township scales within VMS and Ni-Cu-PGE bearing assemblages in a number of specific areas including

In the Kamiskotia area by

- correlating the stratigraphy and the contained VMS mineralization to the upper Blake River assemblage;
- tracing mineralized stratigraphy from the Kam-Kotia to the Jameland deposits;
- recognizing for the first time the alteration signatures of the various Kamiskotia deposits;
- relating a number of the Kamiskotia VMS deposits to synvolcanic faults (e.g., Genex Mine).

In the Ben Nevis area by

- developing stratigraphic and geochemical correlations with the uppermost part of the Blake River assemblage and comparisons with the Noranda and LaRonde camps;
- documenting overprinting relations between VMS and porphyry style mineralization associated with the Clifford stock.

In the Munro and Currie townships areas by

- documenting the regional setting of VMS mineralization in the Kidd–Munro assemblage at the Potter and Potterdoal mines and constructing a stratigraphic sequence in the central part of the assemblage in Munro Township;
- documenting lithologies, geochemical patterns and structural overprinting of the upper Tisdale and lower Blake River assemblages stratigraphy in Currie Township.

In the Shaw Dome area by

- documenting the regional setting of Ni-Cu-PGE mineralization in the Tisdale assemblage;
- indicating the presence in the Shaw Dome of important criteria for generation of magmatic sulphide deposits including fertile komatiitic magma (metal source), proximity to sulphide iron formation (sulphur source), abundant olivine cumulate (heat source and dynamic system), and footwall embayments (physical traps);
- showing that Ni-Cu-PGE deposit-types occur in clusters implying a significant potential for discovery of additional deposits in the Tisdale assemblage (e.g., the Bartlett and Halliday domes).

The Timmins and Kirkland Lake–Larder Lake gold and intrusion subprojects utilized detailed mapping and structural studies, lithogeochemistry and geochronology to provide an improved understanding of the relationships between and the ages of the various assemblages, and the timing of intrusions, structural, alteration and epigenetic gold mineralization episodes. The results of these studies documented the existence of multiple gold mineralizing events at both Timmins and Kirkland Lake.

In the Timmins area, the main structural and gold mineralization events included

- D1 uplift and excision of upper Tisdale stratigraphy with formation of an angular unconformity predating deposition of Porcupine assemblage at 2690 Ma.
- An early, lower grade gold mineralizing event predates the Timiskaming unconformity and may be synchronous with D2, which produced thrusting and folding and early south-over-north dip-slip movement on the Porcupine–Destor deformation zone (PDDZ) between 2685 and 2676 Ma.
- The later main stage of gold mineralization is associated with D3, a protracted event which coincided with the opening of the Timiskaming basin but also overprints the Timiskaming sediments. The D3 folding and faulting are coeval with up to 13 km of left-lateral strike-slip movement on the PDDZ. The main stage of gold mineralization provided most of the ore at the Hollinger-McIntyre, Dome and Hoyle Pond mines. Rhenium-osmium analyses of molybdenite associated with gold mineralization at the McIntyre Mine provided an age of 2672±7 Ma and, at the Dome Mine, 2670±10 Ma.
- D4, produced by transpressional strain, included folding and faulting that preserved Timiskaming assemblages in synclines along the PDDZ and is associated with a late stage gold mineralization event along the Pamour Mine trend.

In the Kirkland Lake–Larder Lake area, the main structural and gold mineralization events, all post-Timiskaming, include

- D2, corresponding to the reverse-dextral (south-over-north) movement along the Larder Lake–Cadillac deformation zone (possibly correlated to the D3 event in Timmins). Gold mineralization hosted by the Larder Lake–Cadillac and Upper Canada deformation zones (e.g., Anoki, McBean and Upper Canada deposits) formed synchronously with D2.
- D3, related to the east-west shortening.
- D4, corresponding to the northwest-southeast shortening. Gold mineralization of the Narrows Break (about 2.5 km north of the Larder Lake–Cadillac deformation zone, and 350 m north of the Kirkland Lake Main Break) is synchronous with D4.
- The Kirkland Lake gold deposits consist of gold and telluride-bearing, sulphide-poor quartz veins associated with the brittle to brittle-ductile Kirkland Lake fault (Main Break) and its subsidiary splays. The association of veins with brittle faults suggest relatively shallow crustal levels of mineralization. Distinct metal signature and mineralization style suggest that Kirkland Lake deposit probably represents a stand-alone hydrothermal system that is unrelated to gold deposits along the Larder Lake–Cadillac deformation zone and its splays. A deep magmatic fluid source (sharing analogies with the alkalic magmatic mineralization systems, as defined by Jensen and Barton 2000) appears most probable for the Kirkland Lake mineralization. Gold-bearing veins could have formed early in the D4 event, synchronously with south-over-north reverse-dextral to reverse movement along the Main Break. Alternatively, mineralization could have pre-dated D4.

A new metamorphic framework has provided additional constraints on the setting of gold deposits and a new tool for gold exploration.

- The metamorphic pattern in the study area is the result of superposition of regional metamorphism on narrow higher grade contact metamorphic aureoles that formed at different times immediately adjacent to granitic intrusions, indicating that most of the granitoids are older than the regional metamorphic event.
- Pre-Timiskaming phases of deformation were less penetrative and occurred at shallower depths in the crust and at lower temperatures than post-Timiskaming deformation.
- Post-Timiskaming deformation, when peak regional metamorphic conditions prevailed, was most conducive to formation of large syn-metamorphic (orogenic) gold deposits. There is a striking spatial relationship of the boundary between the lower and upper greenschist metamorphic zones and a significant number of gold mines. Newly identified high priority targets are defined by the coincidence of metamorphic anomalies with major structural features, specific rock compositions, and moderate to intense deformation.
- The pre-regional metamorphic ages inferred for most of the intrusive plutonic rocks in between the Porcupine–Destor and Larder Lake–Cadillac deformation zones suggests targeting for granite- and porphyry-related gold deposits in this area.

Regional structural patterns are now better understood, in part based upon improved knowledge of the distribution of the stratigraphy and intrusions in conjunction with detailed and regional-scale geophysical surveys including magnetic, gravity and reflection seismic surveys. Major external intrusive units, such as Round Lake and Kenogamissi batholiths, include predominantly synvolcanic phases that occupy anticlinal culminations in common with the situation in Quebec (Daigneault, Mueller and Chown 2004), whereas the late syntectonic intrusions had a relatively minor localized structural effect on the surrounding supracrustal rocks. Regional deformation zones are the loci of major faults, which have been reactivated repeatedly and have exerted control on the distribution of early volcanic ("Keewatin") and late sedimentary assemblages. All assemblages were constructed in an autochthonous fashion and have been locally juxtaposed along regional structures during major ductile deformation events that involved predominantly north-south transpressional shortening. Our geophysical interpretations and conclusions and preliminary interpretations from the Discover Abitibi seismic reflection surveys (Reed, Snyder and Salisbury 2005)

- demonstrate the sense of dip on major structures and lithological units with inversions of magnetic and gravity data;
- demonstrate the sense of dip on major lithological units and major strike-slip faults using reflection seismic data;
- demonstrate a southerly dip for the Porcupine–Destor fault in the Matheson to Nighthawk Lake segment, with a change to steep northerly dip in the Timmins camp;
- verify that the Shaw structure is domal and may be cored by a granitic body;
- indicate higher impedance units (Tisdale assemblage volcanic rocks?) occur in anticlinal structures (D2?) beneath the Porcupine assemblage sedimentary rocks north of Timmins.

This report represents the first comprehensive multidisciplinary synthesis at greenstone belt scale since the widespread acceptance of autochthonous models for greenstone belt evolution (Ayer, Amelin et al. 2002; Thurston 2002). As such, it considerably advances understanding of Abitibi greenstone belt architecture and metallogeny with specific emphasis on copper-zinc, nickel-copper-PGE and gold mineralization and with numerous insights and recommendations that are directly applicable to exploration for these commodities.

References

Ames, D.E., Bleeker, W., Heather, K.B. and Wodicka, N. 1997. Timmins to Sudbury transect: new insights into the regional geology and setting of mineral deposits; *in* Guidebook, Geological Association of Canada, Field Trip B6, p.1-37.

Arndt, N.T. 1977. Thick, layered peridotite-gabbro lava flows in Munro Township, Ontario; Canadian Journal of Earth Sciences, v.14, p.2620-2637.

Arndt, N.T., Naldrett, A.J. and Pyke, D.R. 1977. Komatiitic and iron-rich tholeiitic lavas of Munro Township, northeast Ontario; Journal of Petrology, v.18, p.319-369.

Ayer, J.A., Amelin, Y, Corfu, F., Kamo, S.L., Ketchum, J.W.F., Kwok, K. and Trowell, N. 2002. Evolution of the southern Abitibi greenstone belt based on U-Pb geochronology: autochthonous volcanic construction followed by plutonism, regional deformation and sedimentation; Precambrian Research, v.115, p.63-95.

Ayer, J.A., Barr, E., Bleeker, W., Creaser, R.A., Hall, G., Ketchum, J.W.F., Powers, D., Salier, B., Still, A. and Trowell, N.F. 2003. Discover Abitibi. New geochronological results from the Timmins area: implications for the timing of late-tectonic stratigraphy, magmatism and gold mineralization; Summary of Field Work and Other Activities 2003, Ontario Geological Survey, Open File Report 6120, p.33-1 to 33-11.

Ayer, J.A., Berger, B.R., Hall, L.A.F., Houlé, M., Johns, G.W., Josey, S., Madon, Z., Rainsford, D., Trowell, N.F. and Vaillancourt, C. 2005. Geological compilation of the central Abitibi greenstone belt: Kapuskasing structural zone to the Quebec border; Ontario Geological Survey, Preliminary Map P.3565, scale 1:250 000.

Ayer, J.A., Berger, B.R. and Trowell, N.F. 1999. Geological compilation of the Lake Abitibi area, Abitibi greenstone belt; Ontario Geological Survey, Preliminary Map P.3398, scale 1:100 000.

Ayer, J.A., Ketchum, J.W.F. and Trowell, N.F. 2002. New geochronological and neodymium isotopic results from the Abitibi greenstone belt, with emphasis on the timing and the tectonic implications of Neoarchean sedimentation and volcanism; *in* Summary of Field Work and Other Activities, 2002, Ontario Geological Survey, Open File Report 6100, p.5-1 to 5-16.

Ayer, J.A., Thurston, P.C., Bateman, R., Gibson, H.L., Hamilton, M.A., Hathaway, B., Hocker, S.M., Hudak, G., Lafrance, B., Ispolatov, V., MacDonald, P.J., Péloquin, A.S., Piercey, S.J., Reed, L.E., Thompson, P.H. and Izumi, H. 2005. Digital compilation of maps and data from the Greenstone Architecture Project: Discover Abitibi Initiative; Ontario Geological Survey, Miscellaneous Release—Data 155.

Ayer, J.A., Thurston, P.C., Dubé, B., Gibson, H.L., Hudak, G.J., Lafrance, B., Lesher, C.M., Piercey, S.J., Reed, L.E. and Thompson, P.H. 2004. Discover Abitibi Initiative. Greenstone Architecture Project: Overview of results and belt-scale implications; *in* Summary of Field Work and other Activities 2004, Ontario Geological Survey, Open File Report 6145, p.37-1 to 37-15.

Barnes, S.J. 2004. Introduction to nickel sulphide orebodies and komatiites of the Black Swan area, Yilgarn Craton, Western Australia; Mineralium Deposita, v.39, p.679-783.

Barnes, S.J., Hill, R.E.T., Perring, C.S. and Dowling, S.E. 1999. Komatiite flow fields and associated Ni-sulphide mineralization with examples from the Yilgarn Block, Western Australia; *in* Dynamic processes in magmatic ore deposits and their application to mineral exploration, Geological Association of Canada, Short Course Notes 13, p.159-194.

Barrie, C.T. 1992. Geology of the Kamiskotia area; Ontario Geological Survey, Open File Report 5829, 179p.

——— 1999. The Kidd–Munro Extension Project: Year 3 Report; unpublished report.

Barrie, C.T. and Corfu, F. 1999. The Kidd–Munro Extension Project: results of U-Pb geochronology for Year 1; *in* Summary of Field Work and other Activities, 1998, Ontario Geological Survey, Miscellaneous Paper 169, p.74-81.

Barrie, C.T. and Davis, D.W. 1990. Timing of magmatism and deformation in the Kamiskotia–Kidd Creek area, western Abitibi Subprovince, Canada; Precambrian Research, v.46, p.217-240.

Barrie, C.T., Naldrett, A.J. and Davis, D., 1990. Geochemical constraints on the genesis of the Montcalm gabbroic complex and Ni-Cu deposit, western Abitibi Subprovince, Ontario. Canadian Mineralogist, 28: 451-474.

Bateman, R. 2005a. Precambrian geology of Tisdale Township and parts of Deloro, Mountjoy and Ogden townships; Ontario Geological Survey, Preliminary Map P.3555, scale 1:10 000.

——— 2005b. Precambrian geology, parts of Whitney and Hoyle townships; Ontario Geological Survey, Preliminary Map P.3547—Revised, scale 1:10 000.

Bateman, R., Ayer, J.A., Barr, E., Dubé, B. and Hamilton, M.A. 2004. Discover Abitibi. Gold Subproject 1. Protracted structural evolution of the Timmins–Porcupine gold camp and the Porcupine–Destor deformation zone; *in* Summary of Field Work and Other Activities 2004, Ontario Geological Survey, Open File Report 6145, p.41-1 to 41-10.

Bateman, R., Ayer, J.A., Dubé, B. and Hamilton, M.A. 2005. The Timmins–Porcupine gold camp, northern Ontario: the anatomy of an Archaean greenstone belt and its gold mineralization: Discover Abitibi Initiative; Ontario Geological Survey, Open File Report 6158, 90p.

Bateman, R. and Hagemann, S.G. 2004. Gold mineralization throughout about 45 Ma of Archaean orogenesis: protracted flux of gold in the Golden Mile, Yilgarn Craton, Western Australia. Mineralium Deposita, v.39, p.536-559.

Becker, J.K. and Benn, K. 2003. The Neoarchean Rice Lake Batholith and its place in the tectonomagmatic evolution of the Swayze and Abitibi granite-greenstone belts, northeastern Ontario; Ontario Geological Survey, Open File Report 6105, 42p.

Benn, K. and Peschler, A.P. 2005. A detachment fold model for fault zones in the Late Archean Abitibi greenstone belt; Tectonophysics, v.400, p.85-104.

Berger, B.R. 2002. Geological synthesis of the Highway 101 area, east of Matheson, Ontario; Ontario Geological Survey, Open File Report 6091, 124p.

Blake, T.S. 2001. Cyclic continental mafic tuff and flood basalt volcanism in the Late Archaean Nullagine and Mount Jope supersequences in the eastern Pilbara, Western Australia; Precambrian Research, v.107, p.139-177.

Bleeker, W. 1995. Surface geology of the Porcupine camp; *in* Tectonics and metallogeny of Archean crust in the Abitibi–Kapuskasing–Wawa region; Geological Survey of Canada, Open File 3141, p.13-37.

——— 1999. Structure, stratigraphy, and primary setting of the Kidd Creek volcanogenic massive sulfide deposit: a semi-quantitative reconstruction; *in* The giant Kidd Creek volcanogenic massive sulfide deposit, western Abitibi Subprovince, Canada, Economic Geology Monograph 10, p.71-123.

Bleeker, W. and Parrish, R.R. 1996. Stratigraphy and U-Pb zircon geochronology of Kidd Creek: implications for the formation of giant volcanogenic massive sulphide deposits and tectonic history of the Abitibi greenstone belt; Canadian Journal of Earth Sciences, v.33, p.1213-1231.

Bleeker, W., Parrish, R.R. and Sager-Kinsman, S. 1999. High-precision U-Pb geochronology of the Late Archean Kidd Creek deposit and surrounding Kidd volcanic complex; *in* The giant Kidd Creek volcanogenic massive sulfide deposit, western Abitibi Subprovince, Canada, Economic Geology Monograph 10, p.43-69.

Born, P. 1995. A sedimentary basin analysis of the Abitibi greenstone belt in the Timmins area, northern Ontario, Canada; unpublished PhD thesis, Carleton University, Ottawa, Ontario, 489p.

Boulanger, O. and Chouteau, M. 2001. Constraints in 3D gravity inversion; Geophysical Prospecting, v.49, p.265-280.

Buffam, B.S.W. 1948. Moneta Porcupine Mine; *in* Structural geology of Canadian ore deposits, Canadian Institute of Mining and Metallurgy, p.457-464.

Burrows, D.R. and Spooner, E.T.C. 1986. The McIntyre Cu-Au deposit, Timmins, Ontario, Canada; *in* Proceedings of Gold '86: An international symposium on the geology of gold, Konsult International, Willowdale, Ontario, p.23-39.

Burrows, D.R., Spooner, E.T.C., Wood, P.C. and Jemielita, R.A. 1993. Structural controls on formation of the Hollinger–McIntyre Au-quartz vein system in the Hollinger shear zone, Timmins, southern Abitibi greenstone belt, Ontario; Economic Geology, v.88, p.1643-1663.

Charlewood, G.H. 1964. Geology of deep developments on the main ore zone at Kirkland Lake; Ontario Department of Mines, Geological Circular No.11, 49p.

Cheney, E.S. and Winter, H. de la R. 1995. The late Archean to Mesoproterozoic major unconformity-bounded units of the Kaapvaal Province of southern Africa; Precambrian Research, v.74, p.203-223.

Chown, E.H., Daigneault, R., Mueller, W. and Mortensen, J.K. 1992. Tectonic evolution of the Northern Volcanic Zone, Abitibi belt, Quebec; Canadian Journal of Earth Sciences, v.29, p.2211-2225.

Chown, E.H., Harrap, R. and Moukhsil, A. 2002. The role of granitic intrusions in the evolution of the Abitibi belt, Canada; Precambrian Research, v.115, p.291-310.

Coad, P.R. 1976. The Potter Mine; unpublished MSc thesis, University of Toronto, Toronto, Ontario, 239p.

Corfu, F. 1993. The evolution of the southern Abitibi greenstone belt in light of precise U-Pb geochronology; Economic Geology, v.88, p.1323-1340.

Corfu, F., Jackson, S.J. and Sutcliffe, R.H. 1991. U-Pb ages and tectonic significance of Late Archean alkalic magmatism and nonmarine sedimentation: Timiskaming Group, southern Abitibi belt, Ontario; Canadian Journal of Earth Sciences, v.28, p.489-503.

Corfu, F., Krogh, T.E., Kwok, Y.Y. and Jensen, L.S. 1989. U-Pb zircon geochronology in the southwestern Abitibi greenstone belt, Superior Province; Canadian Journal of Earth Sciences, v.26, p.1747-1763.

Corfu, F. and Noble, S.R. 1992. Genesis of the southern Abitibi greenstone belt, Superior Province, Canada; evidence from zircon Hf isotope analyses using a single filament technique; Geochimica et Cosmochimica Acta, v.56, p.2081-2097.

Daigneault, R., Mueller, W.U. and Chown, E.H. 2004. Abitibi greenstone belt plate tectonics: A history of diachronic arc development, accretion and collision; *in* The Precambrian Earth: tempos and events, Elsevier, Amsterdam, p.88-103.

Davis, D.W. 1982. Optimum linear regression and error estimation applied to U-Pb data; Canadian Journal of Earth Sciences, v.19, p.2141-2149.

——— 2002. U-Pb geochronology of Archean metasedimentary rocks in the Pontiac and Abitibi subprovinces, Quebec, constraints on timing, provenance and regional tectonics; Precambrian Research, v.115, p.97-117.

Davis, W.J., Lacroix, S., Gariépy, C. and Machado, N. 2000. Geochronology and radiogenic isotope geochemistry of plutonic rocks from the central Abitibi Subprovince: significance to the internal subdivision and plutono-tectonic evolution of the Abitibi belt; Canadian Journal of Earth Sciences, v.37, p.117-133.

Davis, W.J., Machado, N., Gariépy, C., Sawyer, E.W. and Benn, K. 1995. U-Pb geochronology of the Opatica tonalite-gneiss belt and its relationship to the Abitibi greenstone belt, Superior Province, Quebec; Canadian Journal of Earth Sciences, v.32, p.113-127.

de Rosen-Spence, A.F. 1976. Stratigraphy, development and petrogenesis of the central Noranda volcanic pile, Noranda, Quebec; unpublished PhD thesis, University of Toronto, Toronto, Ontario, 439p.

Dinel, E. and Fowler, A.D. 2004. Discover Abitibi. Preliminary results of the geology and geochemistry of the volcanic rocks hosting the Hoyle Pond mine, Timmins, Ontario; *in* Summary of Field Work and Other Activities 2004, Ontario Geological Survey, Open File Report 6145, p.46-1 to 46-4.

Dubé, B., Mercier-Langevin, P., Hannington, M.D., Davis, D.W. and Lafrance, B. 2004. Le gisement de sulfures massifs volcanogènes aurifères LaRonde, Abitibi, Québec: altération, minéralisation, genèse et implications pour l'exploration; Ministère des Ressources Naturelles, Faune et Parcs, Québec, Rapport Interimaire, MB2004-03, 112p.

Dubé, B., Mercier-Langevin, P., Lafrance, B., Hannington, M.D., Moorhead, L., Davis, D.W. and Pilote, P. 2003. The Doyon–Bousquet–LaRonde Archean Au-rich VMS gold camp: the example of the world-class LaRonde deposit, Abitibi and its implications for exploration; extended abstract *in* Ore Deposits at Depth, CIM 2003 Field Conference, Timmins, Ontario, Canadian Institute of Mining and Metallurgy, Abstract Volume, p. 3-10.

Dubé, B., Williamson, K. and Malo, M. 2003. Gold mineralization within the Red Lake mine trend: example from the Cochenour–Willans Mine area, Red Lake, Ontario, with new key information from the Red Lake Mine and potential analogy with the Timmins camp; Geological Survey of Canada, Current Research, v.2003-C21, 15p. [available in electronic form only]

Dubé, B., Williamson, K., McNicoll, V.J., Malo, M., Skulski, T., Twomey, T. and Sanborn-Barrie, M. 2004. Timing of gold mineralization in the Red Lake gold camp, northwestern Ontario, Canada: new constraints from U-Pb geochronology at the Goldcorp high-grade zone, Red Lake Mine and at the Madsen Mine; Economic Geology, v.99, p.1611-1641.

Environmental Systems Research Institute, Inc. http://www.esri.ca

Epp, M.S. 1997. Geology, petrography and geochemistry of the Potterdoal Cu-Zn deposit, Kidd–Munro assemblage, Munro Township, Ontario; unpublished MSc thesis, McMaster University, Hamilton, Ontario, 143p.

Epp, M.S. and Crocket, J.H. 1999. Geology and geochemistry of the Potterdoal Cu-Zn deposit, Munro Township, Ontario, *in* The giant Kidd Creek volcanogenic massive sulfide deposit, western Abitibi Subprovince, Canada, Economic Geology Monograph 10, p.593-612.

Ferguson, S.A., Buffam, B.S.W., Carter, O.F., Griffis, A.T., Holmes, T.C., Hurst, M.E., Jones, W.A., Lane, H.C. and Longley, C.S. 1968. Geology and ore deposits of Tisdale Township, District of Cochrane; Ontario Department of Mines, Geological Report 58, 177p.

Frarey, M.J. and Krogh, T.E. 1986. U-Pb zircon ages of late internal plutons of the Abitibi and eastern Wawa subprovinces, Ontario and Quebec; *in* Current Research Part A, Geological Survey of Canada, Paper 86-1A, p.43-48.

Galley, A.G., Pilote, P. and Davis, D.W. 2003. Gold-related subvolcanic Mooshla intrusive complex, Bousquet Mining District, P.Q; *in* Ore Deposits at Depth, CIM 2003 Field Conference, Timmins, Ontario, Canadian Institute of Mining and Metallurgy, Abstract Volume, p.16.

Gamble, A.P.D. 2000. Geology of the Potter Cu-Zn-Co-Ag VMS mineralization and exploration progress report to March 31, 2000 at Millstream Mines Ltd. Potter Mine Exploration project; Dave Gamble Geoservices Inc., unpublished company report, 80p.

Gélinas, L., Brooks, C., Perrault, G., Carignan, J., Trudel, P. and Grasso, F. 1977. Chemostratigraphic divisions within the Abitibi volcanic belt, Rouyn-Noranda, Quebec; *in* Volcanic regimes in Canada, Geological Association of Canada, Special Paper 16, p.265-295.

Geosoft® Inc. http://www.geosoft.com

Gibson, H.L. and Gamble, A.P.D. 2000. A reconstruction of the volcanic environment hosting Archean seafloor and subseafloor VMS mineralization at the Potter Mine, Munro Township, Ontario, Canada; *in* Volcanic environments and massive sulfide deposits, Centre for Ore Deposit Research, University of Tasmania, Hobart, Tasmania, CODES Special Publication 3, p.65-66.

Gibson, H.L. and Watkinson, D.H. 1990. Volcanogenic massive sulphide deposits of the Noranda cauldron and shield volcano, Québec; *in* The northwestern Quebec polymetallic belt: a summary of 60 years of mining exploration, Canadian Institute of Mining and Metallurgy, Special Volume 43, p.119-132.

Gibson, H.L., Watkinson, D.L. and Comba, C.D.A. 1989. Subaqueous phreatomagmatic explosion breccias at Buttercup Hill, Noranda, Quebec; Canadian Journal of Earth Sciences, v.26, p.1428-1439.

Goodwin, A. M. 1977. Archean volcanism in Superior Province, Canadian Shield; *in* Volcanic regimes in Canada, Geological Association of Canada, Special Paper 16, p.205-241.

———1979. Archean volcanic studies in the Timmins–Kirkland Lake–Noranda region of Ontario and Québec; Geological Survey of Canada, Bulletin 278, 51p.

Gosselin, G. 1998. Veines de quartz aurifères précoces à la zone Ouest de la Mine Doyon, Canton de Bousquet, Preissac, Abitibi; unpublished Thèse de maîtrise [MSc thesis], Université du Québec à Chicoutimi, Chicoutimi, Québec, 128p.

Gosselin, P. and Dubé, B. 2005. Gold deposits of Canada: distribution, geological parameters and gold content; Geological Survey of Canada, Open File 4896, 105p.

Goutier, J. 1997. Géologie de la région de Destor; Québec, Ministère des ressources naturelles du Québec, Rapport Géologique RG 96-13, 37p.

GRAV3D 2001. A program library for forward modelling and inversion of gravity data over 3D structures, version 2.0 (*2001*); developed under the consortium research project *Joint/Cooperative Inversion of Geophysical and Geological Data*, UBC-Geophysical Inversion Facility, Department of Earth and Ocean Sciences, University of British Columbia, Vancouver, British Columbia.

Gray, M.D. and Hutchinson, R.W. 2001. New evidence for multiple periods of gold emplacement in the Porcupine mining district, Timmins area, Ontario, Canada; Economic Geology, v.96, p.453-475.

Green, A.H. and Naldrett, A.J. 1981. The Langmuir volcanic peridotite-associated nickel deposits: Canadian equivalents of the western Australian occurrences; Economic Geology, v.76, p.1503-1523.

Groves, D.I., Goldfarb, R.J., Robert, F. and Hart, C.J.R. 2005. Gold deposits in metamorphic belts: overview of current understanding, outstanding problems, future research, and exploration significance; Economic Geology, v.98, p.1-29.

Gupta, V.K. and Ramani, N. 1980. Some aspects of regional-residual separation of gravity anomalies in a Precambrian terrain; Geophysics, v.45, p.1412-1426.

Hall, G.C. 1998. Autochthonous model for gold metallogenesis and exploration in the Yilgarn. Geodynamics and Gold Exploration in the Yilgarn, Workshop Abstracts, Australian Geodynamics Cooperative Research Centre, p.32-35.

Hall, L.A.F. and Houlé, M.G. 2003. Geology and mineral potential of Shaw, Eldorado and Adams townships, Shaw Dome area; *in* Summary of Field Work and Other Activities 2003, Ontario Geological Survey, Open File Report 6120, p.6-1 to 6-4.

Hall, L.A.F., Houlé, M.G. and Tremblay, E. 2004. Precambrian geology of Shaw Township; Ontario Geological Survey, Preliminary Map P.3541, scale 1:20 000.

Hall, L.A.F., MacDonald, C.A. and Dinel, E.R. 2003. Precambrian geology of Deloro Township; Ontario Geological Survey, Preliminary Map P.3528, scale 1:20 000.

Hall, L.A.F. and Smith, M.D. 2002. Precambrian geology of Denton and Carscallen townships, Timmins West area; Ontario Geological Survey, Open File Report 6093, 75p.

Hamilton, M.A., McLelland, J. and Selleck, B. 2004. SHRIMP U-Pb zircon geochronology of the anorthosite-mangerite-charnockite-granite (AMCG) suite, Adirondack mountains, New York: ages of emplacement and metamorphism; *in* Proterozoic tectonic evolution of the Grenville orogen in North America, Geological Society of America, Memoir 197, p.337-355.

Hanes, J.A., Archibald, D.A., Hodgson, C.J. and Robert, F. 1989. Preliminary 40Ar/39Ar geochronology and timing of Archean gold mineralization of the Sigma Mine, Val d'Or Quebec; *in* Current Research, Part C, Geological Survey of Canada, Paper 1989-1C, p.135-142.

Hart, T.R. 1984. The geochemistry and petrogenesis of a metavolcanic and intrusive sequence in the Kamiskotia area, Timmins, Ontario; unpublished MSc thesis, University of Toronto, Toronto, Ontario, 174p.

Hathway, B. 2005. Precambrian geology, parts of Godfrey, Robb, Jamieson, Loveland, Macdiarmid and Thorburn townships; Ontario Geological Survey, Preliminary Map P.3556, scale 1:20 000.

Hathway, B. and Hocker, S.M. 2005. Precambrian geology, parts of Godfrey, Turnbull, Carscallen and Bristol townships; Ontario Geological Survey, Preliminary Map P.3544—Revised, scale 1:10 000.

Hathway, B., Hudak, G. and Hamilton, M.A. 2005. Geological setting of volcanogenic massive sulphide mineralization in the Kamiskotia area: Discover Abitibi Initiative; Ontario Geological Survey, Open File Report 6155, 81p.

Heather, K.B. 1998. New insights on the stratigraphy and structural geology of the southwestern Abitibi greenstone belts: implications for the tectonic evolution and setting of mineral deposits in the Superior Province; *in* The First Age of Giant Ore Formaation: Stratigraphy, Tectonics and Mineralisation in the Lake Archean and Early Proterozoic, Prospectors and Developers Association of Canada, 1998 annual meeting volume, p.63-102.

——— 2001. The geological evolution of the Archean Swayze greenstone belt, Superior Province, Canada; unpublished PhD thesis, Keele University, Keele, Staffordshire, United Kingdom, 370p.

Heather, K.B., Percival, J.A., Moser, D. and Bleeker, W. 1995. Tectonics and metallogeny of Archean crust in the Abitibi–Kapuskasing–Wawa region; Geological Survey of Canada, Open File 3141, 148p.

Hickman, A.H. and Van Kranendonk, M.J. 2004. Diapiric processes in the formation of Archaean continental crust, East Pilbara granite-greenstone terrane, Australia; *in* The Precambrian Earth: tempos and events, Elsevier, Amsterdam, p.118-139.

Hill, R.E.T., Barnes, S.J., Gole, M.J. and Dowling, S.E. 1990. Physical volcanology of komatiites; a field guide to the komatiites of Norseman–Wiluna greenstone belt, Eastern Goldfields Province, Yilgarn Block, Western Australia; Geological Society of Australia, Excursion Guide Book, v.1, p.100.

——— 1995. The volcanology of komatiites as deduced from field relationships in the Norseman–Wiluna greenstone belt, Western Australia; Lithos, v.34, p.159-188.

Hocker, S.M., Thurston, P.C. and Gibson, H.L. 2005a. Volcanic stratigraphy and controls on mineralization in the Genex Mine area, Kamiskotia area: Discover Abitibi Initiative; Ontario Geological Survey, Open File Report 6156, 143p.

——— 2005b. Geochemical, petrographic and compilation data from the Genex Mine area, Kamiskotia area: Discover Abitibi; Ontario Geological Survey, Miscellaneous Release—Data 144.

Hodgson, C.J. 1993. Mesothermal lode-gold deposits; *in* Mineral Deposit Modeling, Geological Association of Canada, Special Paper 40, p.635-678.

Houlé, M.G. and Guilmette, C. 2004. Geology and mineral potential of Carman and Langmuir townships, Shaw Dome area; *in* Summary of Field Work and Other Activities 2004, Ontario Geological Survey, Open File Report 6145, p.7-1 to 7-16.

——— 2005. Precambrian geology, Carman and Langmuir townships; Ontario Geological Survey, Preliminary Map P.3268, scale 1 :20 000.

Houlé, M.G., Hall, L.A.F. and Tremblay, E. 2004. Precambrian geology, Eldorado and Adams townships; Ontario Geological Survey, Preliminary Map P.3542, scale 1:20 000.

Houlé, M.G., Lesher, C.M., Gibson, H.L., Fowler, A.D. and Sproule, R.A. 2001. Physical volcanology of komatiites in the Abitibi greenstone belt; *in* Summary of Field Work and Other Activities 2001, Ontario Geological Survey, Open File Report 6070, p.13-1 to 13-16.

Ispolatov, V.O. 2005. Precambrian geology of Teck Township transect; Ontario Geological Survey, Preliminary Map P.3558, scale 1:10 000.

Ispolatov, V.O. and Lafrance, B. 2005. Precambrian geology of Gauthier Township transect; Ontario Geological Survey, Preliminary Map P.3546—Revised, scale 1:10 000.

Ispolatov, V.O., Lafrance, B., Dubé, B., Hamilton, M.A. and Creaser, R.A. 2005. Geology, structure, and gold mineralization, Kirkland Lake and Larder Lake areas (Gauthier and Teck townships): Discover Abitibi Initiative; Ontario Geological Survey, Open File Report 6159, 170p.

Hyde, R.S. 1980. Sedimentary facies in the Archean Timiskaming Group and their tectonic implications, Abitibi greenstone belt, northeastern Ontario, Canada; Precambrian Research, v.12, p.161-195.

Jackson, S.L. and Fyon, J.A. 1991. The western Abitibi Subprovince in Ontario, *in* Geology of Ontario; Ontario Geological Survey, Special Volume 4, Part 1, p.405-482.

Jackson, S.L., Fyon, J.A. and Corfu, F. 1994. Review of Archean supracrustal assemblages of the southern Abitibi greenstone belt in Ontario, Canada: products of micro-plate interactions within a large-scale plate-tectonic setting; Precambrian Research, v.65, p.183-205.

Jaffey, A.H., Flynn, K.F., Glendenin, L.E., Bentley, W.C. and Essling, A.M. 1971. Precision measurement of half-lives and specific activities of 235U and 238U; Physical Review C, v.4, p.1889-1906.

Jensen, E.P. and Barton, M.D. 2000. Gold deposits related to alkaline magmatism; Reviews in Economic Geology, v.13, p.279-314.

Jensen, L.S. and Langford, F.F. 1985. Geology and petrogenesis of the Archean Abitibi belt in the Kirkland Lake area, Ontario; Ontario Geological Survey, Miscellaneous Paper 123, 130p.

Jiricka, D.E. 1984. Geology of the Hart–McWatters nickel property; unpublished MSc thesis, Laurentian University, Sudbury, Ontario, 94p.

Johns, G.W. 1999. Precambrian geology, Shining Tree area, (east half); Ontario Geological Survey, Preliminary Map P.3389, scale 1:30 000.

Johns, G.W. and Amelin, Y. 1998. Reappraisal of the geology of the Shining Tree area (eastern part), Districts of Sudbury and Timiskaming; *in* Summary of Field Work and Other Activities, 1998, Ontario Geological Survey, Miscellaneous Paper 169, p.43-50.

Johnstone, R.M. 1991. The geology of the northwestern Black River–Matheson area, District of Cochrane; Ontario Geological Survey, Open File Report 5785, 288p.

Kerrich, R., Wyman, D.A., Fan, J. and Bleeker, W. 1999. Boninite series: low Ti tholeiite associations from the 2.7 Ga Abitibi greenstone belt; Earth and Planetary Science Letters, v.164, p.303-316.

Ketchum, J.W. F. Ayer, J.A., van Breemen, O., Pearson, N.J., O'Reilly, S.Y. and Becker, J.K., in press. Pericratonic crustal growth of the southwestern Abitibi subprovince, Canada, Contributions to Mineralogy and Petrology.

Krogh, T.E. 1973. A low contamination method for hydrothermal decomposition of zircon and extraction of U and Pb for isotopic age determinations; Geochimica et Cosmochimica Acta, v.37, p.485-494.

——— 1982. Improved accuracy of U-Pb zircon ages by the creation for more concordant systems using an air abrasion technique; Geochimica et Cosmochimica Acta, v.46, p.637-649.

Laflèche, M.R., Dupuy, C. and Bougault, H. 1992. Geochemistry and petrogenesis of Archean mafic volcanic rocks of the southern Abitibi Belt, Quebec; Precambrian Research, v.57, p.207-241.

Lafrance, B. 2003. Reconstruction d'un environnement du sulfures massifs volcanogènes deforme; exemple archéen de Normetal, Abitibi; Thèse de doctorat [unpublished PhD thesis], Université du Chicoutimi, Chicoutimi, Quebec, 476p.

Lafrance, B., Moorhead, J. and Davis, D. W. 2003. Cadre géologique du camp minier de Doyon–Bousquet–LaRonde; Géologie Québec, Ressources Naturelles du Québec, Étude ET2002-07, 43p.

Larson, M.S. 1996. Physical volcanology and petrogenesis of intrusive and extrusive komatiites in the Shaw Dome area, Abitibi greenstone belt, Ontario, Canada; unpublished MSc thesis, University of Alabama, Tuscaloosa, Alabama, 259p.

Legault, M., Gauthier, M., Jébrak, M., Davis, D.W. and Baillargeon, F. 2002. Evolution of the subaqueous to near-emergent Joutel volcanic complex, Northern volcanic zone, Abitibi Subprovince, Quebec, Canada; Precambrian Research, v.115, p.187-221.

Lesher, C.M., 1989. Komatiite-associated nickel sulphide deposits. Reviews in Economic Geology, 4: 44-101.

Lesher, C.M., Arndt, N.T. and Groves, D.I. 1984. Genesis of komatiite-hosted nickel-sulphide deposits at Kambalda, Western Australia: a distal volcanic model; *in* Sulphide deposits in mafic and ultramafic rocks, Proceedings of IGCP Projects 161 and 91, Third Nickel Sulphide Field Conference, Perth, Western Australia, 23-25 May, 1982, Institute of Mining and Metallurgy, London, p.70-80.

Lesher, C.M., Goodwin, A.M., Campbell, I.H. and Gorton, M.P. 1986. The geochemistry of ore-associated and barren, felsic metavolcanic rocks in the Superior Province, Canada; Canadian Journal of Earth Sciences, v.23, p.222-237.

Lesher, C.M. and Keays, R.R., 2002. Komatiite-associated Ni_Cu-(PGE) deposits; geology, mineralogy, geochemistry and genesis. In: L.J. Cabri (Editor), The geology, geochemistry, mineralogy and mineral beneficiation of platinum-group elements. Canadian Institute of Mining and Metallurgy, pp. 579-617.

Li, Y. and Oldenburg, D.W. 1996. 3-D inversion of magnetic data; Geophysics, v.61, p.394-408.

——— 1998a. 3D inversion of gravity data; Geophysics, v.63, p.109-119.

——— 1998b. Separation of regional and residual magnetic field data; Geophysics, v.63, p.431-439.

Ludwig, K.E. 2001. Users manual for Isoplot/Ex v.2.49: a geochronological toolkit for Microsoft® Excel; University of California–Berkeley, Berkeley, California, Berkeley Geochronology Center, Special Publication No. 1a.

MacDonald, P.J. and Piercey, S.J. 2003. Discover Abitibi. Gold Subproject 3. Preliminary regional geological assessment of porphyry intrusions spatially associated with gold deposits in the western Abitibi Subprovince, Timmins, Ontario; *in* Summary of Field Work and Other Activities 2003, Ontario Geological Survey, Open File Report 6120, p.36-1 to 36-7.

MacDonald, P.J., Piercey, S.J. and Hamilton, M.A. 2004. Discover Abitibi. Gold Subproject 3. Regional geological assessment of porphyry intrusions spatially associated with gold deposits along the Porcupine–Destor deformation zone, western Abitibi Subprovince, Timmins, Ontario; *in* Summary of Field Work and Other Activities 2004, Ontario Geological Survey, Open File Report 6145, p.43-1 to 43-7.

——— 2005. An integrated study of intrusive rocks spatially associated with gold and base metal mineralization in the Abitibi greenstone belt, Timmins area and Clifford Township: Discover Abitibi Initiative; Ontario Geological Survey, Open File Report 6160, 210p.

MAG3D 1998. A program library for forward modelling and inversion of magnetic data over 3D structures, version 3.0 (*1998*); developed under the consortium research project *Joint/Cooperative Inversion of Geophysical and Geological Data*, UBC–Geophysical Inversion Facility, Department of Earth and Ocean Sciences, University of British Columbia, Vancouver, British Columbia.

Mercier-Langevin, P., Dubé, B., Hannington, M.D., Davis, D.W. and Lafrance, B. 2004. Contexte géologique et structural des sulfures massifs volcanogènes aurifères du gisement LaRonde, Abitibi; Ministères des Resources naturelles de la faune et des parcs, Étude ET2003-03, 60p.

Mikucki, E.J. and Roberts, F.I. 2004, Metamorphic petrography of the Kalgoorlie region, Eastern Goldfields granite-greenstone terrane: METPET database; Western Australia Geological Survey, Record 2003/12.

Moritz, R.P. and Crocket, J.H. 1990. Mechanics of formation of the gold-bearing quartz-fuchsite vein at the Dome Mine, Timmins area, Ontario; Canadian Journal of Earth Sciences, v.27, p.1609-1620.

Mortensen, J.K. 1993a. U-Pb geochronology of the eastern Abitibi subprovince. Part 1: Chibougamau–Matagami–Joutel region; Canadian Journal of Earth Sciences, v.30, p.11-28.

——— 1993b. U-Pb geochronology of the eastern Abitibi Subprovince. Part 2: Noranda–Kirkland Lake area; Canadian Journal of Earth Sciences, v.30, p.29-41.

Mueller, W. 1991. Volcanism and related slope to shallow marine volcaniclastic sedimentation: an Archean example, Chibougamau, Quebec, Canada; Precambrian Research, v.49, p.1-22.

Mueller, W., Daigneault, R., Mortensen, J.K. and Chown, E.H. 1996. Archean terrane docking: upper crustal collision tectonics, Abitibi greenstone belt, Quebec, Canada; Tectonophysics, v.265, p.127-150.

Mueller, W., Donaldson, J.A. and Doucet, P. 1994. Volcanic and tectono-plutonic influences on sedimentation in the Archaean Kirkland Basin, Abitibi greenstone belt, Canada; Precambrian Research, v.68, p.201-230.

Mueller, W.U. and Mortensen, J.K. 2002. Age constraints and characteristics of subaqueous volcanic construction, the Archean Hunter Mine Group, Abitibi greenstone belt; Precambrian Research, v.115, p.119-152.

Muir, T.L. 1975. A petrological study of the ultramafic and related rocks of the Shaw Dome, southeast of Timmins, Ontario; unpublished MSc thesis, Queen's University, Kingston, Ontario, 271p.

Naldrett, A.J. 2004. Magmatic sulphide deposits—Geology, geochemistry and exploration; Springer Verlag, Berlin, 727p.

Nunes, P.D., and Jensen, L.S. 1980. Geochronology of the Abitibi metavolcanic belt, Kirkland Lake area – progress report; *in* Summary of geochronology studies 1977–1979, Ontario Geological Survey, Miscellaneous Paper 92, p.32-39.

Oldenburg, D.W., Li, Y. and Ellis, R.G. 1997. Inversion of geophysical data over a copper gold porphyry deposit: a case history for Mt. Milligan; Geophysics, v.62, p.1419-1431.

Ontario Geological Survey 2004a. Ontario airborne geophysical surveys, magnetic data, grid, vector and profile data, central Abitibi Destor-Porcupine–Pipestone faults area (Discover Abitibi); Ontario Geological Survey, Geophysical Data Set 1049.

——— 2004b. Mineral Deposit Inventory Version 2 (MDI2) – October 2004 Release; Ontario Geological Survey, Digital Data.

Paradis, S. 1990. Stratigraphy, volcanology and geochemistry of the New Vauze–Norbec area, central Noranda volcanic complex, Quebec, Canada; unpublished PhD thesis, Carleton University, Ottawa, Ontario, 695p.

Péloquin, A.S. 2000. Reappraisal of the Blake River Group stratigraphy and its place in the Archean volcanic record; Thèse de doctorat [unpublished PhD thesis], Université de Montréal, Montreal, Quebec, 189p.

——— 2005. Precambrian geology of Ben Nevis and Katrine townships; Ontario Geological Survey, Preliminary Map P.3543—Revised, scale 1:20 000.

Péloquin, A.S., Houlé, M.G. and Gibson, H.L. 2005. Geology of the Kidd–Munro assemblage in Munro Township, and the Tisdale and lower Blake River assemblages in Currie Township: Discover Abitibi Initiative; Ontario Geological Survey, Open File Report 6157, 94p.

Péloquin, A.S. and Piercey, S.J. 2003. Discover Abitibi. Base Metal Subproject 3: Geology and base metal mineralization in Ben Nevis, Katrine, and Clifford townships; *in* Summary of Field Work and Other Activities 2003, Ontario Geological Survey, Open File Report 6120, p.41-1 to 41-8.

——— 2005. Geology and base metal mineralization in Ben Nevis, Katrine and Clifford townships: Discover Abitibi Initiative; Ontario Geological Survey, Open File Report 6161, 86p.

Péloquin, A.S., Verpaelst, P., and Gaulin, R. 1989. Le Blake River dans les cantons de Duprat, de Montbray, de Beauchastel et de Dasserat; Ministère de l'Energie et des Ressources du Québec, Rapport Interimaire MB89-64, 89p.

Péloquin, A.S., Verpaelst, P., Ludden, J.N., Dejou, B. and Gaulin, R. 2001. La Stratigraphie du Groupe du Blake River Ouest, Ceinture de l'Abitibi, Québec; Ministère des Ressources Naturelles du Québec, Service Géologique du Nord-Ouest, Étude ET98-03, 37p.

Péloquin, A.S., Verpaelst, P., Paradis, S., Gaulin, R. and Cousineau, P. 1989. Projet Blake River Ouest Cantons de Duprat et de Dufresnoy, SNRC 32D/06; Ministère de l'Energie et des Ressources du Québec, Rapport Interimaire, MB89-02, 176p.

Percival, J.A. and West, G.F. 1994. The Kapuskasing uplift: a geological and geophysical synthesis; Canadian Journal of Earth Sciences, v.31, p.1256-1286.

Piercey, S.J., Hamilton, M.A., Peloquin, A.S. and Chaloux, E. 2004. Discover Abitibi Project, Intrusion Subproject: Updates on studies of the Clifford stock and Blake River Group, Clifford Township; *in* Summary of Field Work and Other Activities 2004, Ontario Geological Survey, Open File Report 6145, p.44-1 to 44-14.

Poulsen, K.H., Robert, F. and Dubé, B. 2000. Geological classification of Canadian gold deposits; Geological Survey of Canada, Bulletin 540, 106p.

Powell, W.G., Carmichael, D.M. and Hodgson, C.J. 1995. Conditions and timing of metamorphism in the southern Abitibi greenstone belt, Quebec; Canadian Journal of Earth Sciences, v.32, p.787-805.

Pressacco, R. 1999. Special project: Timmins ore deposit descriptions; Ontario Geological Survey, Open File Report 5985, 222p.

Pyke, D.R. 1974. Timmins area, districts of Cochrane and Timiskaming; Ontario Division of Mines, Preliminary Map P.941, scale 1:63 360.

——— 1975. Geology of Adams and Eldorado townships, District of Cochrane; Ontario Division of Mines, Report 121, 47p.

——— 1978. Geology of the Redstone River area, District of Timiskaming; Ontario Geological Survey, Report 161, 75p.

——— 1982. Geology of the Timmins area, District of Cochrane; Ontario Geological Survey, Report 219, 141p.

Reed, L.E. 2005a. Gravity and magnetic three-dimensional (3D) modelling: Discover Abitibi Initiative; Ontario Geological Survey, Open File Report 6163, 40p.

——— 2005b. Magnetic and gravity 3D modelling products: Discover Abitibi Initiative; Ontario Geological Survey, Miscellaneous Release—Data 162.

Reed, L.E., Snyder, D.B. and Salisbury, M.H. 2005. Two-dimensional (2D) reflection seismic surveying in the Timmins–Kirkland Lake area, northern Ontario, Canada; acquisition, processing, interpretation: Discover Abitibi Initiative; Ontario Geological Survey, Open File Report 6169, 96p.

Rhéaume, P., Bandyayera, D., Fallara, F., Boudrias, G. and Cheng, L.Z. 2004. Géologie et métallogénie du secteur du lac aux Loutres, synthèse métallogénique d'Urban-Barry (phase 1 de 2); Ministères des Resources naturelles de la faune et des parcs, Rapport RP2004-05, 10p.

Robert, F. 2000. World-class greenstone gold deposits and their exploration; *in* 31st International Geological Congress, August 2000, Rio de Janeiro, Brasil, Vol. de Presentaciones, CD-ROM, doc. SG304e, 4p.

——— 2003. Giant gold deposits of the Abitibi greenstone belt; extended abstract *in* Western Australia gold giants and global gold giants, Centre for Global Metallogeny, University of Western Australia, Perth, Western Australia, MSc Short Course, p.81-90.

——— 2004. Giant gold deposits of the Abitibi greenstone belt and related models; Society of Economic Geologists Thayer Lindsley Lecture at Laurentian University (Sudbury, Ontario, Canada), December 17, 2004.

Robert, F. and Poulsen, K.H. 1997. World-class Archaean gold deposits in Canada: an overview; Australian Journal of Earth Sciences, v.44, p.329-351.

Robert, F., Poulsen, K.H. and Dubé, B. 1997. Gold deposits and their geological classification; *in* Proceedings of Exploration 97: Fourth Decennial International Conference on Mineral Exploration, Prospectors and Developers Association of Canada, Toronto, Ontario, p.209-220.

Robinson, D.J. and Hutchinson, R.W. 1982. Evidence for a volcanogenic-exhalative origin of a massive nickel sulphide deposit at Redstone, Timmins, Ontario; *in* Precambrian sulphide deposits, Geological Association of Canada, Special Paper 25, p.211-254.

Rogers, N., McNicoll, V., van Staal, C.R. and Tomlinson, K.Y. 2000. Lithogeochemical studies in the Uchi–Confederation greenstone belt, northwestern Ontario: implications for Archean tectonics; *in* Current Research, Geological Survey of Canada, No.2000-C16, 2000; 11p. [electronic version only]

Ropchan, J.R., Luinstra, B., Fowler, A.D., Benn, K., Ayer, J., Berger, B., Dahn, R., Labine, R. and Amelin, Y. 2002. Host-rock and structural controls on the nature and timing of gold mineralization at the Holloway Mine, Abitibi Subprovince, Ontario; Economic Geology, v.97, p.291-309.

Schandl, E.S., Davis, D., Gorton, M.P. and Wasteneys, H.A. 1991. Geochronology of hydrothermal alteration around volcanic-hosted massive sulphide deposits in the Superior Province; Ontario Geological Survey, Miscellaneous Paper 156, p.105-120.

Schuster, T. 1995. Galata nickel showing; unpublished BSc thesis, University of Toronto, Toronto, Ontario, 42p.

Scientific Computing and Applications, (John Paine), Adelaide, Australia http://www.scicomap.com

Scott, C.R., Mueller, W.U. and Pilote, P. 2002. Physical volcanology, stratigraphy, and lithogeochemistry of an Archean volcanic arc: evolution from plume-related volcanism to arc rifting of SE Abitibi greenstone belt, Val d'Or, Canada; Precambrian Research, v.115, p.223-260.

Shanmugam, G. 1988. Origin, recognition, and importance of erosional unconformities in sedimentary basins; *in* New perspectives in basin analysis, Springer Verlag, New York, p.83-108.

Sillitoe, R.H. 2002. Some metallogenic features of gold and copper deposits related to alkaline rocks and consequences for exploration; Mineralium Deposita, v.37, p.4-13.

Sproule, R.A., Lesher, C.M., Ayer, J.A., Thurston, P.C. and Herzberg, C.T. 2002. Spatial and temporal variations in the geochemistry of komatiites and komatiitic basalts in the Abitibi greenstone belt; Precambrian Research, v.115, p.153-186.

Sproule, R.A., Lesher, C.M., Houlé, M., Keays, R.R., Ayer, J. and Thurston, P.C., in press. Chalcophile element geochemistry and metallogenesis of komatiitic rocks in the Abitibi greenstone belt, Canada; Economic Geology.

Stacey, J.S. and Kramers, J.D. 1975. Approximation of terrestrial lead isotope evolution by a two-stage model; Earth and Planetary Science Letters, v.26, p.207-221.

Stern, R.A. 1997. The GSC sensitive high resolution ion microprobe (SHRIMP): analytical techniques of zircon U-Th-Pb age determinations and performance evaluation; *in* Radiogenic age and isotopic studies: Report 10, Geological Survey of Canada, Current Research 1997-F, p.1-31.

Stern, R.A. and Amelin, Y. 2003. Assessment of errors in SIMS zircon U-Pb geochronology using a natural zircon standard and NIST SRM 610 glass; Chemical Geology, v.197, p.111-146.

Still, A.C. 2001. Structural setting and controls of gold mineralization at the Macassa Mine, Kirkland Lake, Ontario; unpublished M.Sc. thesis, Queen's University, Kingston, Ontario, 151p.

Stone, M.S. and Stone, W.E. 2000. A crustally contaminated komatiitic dyke-sill-lava complex, Abitibi greenstone belt, Ontario; Precambrian Research, v.102, p.21-46.

Sutcliffe, R.H., Barrie, C.T., Burrows, D.R. and Beakhouse, G.P. 1993. Plutonism in the southern Abitibi Subprovince: a tectonic and petrogenetic framework; Economic Geology, v.88, p.1359-1375.

Thompson, P.H. 2002. Toward a new metamorphic framework for gold exploration in the Timmins area, Central Abitibi greenstone belt; Ontario Geological Survey, Open File Report 6101, 51p.

——— 2003. Toward a new metamorphic framework for gold exploration in the Red Lake greenstone belt; Ontario Geological Survey, Open File Report 6122, 52p.

——— 2005. A new metamorphic framework for gold exploration in the Timmins–Kirkland Lake area, western Abitibi greenstone belt: Discover Abitibi Initiative; Ontario Geological Survey, Open File Report 6162, 104p.

———, in press. Metamorphic constraints on the geological setting, thermal regime and timing of alteration and gold mineralization in the Yellowknife greenstone belt, NWT, Canada; Chapter 14 *in* Gold in the Yellowknife greenstone belt, Northwest Territories: Results of the EXTECH III Multidisciplinary Research Project, Mineral Deposits Division of the Geological Association of Canada.

Thomson, J.E. 1950. Geology of Teck Township and the Kenogami Lake area, Kirkland Lake gold belt; Ontario Department of Mines, Annual Report 1948, v.57, pt.5, p.1-53.

Thurston, P.C. 2002. Autochthonous development of Superior Province greenstone belts?; Precambrian Research, v.115, p.11-36.

Toogood, D.J. 1989. The Upper Canada Mine, an Archean shear-hosted lode gold deposit; Queenston Mining Inc., internal report, p.1-57. (Accessible at the MNDM Mines Library, Sudbury, Ontario.)

Trudel, P. 1978. Géologie de la région de Cléricy, Abitibi-Ouest; Ministère des Ressources Naturelles du Québec, Rapport Final DP598, 150p.

———1979. Le volcanisme archéen et la géologie structurale de a région de Cléricy, Abitibi, Québec; Thèse de doctorat [unpublished PhD thesis], École Polytechnique, Montréal, Québec, 307p.

University of British Columbia Geophysical Inversion Facility http://www.eos.ubc.ca/research/ubcgif/

Vaillancourt, C. 2001. Precambrian geology of the Watabeag Lake area; Ontario Geological Survey, Open File Report 6042, 61p.

Wilkinson, L., Cruden, A.R. and Krogh, T.E. 1999. Timing and kinematics of post-Timiskaming deformation within the Larder Lake–Cadillac deformation zone, southwest Abitibi greenstone belt, Ontario, Canada; Canadian Journal of Earth Sciences, v.36, p.627-647.

Williams, H. and McBirney, A.R. 1979. Volcanology; Freeman, Cooper and Co., San Francisco, 397p.

Williams, H.R., Stott, G.M. and Thurston, P.C. 1992. Tectonic evolution of Ontario: summary and synthesis. Part 1: Revolution in the Superior Province; *in* Geology of Ontario, Ontario Geological Survey, Special Volume 4, Part 2, p.1255-1294.

Wood, P.C., Burrows, D.R., Thomas, A.V. and Spooner, E.T.C. 1986. The Hollinger–McIntyre Au-quartz vein system, Timmins, Ontario, Canada: geologic characteristics, fluid properties and light stable isotope geochemistry; *in* Proceedings of Gold '86: An international symposium on the geology of gold, Konsult International, Toronto, p.56-80.

Zhang, Q., Machado, N., Ludden, J.N. and Moore, D. 1993.Geotectonic constraints from U-Pb ages for the Blake River Group, the Kinojevis Group and the Normetal Mine area, Abitibi, Quebec; Geological Association of Canada–Mineralogical Association of Canada, Annual Meeting, Program with Abstracts, v.18, p.A114.

This page left blank intentionally

Appendix 1

Thermal Ionization Mass Spectrometry (TIMS) Methodology, Results and Data

THERMAL IONIZATION MASS SPECTROMETRY (TIMS) ANALYTICAL METHODS

Uranium-lead geochronological samples for this project were collected during field work in 2003 and 2004 and analyzed at the Jack Satterly Geochronology Laboratory (JSGL) at the University of Toronto. All samples had weathered surfaces removed in the field using a hammer and chisel, and each piece was subsequently washed and dried in the laboratory before further processing. Total rock sample weights committed to crushing were generally in the 10 to 15 kg range. Samples were initially reduced using a jaw crusher, and then taken down to sand-size particles using a disk mill. Wilfley™ (shaking) table, heavy liquid (bromoform and methylene iodide) and magnetic separation (Frantz™ isodynamic separator) techniques were then employed to obtain an initial concentration of zircon and other minerals of high density.

From the least paramagnetic groups, highest quality zircon grains were handpicked under alcohol using a binocular microscope, with preferential individual grain selection made on the basis of clarity, and the absence of cores, cracks, alteration, and (Pb-bearing) inclusions. All zircon fractions were subjected to an air abrasion treatment (Krogh 1982) in order to remove exterior portions of grains that may have experienced post-crystallization Pb-loss. Prior to dissolution, weights of abraded zircons were estimated by use of a scaled digital photographic measurement of the length and breadth of each grain and an estimate of the maximum thickness, together with the known density.

Selected zircons were washed briefly in warm 4N HNO_3, given a brief second cleaning in 7N HNO_3, and then transferred in a single drop of 7N HNO_3 into clean Teflon dissolution vessels together with concentrated hydrofluoric acid and a measured quantity of mixed ^{205}Pb–^{235}U isotopic tracer solution (Krogh 1973). Complete sample dissolution was accomplished over a period of approximately 4 days at a temperature of 195°C. In all cases, zircon grain sizes were sufficiently small such that no ion exchange column chemical isolation and purification of Pb and U was necessary. Instead, fractions were dried down, redissolved in 6N HCl, dried down again with phosphoric acid and loaded directly with silica gel onto outgassed single Re filaments. All of the isotopic compositions of Pb and U were determined on a VG354 mass spectrometer using a Daly detector equipped with a digital ion counting system. System deadtime corrections during the analytical period were 19.5 ns for both Pb and U. Corrections for Daly mass discrimination were 0.05%/a.m.u., while that for thermal mass discrimination was estimated at 0.1%/a.m.u.

Laboratory procedural blanks at the JSGL are routinely at the 0.5 pg and 0.1 pg level or less for Pb and U, respectively. In most cases, the measured total common Pb in the samples was negligible and was assigned the isotopic composition of the lab blank; in a few cases, however, higher common Pb contents could be correlated with the presence of inclusions or minor cracks, and can be interpreted to represent initial common Pb, estimated here after Stacey and Kramers (1975). Comprehensive error estimation was made by propagating all known sources of analytical error, including internal (within-run) ratio variability, uncertainty in the fractionation corrections for Pb and U (based on long-term monitoring of standards), and uncertainties in the quantities and isotopic compositions of the laboratory blank and initial common Pb. The decay constants used for the U/Pb system are those of Jaffey et al. (1971). Age errors in the text, tables and figures are all presented at the 95% confidence level. Error ellipses in the concordia diagrams are shown at the 2σ level. For concordant and near-concordant data having overlapping $^{207}Pb/^{206}Pb$ errors, weighted mean ages were calculated by forcing a regression through the origin of concordia, according to the method of Davis (1982). Other discordia lines and concordia intercept ages were also determined by the regression methods outlined in Davis (1982), using the in-house program ROMAGE. In most cases, the calculated ages and errors using either the Davis (1982) or IsoPlot/Ex (Ludwig 2001) algorithms are equivalent. U/Pb concordia diagrams were generated using the IsoPlot/Ex program of Ludwig (2001).

GEOCHRONOLOGY RESULTS AND DISCUSSION

04BHA-0333 Felsic debris flow, southern Thorburn Township

(NAD83, Zone 17 UTM 453583E, 5395977N; #1 on Figure 2 and Table A1)

In southernmost Thorburn Township, the northeast-facing volcanic succession includes a redeposited volcaniclastic interval. A sample of felsic to intermediate volcaniclastic sandstone was collected from a sand-rich upper portion of a normally graded bed from this unit, and contains coarse plagioclase-lithic clasts as well as altered plagioclase set in a fine matrix of epidote and quartz. Zircon recovery from this volcaniclastic flow was poor; grains were sparse, small, and of generally inferior quality. Nonetheless, individual populations of better quality, colourless to pale pink/yellow, sharply terminated elongate prisms and short, stubby prisms were selected for air abrasion and analyzed. Distinct populations of rounded and pitted zircon grains were also identified and testify to the epiclastic nature of this unit, but they were not dated. Data for two elongate, sharp single prisms (A1, A2) and one short prism (B1) are concordant and yield a weighted mean $^{207}Pb/^{206}Pb$ age of 2712.3±2.8 Ma (84% probability of fit, MSWD = 0.18; Figure 3A; Table A1). Another short prism (B2) is distinctly xenocrystic, but concordant at 2861.4±3.4 Ma, whereas a third stubby prism (B3) shows some Pb-loss (B3; 2% discordant) and is excluded from any age calculation.

The consistent, overlapping and concordant age of 2712.3±2.8 Ma is interpreted to represent the crystallization age of this felsic volcaniclastic unit, and confirms a Kidd–Munro age assignment. The age is also compatible with the younging pattern in these northeast-facing volcanic units, which also include sample 04BHA-0297. However, Ayer et al. (2002) determined an age of 2719.5±1.7 Ma for a dacitic tuff (TB96-1) immediately to the northeast of the present locality, which suggests that a structural break may occur between these two nearby volcanic panels.

03BHA-0381 Rhyolite lapilli tuff, Footprint Lake, northern Loveland Township

A sample of rhyolite lapilli tuff was collected from Noranda diamond drill hole FPT-89-1 (Timmins Resident Geologist's Office, assessment file T-3236), covering the interval 130.85–136.8m (box #20). The purpose of dating this sample was aimed at constraining the age of volcanism in the northern part of the Kamiskotia area, and investigating the nature of the boundary between the Kidd–Munro assemblage in the north and the Blake River and Tisdale assemblages to the south. Although a heavy mineral separate was recovered from this sample, no minerals suitable for dating were observed.

04BHA-0297 Quartz-phyric flow-banded rhyolite, central Loveland Township

(NAD83, Zone 17 UTM 451785E, 5389819N; #2 on Figure 2 and Table 1)

A sample of quartz-phyric, flow-banded rhyolite was collected from a sequence of northeast-facing Kidd–Munro assemblage volcanic units in central Loveland Township. Sample 04BHA-0297 contains quartz and potassium feldspar phenocrysts ranging up to 2 mm in length, within a groundmass dominated by quartz and sericite. Moderate quantities of zircon were recovered from this unit, consisting mostly of stubby to slightly flat, water-clear, pale-brown to colourless, sharply faceted prisms. Rod-like melt and/or apatite inclusions were noted in several grains. Results from three air-abraded single zircon fractions are only slightly discordant (0.5–0.6%), but completely overlap, with $^{207}Pb/^{206}Pb$ ages ranging from 2712.5 to 2715.1 Ma (Z1, Z2, Z4; Figure 3B; Table A1). A fourth fraction (Z3) is 27.6% discordant and, when regressed together, all four fractions yield an upper intercept age of 2714.6±1.2 Ma (36% probability of fit; MSWD = 1.02), which is considered the primary age of eruption of the rhyolite. An age of 2714.6±1.2 Ma for this unit confirms its assignment to the Kidd–Munro assemblage (*see also* 04BHA-0333).

04BHA-0462 Granophyre, Kamiskotia Gabbroic Complex, Robb Township

(NAD83, Zone 17 UTM 451049E, 5381502N; #3 on Figure 2 and Table 1)

In central Robb Township, a granophyric phase from the Upper Zone (Barrie 1992) of the large Kamiskotia Gabbroic Complex (KGC) crops out approximately 1.7 km northwest of Kamiskotia Lake. A representative sample collected from this locality (04BHA-0462) consists of quartz, altered plagioclase, granophyric intergrowth, and minor opaques, chlorite and epidote. Zircon recovery from the sample was sparse, but an adequate number of good quality grains were found for analysis. These comprised colourless to pale pink-brown irregular grain fragments, parts of skeletal grains and rarer faceted crystals showing low-order faces. Conventional isotope dilution U/Pb analyses of three abraded single zircons are concordant to slightly discordant (0.2–0.6%) and yield $^{207}Pb/^{206}Pb$ ages between 2704 and 2706 Ma (Table A1). Weighting of all three analyses yields a mean age of 2704.8±1.4 Ma (53% fit, MSWD = 0.64; Figure 3C), which is considered a robust estimate for the age of crystallization of the Upper Zone of the KGC.

The 2704.8±1.4 Ma age for the KGC Upper Zone granophyre is slightly younger than, but within error of, a 2707±2 Ma age determined for a stratigraphically lower, Middle Zone gabbro dated by Barrie and Davis (1990). The granophyre age is also within error of a 2703.1±1.2 Ma age for one of the lowest dated units (03BHA-0047; this study) of the Kamiskotia Volcanic Complex, which the gabbro and granophyre appear to intrude.

03BHA-0382 Rhyolite, Halfmoon Lake, northeastern Robb Township

(NAD83, Zone 17 UTM 452485E, 5383020N; #4 on Figure 2 and Table 1)

This sample represents a section of rhyolite recovered from diamond drill hole collared west of the Kam-Kotia Mine, at the Falconbridge Halfmoon Project, approximately 200 m south of Halfmoon Lake. Material for U/Pb dating was collected from the 97–100.5 m section of hole R-44-14.

The general zircon population from this sample comprises poor to moderate quality, short, pale- to medium-brown stubby, often ragged, prisms. Better quality grains show sharp, prismatic exteriors although many grains are also broken. A selection of the highest quality, short (2:1 or less) and/or broken, clear and crack-free prisms, essentially devoid of inclusions, were chosen for abrasion and analysis.

Three single grains yield completely overlapping data, straddling concordia and ranging between 0.2 and 0.4% reversely discordant (Figure 3D; Table A1). These results produce a weighted mean $^{207}Pb/^{206}Pb$ age of 2700.0±1.1 Ma (40% probability of fit; MSWD = 0.9), which is interpreted as the primary crystallization age of the rhyolite. The 2700 Ma age for the Halfmoon Lake rhyolite lies within error of the age of felsic volcanic rocks from the Genex Mine (03BHA-0345) and confirms a Blake River assemblage age for the volcanic stratigraphy immediately north and east of Kamiskotia Lake.

03BHA-0384 Felsic lapilli tuff, Kam-Kotia Mine, eastern Robb Township

(NAD83, Zone 17 UTM 455853E, 5381788N; #5 on Figure 2 and Table 1)

This sample of felsic lapilli tuff was collected from outcrop approximately 500 m southeast of the Kam-Kotia Mine in easternmost Robb Township. Zircons recovered from this sample comprise fairly clear, colourless to pale brown short and elongate prism populations. Apatite and fluid inclusions are relatively common. Uranium and Pb isotopic data obtained for four single short prisms are all overlapping and concordant and yield an average $^{207}Pb/^{206}Pb$ age of 2701.1±1.4 Ma (97% probability of fit, MSWD = 0.09; Figure 3E; Table A1). This age, interpreted to reflect the primary crystallization of the tuff, is nearly identical to those obtained from other volcanic units between Halfmoon Lake and the Genex Mine and appear to corroborate a Blake River assemblage age for this sequence.

03BHA-0345 Felsic lapilli tuff, Genex Mine, central Godfrey Township

(NAD83, Zone 17 UTM 458483E, 5369414N; #6 on Figure 2 and Table 1)

A sample of crystal-rich felsic lapilli tuff was collected from an outcrop approximately 800 m south-southwest of the Genex Mine. This sample yielded an abundant population of relatively large, colourless to pale yellow-brown, water-clear, sharply prismatic or euhedral zircon grains. Best quality grains are dominated by short, stubby or equant forms, though subordinate populations having slightly more elongate, or flat, prismatic morphologies are also present. Rod and bubble inclusions are common in many zircons, but were avoided in the final grains chosen for analysis.

Data for three abraded single-grain fractions of colourless to pale yellow, clear, stubby to equant zircons overlap completely, clustering tightly on or slightly above concordia (<0.6% reversely discordant; Figure 3F; Table A1). All three fractions considered together yield a weighted mean $^{207}Pb/^{206}Pb$ age of 2698.6±1.3 Ma (16% probability of fit). This age is considered to represent the best estimate of the primary age of crystallization of the tuff.

An age of 2699±1 Ma for the felsic lapilli tuff at the Genex Mine is entirely consistent with ca. 2700 Ma volcanism dated elsewhere in the region between the Genex and Halfmoon Lake deposits, immediately east and northeast of the Kamiskotia Gabbroic Complex (new results: this report). The age appears to slightly postdate that determined for nearby rhyolites from southwestern Godfrey Township, which were emplaced at 2705±2 Ma (Barrie and Davis 1990). The new U/Pb age determination at 2699 Ma suggests that the felsic volcanic rocks exposed adjacent to the Genex VMS deposit likely represent members of the Blake River assemblage, rather than the Tisdale assemblage as previously thought (Ayer et al. 2002).

03BHA-0047 Felsic lapilli tuff, eastern Turnbull Township

(NAD83, Zone 17 UTM 453921E, 5370435N; #7 on Figure 2 and Table 1)

Sample 03BHA-0047 represents a crystal-rich felsic lapilli tuff from the lower(?) part of the Kamiskotia Volcanic Complex, cropping out on the western flank of the Kamiskotia anticline in eastern Turnbull Township. The unit contains abundant quartz and albitized feldspar phenocrysts (to 1 mm), set in a matrix of quartz-sericite and carbonate, and contains relict volcanic shards. Abundant zircon was recovered from this sample, consisting mostly of clear, small, stubby prisms as well as flat, equant or irregular grains. Three single-grain zircon analyses yielded concordant or near-concordant results (Figure 4A; Table A1). A weighted mean age derived from all three fractions is 2703.1±1.2 Ma (56% probability of fit; MSWD = 0.57), and is considered to represent the primary age of eruption of the tuff. This age is consistent with an interpretation placing the greater Kamiskotia Volcanic Complex stratigraphy within the ca. 2696 to 2703 Ma Blake River assemblage.

96JAA-0094 Rhyolite, Carscallen Township

(NAD83, Zone 17 UTM 449520E, 5363120N; #8 on Figure 2 and Table 1)

Ayer et al. (2002) presented U/Pb geochronological evidence that suggested that rhyolite and related felsic tuffs and volcanic rocks occurring in northern and central Carscallen Township east of the Kamiskotia Gabbroic Complex might be old enough to assign to the upper Kidd–Munro assemblage. This was supported by ages for three single-grain zircon fractions from rhyolite 96JAA-0094, which were concordant to subconcordant and yielded an age of 2712.8±1.2 Ma. Although the unit overlies iron formation at the top of the Deloro assemblage, the general facing directions are consistent with a progression to the north and northeast into rocks mapped as the Kamiskotia Volcanic Complex, which

contrastingly have been dated near 2700 Ma (Barrie and Davis 1990; this study). Further geochronological study of sample 96JAA-0094 was carried out to test whether the true age for the felsic volcanic unit is closer to a Tisdale (ca. 2710–2704 Ma) or Kamiskotia Volcanic Complex–Blake River (ca. 2703–2696) age, and resolve whether the published 2713 Ma age accurately dates the time of volcanism or possibly inheritance.

Three additional good-quality zircon grains were selected from sample 96JAA-0094 for air-abrasion and U/Pb analysis. These included two very fine-grained short, colourless zircon prisms from a subpopulation not analyzed by Ayer et al. (2002). The new isotopic data are presented in Table A1 and are shown graphically, together with the earlier data, in Figure 4B. Data for two of the new analyses (Z1, Z2) are concordant and have overlapping $^{207}Pb/^{206}Pb$ ages. Moreover, these are entirely within error of the two most concordant data of Ayer et al. (2002), shown as shaded ellipses in Figure 4B. A recalculated weighted mean age for only these four analyses is 2712.2±0.9 Ma, which confirms a Kidd–Munro age for this unit. A third single-grain analysis (Z3) is 4% discordant but has a $^{207}Pb/^{206}Pb$ age of 2853.6±1.4 Ma, attesting to the presence of a much older, pre-Abitibi inheritance in this area.

04JAA-0004 Deformed conglomerate, Timiskaming assemblage, northeast Thorneloe Township

(NAD83, Zone 17 UTM 463598E, 5354205N; #9 on Figure 2 and Table 1)

Sample 04JAA-0004 represents a strongly deformed conglomerate collected from the south shore of Kenogamissi Lake in northeastern Thorneloe Township. Dating of zircon in this metasediment was carried out in order to test for the presence of Timiskaming conglomerates west of the Mattagami River fault. The sample contained an abundant assortment of zircon morphological types, ranging from large, rounded grains to sharply euhedral, occasionally elongate (up to ~4:1) whole prisms and fragments, and rare, small, distinctly brown prismatic grains. Results from the analysis of the U/Pb isotopic compositions of seven air-abraded single detrital zircon grains are presented in Figure 4C and Table A1. The oldest zircon population measured is represented by two concordant analyses (rounded grains Z1, Z2) whose $^{207}Pb/^{206}Pb$ ages cluster at 2726.1 and 2727.5 Ma. The youngest igneous grains are represented by two fractions (euhedral grains Z4, Z5) overlapping each other and concordia, having $^{207}Pb/^{206}Pb$ ages of 2684.4 Ma and 2685.0 Ma. Two intermediate-age grains (brownish fragments Z7, Z8) are 0.7 and 1.7% discordant with ages at 2716.1 and 2705.0 Ma, respectively. Fraction Z6 represents a single, discrete short brown prism with high uranium concentration (524 ppm) and very low Th/U (0.07). This zircon yielded a concordant $^{207}Pb/^{206}Pb$ age of 2618.1±2.0 Ma (2σ), and is best interpreted as a grain crystallized during metamorphic heating of this unit (accompanying deformation?). The most rigorous constraint on the age of sedimentation is provided by the precise analysis for grain Z4, implying that deposition of the conglomerate was younger than 2684.4±1.7 Ma (2σ). The older age populations in this sample imply that detritus was shed into the basin from older Abitibi crustal sources such as felsic volcanic rocks of the Deloro, Kidd–Munro and Tisdale assemblages.

The results support the hypothesis that this deformed band of sediments represents the continuation of Timiskaming assemblage and the Porcupine–Destor fault to the west of the Mattagami River fault.

04PCT-0062 Feldspar-phyric lapilli tuff, Deloro Township

(NAD83, Zone 17 UTM 478510E, 5364034N; #10 on Figure 2 and Table 1)

Sample 04PCT-0062 was collected from a sequence of feldspar-phyric lapilli tuffs intercalated with ultramafic volcanic rocks and iron formation exposed along the Deloro Township power line in northwestern Deloro Township. This sample contained very sparse and generally low-quality zircon,

comprising a variety of essentially colourless, euhedral and subhedral grains, occasionally elongate (up to ~4:1), and frequently with numerous cracks or inclusions. Equant morphologies and irregular fragments of zircon are also present, as is a distinct population of finer grained, rounded grains suggestive of sedimentary reworking.

Highest quality, clear, colourless, short or slightly elongate prisms with sharp facets were selected for air-abrasion and analysis. Results of U/Pb geochronology carried out on five fractions from this tuff are presented in Figure 4D and Table A1. The analytical data are variably discordant, with two fractions (Z1, Z5) overlapping concordia. Results from all fractions are collinear, and a free regression of all data results in a calculated upper intercept age of 2724.1±3.7 Ma (65% probability of fit; MSWD = 0.55), and a lower intercept age of 299 Ma. Choosing to exclude the relatively imprecise but concordant analysis for Z5 makes little difference to the upper intercept age or errors, and so the preferred interpretation of the primary age of this feldspar-phyric lapilli tuff is 2724.1±3.7 Ma.

SM85-60 Albitite dike, McIntyre Mine, Tisdale Township

(NAD83, Zone 17 UTM 477860E, 5369470N; #13 on Figure 2 and Table 1)

At the McIntyre Mine in Tisdale Township, albitite dikes transect tholeiitic basalts of the Tisdale assemblage as well as the local, 2689±1 Ma Pearl Lake granitic porphyry. On the basis of geochemical arguments, these dikes were interpreted by Burrows and Spooner (1986) as altered equivalents of lamprophyres, and have been considered petrogenetically unrelated to most regional porphyries (Wood et al. 1986). Moreover, the dikes appear to have intruded late in the tectonic history of the area, are overprinted by hydrothermal alteration, and are themselves crosscut by gold-bearing veins (Burrows and Spooner 1986; Bateman et al. 2004).

Corfu et al. (1989) presented U/Pb isotopic data for five zircon fractions from this dike (sample "Ab" in their study). These authors concluded that the best constraint on the age of the albitite dike was established by the precise multigrain analysis of equant prisms (their analysis #41), as well as two other less precise age determinations on equant single grains (#40, 42). When combined with a discordant analysis of long-prismatic brownish prisms, they obtained an age of 2673+6/–2 Ma (37% probability of fit; Corfu et al. 1989). Inheritance was also noted in one multigrain fraction (#39) comprising subrounded long-prisms, suggesting incorporation of xenocrystic zircons with a minimum age of 2689 Ma. Although slightly imprecise, the 2673 Ma age confirmed that the albitite dike is distinctly younger than, and unrelated to, the nearby Pearl Lake porphyry (2689±1 Ma: Corfu et al. 1989).

Additional, new analyses of single-grain zircon fractions from this sample were sought in order to improve the error on the primary age of dike emplacement, as well as to test a more refined age correlation with another precisely dated albitite dike from the Timmins area (e.g., 04JAA-0010, this study). For this purpose, three more single-grain fractions were analyzed—two abraded equant grains and one subrounded elongate prism—and their results are presented in Table A1 and Figure 4E. The two equant grains (Z1, Z2) are completely overlapping, concordant, and yield an average $^{207}Pb/^{206}Pb$ age of 2672.7±1.3 Ma, while the third fraction (Z4) is 1.4% discordant and has a $^{207}Pb/^{206}Pb$ age of 2694±4 Ma. The new data in Figure 4E (white ellipses) are plotted together with the most concordant data of Corfu et al. (1989; analyses 39–42: shaded ellipses in Figure 4E). Although a total of five analyses cluster on concordia between 2670 and 2676 Ma, a weighted mean calculated for the most precise three analyses (Z1, Z2, 41) yields an age of 2672.8±1.1 Ma, which is interpreted here as the best estimate of the primary age of crystallization of the albitite dike. The older age for the subrounded long prism (Z4) is consistent with the earlier results of Corfu et al. (1989) for this morphology suggesting possible inheritance from units such as the porphyry suite in the McIntyre Mine area (ca. 2688–2691 Ma).

The revised age of 2672.8±1.1 Ma for the albitite dike provides a more robust maximum age estimate for crosscutting gold mineralization at the McIntyre Mine. The dike age is also considered to be identical within error to that of an intermineral dike (interpreted to represent a heavily altered lamprophyre) cutting Timiskaming assemblage units at the Holloway Mine (Ropchan et al. 2002). Also, the emplacement age for SM85-60 appears to be slightly younger than that determined for the compositionally similar albitite dike intruding Tisdale assemblage ultramafic volcanic rocks from Whitney Township (2676.5±1.6 Ma; *see* 04JAA-0010 below).

04JAA-0009 Heterolithic breccia, north Tisdale syncline, western Tisdale Township

This sample was collected to test for the possible presence of Krist formation at the contact between Porcupine assemblage sediments and underlying Tisdale assemblage volcanic rocks in the north Tisdale syncline, western Tisdale Township. Although a heavy mineral separate was recovered from this sample, no datable minerals were observed.

KCR.52 Porcupine greywacke, central Tisdale syncline, Tisdale Township

(NAD83, Zone 17 UTM 479026E, 5372271N; #14 on Figure 2 and Table 1)

A representative band of Porcupine Group greywacke was sampled across the central Tisdale syncline by W. Bleeker (GSC) from Pamour Exploration drill hole NK90-04, over an interval between 320 and 400 feet depth. Here, steeply bedded greywackes overlie mafic volcanic rocks with an intervening transition zone of black argillite (W. Bleeker, GSC, personal communication, 2004). An abundant and varied assortment of zircon was recovered from this sample. Least paramagnetic and best quality populations included large, slightly elongate, colourless to very pale brown prisms with minor rod inclusions, smaller, well-faceted short prisms, medium-brown, euhedral to slightly rounded, short prisms, and elongate (~4:1) square or four-sided clear, colourless prismatic grains.

Six air-abraded single detrital grains yield $^{207}Pb/^{206}Pb$ ages that range narrowly from approximately 2691 to 2700 Ma, although two fractions (A3, C1) are slightly discordant, and one of these is relatively imprecise due to elevated common Pb (A3: Figure 4F; Table A1). The U/Pb geochronological results are consistent with detritus having been sourced in uplifted, older Abitibi assemblages, which, in this sample, appear limited to Blake River assemblage rocks (ca. 2696-2703 Ma), some of the older regional porphyry suite intrusive rocks (ca. 2690–2691 Ma), or even recycled components of Krist formation fragmental volcanic rocks (lower Porcupine assemblage; ca. 2687–2692 Ma). The most robust constraint on the maximum age of deposition for this Porcupine unit is provided by single-grain fraction A1, which is concordant at 2690.9±2.5 Ma (2σ).

04JAA-0003 Fine-grained wacke, Porcupine assemblage, eastern Tisdale Township

(NAD83, Zone 17 UTM 484309E, 5371290N; #15 on Figure 2 and Table 1)

This sample represents a fine-grained greywacke within Beatty formation sandstones of the Porcupine sequence directly underlying the Timiskaming angular unconformity in eastern Tisdale Township. Sample 04JAA-0003 contained an abundant and diverse supply of nonmagnetic zircon, ranging from clear and colourless narrow elongate prisms to large, medium-brown larger grains with or without inclusions. Most grains show some evidence for sedimentary abrasion such as slight rounding of grain edges or pitted surfaces. A selection of high-quality, clear single grains were chosen for air-abrasion and

analysis, and the data are presented in Figure 5A and Table A1. Four of the six zircon analyses are concordant or nearly concordant (>99.4%) and have $^{207}Pb/^{206}Pb$ ages at 2687.2 Ma, 2691.5 Ma, 2720.4 Ma and 2725.5 Ma, a fifth (A3) is slightly more discordant at 2708.3 Ma, while the sixth fraction (A1) is too discordant to be reliable (3.2% discordant). The results suggest that provenance sources for this Beatty formation wacke probably included uplifted and eroded expanses of older Abitibi crust in part including Deloro (ca. 2724–2730 Ma), Stoughton–Roquemaure (2720–2723 Ma), and Tisdale (2704–2710 Ma) assemblages. The youngest identifiable grain places a constraint on sedimentation, indicating that Beatty deposition must have postdated 2687.2±1.6 Ma (2σ).

04ED-198 Quartz-porphyritic sericite schist, Hoyle Pond Mine, Hoyle Township

(NAD83, Zone 17 UTM 492687E, 5377143N; #16 on Figure 2 and Table 1)

At the Hoyle Pond Mine, the local Tisdale volcanic assemblage is a stratigraphic host to a quartz-phyric sericite schist (Dinel and Fowler 2004). From underground at the mine site (–600 m), sample 04ED-198 was collected in order to test the age of the apparently conformable, surrounding mafic to ultramafic Tisdale assemblage volcanic rocks in this area. Petrographic aspects of the sericite schist (e.g., embayed quartz phenocrysts) led Dinel and Fowler (2004) to conclude that the unit is igneous in origin. A moderate yield of tiny, clear to cloudy, colourless to pale brown, elongate (2-4:1) doubly terminated prisms was recovered from this sample. Many of these contained zones of alteration, inclusions and cracks. Two of the better quality colourless prisms and a single brown prism tip broken into two fragments were abraded and analyzed, and the results are shown in Figure 5B and Table A1. Although none of the fractions yielded concordant data, all four of the analyses are collinear and, when regressed together, provide an upper intercept age of 2687.6±2.2 Ma (55% probability of fit; MSWD = 0.59). This age is interpreted as the primary age of crystallization of the schistose felsic volcanic unit, but is at least 14 my younger than the expected age for the enclosing Tisdale assemblage volcanic rocks (ca. 2704–2710 Ma). Because the age for the felsic unit is identical within error to a number of other Timmins porphyry bodies, including a 2684.4±1.9 Ma quartz-albite porphyry from the Hoyle Pond Mine itself (Dinel and Fowler 2004; this study), it seems likely that the quartz-porphyritic schist dated here represents a sheet which intruded the Tisdale volcanic sequence conformably or semi-conformably.

03ED-096A Quartz-feldspar porphyry, Hoyle Pond Mine, Hoyle Township

(NAD83, Zone 17 UTM 492516E, 5377036N; #17 on Figure 2 and Table 1)

The Hoyle Pond porphyry is a small, elongate intrusive body (probably <1.0 x 0.1 km) emplaced into mafic volcanic rocks of the lower Tisdale assemblage. The unit is characterized by euhedral quartz and albite phenocrysts ranging in size from 5 to 18 mm, the latter frequently showing a preferential alignment or trachytic texture, set within a fine-grained microlitic groundmass. The unit carries a strong, penetrative fabric associated with D2 fold structures.

Zircons from the Hoyle Pond porphyry are dominantly short, small square euhedral prisms, occasionally doubly terminated, but frequently broken. Rare, more elongate (up to 4:1) prisms are also present. Most grains are full of inclusions and fractures and are medium-brown in colour, but clear and colourless grains are present. Several clear and crack-free representative short prisms were picked and given a strong air-abrasion treatment. Table A1 and Figure 5C show the U/Pb analytical results for four fractions. Three single-grain analyses (A1b, A1c, A2a) are concordant or nearly concordant (99.5–100.0%) and together yield a weighted mean $^{207}Pb/^{206}Pb$ age of 2684.4±1.9 Ma (54% probability of fit, MSWD = 0.61). This age is considered the best estimate of the timing of crystallization of the Hoyle Pond porphyry, and may also represent the timing of D2 deformation and penetrative S2 fabric development if the body intruded a dilation zone synkinematically. Analysis of a fourth single-grain

fraction (A1a) also overlaps concordia, but has a distinctly higher $^{207}Pb/^{206}Pb$ age at 2695.1±3.3 Ma, and is interpreted as reflecting a mixture of an inherited component (e.g., 2703 Ma or older Tisdale assemblage) and magmatic growth within the porphyry at 2684 Ma. A 2684 Ma age for D2 deformation is consistent with the general observation by Bateman et al. (2004) that folds of this generation occurred after deposition of Porcupine assemblage (<2687.2±1.6 Ma in the Timmins area; M.A. Hamilton, in progress), but before the onset of Timiskaming sedimentation (<ca. 2673 Ma), as noted.

03RJB-18973-10 Sandstone, Porcupine assemblage, Hoyle Township

(NAD83, Zone 17 UTM 492148E, 5375256N; #18 on Figure 2 and Table 1)

A single sample of Hoyle formation sandstone was combined from two separate intersection intervals from Porcupine Joint Venture drill hole 18973 (112–115 m and 128–131 m), collared north of the Pamour Mine near the Hoyle–Whitney townships boundary. This sample, of presumed Porcupine formation affinity, is representative of the sedimentary unit, which, at this locality, is in fault contact with underlying basalts of the lower Tisdale formation.

This sample contained a relatively abundant and mixed population of large and small zircon grains, including clear, colourless to pale- and medium-brown stubby to short prisms, often sharply faceted but occasionally subrounded. Minor flat prisms are also present. Analysis of six strongly air-abraded single grains by TIMS yielded a spread of essentially concordant data of variable precision, having $^{207}Pb/^{206}Pb$ ages of 2725.1±13.3 Ma, 2712.9±5.1 Ma, 2711.5±13.8 Ma, 2704.2±8.6 Ma, 2690.4±5.0 Ma and 2688.2±1.9 Ma (Figure 5D; Table A1). As with the previous sample, the oldest detrital zircon could have been sourced in Deloro assemblage units (ca. 2724–2730 Ma), whereas intermediate age populations could ultimately reflect Kidd–Munro (ca. 2711–2719 Ma) and Tisdale (ca. 2703–2710 Ma) assemblage provenance.

The youngest two detrital zircon ages are within error of each other and are equivalent to the youngest age reported from Porcupine sandstone 03RJB-18972-6 (this report: 2689.5±1.7 Ma). The ages are also consistent with the youngest identified detrital zircons from other Beatty and Hoyle formation units described elsewhere between the Timmins and Kidd Creek areas (2687.2±1.6 Ma, 2690.9±2.5 Ma: M.A. Hamilton, unpublished data; 2691.3±1.5 Ma: W. Bleeker, GSC, personal communication, 2005; 2684.7±6.3 Ma: Bleeker and Parrish 1996).

Ion microprobe (SHRIMP) dating was also carried out on a limited number of detrital zircon grains from this sample. Initial *in situ* characterization of the detrital population, based on 19 concordant or nearly concordant (>97%) analyses reveals a very limited spread of $^{207}Pb/^{206}Pb$ ages, mostly between 2706–2687 Ma, with the exception of two older grains, at 2714 Ma and 2756 Ma. Although the youngest age data are not sufficiently precise to constrain a maximum age of deposition with great certainty, the bulk of the younger zircon detritus clusters near 2690 Ma and clearly substantiates in greater number the results determined by isotope dilution.

As described above for sample 03RJB-18972-6, the similarity of the youngest detrital grain ages with the established ages for Krist formation felsic magmatism (2685–2691.5 Ma: Ayer et al. 2003) suggests that fragmental, calc-alkalic volcanism may have been contemporaneous with parts of early, conformable Porcupine sedimentation. Subsequent greywacke turbidite deposition likely followed shortly after initial Krist magmatism and, in part, represents reworking of the ca. 2690 Ma fragmental debris.

03PJM-131 Quartz-feldspar porphyry, Pamour Mine area, Whitney Township

(NAD83, Zone 17 UTM 489978E, 5373473N; #19 on Figure 2 and Table 1)

As described by MacDonald and Piercey (2003) and MacDonald, Piercey and Hamilton (2005), the recently identified Pamour body southwest of Pamour Mine is a weakly foliated, moderately fresh, quartz- and feldspar-bearing porphyry carrying minor biotite alteration (disseminated fine flakes or 5–20 mm clusters), and little pyrite. Phenocrysts within the porphyry average 1 to 2 mm, but reach up to 5 mm in maximum dimension. This unit sharply intrudes strongly altered (talc-carbonate) ultramafic volcanic rocks of the Hersey Lake formation in the lower Tisdale assemblage. The Pamour porphyry appears to truncate an earlier structural foliation developed in the host rocks, and is itself characterized internally by only a weak fabric, which may have originated by magmatic flow (MacDonald and Piercey 2003; MacDonald, Piercey and Hamilton 2004; 2005; Bateman et al. 2004, 2005, this study). The significance of this is discussed below.

A representative sample of the porphyry was collected for dating from the 340.8 to 392 m interval of Porcupine Joint Venture drill hole 18986. Quartz-feldspar porphyry sample 03PJM-131 yielded a relatively diverse population of poor-quality zircons, comprising small, generally square bipyramids, pale to medium brown in colour, and often cracked, frosted or turbid, with some of the larger grains being slightly rounded (resorbed xenocrysts?). The best-quality (clearest, inclusion- and crack-free) grains were given strong air-abrasion before final selection and analysis, but the results are scattered: three fractions lie on or near concordia between 2680 and 2703 Ma (2 of these fractions have large errors, due in part to elevated common Pb; Table A1; Figure 5E). These data likely reflect varying degrees of zircon inheritance from the Tisdale assemblage or underlying units within porphyry magmatic grains. Two darker brown single grains are both highly discordant (A1b, A1c: Figure 5E). However, the datum for a single brown square bipyramid (fraction A1f) is only slightly discordant (0.5%) and at present provides the best estimate for the age of the sample, at 2677.5±2.0 Ma ($^{207}Pb/^{206}Pb$ age). This interpretation is based on the assumption that analysis A1f itself does not contain inheritance; further, because of its minor discordance, the 2677.5 Ma age could be regarded as a minimum time of emplacement.

Preliminary U/Pb results have been obtained for minor, euhedral pale yellow titanite from this sample. Two initial single-grain fractions are variably discordant, but suggest an upper intercept age of ~2673±11 Ma. Although imprecise, the titanite age is consistent with simple cooling through ca. 600°C following igneous crystallization, as defined by the best zircon age estimate near 2677.5 Ma.

In summary, the best approximation of the age of emplacement of the Pamour porphyry is provisionally estimated at 2677.5±2.0 Ma, though this conclusion is based upon a slightly discordant single analysis. A more robust assessment of the true age of the body is hampered by inheritance and Pb-loss effects. Although younger than most other porphyry intrusions in the Timmins area (ca. 2687–2692 Ma), the ca. 2678 Ma age is entirely consistent with the observation that the Pamour intrusion carries less of a structural fabric than its counterparts and host rocks and may therefore independently provide a minimum age for D2 deformation. This interpretation is supported independently by the age of the Hoyle Pond porphyry (2684.4±1.9 Ma: *see* 03ED-096A above), which may be synchronous with D2 structures. An interesting additional observation is that the ca. 2678 Ma Pamour porphyry age correlates with a distinct population of youngest detrital zircons found within Dome formation sediments of the lowermost Timiskaming Group (2679 Ma: Ayer et al. 2003; Corfu, Jackson and Sutcliffe 1991).

04JAA-0010 Albitite dike cutting Tisdale assemblage ultramafic volcanic rocks, Whitney Township

(NAD83, Zone 17 UTM 491529E, 5372949N; #20 on Figure 2 and Table 1)

South of the Pamour Mine, near the Porcupine–Destor deformation zone (PDDZ) in Whitney Township, an 8 m thick, white albitite dike cutting ultramafic volcanic rocks of the Tisdale assemblage was intersected in drill core (DDH 18979; E. Barr, Placer Dome (CLA) Ltd., Porcupine Joint Venture, personal communication, 2004). Similar, though much thinner dikes were also observed intruding Timiskaming assemblage conglomerates at this locality, but were too small to investigate. Sample 04JAA-0010 was collected from the thick albitite dike and consists of a fine-grained and sugary textured albititic feldspar with 1 to 2% disseminated pyrite and rare, fine-grained quartz phenocrysts. This dike yielded a small but adequate amount of good quality zircon. The best quality grains comprised essentially clear, nearly colourless prismatic forms characterized by (4-5:1) needles ranging up to 300 μm in length, or by short, stubby doubly terminated crystals. Most grains show a small amount of subrounding. Five single, clear and colourless to pale brown single zircons were analyzed for U and Pb; results are presented in Figure 5F and Table A1. The data range from being nearly concordant (0.6–0.7% discordant: A1d, A1e) to moderately discordant (5.5%: A1c). However, data for four of the five fractions are strongly collinear, and regression of these four (A1b to A1e) through the origin yields a tightly constrained upper intercept age of 2676.5±1.6 Ma (95% fit; MSWD = 0.12). Fraction A1a contained elevated total common-Pb levels; the datum for this grain is resultingly imprecise, is almost 2% discordant and has a $^{207}Pb/^{206}Pb$ age of 2665.2±13.9 Ma, falling to the left of the discordia. For these reasons, the datum for fraction A1a is considered spurious and is not included in the age regression.

The age result for the albitite dike in Whitney Township is similar to the provisional age of ca. 2677.5 Ma for the nearby Pamour porphyry (03PJM-131) and the possibility of a genetic relationship between the two is raised. Burrows and Spooner (1986) and Wood et al. (1986), however, have argued, on the basis of geochemical comparisons with other porphyry bodies, that a petrogenetic linkage is doubtful. The 2676.5±1.6 Ma age is almost within error of the revised age for the albitite dike from the McIntyre Mine (SM85-60: 2672.8±1.1 Ma; Corfu et al., 1989; this study). At the McIntyre Mine, the albitite dikes are crosscut by an auriferous vein and alteration system and the albitite dikes, therefore, provide an important maximum age constraint on the timing of gold mineralization.

03RJB-18972-6 Sandstone, Porcupine assemblage, Whitney Township

(NAD83, Zone 17 UTM 491548E, 5372704N; #21 on Figure 2 and Table 1)

This sample was recovered from the 140 to 148 m interval of Porcupine Joint Venture drill hole 18972, and comprised fine sands within a broader section of turbiditic beds between 124 and 152 m. This unit occurs south of the main unit of Timiskaming assemblage sandstone and south of the Porcupine–Destor deformation zone, in rocks previously mapped as the Whitney formation member of the Porcupine assemblage (after Born 1995).

Zircon populations from this sample comprised a variety of clear and colourless, short-prismatic and slightly rounded grains, to pale and darker brown-red varieties as well as a distinct group of well-rounded and pitted grains. Analysis of five strongly air-abraded single grains by TIMS yielded an essentially bimodal clustering of concordant data having $^{207}Pb/^{206}Pb$ ages of 2726.2±1.6 Ma and 2722.9±3.7 Ma, and 2691.6±8.0 Ma, 2689.9±2.4 Ma and 2689.5±1.7 Ma; the datum for a sixth grain (B4) is moderately discordant (3.2%) and has a younger $^{207}Pb/^{206}Pb$ age of 2658.8±1.5 Ma (Figure 6A; Table A1). The older detrital zircon populations likely reflect provenance from sources such as the Deloro assemblage (ca. 2724–2730 Ma), whose present-day exposures are in relatively close proximity. This interpretation is supported, in part, by the euhedral nature of the two measured older grains. The younger ages, at ca.

2690 Ma, are equivalent within error to the age of Krist formation felsic volcanic rocks (2685–2691.5 Ma: Ayer et al. 2003), which are known to occur at the base of the Porcupine assemblage. These ages are also comparable to the emplacement ages of numerous calc-alkaline porphyries in the Timmins area and elsewhere (mostly 2688–2691 Ma: M.A. Hamilton, this study; Ayer et al. 2003; Gray and Hutchinson 2001; Corfu et al. 1989).

The youngest pair of reliable concordant single-grain analyses (A1, B3) permit a provisional maximum age of deposition for the sandstone to be estimated at approximately 2689 Ma. Ancillary *in situ* spot age determinations have also been carried out on 15 additional zircon grains by ion microprobe analysis (SHRIMP II), and are presented in more detail in Figure 11C and in Appendix 2. In summary, the SHRIMP data reveal detrital zircon ages as old as approximately 2750 Ma in this sample, although most cluster between ca. 2740 to 2690 Ma. The younger end of the SHRIMP data spectrum corresponds closely with the youngest ages determined by TIMS (though the individual spot errors for the former are intrinsically less precise), and the most reliable age of deposition for this sandstone remains 2689 Ma. Ion microprobe analysis also yielded a single spot age determination for a grain interior at 2499±9 Ma; although the analysis is concordant (100.3%), this domain is characterized by anomalously high U (ca. 1200 ppm) and the significance of this age remains unclear. Further analytical work is warranted to elucidate the nature of the sparse younger apparent ages.

At present, given the relatively small total number of age determinations, it is impossible to definitively conclude that the unit represents a member of the Porcupine assemblage and not, for example, Timiskaming assemblage. However, the present TIMS and SHRIMP evidence suggest that there is a preponderance of youngest detrital zircon grains at ca. 2690 Ma, and an absence of grains in the range 2685 to 2675 Ma (which would be diagnostic of Timiskaming assemblage). Thus, it is considered most probable that the dated unit from this locality south of the PDDZ represents a sandstone member of the Porcupine assemblage.

C88-17 Felsic volcanic, Whitney Township

(NAD83, Zone 17 UTM 488920E, 5369670N; #22 on Figure 2 and Table 1)

South and east of Timmins, the Shaw Dome has been shown to be cored by rocks of the ca. 2730 to 2724 Ma Deloro assemblage (cf. samples #10, #23: Table 1; Figure 2). However, in south-central Whitney Township, Corfu and Noble (1992) suggested that a felsic volcanic member of comparable age (2725±1 Ma) occurs to the northeast and outside of this structure (their sample C88-17, or "DU-2"). In order to test for possible inheritance and verify the robustness of this age, further U/Pb zircon geochronology was carried out.

This sample contains a large number of zircons, most of which show a relatively uniform morphology (clear, colourless, equant to slightly elongate prisms). These features cast some initial doubt on a xenocrystic control for the age of this sample. Three high-quality air-abraded prisms were analyzed for their U and Pb isotopic compositions and the results are shown in Table A1 and Figure 6B. Data for all of the new fractions are concordant, with two having nearly identical $^{207}Pb/^{206}Pb$ ages (Z-B1, Z-F1: 2724.3, 2724.2 Ma, respectively), while the third fraction, Z-B2 (dashed ellipse), shows a slightly younger but overlapping age of 2718.6 Ma. Figure 6B also shows the excellent agreement between the two most concordant analyses of Corfu and Noble (1992; filled ellipses) and the older two single-grain analyses measured here. Regression of the five-point collinear array of the previous study with the new data (Z-B1, Z-F1) results in an upper intercept age of 2724.6±0.8 Ma (88% probability of fit; MSWD = 0.4), which is identical to, but slightly more precise than, the 2725±1 Ma age of Corfu and Noble (1992). The analysis of fraction Z-B2 is slightly reverse discordant; though marginally younger, the difference is not statistically significant and the analysis is considered spurious.

Therefore, on geochronological grounds, there is no compelling reason to doubt the validity of assigning this unit to the Deloro assemblage. Rather, an alternate rationale such as structural repetition may be a likely explanation for the occurrence of this unit within the younger (Tisdale assemblage) stratigraphy.

03LAH-0627 Mt. Logano quartz-feldspar porphyry, Shaw Township

(NAD83, Zone 17 UTM 492156E, 5365021N; #23 on Figure 2 and Table 1)

The Mt. Logano intrusion represents one of the largest single bodies of quartz-feldspar (albite) porphyry in the Timmins area, exposed south of the Porcupine–Destor deformation zone, on the northern flank of the Shaw Dome in northeastern Shaw Township (Hall and Houlé 2003). This elongate (roughly 1x5 km) unit was sampled in order to establish an age constraint for the southern trend porphyries (terminology of MacDonald and Piercey 2003).

Sample 03LAH-0627 yielded an abundance of high-quality, slender, pale brown to colourless well-terminated prismatic zircons, as well as rarer needle or acicular forms, and flat prisms. The highest quality, air abraded, elongate prisms yielded a very tight agreement of $^{207}Pb/^{206}Pb$ ages with two single-grain fractions overlapping one another and concordia, while a third is somewhat reversely concordant (Figure 6C; Table A1). A fourth single-grain fraction is slightly discordant, has a slightly older $^{207}Pb/^{206}Pb$ age, and probably contains a small amount of inheritance (A1d: Figure 6C). The three concordant and near-concordant fractions provide a well-defined weighted mean $^{207}Pb/^{206}Pb$ age of 2689.0±1.4 Ma, which is interpreted as the primary crystallization age of the Mt. Logano porphyry. Given the similarity in chemistry and field relationships of the intrusions on the northern margin of the Shaw Dome, it is likely that this age is representative of all or most southern trend intrusions.

The 2689 Ma age for the Mt. Logano porphyry is indistinguishable from the majority of ages determined for other porphyritic intrusions from the central, northern, and western trend bodies (2688–2691 Ma (n=7): Corfu et al. 1989; Gray and Hutchinson 2001; Ayer et al. 2003). The Mt. Logano intrusion was also emplaced within error of a number of other regional granitoid plutons, including the potassium feldspar porphyritic Adams stock (2686.4±2.8 Ma: Frarey and Krogh 1986), the Clifford stock and associated felsic dikes (2686.9±1.2 Ma, 2688.5±2.3 Ma: this report), the Clarice Lake pluton (2689±1 Ma: Corfu and Noble 1992), and several plutons in the eastern Abitibi region of Quebec (ca. 2690 Ma: Mortensen 1993b).

03LAH-0161 Felsic to intermediate flow, Shaw Township

(NAD83, Zone 17 UTM 493476E, 5362615N; #24 on Figure 2 and Table 1)

During the 2003 mapping season, a unit of intermediate to felsic metavolcanic rock was sampled by L.A.F. Hall and M.G. Houlé from an outcrop on the northeastern flank of the core of the Shaw Dome, eastern Shaw Township. This aphyric and amygdaloidal flow is interpreted to represent a member of the "Supracrustal Package A" (Hall and Houlé 2003), and a geochronological study of this unit was attempted in order to test whether or not the volcanic package is of probable Deloro assemblage affinity.

Zircon recovery from this sample was remarkably low. Only a few scattered grains were found and most were of very poor quality. One single, clear, brown irregular prism fragment was considered appropriate for analysis and was given a strong air-abrasion treatment. Uranium–lead results for this fraction are provided in Table A1 and Figure 6D. The data are slightly discordant (1.2%), have elevated common-Pb, and yield a measured $^{207}Pb/^{206}Pb$ age of 2727.3±11.9 Ma. If a simple (modern-day) Pb-loss history is assumed for the fraction, then the model $^{207}Pb/^{206}Pb$ age of 2727 Ma confirms that the central part of the Shaw Dome structure contains rocks of the Deloro assemblage (2724–2730 Ma: Ayer et al. 2003).

04MGH-0523 Intermediate volcaniclastic, south-central Langmuir Township

Sample 04MGH-0523 was collected from a sequence of intermediate epiclastic rocks found within "Supracrustal Package B" or "Supracrustal Package C", located in the south-central part of Langmuir Township. Although dating was targeted to resolve Tisdale versus Deloro assemblage ages southeast of the Shaw Dome, no accessory phases were found in the heavy mineral concentrate from this sample that were amenable to U/Pb geochronology.

96TB-099 Fragmental felsic volcanic, southern Langmuir Township

(NAD83, Zone 17 UTM 499477E, 5352378N; #26 on Figure 2 and Table 1)

Because of the same issues related to the occurrence of previously dated Deloro-age rocks—outside of the core of the Shaw Dome and apparently within the adjacent Tisdale stratigraphy—the same approach used with sample C88-17 (see above) was applied here. Namely, the purpose was to test for the possible influence of inherited or xenocrystic zircon grains on the determined age of 2723.4±1.5 Ma (Barrie 1999; Barrie and Corfu 1999) for the fragmental felsic volcanic ("dacite") unit from Langmuir Township (sample 96TB-099).

Three additional clear and colourless single zircon fractions were prepared for this sample, two of which represent euhedral short prisms, while a third is a euhedral, equant grain. The new U and Pb isotopic data for all three analyses cluster tightly on concordia (Table A1; Figure 6E, unshaded ellipses). This cluster overlaps directly with the most concordant three data points of Barrie (1999) and Barrie and Corfu (1999). With the exception of new fraction Z-C, which appears to be marginally older (xenocrystic?), a regression of all 4 points from Barrie and Corfu (1999; shaded ellipses in Fig. 6E) and new analyses Z-G and Z-H yields an upper intercept age of 2723.1±1.3 Ma (69% probability of fit; MSWD = 0.56; lower intercept = 207 Ma). This age is identical to, but slightly more precise than, the previous age of Barrie (1999) and Barrie and Corfu (1999), and confirms that the felsic volcanic at this locality belongs to the Deloro assemblage.

04MGH-0523 Intermediate volcaniclastic, south-central Langmuir Township

Sample 04MGH-0523 was collected from a sequence of intermediate epiclastic rocks found within "Supracrustal Package B" or "Supracrustal Package C", located in the south-central part of Langmuir Township. Although dating was targeted to resolve Tisdale versus Deloro assemblage ages southeast of the Shaw Dome, no accessory phases were found in the heavy mineral concentrate from this sample that were amenable to U/Pb geochronology.

04MGH-0283 Intrusive porphyry, Eldorado Township

(NAD83, Zone 17 UTM 487699E, 5351167N; #27 on Figure 2 and Table 1)

Sample 04MGH-0283 represents a quartz-feldspar porphyry intrusive unit, intersected in drill core (Inco DDH-87615; Box 86, 1574.6–1582.8 feet interval) on the Redstone property in Eldorado Township. The unit is interpreted to occur within Tisdale assemblage stratigraphy in the footwall to the main Redstone property mineralized horizon. Zircons recovered from this sample are abundant and of generally good quality, mostly occurring as slender, elongate prisms up to about 4-5:1 (length:width). Generally, these grains are clear and either colourless or pale-medium brown, and have square, or, more rarely, flat cross-sections. High-quality representative grains were selected for air abrasion and isotopic analysis.

Three individual grains were analyzed for U and Pb and gave highly consistent results, all of which are overlapping and only slightly discordant (0.4–0.6%: Figure 6F; Table A1). A calculated weighted mean age for all three fractions is 2686.2±1.1 Ma (64% probability of fit; MSWD = 0.44), which is interpreted as the primary age of crystallization of the porphyry. A 2686.2±1.1 Ma age for this intrusive is identical to that of the adjacent, large, potassium feldspar porphyritic Adams stock immediately to the west, dated at 2686±3 Ma (Frarey and Krogh 1986), as well as to a number of other porphyry bodies occurring in the Timmins area and elsewhere in the Abitibi greenstone belt.

04PCT-0064 Quartz-phyric gabbro dike, Bartlett Township

(NAD83, Zone 17 UTM 482078E, 5331967N; #28 on Figure 2 and Table 1)

A sample of quartz-phyric gabbro was collected from a dike cutting Deloro assemblage rocks in Bartlett Township. This dike is representative of numerous similar east to west striking dikes, which emanate from the underlying Muskasenda gabbro body and have been interpreted to feed overlying Tisdale assemblage mafic volcanic rocks occurring further to the east (Ayer et al. 2004).

Heavy mineral concentrates from this gabbro yielded very little zircon, except for extremely tiny, clouded and stained grains of relatively low quality. Minor, small blade fragments of very pale brown baddeleyite were also present, and a selection of these were chosen for U/Pb analysis. A dull lustre on all grains suggests the possible presence of fine zircon coatings. Results for four fractions, each comprising 3 small, thin blades of baddeleyite are presented in Table A1 and Figure 7A. All of the data are highly collinear and regress to yield an upper intercept age of 2705.7+4.4/–3.8 Ma (86% probability of fit; MSWD = 0.15) and a lower intercept age of 810 Ma. The Th/U ratios for the analyzed grain fractions range from 0.07 to 0.25. This is relatively high for baddeleyite, but is appropriate for a mixture of baddeleyite and zircon, the latter of which may be present as (late magmatic?) coatings on early igneous baddeleyite grains. This is also supported by the observation that the variation in Pb/U (i.e., Pb-loss) appears to be broadly correlated with Th/U, suggesting that the grains with the greater proportion of zircon rim development or growth also show the highest degree of discordance.

Direct dating of the large, sill-like Muskasenda gabbro has not been carried out previously, but the intrusion is known to enclose an enclave of Deloro assemblage felsic metavolcanic rocks, which have been dated at 2727.9±2.2 Ma (Ayer et al. 2003), thereby providing a maximum age for the younger host gabbro. A primary igneous age of 2705.7+4.4/–3.8 Ma for the east-west gabbro dike presented here establishes with reasonable confidence that the dikes (and by inference the Muskasenda gabbro sill) intruded Deloro assemblage stratigraphy during a period contemporaneous with Tisdale assemblage volcanism.

03JAA-0006 Feldspar porphyry, Discovery outcrop, Teck Township

(NAD83, Zone 17 UTM 571986E, 5333892N; #30 on Figure 2 and Table 1)

A sample of feldspar-porphyritic syenite was collected from an outcrop of Main Break mineralization on the (former) Wright–Hargreaves property. At this locality, the syenite is recognized as one of the youngest porphyries in the region, which cuts Timiskaming assemblage metasediments, but is itself crosscut by Main Break mineralization. Thus, accurate and precise dating of the porphyry offers the opportunity to establish a maximum age for the timing of mineralization.

Zircons recovered from this syenite are modest in number and relatively diverse in appearance. The largest, clear and crack-free grains comprise colourless or pale brown irregular fragments, rarely with prismatic crystal faces. However, the bulk of the sample is dominated by short, colourless to pale brown

subhedral prisms, slightly flat to square in cross-section, but variably cracked and clouded with inclusions. Higher quality representative zircons were selected from each of the main populations and subjected to strong air abrasion treatment. Results for five single-grain fractions are presented in Table A1 and Figure 7B. The U/Pb isotopic data for these zircons is compromised in some cases by a combination of very small grain size and higher-than-average levels of common-Pb. Most analyses are concordant within error, and have $^{207}Pb/^{206}Pb$ ages that fall between ca. 2690 and 2700 Ma (Table A1). Specifically, data from two grains overlap on or near concordia at approximately 2700 Ma (2700.2±2.9 Ma, 2700.6±4.4 Ma: Figure 7B). One analysis sits at 2694.4±7.4 Ma, while two younger analyses reflect an age at about 2690 Ma (2689.6±4.7 Ma, 2689.7±41.3 Ma).

Field relationships at this locality show unequivocally that the syenite porphyry intrudes Timiskaming Group sediments. Where constrained in the Kirkland Lake basin (and elsewhere), the age of deposition of the Timiskaming detritus is considered to be younger than approximately 2679 Ma (e.g., Corfu, Jackson and Sutcliffe 1991); moreover, results presented in this study further constrain the age of Timiskaming basin development to be younger than 2677.7±3.1 Ma or even 2669.6±1.4 Ma (samples 03VOI-0570-1, 03VOI-0422-1, below, respectively). Therefore, by virtue of being consistently older than the unit it intrudes, all of the single-grain zircon analyzed from the crosscutting syenite must be regarded as inherited, xenocrystic grains. Consequently, no absolute age information can be retrieved from the TIMS analyses carried out to date on this sample.

A reconnaissance SEM imaging and SHRIMP study were carried out on representative subpopulations of zircons from this syenite, and are reported elsewhere in detail (Appendix 2). In summary, however, backscatter electron (BSE) imaging of sectioned and polished zircons from sample 03JAA-0006 (*see* Figure 18) confirmed the presence of broad, subhedral to slightly rounded and embayed cores, locally, but not always rimmed by a very thin shell of bright (higher U, Th) exterior zircon growth that is often sharply magmatic. Ion microprobe U/Pb analysis of approximately 20 core domains revealed ages as old as ca. 2729 Ma, but the complete spectrum of ages form a broad cluster near concordia between this age and approximately 2675 Ma. Insufficient data were acquired on the very thin magmatic(?) overgrowths to permit a precise assessment of the timing of the igneous mantling of the xenocrystic cores. The ages determined on the zircon cores are consistent with the established provenance age modes known from Timiskaming detrital grains.

The BSE imaging and *in situ* U/Pb evidence, together with the TIMS results presented above, provide strong support for the interpretation of the bulk of the zircon age data to reflect an inherited, xenocrystic origin, presumably from the host Timiskaming assemblage sediments. The magmatic age of the syenite porphyry remains unclear, although independent new regional age constraints on host Timiskaming supracrustal units suggest that it may be younger than 2678 Ma or even 2670 Ma.

04VOI-4529 Intermineral dike, Teck Township

Sample 04VOI-4529 was collected from an intermineral dike associated with quartz vein mineralization at Macassa. Unfortunately, no accessory phases were found in the heavy mineral concentrate from this sample that were amenable to U/Pb geochronology.

04VOI-1518-4 Crosscutting dike, Teck Township

Sample 04VOI-1518-4 represents a dike which crosscuts a folded contact of syenite porphyries and tuffs, and constrains a maximum age for D4 deformation. Although a heavy mineral separate was recovered from this sample, no datable minerals were observed.

03VOI-0422-1 Trachytic lava, Timiskaming assemblage, Gauthier Township

(NAD83, Zone 17 UTM 587842E, 5332221N; #31 on Figure 2 and Table 1)

Sample 03VOI-0422-1 was collected from a distinct unit of feldspar-phyric trachytic lava from the volcanic-dominated section of the Timiskaming assemblage in central Gauthier Township.

A modest amount of zircon was recovered from this sample, dominated morphologically by small, short (2-3:1), generally cylindrical and often sharply terminated prisms. For the most part, zircons were colourless to brown and free of cracks and inclusions, but distinct cores were visible in some grains and were avoided where possible.

Analytical data for two abraded single grains and one fraction comprising two small grains are 0.3 to 3.2% discordant and yield overlapping $^{207}Pb/^{206}Pb$ ages between 2668.3 and 2670.1 Ma (Table A1). The strongly collinear nature of the data enable a regression line to be fit through the origin that provides an upper intercept age of 2669.6±1.4 Ma (71% probability of fit; MSWD = 0.34; Figure 7C). Two other fractions, consisting of a single, colourless stubby prism (A2) and two small short brown prisms (A4) are only slightly discordant (0.6%), but have distinctly higher $^{207}Pb/^{206}Pb$ ratios than the previous fractions. Their corresponding ages, at 2694 and 2676 Ma, respectively, suggest minor amounts of inheritance—possibly from Porcupine and even earliest Timiskaming sources—although the ages should be regarded as strictly minimum estimates.

The 2669.6±1.4 Ma age for the early Timiskaming assemblage alkaline volcanic rock from Gauthier Township is younger than any previous depositional estimate based on the youngest measured detrital zircons from the Timiskaming Group in the Timmins, Kirkland Lake or Larder Lake areas (Corfu, Jackson and Sutcliffe 1991; Ayer et al. 2003). However, this age is in accord with maximum age estimates of Timiskaming assemblage sandstone and conglomerate deposition from the uppermost Three Nations formation (<2669–2670 Ma: summarized in Ayer et al. 2003). Further work might be aimed at understanding whether real age differences exist between various Timiskaming depocentres that evolved regionally or between one gold camp and another.

03VOI-0570-1 Sandstone, Timiskaming assemblage, Gauthier Township

(NAD83, Zone 17 UTM 589358E, 5331803N; #32 on Figure 2 and Table 1)

Sample 03VOI-0570-1 represents a sandstone member of an overall turbiditic sequence from east-central Gauthier Township, which was collected to confirm or refute a Timiskaming age for this sedimentary assemblage.

This sample contained an abundant yield of zircon of variable morphology, predominantly pale- to medium-brown short prisms up to 2:1 in length:width, and often with minor bubble inclusions. Most grains retain relatively sharp exterior crystal facets and do not show significant evidence for sedimentary abrasion or transport, although a subordinate population of very pale brown, rounded to very well-rounded subequant to slightly elongate grains do occur. Rare examples of colourless elongate needles are also present, as are flat grains and grain fragments.

Zircon grains were selected for laboratory abrasion and analysis from three principal morphological types: 1) short, sharply faceted, medium-brown euhedra, 2) slightly rounded, very pale brown elongate grains, and 3) large, clear, brown fragments. The U/Pb results for six single grains are presented in Table A1 and shown graphically in Figure 7D. Most analyses are either concordant or only slightly discordant (0.6% discordant or less), with one of the two rounded grains showing the oldest $^{207}Pb/^{206}Pb$ age at 2769.8±1.7 Ma. The remaining analyses cluster tightly between 2682 and 2678 Ma, with the youngest identified grain (1b) having a $^{207}Pb/^{206}Pb$ age of 2677.7±3.1 Ma (0.5% discordant).

Based on this relatively small sampling of detrital zircons, the young age of the bulk of the detritus, <2682 Ma, confirms a Timiskaming assemblage affinity for this sandstone. Consequently, the current best estimate for the age of deposition of Timiskaming Group sediments, based on grain fraction 1b, is that sedimentation in the Kirkland Lake area must locally postdate 2677.7±3.1 Ma. This constraint is internally consistent with earlier estimates based on youngest recognizable concordant detrital grains from the Dome formation (<2679 Ma, <2674 Ma: Corfu et al. 1991; Ayer et al. 2003) and the Three Nations formation (<2670-2669 Ma: Bleeker, Parrish and Sager-Kinsman 1999). Notwithstanding this, the additional new age constraint provided by the Timiskaming trachytic flow (*see* 03VOI-0422-1 above) implies that Timiskaming basin development in Gauthier Township may actually be as young as 2670 Ma, a result which remains possible provided that synsedimentary magmatic zircons are either not present or have not yet been analyzed.

03ASP-0083 Polylithic tuff with rhyolite fragments, Katrine Township

Much of the northern and eastern parts of Katrine Township are dominated by massive, pillowed and brecciated andesitic volcanic members of the Blake River Group stratigraphy (Péloquin and Piercey 2003). During the 2003 mapping program in this region, a polylithic tuff breccia, locally containing rhyolite, andesite and jasper fragments, was sampled for geochronological study. Dating of this unit was aimed at elucidating the age of volcanism in the southern (basal?) part of the Blake River Group, as well as possible inheritance ages carried in xenolithic fragments. Although a heavy mineral separate was recovered from this sample, no datable minerals were observed.

03SJP-059-1 Feldspar-phyric dike, Clifford Township

(NAD83, Zone 17 UTM 590369E, 5349181N; #33 on Figure 2 and Table 1)

A felsic, plagioclase-phyric dike, locally intruding andesitic volcanic rocks of the Blake River Group, was sampled approximately 1 km south of the Clifford stock in Clifford Township. This dike is thought to be representative of a broader swarm of east- to northeast-trending dike- and sill-like intrusions found within Blake River Group southeast of the Clifford stock.

Abundant, high-quality zircons were recovered from this sample, comprising populations of colourless to pale brown, water-clear, euhedral long prisms, and stubbier or lozenge-shaped, sharp, doubly terminated grains. Small fluid, melt or apatite inclusions were few in any given zircon grain, but were nearly ubiquitous. Four representative single grains were abraded and analyzed. All analyses are overlapping, and most straddle concordia. Precise analyses obtained for three grains (A1, A3, A4) yield a weighted mean $^{207}Pb/^{206}Pb$ age of 2688.5±2.3 Ma (Table A1; Figure 7E). The fourth fraction (A2) has a high proportion of common-Pb and commensurate large errors, yielding a slightly higher $^{207}Pb/^{206}Pb$ age (2694±5 Ma), and may reflect minor inheritance (dashed ellipse in Figure 7E). Therefore, the data suggest primary crystallization of this dike at 2688.5±2.3 Ma, with the incorporation of xenocrystic zircon from the distinctly older, enclosing Blake River Group units of the ca. 2697 to 2701 Ma Blake River assemblage (Ayer et al. 2002).

Although original observations suggested that the felsic dikes might have been synvolcanic with surrounding Blake River Group andesitic volcaniclastic rocks, the distinctly younger age reported here supports recent field observations concluding that the sheets clearly represent a younger magmatic event (e.g., Piercey et al. 2004). The approximately 10 my gap between these extrusive and intrusive episodes is corroborated by a similar, young age for the nearby Clifford stock (see below), with which the dikes are likely coeval and petrogenetically related.

03SJP-115-1 Monzonite, Clifford stock, Clifford Township

(NAD83, Zone 17 UTM 591133E, 5351000N; #34 on Figure 2 and Table 1)

This sample was collected in order to determine the primary crystallization age of the Clifford stock and to assess its potential age similarity to the surrounding Blake River Group and to ages of other possible subvolcanic intrusive rocks within the Blake River Group. The sample is tonalitic to granodioritic in composition, and is texturally equigranular to weakly porphyritic with some larger 0.5 cm potassium feldspar phenocrysts. Hornblende is the dominant mafic phase, while epidote occurs forming distinct, rounded patches.

The sample yielded abundant colourless to pale brown zircon, dominated by a population of elongate (up to 6:1) cylindrical euhedral grains as well as subordinate, larger, "glassy" broken fragments and elongate flat euhedra. Uranium-lead analyses for three abraded single-grain fractions all overlap, are either concordant or slightly discordant (to 0.7%) and, together, provide a weighted mean $^{207}Pb/^{206}Pb$ age of 2686.9±1.2 Ma (62% probability of fit, MSWD = 0.47; Figure 7F; Table A1).

The age of 2686.9 Ma is interpreted to represent the best estimate of the timing of magmatic crystallization of the Clifford stock, and overlaps with the age determined for the spatially associated east- to northeast-trending felsic dikes exposed south and east of the pluton (*see* 03SJP-059-1 above). As concluded above, the ages demonstrate that the intrusive rocks distinctly postdate volcanism of the Blake River assemblage and, therefore, cannot be considered to be synvolcanic or even late-synvolcanic. The age of the Clifford stock is also similar to that determined for the Clarice Lake pluton (2689±1 Ma: Corfu and Noble 1992), which also intruded the Blake River Group near the Ontario–Quebec border. Emplacement of the Clifford stock appears to have also coincided in time with intrusion of the Lac Dufault pluton in the eastern Abitibi of Quebec and a late, potassium feldspar porphyritic phase of the Lac Abitibi batholith (2690.3+2.2/–2.0 Ma and 2689.8+1.2/–1.1 Ma, respectively: Mortensen 1993b), the potassium feldspar porphyritic Adams stock south of Timmins (2686±3 Ma: Frarey and Krogh 1986), and several gold-related intrusive rocks in the Porcupine Camp (2688–2691 Ma: Corfu et al. 1989).

03ASP-0130-1 Porphyritic rhyolite, Ben Nevis Township

(NAD83, Zone 17 UTM 593407E, 5350603N; #35 on Figure 2 and Table 1)

A porphyritic, intrusive rhyolite, interpreted to be a synvolcanic cryptodome within the Blake River Group, was sampled east of the Clifford stock on the axis of the Clifford antiform. A precise age for this unit would test the synvolcanic nature of this unit, establish the timing of a component of Blake River Group volcanism in eastern Clifford Township and permit correlation with similar units in Ben Nevis Township as well as the Noranda district of Quebec.

This sample is characterized by two principal zircon populations: clear and colourless, short, small, square prisms; and larger, slightly more elongate, pale brown equivalents. Three analyses of the best quality, air-abraded prismatic grains from the smaller size fraction (two single grains and one fraction comprising three smaller zircons) yield a narrow range of $^{207}Pb/^{206}Pb$ ages (2694.9 – 2696.6 Ma) that are only slightly discordant (0.1–0.3%). A fourth single-grain analysis (fraction A2a) is just over 1% discordant (Figure 8A; Table A1). Regression of all four analyses suggests an upper intercept age of 2699.8±3.6 Ma with a lower intercept of approximately 1639 (± 240) Ma (75% probability of fit; MSWD = 0.28). A simple weighted mean $^{207}Pb/^{206}Pb$ age calculation for the three most concordant analyses yields an age of 2696.4±1.2 Ma (68% probability of fit; MSWD = 0.38). However, as all fractions appear to demonstrate a small degree of discordance, and given the present data set, the more conservative age of 2699.8±3.6 Ma is regarded as the most robust estimate for the primary crystallization of the rhyolite porphyry.

An age of 2699.8±3.6 Ma for the rhyolite is in good agreement with the principal range of ages published for the Blake River assemblage (2697–2701 Ma: summarized in Ayer et al. 2002) and confirms the synvolcanic nature of this specific occurrence of felsic magmatism. On the basis of the age estimate alone, particularly with the current error levels, it is difficult to place the timing of the Clifford Township volcanism either early or late within the overall Blake River Group stratigraphic sequence.

03ASP-0179-1 Massive rhyolite, Ben Nevis Township

(NAD83, Zone 17 UTM 599636E, 5352799N; #36 on Figure 2 and Table 1)

Sample 03ASP-0179-1 represents a massive, columnar jointed rhyolite flow, collected in the Canagau Mine area, to establish the timing of felsic Blake River Group volcanism in Ben Nevis Township.

Small, pale yellow, sharply faceted doubly terminated subequant zircon prisms are moderately abundant in the sample. Three multigrain fractions, comprising between three and six abraded grains each, yield a collinear array ranging from being concordant to almost 5% discordant (Figure 8B; Table A1). Regression of all three analyses defines an upper intercept age of 2696.6±1.3 Ma (50% probability of fit; MSWD = 0.45) with an essentially zero-age lower intercept (90±120 Ma). The 2696.6 Ma age is interpreted to represent the primary age of crystallization of the rhyolite. This age is equivalent to that of the youngest volcanic members of the Blake River assemblage recognized elsewhere (2697–2701 Ma: Ayer et al. 2002). In detail, the Ben Nevis Township rhyolite appears to be younger than the principal phases of volcanism identified in the Misema and Noranda "subgroups" of the Blake River Group. The closest possible coeval related units include volcanic members in the Reneault–Dufresnoy (2696±1.1 Ma) and Bousquet (2694±2 Ma) formations of the Blake River Group in Quebec. Stratigraphic correlations for the Blake River Group are therefore strengthened between the current study area and the Noranda region of Quebec.

C89-7 Pegmatitic gabbro sill, Ghost Range complex, Lamplugh Township

(NAD83, Zone 17 UTM 585970E, 5376800N; #38 on Figure 2 and Table 1)

Uranium-lead (U/Pb) isotopic data for this differentiated gabbroic sill were originally presented by Corfu (1993), and the data are reproduced here (shaded ellipses: Figure 8C). The dated phases comprised mostly single grains of fragmented, euhedral and partly turbid zircon, and brown, translucent to opaque baddeleyite. All analyses were variably discordant, but a fit through the most discordant zircon analysis (3z) and a subgroup of the cluster near concordia (1z, 4bd) yielded an upper intercept age of 2713+7/–5 Ma (Corfu 1993) and a lower intercept age of ca. 1250 Ma.

Analysis of additional fractions from this sample was warranted by the desire to improve the precision of the original age determination in the context of the surrounding stratigraphy, as well as to assess correlation with the newly dated 2706.8±1.2 Ma Centre Hill mafic to ultramafic complex in Munro Township (*see* 04JAA-0002 above). Two fractions of tiny baddeleyite fragments were picked from the residues of the original Corfu study, enough to comprise roughly 1 μg each. Because the grains showed a very dull lustre, each fraction was given a brief wash in concentrated HF to remove any possible overgrowths of zircon (late magmatic or metamorphic) which might be carrying a Pb-loss signature resulting from a 1250 Ma or even younger isotopic disturbance. The resulting two analyses (Bd-1, Bd-2: Figure 8C; Table A1) are more concordant (~99.1–98.9%) than the previous three baddeleyite analyses from this sample, but, like two of those baddeleyite (and one of the zircon) analyses, these new data fall to the right of the aforementioned regression of Corfu (1993). Assuming only a recent Pb-loss event to have affected the most concordant baddeleyites, then regression of analyses Bd-1, Bd-2 and 5bd through the origin yields an upper intercept age of 2712.4±1.1 Ma (*see* Figure 8C, inset), which is almost identical to

the original Corfu (1993) age, only more precise. Regression of the more discordant, turbid and cracked zircon analyses (2z, 3z) together with those for the older four baddeleyites (5bd, 6bd, Bd-1 and Bd-2) results in an unrealistically old upper intercept age (2724 Ma), which is greater than the accepted age of the host Kidd–Munro assemblage volcanic rocks (ca. 2719–2711 Ma: Nunes and Jensen 1980; Corfu et al. 1989; Barrie and Davis 1990; Corfu and Noble 1992; Corfu 1993; Ayer et al. 2002). This fact, combined with the agreement to the earlier Corfu (1993) result, suggests that the 2712.4±1.1 Ma age represents an accurate and precise estimate of the timing of emplacement of the Ghost Range sill.

The age for the Ghost Range gabbroic complex is now considered distinct and separate from the age of other mafic to ultramafic complexes found elsewhere in the Kidd–Munro assemblage, including the 2706.8±1.2 Ma Centre Hill complex (this report), the Munro–Warden sill (2704.9±1.9 Ma: Barrie 1999), the Dundonald mafic to ultramafic sill (2707+3/–2 Ma: Barrie and Corfu 1999), as well as the 2707 to 2705 Ma Kamiskotia Gabbroic Complex (2707±2 Ma gabbro: Barrie and Davis 1990; Corfu and Noble 1992; 2704.8±1.5 Ma granophyre: this report). Regional mafic to ultramafic intrusions elsewhere in the Timmins–Kidd Creek area also include the Mann mafic to ultramafic intrusion in Mann Township (2704 .0±4.9 Ma; Barrie 1999) and a dunite differentiate from Deloro Township (2707+3/–2 Ma; Corfu and Noble 1992; Corfu 1993), both of which are distinctly younger than the Ghost Range sill age refined here.

04JAA-0001 Quartz-phyric felsic flow, southwest Munro Township

This sample was collected to establish a precise age for the base of the Kidd–Munro assemblage in Munro Township. Unfortunately, no datable accessory phases were found in the heavy mineral concentrate processed from this sample.

04JAA-0002 Leucogabbro, Centre Hill complex, north-central Munro Township

(NAD83, Zone 17 UTM 558199E, 5383067N; #39 on Figure 2 and Table 1)

A coarse-grained variety of leucogabbro exists in the upper fractionated portions of the Centre Hill mafic to ultramafic complex. A sample of this unit was collected for dating purposes to test the hypothesis that the Centre Hill complex might represent a synvolcanic intrusion related to the VMS mineralization in the overlying Potter Mine.

The Centre Hill leucogabbro contained a moderately abundant population of both zircon and baddeleyite. Zircon occurs as large, colourless, sometimes cloudy, subhedral to anhedral grains with square cross-sections or as skeletal grains with flat, flange-like or partly hollow crystals. Some crystals are fragments of larger euhedra and many grains are cracked. Discrete, smaller and rounded, xenocrystic zircons are also present and were excluded from analysis. Baddeleyite grains in this sample occur as fine- to medium-grained, brown, striated blocky and blade varieties. Most baddeleyite grains show a dull lustre suggestive of a fine-grained partial overgrowth or replacement by fine-grained zircon, an observation confirmed by secondary electron imaging.

Isotope dilution results for two zircon single-grain analyses are shown in Table A1 and Figure 8D. The data are only slightly discordant (0.4–0.5%) and have identical $^{207}Pb/^{206}Pb$ ages at 2706.6 and 2706.9 Ma. Results for two analyzed single grains of baddeleyite (unabraded) are slightly more discordant (1.0–1.4%) but yield similar $^{207}Pb/^{206}Pb$ ages as the zircon analyses. Regression of all four analyses results in an upper intercept age of 2706.8±1.2 Ma with a very high probability of fit (94%; MSWD = 0.13). The regression is anchored through the origin and the goodness of fit for this discordia suggests that the Pb-loss behaviour observed in the baddeleyites is a result of modern (zero-age) disturbances and not an older secondary Pb-loss event. Thus, the partial zircon frosting present on the baddeleyites likely reflects local, late saturation of the magma in silica rather than a younger metamorphic reaction.

A primary magmatic crystallization age of 2706.8±1.2 Ma for leucogabbro from the Centre Hill mafic to ultramafic complex is similar in age to the nearby Munro–Warden sill at 2704.9±1.9 Ma (Barrie 1999), the Middle Zone gabbro of the Kamiskotia Gabbroic Complex (2707±2 Ma: Barrie and Davis 1990), and the mafic Dundonald sill (2707+3/–2 Ma: Barrie and Corfu 1999) all of which were emplaced into slightly older rocks of the Kidd–Munro assemblage.

Table A1. U/Pb isotopic data for zircon from sample localities in the southern Abitibi greenstone belt, Ontario.

Sample Fraction	Analysis no.	Description (# = location on Figure 2 & Table 1)	Weight (mg)	U (ppm)	Th/U	Pb* (pg)	Pb_C (pg)	$^{206}Pb/^{204}Pb$	$^{206}Pb/^{238}U$	± 2σ	$^{207}Pb/^{235}U$	± 2σ	$^{207}Pb/^{206}Pb$	± 2σ	$^{207}Pb/^{206}Pb$ Age (Ma)	± 2σ	Disc. (%)	Corr. Coeff.
04BHA-0333		***#1, Felsic debris flow, south Thornburn Twp.***																
A1	MAH4098	1 clr, cls-ppink sharp, elong	0.0002	82	0.59	9.0	0.5	1018	0.52258	0.00399	13.4540	0.1165	0.18672	0.00063	2713.5	5.5	0.2	0.9223
A2	MAH4099	1 clr, cls-ppink sharp, elong	0.0001	81	0.55	4.9	0.6	488	0.52458	0.00713	13.5002	0.2075	0.18665	0.00109	2712.9	9.7	-0.3	0.9256
B1	MAH4080	1 clr, cls-pyell, stubby, sharp	0.0008	39	0.42	17.9	0.8	1244	0.52076	0.00250	13.3909	0.0752	0.18650	0.00046	2711.5	4.1	0.4	0.8996
B2	MAH4081	1 clr, pbr, stubby, sharp	0.0004	133	0.57	33.7	1.5	1296	0.55605	0.00167	15.6682	0.0631	0.20436	0.00043	2861.4	3.4	0.5	0.8603
B3	MAH4082	1 clr, cls-ppink, stubby, sharp	0.0004	88	0.87	22.9	0.6	2208	0.50485	0.00201	12.7341	0.0567	0.18294	0.00034	2679.7	3.1	2.0	0.9088
04BHA-0297		***#2, Qz-fsp phyric felsic flow, central Loveland Twp.***																
Z1	DWD4689	1 clr, cls, stubby, with rod melt incl	0.0040	55	0.51	130.0	1.5	4963	0.52093	0.00171	13.4103	0.0455	0.18671	0.00030	2713.4	2.6	0.5	0.8846
Z2	DWD4690a	1 clr, cls, eq, with rod incl	0.0020	59	0.51	69.6	3.3	1221	0.52036	0.00199	13.3884	0.0641	0.18660	0.00051	2712.5	4.5	0.5	0.8211
Z3	DWD4691	1 clr, cls, eq	0.0015	89	0.50	57.6	0.6	5678	0.37736	0.00134	9.6567	0.0367	0.18560	0.00020	2703.5	1.7	27.6	0.9609
Z4	MAH4097a	1 clr, cls, stubby	0.0016	105	0.63	102.2	0.8	6778	0.52078	0.00135	13.4203	0.0392	0.18690	0.00018	2715.1	1.6	0.6	0.9433
04BHA-0462		***#3, Granophyre, Kamiskotia gabbro, Robb Twp.***																
A1a	MAH4102	1 clr, cls, elong	0.0007	100	0.37	39.4	0.6	3883	0.51833	0.00151	13.2758	0.0435	0.18576	0.00026	2705.0	2.3	0.6	0.9073
A1b	MAH4107	1 clr, cls-pbr, irreg frag	0.0012	169	0.78	123.6	0.8	8591	0.51983	0.00182	13.3038	0.0464	0.18561	0.00031	2703.7	2.7	0.2	0.8870
A1c	MAH4108	1 clr, cls, elong	0.0006	73	0.48	27.3	1.2	1337	0.51847	0.00184	13.2892	0.0608	0.18590	0.00041	2706.2	3.7	0.6	0.8817
03BHA-0382		***#4, Rhyolite, Robb Twp.***																
A1	MAH4046	1 clr, pbr-br, short, sharp prism	0.0005	103	0.46	30.2	0.5	3486	0.52182	0.00153	13.3257	0.0433	0.18521	0.00026	2700.1	2.3	-0.3	0.9020
A2	MAH4047	1 clr, pbr-br, short, sharp prism	0.0003	237	0.41	37.3	0.7	3273	0.52189	0.00158	13.3195	0.0459	0.18510	0.00022	2699.1	2.0	-0.4	0.9407
A3	MAH4048	1 clr, pbr-br, short, sharp prism	0.0003	178	0.40	30.0	0.4	4760	0.52154	0.00162	13.3268	0.0446	0.18533	0.00025	2701.1	2.2	-0.2	0.9152
03BHA-0384		***#5, Felsic lapilli tuff, Robb Twp.***																
A1	MAH4018	1 elong (3:1) clr, cls, prism, minor incl.	0.0016	23	0.56	22.5	2.6	491	0.51943	0.00246	13.2770	0.1128	0.18539	0.00106	2701.6	9.4	0.2	0.7709
A2	MAH4019	1 sl. elong (2:1) clr, pbr, prism, minor incl.	0.0019	333	0.79	392.6	1.8	11499	0.51914	0.00238	13.2671	0.0621	0.18535	0.00027	2701.3	2.4	0.3	0.9515
A3	MAH4020	1 eq, clr, cls, prism, minor incl.	0.0014	77	0.59	66.8	1.4	2631	0.52009	0.00155	13.2897	0.0453	0.18533	0.00029	2701.1	2.5	0.1	0.8920
A4	MAH4021	1 sl. elong (2:1), cls-pbr, clr, prism	0.0016	64	0.59	61.3	2.8	1215	0.51969	0.00195	13.2719	0.0641	0.18522	0.00046	2700.2	4.1	0.1	0.8634
03BHA-0345		***#6, Felsic lapilli tuff, Godfrey Twp.***																
A1a	MAH4043	1 clr, cls-pyell, stubby to eq prism	0.0014	36	0.53	29.8	5.8	305	0.52159	0.00236	13.3108	0.1669	0.18509	0.00174	2699.0	15.6	-0.3	0.7847
A1b	MAH4044	1 clr, cls-pyell, stubby to eq prism	0.0011	28	0.56	18.2	0.3	3097	0.52148	0.00222	13.3197	0.0615	0.18525	0.00027	2700.4	2.4	-0.2	0.9508
A1c	MAH4045	1 clr, cls-pyell, stubby to eq prism	0.0014	26	0.51	22.3	0.3	4524	0.52247	0.00199	13.3218	0.0542	0.18493	0.00021	2697.5	1.9	-0.5	0.9597
03BHA-0047		***#7, Felsic lapilli tuff, eastern Turnbull Twp.***																
Z1	DWD4686	1 clr, cls, eq, flat	0.0020	75	0.49	87.7	0.8	6342	0.51661	0.00199	13.2165	0.0541	0.18555	0.00021	2703.1	1.9	0.8	0.9597
Z2	DWD4687c	1 clr, cls, short prism, with rod incl	0.0021	85	0.52	105.0	0.8	7173	0.51838	0.00162	13.2669	0.0437	0.18562	0.00024	2703.7	2.2	0.5	0.9187
Z3	DWD4688b	1 clr, cls, irregular	0.0019	33	0.47	36.3	0.7	2985	0.51844	0.00266	13.2509	0.0682	0.18537	0.00039	2701.5	3.5	0.4	0.9163
96JAA-094		***#8, Rhyolite, Carscallen Twp. (Ayer et al., 2002)***																
Z1	MAH5037b	1 clr, cls, short prism	0.0003	114	0.75	22.8	0.6	1948	0.52239	0.00221	13.4218	0.0618	0.18634	0.00039	2710.2	3.5	0.0	0.8898
Z2	MAH5038	1 clr, cls, short prism	0.0007	86	0.50	35.7	0.4	4552	0.52297	0.00163	13.4469	0.0466	0.18649	0.00020	2711.4	1.7	0.0	0.9545
Z3	MAH5034a	1 clr, cls-pbr, gemmy, sharp short prism	0.0010	137	0.75	88.4	0.4	10602	0.53427	0.00118	14.9828	0.0384	0.20339	0.00018	2853.6	1.4	4.1	0.9437
04JAA-0004		***#9, Deformed Timiskaming conglomerate, northeastern Thorneloe Twp.***																
Z1	DWD4692	1 large clr, pbr, eq and irreg	0.0320	26	0.60	509.8	2.9	9820	0.52459	0.00140	13.6092	0.0407	0.18815	0.00016	2726.1	1.4	0.3	0.9600
Z2	DWD4693	1 clr, cls, rounded 2:1 prism	0.0086	45	0.57	236.3	1.6	8389	0.52325	0.00234	13.5863	0.0635	0.18832	0.00018	2727.5	1.6	0.7	0.9795
Z4	DWD4695	1 clr, cls, euh, eq	0.0024	48	0.60	69.3	0.4	8744	0.51474	0.00137	13.0202	0.0388	0.18346	0.00019	2684.4	1.7	0.3	0.9374
Z5	DWD4696	1 clr, cls, euh, long prism	0.0005	84	0.67	25.4	0.4	3344	0.51340	0.00221	12.9914	0.0589	0.18353	0.00027	2685.0	2.4	0.6	0.9468
Z6	DWD4697	1 clr, bm, prism	0.0005	524	0.07	134.5	1.3	6484	0.49942	0.00124	12.1383	0.0341	0.17627	0.00021	2618.1	2.0	0.3	0.9017
Z7	MAH4091	1 clr, pbr, subeq, frag	0.0025	138	0.96	224.4	1.5	7982	0.52022	0.00123	13.4140	0.0362	0.18701	0.00019	2716.1	1.7	0.7	0.9294
Z8	MAH4092	1 clr, pbr, small subeq, frag	0.0004	326	0.81	81.0	0.8	5186	0.51263	0.00127	13.1302	0.0363	0.18576	0.00024	2705.0	2.1	1.7	0.8865

Table A1. continued

Sample Fraction	Analysis no.	Description (# = location on Figure 2 & Table 1)	Weight (mg)	U (ppm)	Th/U	Pb* (pg)	Pb_C (pg)	$^{206}Pb/^{204}Pb$	$^{206}Pb/^{238}U$	± 2σ	$^{207}Pb/^{235}U$	± 2σ	$^{207}Pb/^{206}Pb$	± 2σ	$^{207}Pb/^{206}Pb$ Age (Ma)	± 2σ	Disc. (%)	Corr. Coeff.
04PCT-0062		***#10, Feldspar-phyric lapilli tuff, Deloro Twp.***																
Z1	MAH5008	1 clr, cls, small elong prism	0.0002	188	0.35	16.3	0.7	1432	0.52307	0.00233	13.5501	0.0701	0.18788	0.00041	2723.7	3.6	0.5	0.9068
Z2	MAH5010	1 clr, cls short prism	0.0001	197	0.39	13.7	1.0	831	0.51974	0.00263	13.4544	0.0883	0.18775	0.00065	2722.5	5.7	1.1	0.8561
Z3	MAH5011	1 clr, cls-pbr large short prism	0.0004	197	0.42	44.5	1.1	2308	0.50543	0.00142	13.0553	0.0441	0.18734	0.00030	2718.9	2.6	3.7	0.8834
Z4	MAH5012a	1 clr, cls-pbr short prism	0.0001	270	0.37	13.7	1.2	703	0.51036	0.00275	13.2206	0.0954	0.18788	0.00078	2723.7	6.8	2.9	0.8235
Z5	MAH5016a	1 clr, cls short prism	0.0001	112	0.41	7.2	1.0	425	0.52344	0.00476	13.5222	0.1655	0.18736	0.00126	2719.1	11.1	0.2	0.8418
SM85-60		***#13, Albitite dyke, McIntyre mine, Tisdale Twp. (Corfu et al., 1989)***																
Z1	MAH5019b	1 clr, cls, eq, subrnd	0.0029	59	0.59	102.2	1.4	3998	0.51306	0.00153	12.8857	0.0407	0.18215	0.00029	2672.6	2.7	0.1	0.8650
Z2	MAH5020b	1 clr, cls, square prism	0.0038	80	0.63	182.0	0.9	11255	0.51229	0.00163	12.8679	0.0443	0.18218	0.00017	2672.8	1.6	0.3	0.9623
Z4	MAH5021b	1 clr, cls, short prism, subrnd	0.0007	115	0.57	44.7	1.1	2283	0.51165	0.00165	13.0207	0.0537	0.18457	0.00040	2694.4	3.6	1.4	0.8554
KCR.52		***#14, Porcupine greywacke, north-central Tisdale Twp. (W. Bleeker)***																
A1	MAH5029	1 clr, lrg, sl. elong, cls-pbr, subhed, rod incl	0.0046	45	0.54	122.5	1.0	6622	0.51709	0.00222	13.1314	0.0573	0.18418	0.00027	2690.9	2.5	0.2	0.9410
A2	MAH5030	1 clr, sl. elong, cls-pbr, subhed, incl	0.0015	28	0.35	24.3	0.6	2382	0.51852	0.00228	13.2358	0.0626	0.18513	0.00042	2699.4	3.8	0.3	0.8777
A3	MAH5035a	1 clr, sl. elong, cls-pbr, subhed	0.0014	31	0.85	27.1	2.3	631	0.50882	0.00196	12.9806	0.0879	0.18502	0.00083	2698.4	7.4	2.1	0.7751
A4	MAH5036e	1 clr, sl. elong, cls-pbr, subhed, incl	0.0011	72	0.35	44.9	0.5	5175	0.51935	0.00166	13.2577	0.0457	0.18514	0.00023	2699.5	2.0	0.1	0.9351
C1	MAH5031b	1 clr, med br, short pr,	0.0009	281	0.47	147.1	0.7	12489	0.51409	0.00122	13.0669	0.0355	0.18434	0.00016	2692.3	1.4	0.8	0.9537
E1	MAH5032a	1 clr, cls, elong/needle, small incl	0.0005	104	0.58	31.1	0.9	2045	0.51780	0.00180	13.1883	0.0531	0.18472	0.00032	2695.8	2.8	0.3	0.9050
04JAA-0003		***#15, Porcupine below unconformity, eastern Tisdale Twp.***																
A1	MAH4070	1 clr, pbr, short pr	0.0045	141	0.73	374.2	1.3	15237	0.49221	0.00160	12.1977	0.0419	0.17973	0.00019	2650.4	1.8	3.2	0.9493
A3	MAH4072	1 clr, pbr, eq	0.0014	27	0.86	23.1	1.1	1174	0.51550	0.00275	13.2298	0.0804	0.18614	0.00053	2708.3	4.7	1.3	0.8853
A5	MAH4112a	1 clr, pbr, eq	0.0021	84	0.74	110.7	0.8	7083	0.52309	0.00150	13.5234	0.0424	0.18750	0.00020	2720.4	1.7	0.4	0.9434
A6	MAH5003	1 clr, cls, eq and irreg	0.0037	65	0.86	149.4	1.1	7482	0.51432	0.00123	13.0321	0.0357	0.18377	0.00018	2687.2	1.6	0.6	0.9361
A7	MAH5004	1 clr, cls, ovoidal, with rod incl	0.0008	104	0.95	50.7	0.7	3860	0.51670	0.00146	13.1265	0.0425	0.18425	0.00020	2691.5	1.8	0.3	0.9424
A8	MAH5007	1 clr, cls, sl. irreg ovoidal, with minor incl	0.0004	140	0.83	34.0	1.0	1751	0.52439	0.00154	13.5995	0.0506	0.18809	0.00034	2725.5	3.0	0.3	0.8766
04ED-198		***#16, Quartz-phyric felsic schist, Hoyle Twp.***																
Z1	MAH5009	1 clr, cls, elong prism	0.0002	245	0.07	22.5	1.3	1125	0.49260	0.00161	12.4635	0.0581	0.18351	0.00048	2684.8	4.3	4.6	0.8373
Z2	MAH5015a	1 clr, cls-pbr, elong prism, minor incl	0.0001	245	0.07	13.0	1.0	852	0.51151	0.00254	12.9347	0.0855	0.18340	0.00066	2683.9	5.9	0.9	0.8451
Z3a	MAH5013a	1 clr, pbr, tip frag	0.0004	240	0.10	49.0	0.9	3398	0.50193	0.00127	12.7066	0.0378	0.18360	0.00024	2685.7	2.2	2.9	0.9014
Z3b	MAH5014a	1 clr, pbr, tip frag	0.0002	235	0.12	17.5	0.8	1331	0.41971	0.00150	10.5312	0.0484	0.18198	0.00043	2671.0	3.9	18.2	0.8649
03ED-96A		***#17, Quartz-feldspar porphyry, Hoyle Pond Mine, Hoyle Twp.***																
A1a	MAH4034	1 small, square, elong, clr, cls, prism	0.0010	36	0.03	19.6	0.7	1721	0.51727	0.00217	13.1696	0.0626	0.18465	0.00037	2695.1	3.3	0.3	0.9050
A1b	MAH4035	1 small, square, elong, clr, cls, prism; minor fra	0.0006	39	0.02	12.5	0.6	1285	0.51627	0.00268	13.0623	0.0783	0.18350	0.00047	2684.8	4.2	0.1	0.9067
A1c	MAH4036a	1 small, square, elong, clr, cls, prism	0.0006	51	0.06	16.6	0.9	1194	0.51599	0.00260	13.0364	0.0777	0.18324	0.00046	2682.4	4.2	0.0	0.9092
A2a	MAH4113a	1 small, square, elong, clr, cls, prism; minor fra	0.0003	141	0.04	24.5	0.8	1850	0.51386	0.00194	13.0040	0.0582	0.18354	0.00033	2685.1	3.0	0.5	0.9201
03RJB-18973-10		***#18, Porcupine sandstone, Hoyle Twp.***																
A1	MAH4003	1 clr, pbr, flat subrnd	0.0008	342	1.43	181.6	1.3	6525	0.51304	0.00124	13.0074	0.0356	0.18388	0.00021	2688.2	1.9	0.8	0.9111
A2	MAH4004	1 clr, cls, subrnd	0.0003	74	1.29	13.4	1.9	359	0.52377	0.00508	13.5797	0.1878	0.18804	0.00152	2725.1	13.3	0.4	0.8200
B1	MAH4093	1 clr, cls, sl elong prism, sl rounded	0.0010	67	0.63	39.9	2.4	937	0.51732	0.00149	13.1333	0.0632	0.18413	0.00056	2690.4	5.0	0.1	0.7991
B2	MAH4094	1 clr, pbr, sl elong prism, sl rounded	0.0009	44	0.53	23.3	1.2	1114	0.52234	0.00231	13.4431	0.0721	0.18666	0.00058	2712.9	5.1	0.2	0.8139
B3	MAH4095a	1 clr, cls, sharp	0.0004	43	0.40	11.3	1.2	548	0.52149	0.00363	13.3502	0.1261	0.18567	0.00097	2704.2	8.6	-0.1	0.8394
B4	MAH4096a	1 clr, bm, prism	0.0003	39	0.36	7.5	1.3	343	0.52272	0.00464	13.4410	0.1828	0.18649	0.00156	2711.5	13.8	0.0	0.8042
03PJM-131		***#19, Quartz-feldspar porphyry, Pamour drill hole, Whitney Twp.***																
A1a	MAH4037	1 small, square, clr, cls bipyramid	0.0004	22	0.06	5.3	1.0	349	0.51664	0.00592	13.1151	0.2009	0.18411	0.00153	2690.3	13.8	0.2	0.8453
A1b	MAH4038r	1 small, square, clr, brn bipyramid	0.0004	337	0.74	70.1	1.8	2146	0.48594	0.00136	12.0108	0.0424	0.17926	0.00040	2646.0	3.7	4.3	0.7806
A1c	MAH4039	1 small, square, clr, brn bipyramid	0.0003	634	0.19	112.7	0.5	12965	0.48000	0.00107	11.6905	0.0295	0.17664	0.00018	2621.6	1.7	4.3	0.9138
A1d	MAH4061a	3 small, square, clr, cls bipyramid	0.0006	38	0.02	12.7	0.5	1711	0.51637	0.00281	13.2065	0.0786	0.18549	0.00038	2702.6	3.4	0.9	0.9378
A1e	MAH4062	3 small, square, clr, cls bipyramid	0.0006	74	0.02	24.9	11.3	156	0.51667	0.00313	13.0378	0.3225	0.18302	0.00354	2680.4	32.2	-0.2	0.9134
A1f	MAH4114	1 small, square, clr, brn bipyramid	0.0005	348	0.59	100.9	1.6	3491	0.51235	0.00113	12.9059	0.0354	0.18269	0.00022	2677.5	2.0	0.5	0.9000

Table A1. continued

Sample Fraction	Analysis no.	Description (# = location on Figure 2 & Table 1)	Weight (mg)	U (ppm)	Th/U	Pb* (pg)	Pb_C (pg)	$^{206}Pb/^{204}Pb$	$^{206}Pb/^{238}U$	± 2σ	$^{207}Pb/^{235}U$	± 2σ	$^{207}Pb/^{206}Pb$	± 2σ	$^{207}Pb/^{206}Pb$ Age (Ma)	± 2σ	Disc. (%)	Corr. Coeff.
04JAA-0010		***#20, Albitite dyke, Whitney Twp.***																
A1a	MAH4073	1 clr, cls-pbr, short, sl. flat prism	0.0010	107	0.69	64.3	9.1	400	0.50203	0.00212	12.5528	0.1391	0.18135	0.00152	2665.2	13.9	1.9	0.7523
A1b	MAH4074	1 clr, cls-pbr short prism	0.0013	72	0.63	53.9	2.2	1381	0.49292	0.00163	12.4058	0.0530	0.18254	0.00052	2676.0	4.7	4.2	0.7437
A1c	MAH4075	1 clr, cls short prism	0.0010	101	0.61	57.1	2.0	1615	0.48630	0.00127	12.2369	0.0451	0.18250	0.00036	2675.7	3.3	5.5	0.8578
A1d	MAH4079	1 clr, cls-pbr short prism	0.0010	69	0.70	43.3	1.5	1597	0.51123	0.00177	12.8739	0.0540	0.18264	0.00039	2677.0	3.5	0.7	0.8613
A1e	MAH4085	1 clr, cls-pbr short prism	0.0007	105	0.73	47.5	0.8	3275	0.51150	0.00154	12.8789	0.0422	0.18261	0.00029	2676.8	2.6	0.6	0.8756
03RJB-18972-6		***#21, Porcupine? sandstone, Whitney Twp.***																
A1	MAH4001	1 cls, clr, subrnd	0.0012	151	1.40	130.1	1.9	3220	0.51714	0.00211	13.1246	0.0572	0.18407	0.00027	2689.9	2.4	0.1	0.9434
A2	MAH4002	1 cls, clr, subrnd	0.0003	151	1.12	26.9	2.2	630	0.51500	0.00249	13.0844	0.0941	0.18427	0.00089	2691.6	8.0	0.6	0.7433
B1	MAH4103	1 clr, cls frag of euh	0.0029	97	0.61	170.9	0.7	13728	0.52436	0.00130	13.6039	0.0375	0.18816	0.00018	2726.2	1.6	0.4	0.9359
B2	MAH4104a	1 clr, cls frag of euh	0.0008	35	0.38	16.5	0.7	1325	0.52450	0.00255	13.5809	0.0766	0.18779	0.00042	2722.9	3.7	0.2	0.9199
B3	MAH4105a	1 clr, pbr frag	0.0009	214	1.22	135.3	0.9	7146	0.51492	0.00123	13.0650	0.0358	0.18402	0.00018	2689.5	1.7	0.5	0.9328
B4	MAH4106	1 small, clr, cls frag	0.0006	679	2.20	289.5	1.3	9356	0.49407	0.00095	12.3057	0.0289	0.18064	0.00016	2658.8	1.5	3.2	0.9313
C88-17		***#22, Felsic volcanic, Whitney Twp. (Corfu & Noble, 1992)***																
Z-B1	MAH5048	1 clr, cls, eq	0.0007	37	0.53	15.0	0.9	987	0.52477	0.00252	13.5990	0.0820	0.18795	0.00054	2724.3	4.8	0.2	0.8827
Z-B2	MAH5049c	1 clr, cls, long prism	0.0004	80	0.43	17.6	0.9	1162	0.52576	0.00299	13.5780	0.0884	0.18730	0.00050	2718.6	4.4	-0.2	0.9145
Z-F1	MAH5050	1 clr, cls, eq	0.0002	105	0.35	14.0	0.6	1322	0.52497	0.00257	13.6033	0.0773	0.18794	0.00043	2724.2	3.8	0.2	0.9162
03LAH-0627		***#23, Quartz porphyry, Mt. Logano intrusion, Shaw Twp.***																
A1a	MAH4031	1 clr, cls elong sharp prism euh (>4:1)	0.0018	77	0.27	78.1	0.7	6713	0.51853	0.00119	13.1570	0.0346	0.18403	0.00021	2689.5	1.9	-0.2	0.8970
A1b	MAH4032	1 clr, pbr, sl. elong sharp prism euh	0.0008	63	0.58	30.0	0.6	2769	0.51790	0.00163	13.1302	0.0468	0.18388	0.00028	2688.1	2.5	-0.1	0.9073
A1c	MAH4033a	1 clr, cls elong sharp prism euh; incl.	0.0016	52	0.40	46.9	5.6	505	0.51909	0.00163	13.1542	0.1007	0.18379	0.00103	2687.4	9.3	-0.4	0.7666
A1d	MAH4063b	1 clr, cls elong sharp prism euh; fluid? incl.	0.0018	90	0.56	94.3	0.3	15236	0.51517	0.00188	13.0939	0.0517	0.18434	0.00019	2692.3	1.7	0.6	0.9653
03LAH-0161		***#24, Felsic-intermediate flow, Shaw Twp.***																
A3	MAH4030	1 clr, bm irregular prism frag	0.0005	346	0.34	91.5	14.7	380	0.52044	0.00174	13.5112	0.1295	0.18829	0.00136	2727.3	11.9	1.2	0.7904
96TB-099		***#26, Felsic fragmental, south Langmuir, Langmuir Twp. (Barrie & Corfu, 1999)***																
Z-C	MAH5022	1 clr, cls, euh short prism	0.0021	86	0.48	107.3	0.9	6797	0.52526	0.00165	13.6235	0.0465	0.18811	0.00019	2725.7	1.6	0.2	0.9578
Z-G	MAH5023	1 clr, cls, eq	0.0005	65	0.64	20.8	0.6	1868	0.52400	0.00201	13.5591	0.0601	0.18767	0.00032	2721.9	2.8	0.3	0.9250
Z-H	MAH5024c	1 clr, cls, broken euh prism	0.0003	78	0.45	14.7	0.9	962	0.52466	0.00270	13.5812	0.0933	0.18774	0.00076	2722.5	6.7	0.2	0.8091
04MGH-0283		***#27, Quartz-feldspar porphyry, Eldorado Twp.***																
A1a	MAH4076	1 clr, cls-pbr, elong prism frag	0.0041	72	0.16	159.9	0.6	15116	0.51501	0.00114	13.0377	0.0326	0.18360	0.00019	2685.7	1.7	0.4	0.9130
A1b	MAH4077	1 clr, cls-pbr, elong prism frag	0.0021	72	0.24	83.3	1.1	4379	0.51382	0.00143	13.0097	0.0385	0.18363	0.00028	2686.0	2.6	0.6	0.8568
A1c	MAH4078	1 clr, cls, small elong prism	0.0006	122	0.22	40.4	0.6	3893	0.51476	0.00142	13.0405	0.0411	0.18373	0.00021	2686.9	1.9	0.5	0.9324
A4	MAH4056r	1 large, pbr, faceted lozenge; incl	0.0133	33	0.40	250.6	17.4	848	0.51429	0.00218	13.0406	0.0779	0.18390	0.00062	2688.4	5.6	0.6	0.8317
04PCT-0064		***#28, Quartz-phyric gabbro dyke, Bartlett Twp.***																
Bd-1	MAH4100	3 small, thin, pbr blade frags, frosted?	0.0001	267	0.11	14.3	0.8	1072	0.51202	0.00273	13.0622	0.0817	0.18502	0.00053	2698.4	4.7	1.5	0.8889
Bd-2	MAH4101a	3 small, thin, pbr blade frags, frosted?	0.0001	726	0.07	34.6	1.0	2198	0.51227	0.00168	13.0775	0.0496	0.18515	0.00032	2699.6	2.8	1.5	0.8937
Bd-3	MAH5005	3 small, thin, pbr blade frags, frosted?	0.0002	303	0.25	32.5	1.2	1704	0.49792	0.00135	12.6228	0.0451	0.18386	0.00035	2688.0	3.1	3.8	0.8533
Bd-4	MAH5006a	3 small, thin, pbr blade frags, frosted?	0.0001	287	0.12	21.7	1.2	1131	0.51613	0.00184	13.1874	0.0625	0.18531	0.00051	2701.0	4.5	0.8	0.8186
03JAA-0006		***#30, Feldspar porphyry, discovery outcrop, Teck Twp.***																
Z1	MAH4014	1 large clr, cls-pbr, frag	0.0043	51	0.65	134.2	4.0	1838	0.52156	0.00135	13.3202	0.0453	0.18523	0.00033	2700.2	2.9	-0.3	0.8614
Z2	MAH4015	1 large clr, cls-pbr, frag	0.0033	70	0.37	134.6	7.8	1021	0.51880	0.00129	13.1645	0.0572	0.18403	0.00052	2689.6	4.7	-0.2	0.7869
Z3	MAH4066	1 small clr, cls-pbr, frag	0.0005	22	0.80	6.6	0.2	1660	0.52193	0.00548	13.3326	0.1426	0.18527	0.00049	2700.6	4.4	-0.3	0.9688
Z4	MAH4016	1 small clr, cls-pbr, subhedra	0.0004	66	0.22	13.0	7.3	125	0.51184	0.00444	12.9887	0.4148	0.18405	0.00456	2689.7	41.3	1.1	0.8674
Z5	MAH4017	1 small clr, cls-pbr, subhedra	0.0007	208	0.46	88.6	8.2	635	0.51748	0.00136	13.1696	0.0802	0.18458	0.00083	2694.4	7.4	0.3	0.7444

Table A1. continued

Sample Fraction	Analysis no.	Description (# = location on Figure 2 & Table 1)	Weight (mg)	U (ppm)	Th/U	Pb* (pg)	Pb_C (pg)	$^{206}Pb/^{204}Pb$	$^{206}Pb/^{238}U$	± 2σ	$^{207}Pb/^{235}U$	± 2σ	$^{207}Pb/^{206}Pb$	± 2σ	$^{207}Pb/^{206}Pb$ Age (Ma)	± 2σ	Disc. (%)	Corr. Coeff.
03VOI-0422-1		***#31, Trachyte, Timiskaming Group, Gauthier Twp.***																
A1	MAH4040	1 clr, cls, small, stubby prism	0.0003	107	0.66	16.1	0.4	2359	0.51157	0.00231	12.8293	0.0624	0.18189	0.00030	2670.1	2.8	0.3	0.9401
A2	MAH4041r	1 clr, cls, small, stubby prism	0.0006	74	0.40	27.3	0.8	2114	0.51571	0.00160	13.1224	0.0488	0.18455	0.00031	2694.2	2.8	0.6	0.8938
A3	MAH4042a	1 clr, bm, small, 2:1 prism	0.0003	478	0.53	69.1	2.7	1440	0.50561	0.00135	12.6658	0.0480	0.18169	0.00040	2668.3	3.6	1.4	0.8224
A4	MAH4064a	2 clr, bm, small, 2:1 prism	0.0003	356	0.66	74.8	3.4	1239	0.51170	0.00131	12.8828	0.0499	0.18260	0.00047	2676.6	4.3	0.6	0.7471
A5	MAH4065	2 clr, bm, small, 2:1 prism	0.0003	277	0.69	48.6	0.4	7586	0.49685	0.00134	12.4571	0.0370	0.18184	0.00022	2669.7	2.0	3.2	0.9166
03VOI-570-1		***#32, Timiskaming sandstone, Gauthier Twp.***																
1a	MAH4049	1 clr, med-brn, sharp, subeq euh prism	0.0026	169	0.63	267.1	0.4	35802	0.51336	0.00127	12.9593	0.0357	0.18309	0.00017	2681.0	1.5	0.5	0.9440
1b	MAH4050	1 clr, med-brn, sharp, subeq euh prism	0.0026	122	0.83	193.6	0.4	23858	0.51235	0.00172	12.9073	0.0410	0.18271	0.00034	2677.7	3.1	0.5	0.8370
2a	MAH4051	1 clr, pbr, subrnd, sl. elong, prism	0.0015	97	0.36	84.6	0.5	9801	0.53342	0.00171	14.2115	0.0489	0.19323	0.00019	2769.8	1.7	0.6	0.9567
2b	MAH4109	1 clr, pbr, subrnd, sl. elong, prism	0.0007	73	0.47	29.4	0.5	3500	0.51450	0.00199	12.9986	0.0543	0.18324	0.00023	2682.4	2.0	0.3	0.9560
3a	MAH4052	1 large clr, brn, sharp frag	0.0041	145	0.83	368.3	0.6	30646	0.51284	0.00146	12.9239	0.0401	0.18277	0.00016	2678.2	1.5	0.4	0.9581
3b	MAH4110	1 large clr, brn, sharp frag	0.0049	74	0.71	221.0	1.5	8024	0.51216	0.00107	12.9136	0.0322	0.18287	0.00016	2679.1	1.5	0.6	0.9411
03SJP-115-1		***#34, Clifford stock monzogranite, Clifford Twp.***																
Z1	MAH4010	1 cls-pbr, clr, elong euh prism (>4:1); minor inc	0.0025	141	0.48	207.3	2.2	5337	0.51364	0.00292	13.0176	0.0758	0.18381	0.00023	2687.6	2.1	0.7	0.9770
Z2	MAH4007	1 large, pbr, clr, frag; minor incl, frac	0.0008	147	1.02	74.0	2.1	1796	0.51737	0.00209	13.1081	0.0576	0.18375	0.00043	2687.0	3.9	0.0	0.8507
Z3	MAH4012	1 large, cls, clr, frag; minor incl, frac	0.0014	102	0.51	85.8	1.2	4154	0.51660	0.00230	13.0819	0.0612	0.18366	0.00022	2686.2	2.0	0.1	0.9668
03ASP-130-1		***#35, Porphyritic rhyolite, Clifford Twp.***																
A1a	MAH4022	1 clr, pbr, short, stubby euh prism	0.0016	244	0.49	225.9	7.3	1756	0.51867	0.00112	13.2145	0.0422	0.18478	0.00033	2696.3	2.9	0.1	0.8515
A1b	MAH4023c	1 clr, pbr, short, stubby euh prism	0.0010	239	0.45	146.1	6.3	1348	0.51746	0.00111	13.1732	0.0472	0.18463	0.00040	2694.9	3.6	0.3	0.8231
A1d	MAH4058	3 clr, pbr, short, stubby euh prism	0.0024	124	0.53	177.5	0.4	27790	0.51810	0.00115	13.2031	0.0338	0.18482	0.00016	2696.6	1.5	0.2	0.9407
A2a	MAH4024	1 clr, pbr, short, stubby euh prism	0.0012	252	0.56	177.8	2.6	3901	0.51036	0.00127	12.8882	0.0374	0.18315	0.00022	2681.6	2.0	1.1	0.9103
03ASP-0179-1		***#36, Massive rhyolite, Ben Nevis Twp.***																
A1	MAH4053b	3 small, pyell, sharp subeq prisms	0.0007	102	0.46	39.9	0.4	6519	0.51917	0.00168	13.2323	0.0464	0.18485	0.00019	2696.9	1.7	0.1	0.9588
A2	MAH4054	6 v.small, pyell, shrp, subeq prisms	0.0007	298	0.58	119.0	1.1	6132	0.49406	0.00121	12.5774	0.0349	0.18464	0.00020	2694.9	1.8	4.8	0.9216
A3	MAH4055c	6 v.small, pyell, shrp, subeq prisms	0.0007	126	0.55	52.0	0.6	4734	0.51234	0.00130	13.0484	0.0385	0.18471	0.00019	2695.7	1.7	1.3	0.9394
C89-7		***#38, Pegmatitic gabbro, Ghost Range sill, Lamplugh Twp. (Corfu, 1993)***																
Bd-1	MAH5025	3 small, thin, br blade frags, frosted; HF etchec	0.0010	313	0.07	168.2	5.1	2057	0.51761	0.00157	13.3232	0.0492	0.18668	0.00030	2713.1	2.6	1.1	0.9053
Bd-2	MAH5026	3 small, thin, br blade frags, frosted; HF etchec	0.0010	209	0.06	112.2	0.8	8777	0.51825	0.00101	13.3358	0.0318	0.18663	0.00016	2712.7	1.4	0.9	0.9391
04JAA-0002		***#39 Leucogabbro, Centre Hill complex, north-central Munro Twp.***																
Z2	MAH4068	1 clr, cls square skeletal flange	0.0004	119	1.73	33.7	0.5	3365	0.51971	0.00180	13.3245	0.0505	0.18595	0.00024	2706.6	2.1	0.4	0.9418
Z3	MAH5001a	1 clr, cls euh, skeletal	0.0008	287	1.26	149.6	5.9	1246	0.51897	0.00134	13.3073	0.0595	0.18597	0.00056	2706.9	5.0	0.5	0.7613
Bd-1	MAH4069a	1 unabr, frosted?	0.0001	135	0.14	10.2	0.9	688	0.51421	0.00306	13.1697	0.1035	0.18575	0.00075	2704.9	6.7	1.4	0.8626
Bd-3	MAH5002	1 unabr, large blade frag	0.0009	288	0.18	148.3	2.0	4409	0.51648	0.00116	13.2446	0.0358	0.18599	0.00020	2707.0	1.8	1.0	0.9221

Notes:

All analyzed fractions represent least magnetic, air-abraded single zircon grains, free of inclusions, cores or cracks, unless otherwise noted.

Abbreviations: clr - clear; cls - colourless; pyell - pale yellow; brn - brown; pbr - pale brown; eq - equant; subeq - subequant; elong - elongate; euh - euhedral; prism - prismatic; frag - fragment; frac. - fracture(s); subrnd - subrounde

Pb* is total amount (in picograms) of radiogenic Pb.

Pb_C is total measured common Pb (in picograms) assuming the isotopic composition of laboratory blank: 206/204 - 18.221; 207/204 - 15.612; 208/204 - 39.360 (errors of 2%).

Pb/U atomic ratios are corrected for spike, fractionation, blank, and, where necessary, initial common Pb; $^{206}Pb/^{204}Pb$ is corrected for spike and fractionation.

Th/U is model value calculated from radiogenic 208Pb/206Pb ratio and 207Pb/206Pb age assuming concordance.

Disc. (%) - per cent discordance for the given 207Pb/206Pb age.

Uranium decay constants are from Jaffey et al. (1971).

Appendix 2

Sensitive High-Resolution Ion Microprobe (SHRIMP) Methodology and Data

SENSITIVE HIGH RESOLUTION ION MICROPROBE (SHRIMP) ANALYTICAL METHODS

Zircon grains were analyzed using the J.C. Roddick SHRIMP II ion microprobe analytical facility at the Geological Survey of Canada, Ottawa, during two analytical sessions in October and November, 2004. Zircons were arranged along with fragments of the GSC laboratory zircon reference standard (BR266/z6266; 910 ppm U, $^{206}Pb/^{238}U$ isotope dilution age = 559 Ma), cast in epoxy grain mounts (GSC mounts IP339, 343), and polished sufficiently with diamond compound to reveal the grain centres. The mount was then cleaned, coated with approximately 10 nm of high purity gold, and individual zircon grains were imaged with a Cambridge Instruments S360 scanning electron microscope equipped with cathodoluminescence (CL) and backscatter (BSE) detectors to identify complexities of internal structure and compositional zoning, cracks, inclusions and fractures. U/Pb isotopic spot analyses within the zircons were carried out following the general SHRIMP methods outlined in Stern (1997) and Hamilton, McLelland and Selleck (2004). Data were acquired using a mass-filtered O^- primary beam and apertures of sufficient size to effect sputtering diameters of approximately 12x15 and 25x30 µm. Primary O^- beam currents during these sessions were roughly 1.3 nÅ (small spot size) and 15 nÅ (large spot size), while mass resolution was routinely in the range 5250 to 5500.

Peak count rates were measured sequentially over nine mass stations for Zr^+, Pb^+, U^+ and Th+ (plus background) averaged through five to seven scans, using an electron multiplier in pulse-counting mode (27–30 ns deadtime). The 1σ uncertainties in the zircon Pb/U ratios shown in Table A2 reflect, in part, an external error of ±1.0–1.3% resulting from the within-session calibration of the BR266 zircon standard (Stern and Amelin 2003). Correction of the measured isotopic ratios for common Pb was estimated from monitored ^{204}Pb counts; in all cases, the background-corrected ^{204}Pb counts were low and an independently determined surface blank composition was assumed (Stern 1997).

Table A2. Ion microprobe (SHRIMP II) U-Th-Pb data for Abitibi zircons.

Spot	U (ppm)	Th (ppm)	Th/U	Pb* (ppm)	^{204}Pb (ppb)	^{206}Pb/^{204}Pb	f206 (%)	^{207}Pb/^{235}U ± 1σ	^{206}Pb/^{238}U ± 1σ	^{207}Pb/^{206}Pb ± 1σ	^{207}Pb/^{206}Pb ± 1σ Age (Ma)	Disc. (%)	Corr. Coeff.
97JAA-106, ***Rhyolite, Deloro assemblage, Shining Tree area, Macmurchy Township (E487060, N5275406; see Ayer et al., 2002).***													
15.1	136	91	0.687	84	7	8115	0.21	13.4740 ± 0.3077	0.51160 ± 0.00991	0.19101 ± 0.00189	2750.9 ± 16.4	3.9	0.903
8.1	194	70	0.372	107	4	18965	0.09	13.0916 ± 0.2480	0.50011 ± 0.00799	0.18986 ± 0.00159	2740.9 ± 13.8	5.6	0.899
2.1	141	49	0.362	78	1	46468	0.04	13.1258 ± 0.2585	0.50186 ± 0.00818	0.18969 ± 0.00174	2739.5 ± 15.2	5.2	0.886
19.1	213	129	0.627	127	9	10580	0.16	13.2750 ± 0.2704	0.50900 ± 0.00916	0.18915 ± 0.00143	2734.8 ± 12.5	3.7	0.930
11.1	172	61	0.365	97	1	102249	0.02	13.2249 ± 0.2235	0.50736 ± 0.00736	0.18905 ± 0.00133	2733.9 ± 11.6	3.9	0.911
14.1	293	119	0.421	171	1	179533	0.01	13.4682 ± 0.2086	0.51924 ± 0.00731	0.18812 ± 0.00093	2725.8 ± 8.1	1.3	0.949
3.1	279	127	0.471	158	6	18464	0.09	12.9750 ± 0.2232	0.50115 ± 0.00743	0.18778 ± 0.00133	2722.8 ± 11.7	4.6	0.913
16.1	370	193	0.540	213	3	48403	0.04	12.9360 ± 0.2325	0.49994 ± 0.00813	0.18766 ± 0.00110	2721.8 ± 9.7	4.8	0.946
6.1	149	52	0.364	84	1	86356	0.02	13.0874 ± 0.2413	0.50740 ± 0.00796	0.18707 ± 0.00148	2716.6 ± 13.1	3.2	0.904
1.1	412	193	0.484	232	5	32520	0.05	12.8121 ± 0.2239	0.49698 ± 0.00741	0.18697 ± 0.00139	2715.7 ± 12.3	5.1	0.907
12.1	184	81	0.455	108	3	24004	0.07	13.4759 ± 0.2356	0.52409 ± 0.00769	0.18649 ± 0.00147	2711.4 ± 13.0	-0.2	0.895
7.1	116	36	0.317	66	1	100000	0.02	13.1974 ± 0.2266	0.51531 ± 0.00756	0.18575 ± 0.00135	2704.9 ± 12.0	1.2	0.908
18.1	135	62	0.478	79	11	5424	0.32	13.3194 ± 0.2882	0.52084 ± 0.00960	0.18547 ± 0.00172	2702.4 ± 15.4	0.0	0.906
9.1	530	344	0.670	302	8	26226	0.07	12.2713 ± 0.1776	0.48209 ± 0.00647	0.18461 ± 0.00074	2694.7 ± 6.6	7.1	0.962
13.1	211	164	0.802	133	1	100000	0.02	13.2321 ± 0.2165	0.52141 ± 0.00752	0.18406 ± 0.00113	2689.8 ± 10.2	-0.7	0.928
20.1	343	191	0.574	179	3	42017	0.04	11.4825 ± 0.2468	0.45337 ± 0.00889	0.18369 ± 0.00123	2686.5 ± 11.1	12.3	0.951
4.1	347	143	0.424	196	9	16567	0.11	12.6757 ± 0.2039	0.50450 ± 0.00733	0.18222 ± 0.00097	2673.2 ± 8.9	1.8	0.944
96TB-0079, ***Dacite footwall to Langmuir #2 Ni mine, Lower Tisdale assemblage, Langmuir Township (see Barrie and Corfu, 1999), # 25 on Fig. 2.***													
4.1	119	56	0.484	69	1	39573	0.04	13.3650 0.2908	0.50249 0.00740	0.19290 0.00276	2767.1 23.6	6.3	0.759
2.2	88	83	0.974	55	3	11053	0.16	13.1610 0.2692	0.49639 0.00826	0.19229 0.00192	2761.8 16.5	7.2	0.874
19.1	289	152	0.544	160	46	2612	0.66	12.7760 0.2102	0.48506 0.00695	0.19103 0.00124	2751.0 10.7	8.9	0.920
15.1	137	95	0.714	87	0	952381	0.00	13.9360 0.2866	0.52919 0.00726	0.19099 0.00262	2750.7 22.7	0.6	0.750
4.3	74	33	0.462	41	0	100000	0.02	12.9510 0.2927	0.49270 0.00957	0.19064 0.00179	2747.7 15.5	7.3	0.911
17.2	247	22	0.094	131	28	3785	0.46	13.2930 0.2527	0.50694 0.00872	0.19018 0.00118	2743.7 10.3	4.4	0.946
13.3	156	100	0.662	90	25	2559	0.68	12.6690 0.3153	0.48359 0.01033	0.19000 0.00197	2742.2 17.2	8.8	0.911
5.1	169	65	0.397	96	7	9909	0.18	13.3450 0.2538	0.50958 0.00667	0.18994 0.00233	2741.6 20.3	3.9	0.769
18.1	370	18	0.049	194	16	10223	0.17	13.2200 0.2453	0.50589 0.00875	0.18952 0.00092	2738.0 8.0	4.4	0.966
17.1	387	19	0.052	205	42	4055	0.43	13.3660 0.2458	0.51169 0.00602	0.18945 0.00241	2737.4 21.1	3.3	0.727
9.1.2	542	47	0.089	279	27	8553	0.20	12.8650 0.2652	0.49364 0.00977	0.18902 0.00072	2733.6 6.3	6.5	0.983
3.1	138	47	0.348	79	5	12625	0.14	13.3460 0.2946	0.51334 0.00721	0.18855 0.00290	2729.6 25.5	2.6	0.723
11.1	513	511	1.030	346	17	14090	0.12	13.7840 0.2015	0.53094 0.00616	0.18829 0.00142	2727.3 12.5	-0.8	0.858
9.1	670	55	0.085	373	10	31114	0.06	13.8360 0.2015	0.53351 0.00640	0.18810 0.00129	2725.6 11.4	-1.4	0.883
14.2	132	100	0.788	82	7	8506	0.20	13.2020 0.2472	0.50933 0.00818	0.18799 0.00147	2724.6 13.0	3.2	0.910
21.1	167	190	1.178	109	33	2198	0.79	13.1450 0.2859	0.50814 0.00929	0.18762 0.00182	2721.4 16.1	3.3	0.897
22.1	45	27	0.624	26	5	4097	0.42	12.5570 0.3204	0.48559 0.00932	0.18755 0.00273	2720.8 24.2	7.5	0.824
8.1	670	63	0.098	364	26	11692	0.15	13.4520 0.1826	0.52076 0.00571	0.18735 0.00127	2719.1 11.2	0.8	0.870
6.1	233	126	0.559	133	9	10442	0.17	12.7310 0.2316	0.49600 0.00611	0.18615 0.00222	2708.5 19.9	5.0	0.759
15.2	557	70	0.130	294	4	60533	0.03	12.8570 0.1984	0.50244 0.00599	0.18560 0.00156	2703.5 14.0	3.6	0.840
8.2	935	34	0.038	462	54	7186	0.24	12.1260 0.1820	0.48237 0.00661	0.18232 0.00085	2674.1 7.7	6.2	0.951

Uncertainties are reported at 1σ (absolute) and are calculated by numerical propagation of all known sources of error.
Pb* = radiogenic Pb; f206 (%): Percentage of 206Pb which is common.
Disc (%) = Percent discordance along a chord to origin for the given 207Pb/206Pb age; Corr. Coeff. = Correlation coefficient (rho).

Table A2. continued

Spot	U (ppm)	Th (ppm)	Th/U	Pb* (ppm)	^{204}Pb (ppb)	^{206}Pb/^{204}Pb	f206 (%)	^{207}Pb/^{235}U ± 1σ	^{206}Pb/^{238}U ± 1σ	^{207}Pb/^{206}Pb ± 1σ	^{207}Pb/^{206}Pb ± 1σ Age (Ma)	Disc. (%)	Corr. Coeff.
98JAA-0011, ***Felsic to intermediate tuff, upper Tisdale assemblage, NW Cleaver Township (see Ayer et al., 2002), #29 on Fig. 2.***													
3.1	58	31	0.558	35	2	14457	0.12	13.5389 ± 0.3464	0.51957 ± 0.00844	0.18899 ± 0.00337	2733.4 ± 29.7	1.6	0.722
9.1	96	43	0.462	54	0	100000	0.02	12.8633 ± 0.2995	0.49369 ± 0.00943	0.18897 ± 0.00210	2733.2 ± 18.4	6.5	0.880
13.1	65	44	0.690	39	7	4307	0.40	13.0050 ± 0.4352	0.49962 ± 0.01064	0.18878 ± 0.00439	2731.6 ± 38.9	5.3	0.724
11.1	69	43	0.645	41	0	100000	0.02	12.9105 ± 0.3544	0.49775 ± 0.01166	0.18812 ± 0.00220	2725.8 ± 19.4	5.4	0.907
10.1	104	58	0.577	62	5	8548	0.20	13.3259 ± 0.3271	0.51466 ± 0.00989	0.18779 ± 0.00245	2722.9 ± 21.7	2.1	0.849
7.1	95	58	0.634	56	3	14950	0.12	13.0227 ± 0.2855	0.50302 ± 0.00858	0.18777 ± 0.00222	2722.7 ± 19.6	4.3	0.846
5.1	94	67	0.728	58	2	19231	0.09	13.1446 ± 0.2568	0.50790 ± 0.00822	0.18770 ± 0.00171	2722.1 ± 15.1	3.3	0.887
2.1	174	69	0.413	96	1	100000	0.02	12.7455 ± 0.2881	0.49295 ± 0.00988	0.18752 ± 0.00155	2720.6 ± 13.7	6.1	0.932
6.1	128	104	0.841	79	8	7253	0.24	12.9252 ± 0.2301	0.50048 ± 0.00762	0.18730 ± 0.00141	2718.6 ± 12.4	4.6	0.908
12.1	69	32	0.480	39	8	3512	0.49	12.9101 ± 0.3561	0.50451 ± 0.00887	0.18559 ± 0.00356	2703.5 ± 32.0	3.2	0.725
8.1	73	36	0.506	42	1	30139	0.06	12.8817 ± 0.3391	0.50347 ± 0.01043	0.18557 ± 0.00257	2703.3 ± 23.1	3.4	0.853
1.1	75	45	0.624	42	5	5984	0.29	12.4037 ± 0.3416	0.48635 ± 0.00918	0.18497 ± 0.00330	2697.9 ± 29.8	6.4	0.766
14.1	56	35	0.644	32	4	5471	0.32	12.4150 ± 0.3731	0.48686 ± 0.00957	0.18494 ± 0.00378	2697.7 ± 34.1	6.3	0.739
4.1	41	24	0.593	24	6	3021	0.57	12.7930 ± 0.5043	0.51047 ± 0.01348	0.18176 ± 0.00475	2669.0 ± 44.0	0.5	0.753
15.1	56	24	0.451	31	13	1816	0.95	12.3250 ± 0.3554	0.49615 ± 0.00908	0.18017 ± 0.00362	2654.5 ± 33.7	2.6	0.722
3D-CG, ***Heterolithic volcanic tuff/breccia flow, Porcupine/Timiskaming? assemblage, Holloway Mine, Holloway Township (see Ropchan et al., 2002), # 37 on Fig. 2.***													
4.1	137	162	1.221	95	5	11276	0.15	14.1220 ± 0.2597	0.52153 ± 0.00827	0.19639 ± 0.00148	2796.4 ± 12.4	4.0	0.913
10.1	319	205	0.663	199	5	28547	0.06	13.9350 ± 0.2421	0.52869 ± 0.00803	0.19117 ± 0.00129	2752.2 ± 11.2	0.7	0.923
9.2	351	131	0.386	201	5	33490	0.05	13.4180 ± 0.2344	0.51381 ± 0.00776	0.18941 ± 0.00134	2737.0 ± 11.7	2.9	0.915
8.1	197	224	1.175	129	6	14368	0.12	13.2030 ± 0.2667	0.50669 ± 0.00836	0.18899 ± 0.00185	2733.4 ± 16.2	4.1	0.877
20.1	115	51	0.453	66	15	3314	0.52	13.1419 ± 0.2897	0.50548 ± 0.00922	0.18856 ± 0.00195	2729.6 ± 17.1	4.1	0.886
1.1	98	78	0.830	59	8	5419	0.32	12.7820 ± 0.2888	0.49878 ± 0.00807	0.18587 ± 0.00258	2705.9 ± 23.1	4.4	0.793
2.1	192	217	1.165	127	4	19635	0.09	13.0040 ± 0.4197	0.50850 ± 0.01211	0.18547 ± 0.00353	2702.4 ± 31.7	2.4	0.811
14.1	459	1429	3.219	425	5	44603	0.04	13.1810 ± 0.2537	0.51708 ± 0.00835	0.18488 ± 0.00160	2697.1 ± 14.4	0.5	0.895
6.1	862	1815	2.174	698	8	49900	0.04	13.2600 ± 0.2156	0.52030 ± 0.00752	0.18484 ± 0.00108	2696.8 ± 9.7	-0.2	0.934
18.1	580	358	0.637	339	8	32573	0.05	12.6996 ± 0.2046	0.49831 ± 0.00725	0.18484 ± 0.00098	2696.8 ± 8.8	4.1	0.945
13.1	144	92	0.661	84	7	9003	0.19	12.7100 ± 0.2881	0.49908 ± 0.00866	0.18470 ± 0.00232	2695.5 ± 20.9	3.9	0.835
17.1	503	375	0.769	301	10	22168	0.08	12.6830 ± 0.1983	0.49905 ± 0.00736	0.18432 ± 0.00068	2692.1 ± 6.1	3.7	0.972
12.1	436	1079	2.555	352	8	23714	0.07	12.5270 ± 0.2030	0.49434 ± 0.00722	0.18378 ± 0.00100	2687.3 ± 9.0	4.4	0.943
15.1	223	148	0.684	134	6	17030	0.10	12.8780 ± 0.2248	0.50932 ± 0.00762	0.18338 ± 0.00134	2683.7 ± 12.1	1.4	0.910
19.1	268	158	0.608	156	8	14620	0.12	12.6676 ± 0.2447	0.50145 ± 0.00826	0.18322 ± 0.00151	2682.2 ± 13.7	2.8	0.906
3.1	93	114	1.271	62	11	3577	0.48	12.8400 ± 0.2819	0.50857 ± 0.00870	0.18311 ± 0.00216	2681.3 ± 19.6	1.4	0.846
16.1	126	134	1.094	82	5	10321	0.17	12.7630 ± 0.2676	0.50600 ± 0.00863	0.18294 ± 0.00187	2679.7 ± 17.0	1.8	0.875
7.1	121	107	0.915	76	4	12821	0.14	12.7410 ± 0.2829	0.50526 ± 0.00860	0.18288 ± 0.00225	2679.2 ± 20.5	1.9	0.836
5.1	233	282	1.250	157	10	10487	0.17	12.8930 ± 0.2226	0.51221 ± 0.00773	0.18256 ± 0.00122	2676.3 ± 11.1	0.5	0.923

Uncertainties are reported at 1σ (absolute) and are calculated by numerical propagation of all known sources of error.
Pb* = radiogenic Pb; f206 (%): Percentage of 206Pb which is common.
Disc (%) = Percent discordance along a chord to origin for the given 207Pb/206Pb age; Corr. Coeff. = Correlation coefficient (rho).

Table A2. continued

Spot	Struct. Dom.	U (ppm)	Th (ppm)	Th/U	Pb* (ppm)	^{204}Pb (ppb)	^{206}Pb/^{204}Pb	f206 (%)	^{207}Pb/^{235}U ± 1σ	^{206}Pb/^{238}U ± 1σ	^{207}Pb/^{206}Pb ± 1σ	^{207}Pb/^{206}Pb ± 1σ Age (Ma)	Disc. (%)	Corr. Coeff.
99JAA-0057, *Heterolithic volcanic breccia, Timiskaming assemblage, Swayze Township (E038175, N5297199; see Ayer, Ketchum and Trowell 2002)*														
13.1	sharp, elong igneous frag	62	64	1.065	41	37	753	2.30	13.4560 ± 0.4039	0.50635 ± 0.00866	0.19274 ± 0.00436	2765.7 ± 37.6	5.5	0.664
6.1	core	78	54	0.721	48	4	8777	0.20	13.5290 ± 0.3494	0.51718 ± 0.01130	0.18973 ± 0.00215	2739.8 ± 18.7	2.3	0.901
9.1	sharp, elong igneous frag	123	150	1.259	83	5	11342	0.15	13.1660 ± 0.2729	0.50643 ± 0.00898	0.18855 ± 0.00165	2729.6 ± 14.5	3.9	0.908
17.1	center; v. rounded grain	100	94	0.966	64	6	7820	0.22	13.0290 ± 0.2667	0.50696 ± 0.00880	0.18639 ± 0.00166	2710.6 ± 14.8	3.0	0.902
18.1	center; slightly rounded exterior	80	30	0.385	45	9	3785	0.46	12.8790 ± 0.2856	0.50277 ± 0.00842	0.18578 ± 0.00234	2705.2 ± 20.9	3.6	0.827
8.1	center; fairly rounded exterior	570	595	1.077	259	121	1582	1.10	9.9071 ± 0.2706	0.38687 ± 0.00760	0.18573 ± 0.00310	2704.7 ± 27.8	25.8	0.795
1.1	core	599	801	1.381	432	6	49603	0.04	13.6090 ± 0.1944	0.53182 ± 0.00718	0.18559 ± 0.00061	2703.5 ± 5.4	-2.1	0.974
11.1	sharp, elong igneous frag	151	166	1.132	98	6	10549	0.16	12.9580 ± 0.2484	0.50641 ± 0.00841	0.18558 ± 0.00143	2703.4 ± 12.8	2.8	0.917
16.1.2	center or core?; prism. grain exterior	96	70	0.753	56	5	7430	0.23	12.4050 ± 0.3098	0.48479 ± 0.00886	0.18559 ± 0.00276	2703.4 ± 24.8	6.9	0.806
12.1	elong., slightly rounded	52	54	1.081	32	10	2171	0.80	12.3340 ± 0.3274	0.48207 ± 0.00831	0.18556 ± 0.00337	2703.2 ± 30.3	7.5	0.735
15.1	center; fairly rounded exterior	209	319	1.575	150	11	8527	0.20	13.0330 ± 0.2335	0.51073 ± 0.00784	0.18508 ± 0.00139	2698.9 ± 12.5	1.8	0.909
5.1	core? of rounded gr	799	417	0.539	479	28	12887	0.13	13.3800 ± 0.2043	0.52508 ± 0.00759	0.18481 ± 0.00064	2696.6 ± 5.7	-1.1	0.975
4.1	center or core?	108	62	0.599	64	8	6077	0.29	13.1460 ± 0.2543	0.51594 ± 0.00788	0.18479 ± 0.00187	2696.4 ± 16.8	0.7	0.855
10.1	center; slightly rounded exterior	312	492	1.629	224	4	31918	0.05	12.8420 ± 0.2216	0.50812 ± 0.00793	0.18330 ± 0.00103	2683.0 ± 9.4	1.6	0.946
14.1	embayment on long prism	272	42	0.159	136	18	6128	0.28	11.9600 ± 0.2151	0.47630 ± 0.00778	0.18211 ± 0.00105	2672.2 ± 9.6	7.3	0.948
2.1	angular, core? In rounded elong grain	407	110	0.280	219	104	1695	1.02	12.4140 ± 0.2016	0.50195 ± 0.00693	0.17936 ± 0.00125	2647.0 ± 11.7	1.1	0.904
03JAA-0006, *Syenitic feldspar porphyry, Discovery outcrop, Kirkland Lake, Teck Township (E571986, N5333892), #30 on Fig. 2.*														
10.1	core	75	30	0.410	43	5	6273	0.28	13.0790 ± 0.2901	0.50333 ± 0.00822	0.18846 ± 0.00247	2728.8 ± 21.8	4.5	0.810
12.1	core	178	92	0.532	101	2	30931	0.06	12.7280 ± 0.2140	0.49148 ± 0.00709	0.18782 ± 0.00132	2723.2 ± 11.6	6.5	0.910
9.1	core	163	100	0.633	96	22	3148	0.55	12.9370 ± 0.2371	0.50255 ± 0.00737	0.18670 ± 0.00174	2713.3 ± 15.4	4.0	0.864
4.1	core	175	84	0.494	101	1	134771	0.01	12.9420 ± 0.2522	0.50412 ± 0.00793	0.18620 ± 0.00181	2708.9 ± 16.1	3.5	0.870
2.1	core	347	208	0.619	199	6	24704	0.07	12.4840 ± 0.2555	0.48747 ± 0.00786	0.18574 ± 0.00199	2704.8 ± 17.8	6.5	0.854
13.1	core	97	33	0.350	55	5	8063	0.22	13.2120 ± 0.2725	0.51623 ± 0.00880	0.18562 ± 0.00180	2703.7 ± 16.1	0.9	0.885
5.1	core?	157	67	0.441	88	2	26889	0.06	12.6760 ± 0.2226	0.49559 ± 0.00743	0.18551 ± 0.00139	2702.8 ± 12.4	4.9	0.906
17.1	core?	273	188	0.710	160	10	11639	0.15	12.5840 ± 0.2298	0.49243 ± 0.00779	0.18534 ± 0.00137	2701.3 ± 12.2	5.4	0.917
11.1	core	619	485	0.809	371	24	10810	0.16	12.6740 ± 0.2117	0.49609 ± 0.00785	0.18529 ± 0.00070	2700.8 ± 6.2	4.7	0.975
6.1	core	345	126	0.376	196	3	44984	0.04	13.0320 ± 0.3851	0.51240 ± 0.01055	0.18446 ± 0.00346	2693.4 ± 31.4	1.2	0.776
1.1	core	256	92	0.372	143	15	7465	0.23	12.8220 ± 0.2049	0.50490 ± 0.00705	0.18418 ± 0.00114	2690.9 ± 10.3	2.5	0.923
18.2	rim	1027	471	0.474	591	7	63052	0.03	12.8960 ± 0.1934	0.50977 ± 0.00704	0.18347 ± 0.00080	2684.5 ± 7.2	1.3	0.958
19.1	core	672	198	0.305	362	16	17928	0.10	12.4210 ± 0.1825	0.49430 ± 0.00681	0.18225 ± 0.00067	2673.5 ± 6.1	3.8	0.969
3.1	magmatic?	492	459	0.965	301	73	2865	0.61	12.1440 ± 0.1859	0.49035 ± 0.00664	0.17962 ± 0.00102	2649.4 ± 9.4	3.5	0.931
14.1	rim	234	55	0.243	129	14	7567	0.23	12.7160 ± 0.2316	0.51568 ± 0.00833	0.17884 ± 0.00119	2642.1 ± 11.1	-1.8	0.932

Uncertainties are reported at 1σ (absolute) and are calculated by numerical propagation of all known sources of error.
Pb* = radiogenic Pb; f206 (%): Percentage of 206Pb which is common.
Disc (%) = Percent discordance along a chord to origin for the given 207Pb/206Pb age; Corr. Coeff. = Correlation coefficient (rho).

Table A2. continued

Spot	U (ppm)	Th (ppm)	Th/U	Pb* (ppm)	^{204}Pb (ppb)	^{206}Pb/^{204}Pb	f206 (%)	^{207}Pb/^{235}U ± 1σ	^{206}Pb/^{238}U ± 1σ	^{207}Pb/^{206}Pb ± 1σ	^{207}Pb/^{206}Pb ± 1σ Age (Ma)	Disc. (%)	Corr. Coeff.
BNB01-T-01, ***Timiskaming sandstone, basal Dome Formation, above Greenstone Nose unconformity, Dome Mine, Tisdale Township (see Ayer et al., 2003), #12 on Fig. 2.***													
45.1	55	24	0.438	34	35	738	2.35	14.5948 ± 0.2543	0.53385 ± 0.00641	0.19828 ± 0.00222	2812.1 ± 18.4	2.4	0.770
15.1	148	73	0.505	89	5	12241	0.14	14.1151 ± 0.1822	0.51955 ± 0.00595	0.19704 ± 0.00092	2801.9 ± 7.7	4.6	0.933
43.1	78	46	0.616	49	6	5631	0.31	14.5544 ± 0.2138	0.53812 ± 0.00668	0.19616 ± 0.00126	2794.5 ± 10.6	0.8	0.900
38.1	87	46	0.543	53	18	2260	0.77	14.2327 ± 0.2895	0.53139 ± 0.00628	0.19426 ± 0.00294	2778.5 ± 25.0	1.4	0.674
23.1	31	25	0.850	19	7	1868	0.93	13.2719 ± 0.3351	0.50965 ± 0.00806	0.18887 ± 0.00336	2732.3 ± 29.6	3.4	0.715
12.1	60	48	0.823	36	2	13252	0.13	12.8256 ± 0.2256	0.49325 ± 0.00665	0.18859 ± 0.00184	2729.9 ± 16.1	6.4	0.836
36.1	48	20	0.440	27	16	1317	1.32	13.0093 ± 0.3018	0.50123 ± 0.00896	0.18824 ± 0.00240	2726.9 ± 21.1	4.8	0.839
44.1	44	44	1.016	28	38	512	3.39	12.8383 ± 0.3253	0.49582 ± 0.00723	0.18779 ± 0.00356	2722.9 ± 31.6	5.7	0.669
48.1	36	26	0.751	22	36	451	3.85	13.0856 ± 0.3409	0.50584 ± 0.00819	0.18762 ± 0.00347	2721.4 ± 30.8	3.7	0.710
32.1	232	150	0.667	143	6	16218	0.11	13.5547 ± 0.1640	0.52416 ± 0.00574	0.18755 ± 0.00074	2720.8 ± 6.5	0.2	0.946
46.1	63	77	1.267	42	23	1197	1.45	12.8406 ± 0.2095	0.49804 ± 0.00585	0.18699 ± 0.00186	2715.9 ± 16.5	4.9	0.796
50.1	200	168	0.870	125	44	1988	0.87	13.0931 ± 0.1695	0.50823 ± 0.00588	0.18685 ± 0.00085	2714.6 ± 7.5	2.9	0.937
21.2	38	31	0.836	24	4	3979	0.44	13.0899 ± 0.3391	0.50813 ± 0.00837	0.18684 ± 0.00337	2714.5 ± 30.0	3.0	0.723
10.1	219	182	0.856	135	3	28662	0.06	12.9054 ± 0.1541	0.50311 ± 0.00547	0.18604 ± 0.00070	2707.5 ± 6.2	3.6	0.951
22.1	154	129	0.864	96	4	17036	0.10	13.0358 ± 0.1788	0.50842 ± 0.00632	0.18596 ± 0.00083	2706.8 ± 7.4	2.6	0.947
16.1	80	74	0.956	50	5	6415	0.27	12.8268 ± 0.1925	0.50044 ± 0.00597	0.18589 ± 0.00144	2706.2 ± 12.8	4.1	0.859
24.1	525	47	0.093	285	5	44623	0.04	13.3422 ± 0.1495	0.52069 ± 0.00545	0.18584 ± 0.00054	2705.7 ± 4.8	0.2	0.967
37.1	143	133	0.965	90	13	4752	0.37	12.9223 ± 0.1759	0.50471 ± 0.00594	0.18569 ± 0.00103	2704.4 ± 9.2	3.2	0.915
28.1	288	91	0.325	163	10	12203	0.14	13.2393 ± 0.1693	0.51718 ± 0.00568	0.18566 ± 0.00099	2704.1 ± 8.8	0.8	0.911
19.1	429	193	0.464	252	3	56370	0.03	13.2676 ± 0.1474	0.51837 ± 0.00538	0.18563 ± 0.00053	2703.8 ± 4.7	0.5	0.967
27.1	156	75	0.499	90	3	22507	0.08	13.0568 ± 0.1898	0.51032 ± 0.00656	0.18556 ± 0.00099	2703.2 ± 8.9	2.0	0.931
30.1	86	55	0.666	52	5	7351	0.24	13.1598 ± 0.1903	0.51478 ± 0.00630	0.18541 ± 0.00117	2701.8 ± 10.5	1.1	0.901
47.1	190	164	0.893	118	49	1705	1.02	12.9085 ± 0.1638	0.50542 ± 0.00558	0.18523 ± 0.00093	2700.3 ± 8.3	2.9	0.920
49.1	121	25	0.210	66	195	293	5.92	13.2125 ± 0.2699	0.51744 ± 0.00624	0.18519 ± 0.00279	2699.9 ± 25.1	0.5	0.683
40.1	130	74	0.590	77	19	3065	0.57	13.0119 ± 0.2397	0.50996 ± 0.00827	0.18506 ± 0.00129	2698.7 ± 11.5	1.9	0.927
6.1	123	56	0.467	71	2	28401	0.06	12.9772 ± 0.2038	0.50880 ± 0.00607	0.18498 ± 0.00163	2698.1 ± 14.6	2.1	0.830
21.1	37	20	0.569	21	1	19395	0.09	12.8458 ± 0.2301	0.50381 ± 0.00676	0.18493 ± 0.00191	2697.6 ± 17.1	3.0	0.821
14.1	101	45	0.457	58	5	8379	0.21	12.9333 ± 0.1867	0.50741 ± 0.00575	0.18486 ± 0.00141	2697.0 ± 12.7	2.3	0.851
4.1	142	103	0.753	85	5	12847	0.14	12.7812 ± 0.2486	0.50156 ± 0.00793	0.18482 ± 0.00176	2696.6 ± 15.8	3.4	0.874
29.1	160	107	0.689	98	6	11989	0.15	13.1507 ± 0.1706	0.51622 ± 0.00584	0.18476 ± 0.00094	2696.1 ± 8.4	0.6	0.921
35.1	234	157	0.695	141	21	4959	0.35	12.9260 ± 0.1975	0.50741 ± 0.00689	0.18476 ± 0.00102	2696.1 ± 9.2	2.3	0.933
17.1	332	204	0.634	198	4	36036	0.05	12.9764 ± 0.1554	0.50942 ± 0.00568	0.18475 ± 0.00059	2696.0 ± 5.3	1.9	0.964
25.1	301	230	0.787	185	4	29360	0.06	12.9560 ± 0.1566	0.50888 ± 0.00551	0.18465 ± 0.00077	2695.1 ± 6.9	2.0	0.940
9.1	139	70	0.520	80	7	8469	0.21	12.8234 ± 0.2271	0.50489 ± 0.00581	0.18421 ± 0.00223	2691.1 ± 20.1	2.5	0.735
11.1	374	323	0.892	235	4	45434	0.04	12.9530 ± 0.1571	0.51001 ± 0.00553	0.18420 ± 0.00078	2691.1 ± 7.0	1.6	0.938
41.1	639	517	0.837	397	17	16345	0.11	12.9430 ± 0.1487	0.50963 ± 0.00560	0.18420 ± 0.00041	2691.0 ± 3.7	1.6	0.981
7.2	40	23	0.589	22	2	6982	0.25	12.0634 ± 0.2617	0.47505 ± 0.00638	0.18418 ± 0.00284	2690.8 ± 25.7	8.3	0.708
2.1	120	106	0.910	74	1	100000	0.02	12.6243 ± 0.1643	0.49715 ± 0.00565	0.18417 ± 0.00093	2690.8 ± 8.4	4.0	0.922

continued…

Uncertainties are reported at 1σ (absolute) and are calculated by numerical propagation of all known sources of error.
Pb* = radiogenic Pb; f206 (%): Percentage of 206Pb which is common.
Disc (%) = Percent discordance along a chord to origin for the given 207Pb/206Pb age; Corr. Coeff. = Correlation coefficient (rho).

Table A2. continued

Spot	U (ppm)	Th (ppm)	Th/U	Pb* (ppm)	^{204}Pb (ppb)	^{206}Pb/^{204}Pb	f206 (%)	^{207}Pb/^{235}U ± 1σ	^{206}Pb/^{238}U ± 1σ	^{207}Pb/^{206}Pb ± 1σ	^{207}Pb/^{206}Pb ± 1σ Age (Ma)	Disc. (%)	Corr. Coeff.
BNB01-T-01, *Timiskaming sandstone, continued...*													
26.1	157	50	0.330	87	9	7812	0.22	12.7898 ± 0.1778	0.50380 ± 0.00610	0.18412 ± 0.00101	2690.4 ± 9.1	2.7	0.920
1.1	313	168	0.554	180	0	490196	0.00	12.6528 ± 0.2772	0.49875 ± 0.01037	0.18399 ± 0.00088	2689.2 ± 7.9	3.6	0.976
20.1	118	81	0.706	71	2	25920	0.07	12.8321 ± 0.1707	0.50584 ± 0.00575	0.18398 ± 0.00104	2689.1 ± 9.4	2.3	0.907
5.1	103	44	0.440	58	3	13180	0.13	12.7874 ± 0.2255	0.50453 ± 0.00563	0.18382 ± 0.00227	2687.6 ± 20.5	2.5	0.721
33.1	154	32	0.217	84	15	4649	0.37	12.8797 ± 0.1764	0.50834 ± 0.00593	0.18376 ± 0.00108	2687.1 ± 9.7	1.7	0.905
34.1	160	29	0.185	86	16	4493	0.39	12.8608 ± 0.1761	0.50897 ± 0.00595	0.18326 ± 0.00107	2682.6 ± 9.7	1.4	0.907
18.1	85	107	1.300	57	10	3634	0.48	12.7840 ± 0.2465	0.50623 ± 0.00722	0.18316 ± 0.00207	2681.7 ± 18.9	1.9	0.813
42.1	135	67	0.512	77	18	3193	0.54	12.6231 ± 0.1734	0.50021 ± 0.00546	0.18303 ± 0.00130	2680.5 ± 11.8	3.0	0.859
13.1	122	102	0.862	76	3	19493	0.09	12.7436 ± 0.2024	0.50612 ± 0.00605	0.18262 ± 0.00166	2676.8 ± 15.1	1.7	0.824
7.1	95	81	0.882	59	4	11361	0.15	12.6712 ± 0.2043	0.50336 ± 0.00633	0.18257 ± 0.00158	2676.4 ± 14.4	2.2	0.847
8.1	239	177	0.762	145	7	14172	0.12	12.6678 ± 0.1621	0.50371 ± 0.00588	0.18240 ± 0.00073	2674.8 ± 6.6	2.1	0.951
3.1	36	27	0.773	22	5	3390	0.51	12.4106 ± 0.3111	0.49547 ± 0.00991	0.18167 ± 0.00233	2668.1 ± 21.4	3.4	0.862
31.1	214	101	0.488	124	6	15929	0.11	12.7718 ± 0.1617	0.51023 ± 0.00567	0.18154 ± 0.00088	2667.0 ± 8.1	0.4	0.925
39.1	41	32	0.813	25	14	1311	1.32	12.4788 ± 0.2851	0.50154 ± 0.00665	0.18045 ± 0.00307	2657.1 ± 28.5	1.7	0.674
02JAA-0017, *Timiskaming sandstone detrital zircons in auriferous quartz vein, Sedimentary Trough, Dome Mine, Tisdale Township (see Ayer et al., 2003), #11 on Fig. 2.*													
15.1	145	98	0.704	89	19	3315	0.52	13.2612 ± 0.1963	0.51536 ± 0.00679	0.18663 ± 0.00099	2712.7 ± 8.8	1.5	0.935
5.1	106	62	0.602	63	9	5409	0.32	13.0691 ± 0.1830	0.50925 ± 0.00610	0.18613 ± 0.00110	2708.3 ± 9.8	2.5	0.908
12.1	133	129	1.001	85	23	2470	0.70	12.8698 ± 0.1986	0.50291 ± 0.00658	0.18560 ± 0.00124	2703.6 ± 11.1	3.5	0.903
6.1	147	95	0.667	87	17	3714	0.47	12.8510 ± 0.2178	0.50349 ± 0.00589	0.18512 ± 0.00201	2699.3 ± 18.1	3.2	0.771
17.1	127	59	0.478	73	29	1908	0.91	12.9095 ± 0.1851	0.50585 ± 0.00593	0.18509 ± 0.00128	2699.0 ± 11.5	2.7	0.878
9.1	153	79	0.534	90	7	9626	0.18	13.0864 ± 0.1713	0.51281 ± 0.00606	0.18508 ± 0.00080	2698.9 ± 7.2	1.4	0.945
16.1	46	36	0.817	27	31	632	2.74	12.2766 ± 0.3032	0.48109 ± 0.00740	0.18508 ± 0.00324	2698.9 ± 29.2	7.5	0.712
18.1	190	196	1.065	123	6	13576	0.13	12.9620 ± 0.1519	0.50939 ± 0.00550	0.18455 ± 0.00063	2694.2 ± 5.6	1.8	0.958
10.1	70	36	0.540	41	4	6856	0.25	12.9149 ± 0.1770	0.50779 ± 0.00575	0.18446 ± 0.00118	2693.4 ± 10.7	2.1	0.885
8.1	102	89	0.902	64	9	4832	0.36	12.8026 ± 0.1703	0.50502 ± 0.00556	0.18386 ± 0.00115	2688.0 ± 10.3	2.4	0.885
1.1	53	40	0.774	30	10	2087	0.83	11.9253 ± 0.2537	0.47133 ± 0.00693	0.18350 ± 0.00250	2684.8 ± 22.7	8.8	0.772
2.1	167	122	0.751	99	21	3461	0.50	12.4402 ± 0.1622	0.49473 ± 0.00552	0.18237 ± 0.00101	2674.6 ± 9.2	3.8	0.908
11.1	97	72	0.765	59	8	5259	0.33	12.7148 ± 0.1837	0.50593 ± 0.00588	0.18227 ± 0.00132	2673.6 ± 12.1	1.6	0.867
13.1	171	117	0.711	103	14	5465	0.32	12.7737 ± 0.1783	0.50836 ± 0.00592	0.18224 ± 0.00116	2673.4 ± 10.6	1.1	0.892
7.1	226	212	0.969	142	20	4847	0.36	12.6431 ± 0.1646	0.50438 ± 0.00559	0.18180 ± 0.00101	2669.4 ± 9.3	1.7	0.905
19.1	192	182	0.979	122	24	3523	0.49	12.6586 ± 0.4506	0.50510 ± 0.01755	0.18176 ± 0.00082	2669.0 ± 7.5	1.5	0.992
14.1	164	118	0.742	99	19	3676	0.47	12.6198 ± 0.1610	0.50385 ± 0.00550	0.18166 ± 0.00098	2668.1 ± 9.0	1.7	0.908
3.1	163	102	0.648	95	13	5218	0.33	12.4321 ± 0.1545	0.49640 ± 0.00543	0.18164 ± 0.00085	2667.9 ± 7.8	3.2	0.928
20.1	100	51	0.532	57	43	1022	1.70	12.5801 ± 0.2143	0.50472 ± 0.00693	0.18077 ± 0.00154	2660.0 ± 14.2	1.2	0.868

Uncertainties are reported at 1σ (absolute) and are calculated by numerical propagation of all known sources of error.
Pb* = radiogenic Pb; f206 (%): Percentage of 206Pb which is common.
Disc (%) = Percent discordance along a chord to origin for the given 207Pb/206Pb age; Corr. Coeff. = Correlation coefficient (rho).

Table A2. continued

Spot	U (ppm)	Th (ppm)	Th/U	Pb* (ppm)	^{204}Pb (ppb)	^{206}Pb/^{204}Pb	f206 (%)	^{207}Pb/^{235}U ± 1σ	^{206}Pb/^{238}U ± 1σ	^{207}Pb/^{206}Pb ± 1σ	^{207}Pb/^{206}Pb ± 1σ Age (Ma)	Disc. (%)	Corr. Coeff.
04JAA-0003, *Porcupine assemblage wacke, below Timiskaming unconformity, Porcupine Syncline, E Tisdale Twp.(E484309, N5371290), #15 on Fig. 2.*													
40.3	47	28	0.627	28	17	1225	1.42	13.1885 ± 0.3651	0.49710 ± 0.00734	0.19242 ± 0.00416	2763.0 ± 36.0	7.1	0.631
25.1	111	72	0.671	67	8	6057	0.29	13.4285 ± 0.2212	0.51073 ± 0.00641	0.19069 ± 0.00176	2748.2 ± 15.3	3.9	0.831
47.1	21	14	0.680	12	9	994	1.74	13.3984 ± 0.4068	0.51039 ± 0.00838	0.19039 ± 0.00449	2745.6 ± 39.3	3.9	0.638
5.1	48	29	0.623	29	4	5150	0.34	13.3587 ± 0.2496	0.50988 ± 0.00708	0.19002 ± 0.00207	2742.3 ± 18.0	3.8	0.816
38.1	59	54	0.937	37	8	3306	0.52	13.1459 ± 0.2805	0.50412 ± 0.00688	0.18913 ± 0.00280	2734.6 ± 24.6	4.6	0.726
16.1	70	29	0.429	41	7	4312	0.40	13.3076 ± 0.2340	0.51240 ± 0.00707	0.18836 ± 0.00175	2727.9 ± 15.4	2.7	0.851
42.1	46	69	1.558	32	2	10208	0.17	13.1189 ± 0.2335	0.50548 ± 0.00686	0.18823 ± 0.00187	2726.8 ± 16.5	4.0	0.833
24.1	59	32	0.559	35	9	2805	0.62	13.1576 ± 0.2221	0.50746 ± 0.00620	0.18805 ± 0.00192	2725.2 ± 17.0	3.6	0.799
9.1	136	78	0.590	82	9	6955	0.25	13.4287 ± 0.1814	0.51792 ± 0.00581	0.18805 ± 0.00118	2725.2 ± 10.4	1.6	0.888
45.1	116	116	1.038	77	16	3349	0.52	13.5210 ± 0.2127	0.52211 ± 0.00606	0.18782 ± 0.00174	2723.2 ± 15.4	0.7	0.811
34.1	62	70	1.176	41	11	2355	0.74	13.0487 ± 0.2367	0.50467 ± 0.00678	0.18752 ± 0.00199	2720.6 ± 17.6	3.9	0.814
14.1	28	22	0.812	17	8	1625	1.07	13.3108 ± 0.3069	0.51487 ± 0.00717	0.18750 ± 0.00313	2720.4 ± 27.8	1.9	0.695
23.1	42	20	0.489	24	4	4229	0.41	13.0867 ± 0.2295	0.50718 ± 0.00668	0.18714 ± 0.00188	2717.2 ± 16.7	3.3	0.823
31.1	30	24	0.813	19	9	1559	1.11	13.2833 ± 0.3410	0.51499 ± 0.00894	0.18707 ± 0.00315	2716.6 ± 28.1	1.7	0.758
28.1	51	39	0.787	32	13	1762	0.98	13.3381 ± 0.3334	0.51721 ± 0.01028	0.18704 ± 0.00241	2716.3 ± 21.4	1.3	0.859
35.1	59	46	0.814	37	9	2921	0.59	13.3254 ± 0.3770	0.51702 ± 0.00824	0.18693 ± 0.00401	2715.3 ± 35.8	1.3	0.658
8.1	79	70	0.910	49	6	5304	0.33	12.8575 ± 0.1921	0.49892 ± 0.00601	0.18691 ± 0.00139	2715.1 ± 12.3	4.7	0.869
32.1	104	94	0.928	65	8	5453	0.32	12.9278 ± 0.2438	0.50213 ± 0.00828	0.18673 ± 0.00137	2713.6 ± 12.1	4.1	0.923
4.1	86	45	0.538	50	0	250627	0.01	12.9809 ± 0.1962	0.50469 ± 0.00632	0.18654 ± 0.00131	2711.9 ± 11.7	3.5	0.887
20.1	38	40	1.069	25	10	1667	1.04	12.8550 ± 0.2821	0.49999 ± 0.00750	0.18647 ± 0.00266	2711.3 ± 23.7	4.4	0.765
2.1	131	84	0.658	80	7	7813	0.22	13.2296 ± 0.1864	0.51498 ± 0.00644	0.18632 ± 0.00095	2709.9 ± 8.5	1.4	0.933
12.1	101	96	0.984	66	12	3831	0.45	13.4597 ± 0.2007	0.52418 ± 0.00598	0.18623 ± 0.00154	2709.2 ± 13.7	-0.3	0.835
41.1	71	72	1.059	46	9	3491	0.50	13.0627 ± 0.3300	0.50877 ± 0.00729	0.18621 ± 0.00355	2709.0 ± 31.8	2.6	0.662
32.2	171	113	0.686	103	9	8636	0.20	13.0534 ± 0.1734	0.50859 ± 0.00558	0.18615 ± 0.00116	2708.4 ± 10.4	2.6	0.884
6.1	123	80	0.672	74	2	33445	0.05	13.1015 ± 0.2039	0.51061 ± 0.00644	0.18609 ± 0.00143	2707.9 ± 12.7	2.2	0.872
27.1	96	82	0.882	61	7	6496	0.27	13.1786 ± 0.1914	0.51368 ± 0.00607	0.18607 ± 0.00132	2707.7 ± 11.7	1.6	0.875
50.1	51	38	0.772	31	7	3124	0.56	13.1925 ± 0.2270	0.51437 ± 0.00720	0.18602 ± 0.00157	2707.3 ± 14.0	1.4	0.874
49.1	36	20	0.571	21	20	800	2.17	12.9251 ± 0.3722	0.50479 ± 0.01012	0.18571 ± 0.00340	2704.5 ± 30.6	3.2	0.776
39.1	72	66	0.949	46	8	3883	0.45	13.0654 ± 0.2781	0.51041 ± 0.00639	0.18565 ± 0.00292	2704.0 ± 26.2	2.1	0.681
48.1	109	41	0.390	63	28	1762	0.98	13.2091 ± 0.1845	0.51638 ± 0.00575	0.18552 ± 0.00133	2702.9 ± 11.9	0.9	0.861
17.1	110	96	0.903	69	4	11857	0.15	12.9174 ± 0.1698	0.50523 ± 0.00591	0.18543 ± 0.00087	2702.1 ± 7.8	3.0	0.935
36.1	352	229	0.672	217	7	22789	0.08	13.3655 ± 0.1580	0.52290 ± 0.00558	0.18538 ± 0.00073	2701.6 ± 6.5	-0.4	0.944
46.1	160	100	0.647	96	5	13139	0.13	13.0680 ± 0.1525	0.51172 ± 0.00539	0.18521 ± 0.00072	2700.1 ± 6.5	1.6	0.944
11.1	153	214	1.442	106	1	100000	0.02	12.9498 ± 0.1556	0.50750 ± 0.00552	0.18507 ± 0.00072	2698.8 ± 6.5	2.4	0.946
19.1	67	50	0.781	40	8	3443	0.50	12.7695 ± 0.2116	0.50046 ± 0.00649	0.18506 ± 0.00163	2698.7 ± 14.6	3.7	0.849
33.2	179	142	0.818	114	3	25050	0.07	13.2895 ± 0.1781	0.52106 ± 0.00639	0.18498 ± 0.00075	2698.0 ± 6.7	-0.3	0.954
43.1	18	8	0.481	10	29	285	6.08	12.6290 ± 0.5315	0.49537 ± 0.00869	0.18490 ± 0.00668	2697.3 ± 60.9	4.7	0.524
7.1	112	118	1.089	72	4	13263	0.13	12.8922 ± 0.1968	0.50572 ± 0.00648	0.18489 ± 0.00126	2697.3 ± 11.3	2.7	0.896

continued…

Uncertainties are reported at 1σ (absolute) and are calculated by numerical propagation of all known sources of error.
Pb* = radiogenic Pb; f206 (%): Percentage of 206Pb which is common.
Disc (%) = Percent discordance along a chord to origin for the given 207Pb/206Pb age; Corr. Coeff. = Correlation coefficient (rho).

Table A2. continued

Spot	U (ppm)	Th (ppm)	Th/U	Pb* (ppm)	^{204}Pb (ppb)	^{206}Pb/^{204}Pb	f206 (%)	^{207}Pb/^{235}U ± 1σ	^{206}Pb/^{238}U ± 1σ	^{207}Pb/^{206}Pb ± 1σ	^{207}Pb/^{206}Pb ± 1σ Age (Ma)	Disc. (%)	Corr. Coeff.
04JAA-0003, *Porcupine assemblage wacke, continued...*													
37.2	224	141	0.649	135	16	5992	0.29	13.0152 ± 0.1771	0.51089 ± 0.00624	0.18477 ± 0.00086	2696.1 ± 7.7	1.6	0.941
15.2	76	66	0.894	48	4	8514	0.20	13.0175 ± 0.2057	0.51101 ± 0.00673	0.18475 ± 0.00134	2696.0 ± 12.0	1.6	0.890
29.1	131	177	1.396	90	3	16776	0.10	12.9752 ± 0.1737	0.50949 ± 0.00594	0.18471 ± 0.00097	2695.6 ± 8.7	1.9	0.921
21.1	113	34	0.314	64	3	14312	0.12	13.1206 ± 0.1816	0.51630 ± 0.00601	0.18431 ± 0.00113	2692.0 ± 10.2	0.4	0.897
3.1	141	166	1.216	93	2	33979	0.05	12.8584 ± 0.1759	0.50701 ± 0.00583	0.18394 ± 0.00112	2688.7 ± 10.1	2.0	0.896
15.1	90	109	1.257	61	3	15542	0.11	13.0198 ± 0.1807	0.51357 ± 0.00604	0.18387 ± 0.00111	2688.1 ± 10.0	0.7	0.902
37.1	287	127	0.457	165	15	8215	0.21	12.9250 ± 0.1659	0.50985 ± 0.00591	0.18386 ± 0.00078	2688.0 ± 7.1	1.5	0.944
13.1	92	91	1.021	58	3	14815	0.12	12.7417 ± 0.1780	0.50268 ± 0.00595	0.18384 ± 0.00112	2687.8 ± 10.1	2.8	0.902
18.1	91	76	0.866	57	7	6134	0.28	12.9223 ± 0.1885	0.50983 ± 0.00624	0.18383 ± 0.00120	2687.7 ± 10.9	1.4	0.895
33.1	128	63	0.508	77	6	9925	0.18	13.2518 ± 0.2042	0.52323 ± 0.00733	0.18369 ± 0.00090	2686.5 ± 8.2	-1.2	0.949
22.1	89	74	0.855	56	6	6055	0.29	12.8801 ± 0.1853	0.50893 ± 0.00588	0.18355 ± 0.00133	2685.2 ± 12.1	1.5	0.866
40.1	28	19	0.676	17	12	1116	1.55	13.1588 ± 0.3351	0.52020 ± 0.00791	0.18346 ± 0.00341	2684.4 ± 31.1	-0.7	0.689
44.1	212	145	0.706	128	17	5462	0.32	12.9223 ± 0.1622	0.51163 ± 0.00564	0.18318 ± 0.00087	2681.9 ± 7.9	0.8	0.926
26.1	137	127	0.958	87	16	3832	0.45	12.8940 ± 0.1891	0.51074 ± 0.00593	0.18310 ± 0.00140	2681.2 ± 12.7	1.0	0.857
10.1	69	68	1.022	43	7	4079	0.43	12.4655 ± 0.1881	0.49381 ± 0.00598	0.18309 ± 0.00139	2681.0 ± 12.7	4.2	0.866
30.1	93	79	0.869	58	10	4067	0.43	12.6618 ± 0.2124	0.50398 ± 0.00688	0.18221 ± 0.00149	2673.1 ± 13.6	1.9	0.875
1.2	476	290	0.630	267	7	29028	0.06	12.0295 ± 0.1367	0.48346 ± 0.00514	0.18046 ± 0.00052	2657.1 ± 4.8	5.2	0.968
40.2	26	15	0.581	15	24	503	3.44	12.4562 ± 0.4154	0.50693 ± 0.00796	0.17821 ± 0.00491	2636.3 ± 46.5	-0.3	0.574
1.1	157	146	0.957	92	2	25887	0.07	11.5292 ± 0.2135	0.47093 ± 0.00668	0.17756 ± 0.00182	2630.2 ± 17.2	6.5	0.835
03RJB-18972-6, *Porcupine sandstone, south of PDDZ, Whitney Township (E491548, N5372704), # 21 on Fig. 2.*													
7.1	95	61	0.663	58	24	1731	1.00	13.3490 ± 0.1899	0.50845 ± 0.00571	0.19041 ± 0.00142	2745.7 ± 12.3	4.2	0.855
12.1	188	93	0.509	111	12	7085	0.25	13.4732 ± 0.1649	0.51573 ± 0.00568	0.18947 ± 0.00079	2737.6 ± 6.8	2.5	0.942
8.1	452	326	0.745	283	17	11767	0.15	13.6085 ± 0.1527	0.52224 ± 0.00560	0.18899 ± 0.00042	2733.4 ± 3.7	1.1	0.980
3.1	325	89	0.281	187	8	17652	0.10	13.7067 ± 0.1501	0.52733 ± 0.00546	0.18852 ± 0.00047	2729.3 ± 4.1	0.0	0.974
6.1	157	40	0.263	88	23	3041	0.57	13.4030 ± 0.1865	0.51748 ± 0.00645	0.18785 ± 0.00091	2723.4 ± 8.0	1.6	0.939
15.1	96	38	0.408	55	18	2387	0.73	13.1765 ± 0.1945	0.51096 ± 0.00649	0.18703 ± 0.00114	2716.2 ± 10.1	2.5	0.912
13.1	105	80	0.792	63	23	1941	0.89	12.7006 ± 0.1857	0.49712 ± 0.00555	0.18529 ± 0.00151	2700.8 ± 13.5	4.5	0.833
14.1	77	35	0.468	44	11	2947	0.59	13.0331 ± 0.1819	0.51018 ± 0.00582	0.18528 ± 0.00125	2700.7 ± 11.2	2.0	0.877
2.1	237	490	2.136	187	11	9438	0.18	13.1180 ± 0.1500	0.51520 ± 0.00547	0.18467 ± 0.00058	2695.2 ± 5.2	0.7	0.963
4.1	494	994	2.078	388	24	9092	0.19	13.1558 ± 0.1406	0.51725 ± 0.00529	0.18447 ± 0.00038	2693.4 ± 3.4	0.3	0.982
5.2	204	293	1.488	143	6	14795	0.12	13.0101 ± 0.1497	0.51216 ± 0.00546	0.18424 ± 0.00059	2691.4 ± 5.3	1.2	0.961
10.1	613	371	0.625	367	44	6205	0.28	13.0607 ± 0.1963	0.51418 ± 0.00620	0.18422 ± 0.00140	2691.3 ± 12.6	0.8	0.866
5.3	523	1088	2.149	414	19	11943	0.15	13.1099 ± 0.1482	0.51625 ± 0.00550	0.18418 ± 0.00049	2690.9 ± 4.5	0.3	0.972
1.1	742	431	0.600	449	37	8985	0.19	13.1345 ± 0.2367	0.51999 ± 0.00767	0.18320 ± 0.00159	2682.0 ± 14.4	-0.8	0.879
6.2	269	49	0.186	133	29	3743	0.46	11.7457 ± 0.1599	0.47106 ± 0.00568	0.18084 ± 0.00090	2660.6 ± 8.3	7.8	0.931
11.1	1176	743	0.653	649	33	14828	0.12	10.8083 ± 0.1793	0.47765 ± 0.00767	0.16412 ± 0.00043	2498.5 ± 4.4	-0.9	0.988

Uncertainties are reported at 1σ (absolute) and are calculated by numerical propagation of all known sources of error.
Pb* = radiogenic Pb; f206 (%): Percentage of 206Pb which is common.
Disc (%) = Percent discordance along a chord to origin for the given 207Pb/206Pb age; Corr. Coeff. = Correlation coefficient (rho).

Table A2. continued

Spot	U (ppm)	Th (ppm)	Th/U	Pb* (ppm)	^{204}Pb (ppb)	^{206}Pb/^{204}Pb	f206 (%)	^{207}Pb/^{235}U ± 1σ	^{206}Pb/^{238}U ± 1σ	^{207}Pb/^{206}Pb ± 1σ	^{207}Pb/^{206}Pb ± 1σ Age (Ma)	Disc. (%)	Corr. Coeff.
03RJB-18973-10, *Porcupine sandstone, Hoyle Formation, Hoyle Township (E492148, N5375256), #18 on Fig. 2.*													
12.1	196	122	0.640	122	16	5577	0.31	13.9474 ± 0.1771	0.52789 ± 0.00568	0.19162 ± 0.00106	2756.2 ± 9.1	1.1	0.902
3.1	90	14	0.166	49	12	3341	0.52	13.1819 ± 0.2670	0.51187 ± 0.00742	0.18678 ± 0.00233	2714.0 ± 20.7	2.2	0.792
14.1	30	18	0.601	18	6	2119	0.82	13.2186 ± 0.2601	0.51571 ± 0.00697	0.18590 ± 0.00236	2706.2 ± 21.1	1.1	0.768
13.1	176	216	1.267	118	7	11056	0.16	12.9640 ± 0.1551	0.50652 ± 0.00555	0.18563 ± 0.00067	2703.8 ± 6.0	2.8	0.954
4.2	51	19	0.378	29	16	1411	1.23	13.0893 ± 0.2596	0.51179 ± 0.00653	0.18549 ± 0.00254	2702.6 ± 22.7	1.7	0.730
18.1	74	53	0.744	45	26	1240	1.40	12.9692 ± 0.2093	0.50714 ± 0.00631	0.18547 ± 0.00164	2702.4 ± 14.7	2.6	0.840
17.1	105	62	0.610	62	15	3173	0.55	12.9618 ± 0.1936	0.50701 ± 0.00650	0.18541 ± 0.00115	2701.9 ± 10.3	2.6	0.911
8.1	157	37	0.240	86	4	19365	0.09	13.0178 ± 0.1634	0.50926 ± 0.00588	0.18539 ± 0.00068	2701.7 ± 6.1	2.2	0.957
4.1	141	26	0.188	78	15	4148	0.42	13.2411 ± 0.1618	0.51932 ± 0.00556	0.18492 ± 0.00087	2697.5 ± 7.8	0.1	0.924
1.1	145	90	0.644	86	5	12780	0.14	12.7861 ± 0.1703	0.50225 ± 0.00589	0.18464 ± 0.00093	2695.0 ± 8.3	3.2	0.927
5.1	172	57	0.341	97	3	25349	0.07	13.0691 ± 0.1626	0.51337 ± 0.00568	0.18463 ± 0.00083	2695.0 ± 7.4	1.1	0.934
16.1	65	28	0.447	37	16	1762	0.98	12.8809 ± 0.2045	0.50673 ± 0.00619	0.18436 ± 0.00161	2692.5 ± 14.5	2.3	0.838
10.1	182	63	0.356	102	12	6731	0.26	12.9400 ± 0.1717	0.50919 ± 0.00624	0.18431 ± 0.00070	2692.0 ± 6.3	1.8	0.959
7.1	170	53	0.322	95	10	7458	0.23	12.9069 ± 0.1779	0.50790 ± 0.00603	0.18431 ± 0.00104	2692.0 ± 9.4	2.0	0.913
11.1	187	148	0.819	115	11	7592	0.23	12.8783 ± 0.1614	0.50741 ± 0.00566	0.18408 ± 0.00083	2690.0 ± 7.4	2.0	0.935
15.1	32	9	0.297	17	7	2040	0.85	12.7847 ± 0.2384	0.50432 ± 0.00641	0.18386 ± 0.00223	2688.0 ± 20.2	2.5	0.763
9.1	158	79	0.516	92	8	8696	0.20	12.9676 ± 0.1509	0.51194 ± 0.00538	0.18371 ± 0.00071	2686.7 ± 6.4	1.0	0.945
2.1	155	31	0.205	84	18	3840	0.45	12.8251 ± 0.2400	0.50863 ± 0.00823	0.18288 ± 0.00139	2679.1 ± 12.6	1.3	0.915
6.1	223	118	0.548	132	11	8979	0.19	12.9491 ± 0.1569	0.51383 ± 0.00546	0.18278 ± 0.00085	2678.2 ± 7.7	0.2	0.925

Uncertainties are reported at 1σ (absolute) and are calculated by numerical propagation of all known sources of error.
Pb* = radiogenic Pb; f206 (%): Percentage of 206Pb which is common.
Disc (%) = Percent discordance along a chord to origin for the given 207Pb/206Pb age; Corr. Coeff. = Correlation coefficient (rho).

Metric Conversion Table

Conversion from SI to Imperial			Conversion from Imperial to SI		
SI Unit	*Multiplied by*	*Gives*	*Imperial Unit*	*Multiplied by*	*Gives*
		LENGTH			
1 mm	0.039 37	inches	1 inch	**25.4**	mm
1 cm	0.393 70	inches	1 inch	**2.54**	cm
1 m	3.280 84	feet	1 foot	**0.304 8**	m
1 m	0.049 709	chains	1 chain	20.116 8	m
1 km	0.621 371	miles (statute)	1 mile (statute)	**1.609 344**	km
		AREA			
1 cm^2	0.155 0	square inches	1 square inch	**6.451 6**	cm^2
1 m^2	10.763 9	square feet	1 square foot	**0.092 903 04**	m^2
1 km^2	0.386 10	square miles	1 square mile	2.589 988	km^2
1 ha	2.471 054	acres	1 acre	0.404 685 6	ha
		VOLUME			
1 cm^3	0.061 023	cubic inches	1 cubic inch	**16.387 064**	cm^3
1 m^3	35.314 7	cubic feet	1 cubic foot	0.028 316 85	m^3
1 m^3	1.307 951	cubic yards	1 cubic yard	0.764 554 86	m^3
		CAPACITY			
1 L	1.759 755	pints	1 pint	0.568 261	L
1 L	0.879 877	quarts	1 quart	1.136 522	L
1 L	0.219 969	gallons	1 gallon	**4.546 090**	L
		MASS			
1 g	0.035 273 962	ounces (avdp)	1 ounce (avdp)	28.349 523	g
1 g	0.032 150 747	ounces (troy)	1 ounce (troy)	**31.103 476 8**	g
1 kg	2.204 622 6	pounds (avdp)	1 pound (avdp)	**0.453 592 37**	kg
1 kg	0.001 102 3	tons (short)	1 ton (short)	**907.184 74**	kg
1 t	1.102 311 3	tons (short)	1 ton (short)	**0.907 184 74**	t
1 kg	0.000 984 21	tons (long)	1 ton (long)	**1016.046 908 8**	kg
1 t	0.984 206 5	tons (long)	1 ton (long)	**1.016 046 90**	t
		CONCENTRATION			
1 g/t	0.029 166 6	ounce (troy)/ ton (short)	1 ounce (troy)/ ton (short)	34.285 714 2	g/t
1 g/t	0.583 333 33	pennyweights/ ton (short)	1 pennyweight/ ton (short)	1.714 285 7	g/t

OTHER USEFUL CONVERSION FACTORS

	Multiplied by	
1 ounce (troy) per ton (short)	31.103 477	grams per ton (short)
1 gram per ton (short)	0.032 151	ounces (troy) per ton (short)
1 ounce (troy) per ton (short)	20.0	pennyweights per ton (short)
1 pennyweight per ton (short)	0.05	ounces (troy) per ton (short)

Note: Conversion factors which are in bold type are exact. The conversion factors have been taken from or have been derived from factors given in the Metric Practice Guide for the Canadian Mining and Metallurgical Industries, published by the Mining Association of Canada in co-operation with the Coal Association of Canada.

ISSN 0826-9580
ISBN 0-7794-8652-8

Chart A. Magnetic and Gravity Three-Dimensional (3D) Modelling Images

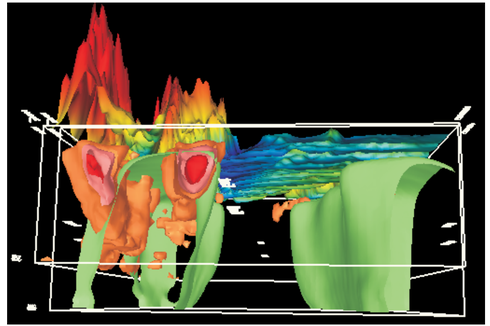

Figure 31. View (looking west from somewhat below the horizon) of 3D inversion of the magnetic and positive gravity data for the Curric Township area. Amplitude-enhanced magnetic data are set above the surface. The magnetic data in lower Blake River assemblage mafic volcanic rocks to the south show 2 limbs of a syncline within a south-dipping gravity high also marking these volcanic rocks. The northern two-thirds of the area (in Tisdale assemblage mafic volcanic rocks) shows a bimodal high low and high-gravity response and low magnetic response. This image suggests a vertical to steep north dip on the northern higher density mafic volcanic rocks.

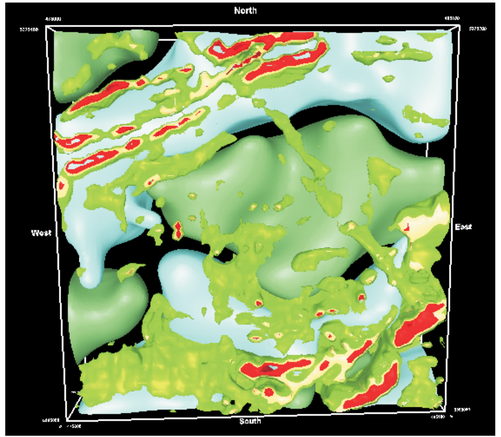

Figure 32. Overhead view of the combined magnetic and gravity shells in parts of Tisdale and Deloro townships; see text for a more detailed explanation.

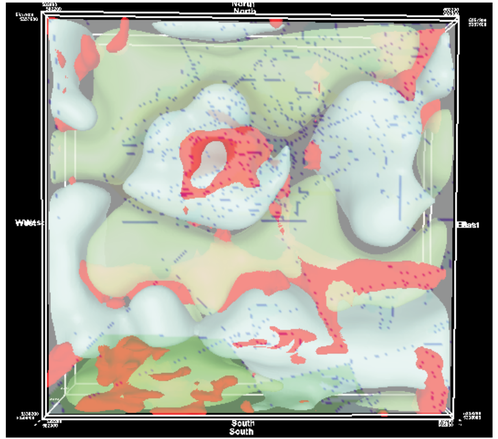

Figure 33. Three-dimensional overhead view of the Clifford stock and surrounding area (4 townships of Clifford, Ben Nevis, Arnold and Katrine). The positive gravity surface is light green, the negative gravity surface is light blue and the magnetic surface is red. Overlying is a transparent image of the geology (*after* Ayer et al. 2005). The Clifford stock (in a faded red) is surrounded by a doughnut-shaped magnetic high (the magnetic margins of the stock), which is then surrounded by a doughnut-shaped gravity low (reflecting surrounding felsic volcanic rocks), followed by a gravity high (from mafic to intermediate volcanic rocks). A separate 3D section (Figure 34) shows the magnetic aureole plunges to the southeast.

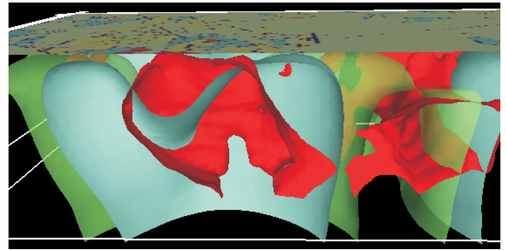

Figure 34. North-south slice through the 3D magnetic (red) and negative gravity (blue) and positive gravity (green) image of the Clifford stock and surrounding area. The view looks east with the surface geology just visible at the top of the image. With reference to Figure 33, the slice cuts the east side of the magnetic anomaly and does not intersect the hole in the doughnut that marks the core of the intrusion. The depression in the blue gravity surface implies a gravity high, not fully developed by the isosurfaces presented here, which is occupied by the magnetic high. As noted in Figure 33, the gravity low identifies the felsic volcanic rocks surrounding the stock. Note, the magnetic body marking the edge of the stock, plunges south, apparently across the density low of the felsic volcanic rocks.

FedNor Canada

Ontario
Northern Ontario Heritage Fund
Fonds du patrimoine du Nord de l'Ontario

Discover Abitibi
A project of innovation, cooperation and revitalization

Découvrons l' Abitibi
Un projet d' innovation, de coopération et de renouvellement

Discover Abitibi Initiative
The Discover Abitibi Initiative is a regional, cluster economic development project based on geoscientific investigations of the western Abitibi greenstone belt. The initiative, centred on the Kirkland Lake and Timmins mining camps, will complete 19 projects developed and directed by the local stakeholders. FedNor, Northern Ontario Heritage Fund Corporation, municipalities and private sector investors have provided the funding for the initiative.

Initiative Découvrons l'Abitibi
L'initiative *Découvrons l'Abitibi* est un projet de développement économique régional dans une grappe d'industries, projet fondé sur des études géoscientifiques de la ceinture de roches vertes de l'Abitibi occidental. Cette initiative, centrée sur les zones minières de Kirkland Lake et de Timmins, mènera à bien 19 projets élaborés et dirigés par des intervenants locaux. FedNor, la Société de gestion du Fonds du patrimoine du Nord de l'Ontario, municipalités et des investisseurs du secteur privé ont fourni les fonds de cette initiative.

Timmins

KIRKLAND LAKE
THE RIGHT ENVIRONMENT

Accompanies OFR 6154

Figure 2. Distribution of lithotectonic assemblages, intrusions, major structures and U/Pb ages in the Timmins to Kirkland Lake study area.

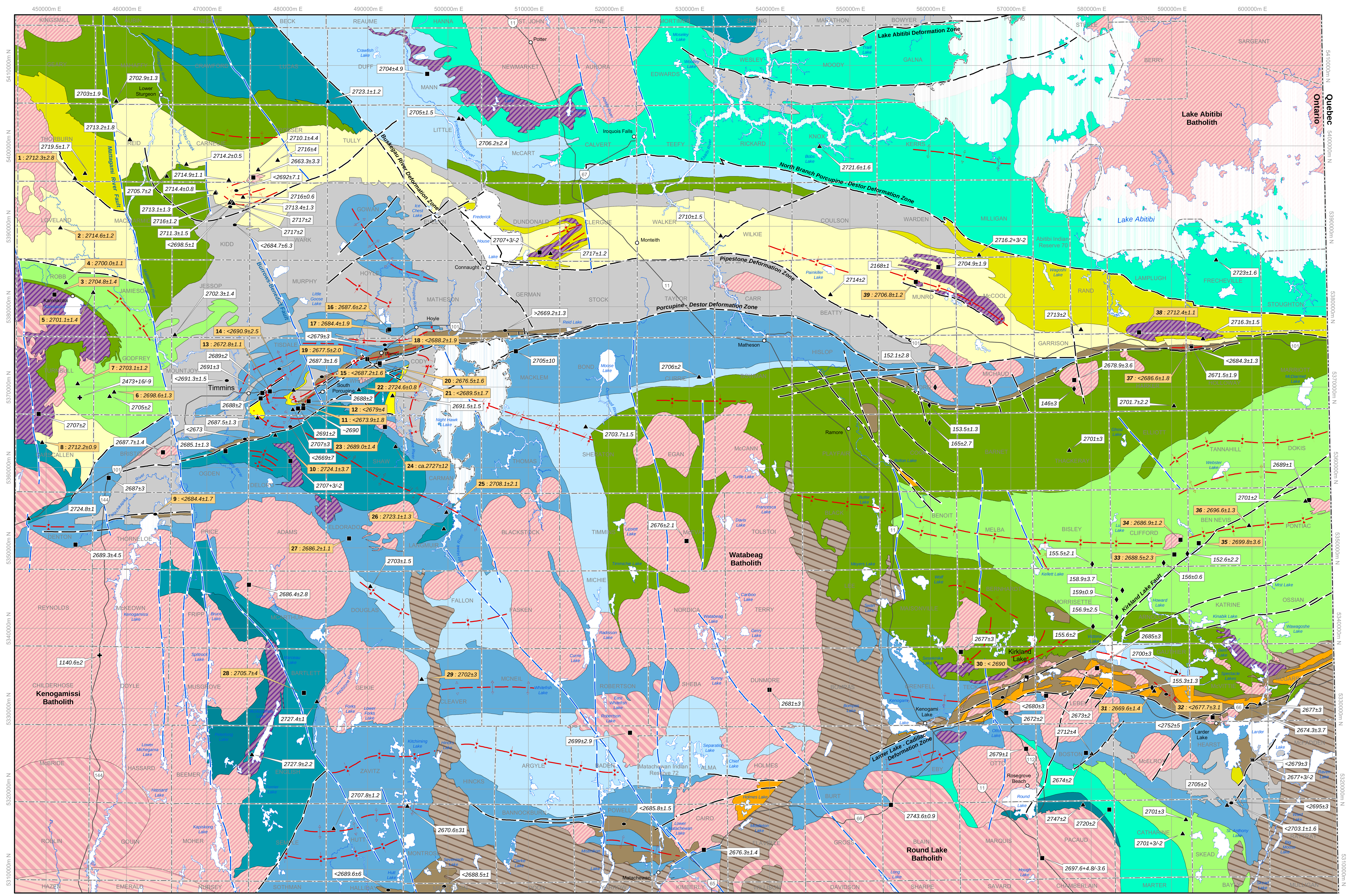

HURONIAN COVER

ABITIBI ASSEMBLAGES

Timiskaming (2676 to 2670 Ma)
- Sedimentary
- Volcanic

UNCONFORMITY

Porcupine (2690 to 2685 Ma)
- Sedimentary
- Volcanic

UNCONFORMITY

Blake River (2704 to 2696 Ma)
- Upper Unit
- Lower Unit

Tisdale (2710 to 2704 Ma)
- Upper Unit
- Lower Unit

Kidd-Munro (2719 to 2711 Ma)
- Upper Unit
- Lower Unit

Stoughton-Roquemaure (2723 to 2720 Ma)

Deloro (2730 to 2724 Ma)

Pacaud (2750 to 2735 Ma)

Intrusive
- Late tectonic (2670 to 2660 Ma)
- Syntectonic (2695 to 2670 Ma)
- Synvolcanic felsics to intermediate (2745 to 2696 Ma)
- Synvolcanic mafic to ultramafic (2740 to 2700 Ma)

SYMBOLS

- Town
- Assemblage boundary
- Post Archean fault
- Archean fault
- Synform, Antiform (unknown generation)
- Synform, Antiform (1st generation)
- Synform, Antiform (2nd generation)
- Synform (3rd generation)

0 2.5 5 10 15 20
Kilometers

GEOCHRONOLOGY SAMPLE

- Volcanic
- Intrusive
- Sedimentary
- Diabase
- Kimberlite

2674.3±3.7 Previous geochronology sample age

1 : 2712.3±2 DA geochronology sample number and age

"<" indicates the maximum (inferred) depositional age based on the youngest detrial zircon analyzed.

1 - 04BHA-0333	**14** - KCR.52	**27** - 04MGH-0283
2 - 04BHA-0297	**15** - 04JAA-0003	**28** - 04PCT-0064
3 - 04BHA-0462	**16** - 04ED-198	**29** - 98JAA-0011
4 - 03BHA-0382	**17** - 03ED-096A	**30** - 03JAA-0006
5 - 03BHA-0384	**18** - 03RJB-18973-10	**31** - 03VOI-0422-1
6 - 03BHA-0345	**19** - 03PJM-131	**32** - 03VOI-0570-1
7 - 03BHA-0047	**20** - 04JAA-0010	**33** - 03SJP-059-01
8 - 96JAA-0094	**21** - 03RJB-18972-6	**34** - 03SJP-115-1
9 - 04JAA-0004	**22** - C88-17 (DU-2)	**35** - 03ASP-0130-1
10 - 04PCT-0062	**23** - 03LAH-0627	**36** - 03ASP-0179-1
11 - 02JAA-0017	**24** - 03LAH-0161	**37** - 3D-CG
12 - BNB01-T-01	**25** - 96TB-079	**38** - C89-7
13 - SM85-60	**26** - 96TB-099	**39** - 04JAA-0002

Discover Abitibi Initiative
The Discover Abitibi Initiative is a regional, cluster economic development project based on geoscientific investigations of the western Abitibi greenstone belt. The initiative, centred on the Kirkland Lake and Timmins mining camps, will complete 19 projects developed and directed by the local stakeholders. FedNor, Northern Ontario Heritage Fund Corporation, municipalities and private sector investors have provided the funding for the initiative.

Initiative Découvrons l'Abitibi
L'initiative *Découvrons l'Abitibi* est un project de développment économique régional dans une grappe d'industries, projet fondé sur des études géoscientifiques de la ceinture de roches vertes de l'Abitibi occidental. Cette initiative, centrée sur les zones minières de Kirkland Lake et de Timmins, mènera à bien 19 projets élaborés et dirigés par des intervenants locaux. FedNor, la Société de gestion du Fonds du patrimoine du Nord de l'Ontario, municipalités et des investisseurs du secteur privé ont fourni les fonds de cette initiative.

Accompanies OFR 6154

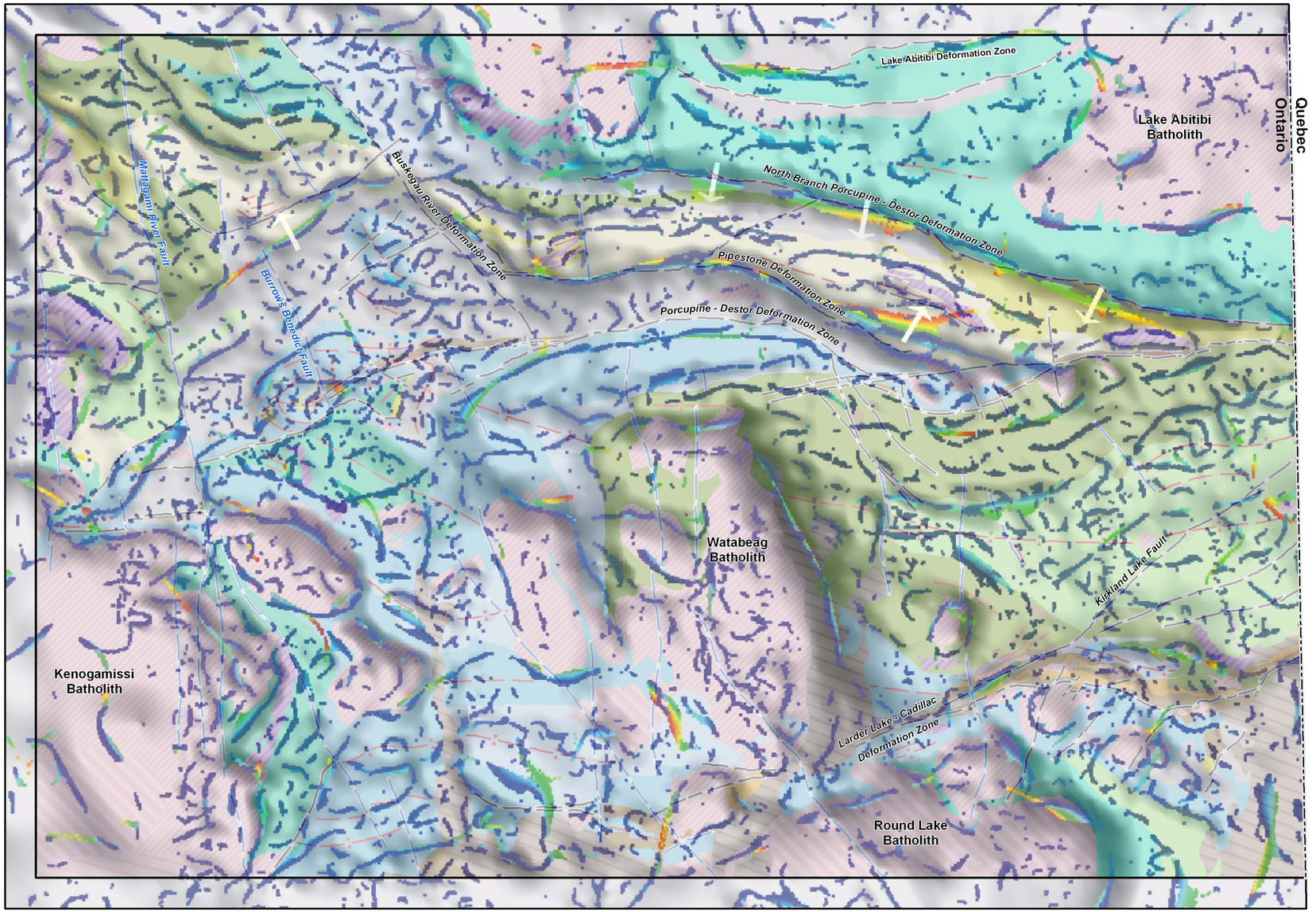

Figure 19. Gravity worms with assemblage and structural map of the study area.

HURONIAN COVER

ABITIBI ASSEMBLAGES

Timiskaming (2676 to 2670 Ma)
- Sedimentary
- Volcanic

UNCONFORMITY

Porcupine (2690 to 2685 Ma)
- Sedimentary
- Volcanic

UNCONFORMITY

Blake River (2704 to 2696 Ma)
- Upper Unit
- Lower Unit

Tisdale (2710 to 2704 Ma)
- Upper Unit
- Lower Unit

Kidd-Munro (2719 to 2711 Ma)
- Upper Unit
- Lower Unit

Stoughton-Roquemaure (2723 to 2720 Ma)

Deloro (2730 to 2724 Ma)

Pacaud (2750 to 2735 Ma)

Intrusive
- Late tectonic (2670 to 2660 Ma)
- Syntectonic (2695 to 2670 Ma)
- Synvolcanic felsics to Intermediate (2745 to 2696 Ma)
- Synvolcanic mafic to ultramafic (2740 to 2700 Ma)

Bouguer Gravity in Shaded Image
- Gravity worms (see text for explanation)
- Dark grey = near surface expression
- Blue/Green/Red expression at progressively deeper levels
- Arrow in direction of dip

SYMBOLS
- Assemblage boundary
- Post Archean fault
- Archean fault
- Synform, Antiform (unknown generation)
- Synform, Antiform (1st generation)
- Synform, Antiform (2nd generation)
- Synform (3rd generation)

0 2.5
Kilometers

FedNor Canada

Ontario
Northern Ontario Heritage Fund
Fonds du patrimoine du Nord de l'Ontario

Discover Abitibi
A project of innovation, cooperation and revitalization
Découvrons l' Abitibi
Un projet d' innovation, de coopération et de renouvellement

Discover Abitibi Initiative
The Discover Abitibi Initiative is a regional, cluster economic development project based on geoscientific investigations of the western Abitibi greenstone belt. The initiative, centred on the Kirkland Lake and Timmins mining camps, will complete 19 projects developed and directed by the local stakeholders. FedNor, Northern Ontario Heritage Fund Corporation, municipalities and private sector investors have provided the funding for the initiative.

Initiative Découvrons l'Abitibi
L'initiative *Découvrons l'Abitibi* est un project de développment économique régional dans une grappe d'industries, projet fondé sur des études géoscientifiques de la ceinture de roches vertes de l'Abitibi occidental. Cette initiative, centrée sur les zones minières de Kirkland Lake et de Timmins, mènera à bien 19 projets élaborés et dirigés par des intervenants locaux. FedNor, la Société de gestion du Fonds du patrimoine du Nord de l'Ontario, municipalités et des investisseurs du secteur privé ont fourni les fonds de cette initiative.

Timmins

KIRKLAND LAKE
THE RIGHT ENVIRONMENT

Accompanies OFR 6154